

**The characterisation of human $\gamma\delta$ T cells in
health and disease;**

**Do $V\gamma 9V\delta 2$ T cells play a role in the
pathogenesis of Bisphosphonate-Related
Osteonecrosis of the Jaw (BRONJ)?**

Paul Leo Ryan

Research Thesis submitted in partial fulfilment of

The Degree of Doctor of Philosophy

Centre for Adult Oral Health, Institute of Dentistry

Barts and The London School of Medicine and Dentistry

Queen Mary University of London

August 2014

Statement of originality

I, Paul Leo Ryan, confirm that the research included within this thesis is my own work or that where it has been carried out in collaboration with, or supported by others, that this is duly acknowledged below and my contribution indicated. Previously published material is also acknowledged below.

I attest that I have exercised reasonable care to ensure that the work is original, and does not to the best of my knowledge break any UK law, infringe any third party's copyright or other Intellectual Property Right, or contain any confidential material.

I accept that the College has the right to use plagiarism detection software to check the electronic version of the thesis.

I confirm that this thesis has not been previously submitted for the award of a degree by this or any other university.

The copyright of this thesis rests with the author and no quotation from it or information derived from it may be published without the prior written consent of the author.

Signature:

A handwritten signature in black ink that reads "Paul Ryan". The signature is written in a cursive style with a large initial 'P' and 'R'.

Date 21.08.14

Details of collaboration and publications

Collaborations

In the assistance of clinical sample collection;

Dr Leo Cheng – Oral and Maxillofacial Surgery, Barts Health NHS Trust, The Royal London Hospital, 3rd Floor Alexandra House, Whitechapel, E1 1BB.

Professor Ali Jawad – Consultant Rheumatologist, The Royal London Hospital, Barts Health NHS Trust, Queen Mary University of London, London, E1 4AD.

Dr Stefano Fedele, Professor Stephen Porter and Dr Pok Lam Fung, Unit of Oral Medicine and Special Care Dentistry, UCL Eastman Dental Institute, Oral Medicine Unit, 256 Gray's Inn Road, London, WC1X 8LD.

Publications

Presentation at academic conferences

1. Ryan P, Bergmeier LA and Pennington DJP – Phenotypic characterisation of Human V γ 9V δ 2 T cells; 15th International Congress of Immunology, Milan, Italy 2013.
2. Ryan P, Bergmeier LA and McKay IJ – Bisphosphonate related osteonecrosis of the Jaw – An immunological based phenomenon; 5th International $\gamma\delta$ T cell conference, Freiberg, Germany 2012.
3. Ryan P, Bergmeier LA and McKay IJ – Bisphosphonate-related osteonecrosis of the Jaw – An immunological based phenomenon; NIHR Wellcome Trust Dental Academic meeting May 2012.

Abstract

Bisphosphonate-Related Osteonecrosis of the Jaw (BRONJ) is a chronic necrosis of the jawbone that occurs in \approx 1-5% of patients receiving bisphosphonate medication for conditions such as osteoporosis and certain cancers. Although the pathogenesis of BRONJ is still uncertain, several recent theories have emerged; these include vascular disruption of the jaw tissue; inappropriate osteoclast activation; and direct cytotoxicity of jaw epithelium. However, despite bisphosphonates having well-documented stimulatory effects on immune cells, and BRONJ being associated with oral microbial infections, an immune-mediated pathology for BRONJ has largely been ignored.

Bisphosphonates activate human $\gamma\delta$ T cells, specifically those that use T cell receptor (TCR) γ -chain variable-region-9, and TCR δ -chain variable-region-2 ($V\gamma 9V\delta 2$ T cells). These unconventional T cells typically account for \approx 1-5% of circulating lymphocytes, make protective responses to microbial challenge, and are promising candidates for cancer immunotherapy. In the context of BRONJ, we have hypothesised that bisphosphonate-mediated activation of jaw-associated $V\gamma 9V\delta 2$ T cells, in the presence of oral microbiota, may drive the disruption of bone turnover that is central to the disease process.

On initiation of these studies, it quickly became apparent that traditional characterisation of $V\gamma 9V\delta 2$ T cells using CD27/CD45RA was demonstrably sub-optimal, while phenotypic analysis of 63 healthy volunteers revealed an unexpected and surprising degree of $V\gamma 9V\delta 2$ T cell heterogeneity; both of which are likely to confuse assessment of disease scenarios. Thus, this thesis describes the novel phenotypic and functional characterisation of $V\gamma 9V\delta 2$ T

cells using alternative surface markers and methods of analysis. This reveals that different sets of individuals have different V γ 9V δ 2 T cell “profiles” that predict very different functional capabilities and responses to immunotherapeutic interventions. Using this improved definition of V γ 9V δ 2 T cells, this thesis then describes preliminary investigations of V γ 9V δ 2 T cell development in the human neonatal thymus, and assesses the involvement of V γ 9V δ 2 T cells in a small cohort of eight BRONJ patients.

Dedication

To the memory of my late father John Ryan BDS NUI and my late uncle Father Martin (Monty) Ryan who sadly passed before completing this work. You have been both a great example and inspiration as individuals in my life and a source of strength and encouragement.

Acknowledgements

My initial thanks are to my supervisors; Professor Daniel Pennington and Dr Lesley Bergmeier who have been a constant source of help and in guiding me throughout the PhD. I am immensely grateful to you both for keeping me on track throughout and for constantly challenging me in the pursuit of scientific excellence. I am fortunate to have had such inspirational and first-class supervisors. My thanks also go my initial supervisor Dr Ian McKay and to past and current Deans; Professors Farida Fortune, Paul Wright and Mike Curtis for believing in me and encouraging me in my career. In addition my thanks are extended to my collaborators; Professor Ali Jawad and Dr Leo Cheng within Barts and The London School of Medicine and Dentistry as well as to Dr Stefano Fedele, Dr Pok Lam Fung and Professor Stephen Porter at The Eastman Dental Institute all of whom have helped in advising and providing direction to the project.

In the laboratory my thanks go to Dr Gary Warnes, Dr Guglielmo Rosignoli and Mr Will Day for their help in flow cytometry and to Dr Charles Mein and Rosamund Nuamah at the genome centre for assistance in performing the gene microarray.

To my fellow PhD students in the Institute of Dentistry and in the Pennington Lab in particular my thanks for your help and support throughout and in particular to Samiul, Capucine, Natalia, and Margarida. To post-docs Nital, Claire and Neil who have always been supportive and in helping me troubleshoot problems and always finding the time to answer a question.

To my colleagues and supervisors in the Dental Institute for being supportive and understanding of the challenges of a basic science PhD. My thanks to Dr Wendy Turner, Dr Shakeel Shahdad and Dr Phil Taylor and also my gratitude goes to Dr Gary Pollock who sadly is no longer with us but as my initial Clinical supervisor was always understanding of the challenges of a PhD.

I would also like to thank my funding body; The Wellcome Trust and The Faculty of Dental Surgery (Royal College of Surgeons of England) who have provided the funding for this research.

To my immediate family, Mum and Kevin and to those who have always been there for me throughout. Your constant love and understanding has been a great source of strength. In addition, my thanks to my close school friends who have always been there to distract me when I needed a break. You have all contributed in helping me achieve this work.

My final thanks go to Cecilia who has been there throughout for me and in understanding the ups and downs of doing a PhD. Your constant support and love have been unwavering. I am grateful to you for always helping me to find perspective and to understand how fortunate I am to have been able to carry out the following work.

Table of Contents

Title page	1
Statement of originality	2
Details of collaboration and publications	3
Collaborations	3
Publications	3
Abstract	4
Dedication	6
Acknowledgements	7
Table of Contents	9
List of Figures	20
List of Tables	24
Abbreviations	25
Chapter 1 Thesis overview	30
Introduction	35
1.1 The Immune System	35
1.1.1 The Innate Immune System	35
1.1.2 The Adaptive Immune System	36
1.2 Human $\gamma\delta$ T cells	38
1.2.1 Human $\gamma\delta$ T cell subsets	40
1.2.2 V δ 1 T cells	40
1.2.3 V δ 2 T cells	41
1.3 Development of human $\gamma\delta$ T cells	43
1.4 Function of $\gamma\delta$ T cells	43
1.4.1 Unique responses to microbial infection	44

1.4.2	Protective response in young animals	44
1.4.3	Immunosurveillance of cancer	45
1.4.4	Immunoregulation	46
1.5	Functional plasticity of V γ 9V δ 2 T cells	48
1.6	$\gamma\delta$ T cells and memory responses	48
1.7	Differentiation pathway of V γ 9V δ 2 T cells.....	51
1.8	$\gamma\delta$ T cell homeostasis.....	52
1.9	Role of the thymus.....	53
1.10	Variation in $\gamma\delta$ T cell number.....	53
1.10.1	Age	54
1.10.2	Gender.....	54
1.10.3	Ethnicity/race and environmental exposure	56
1.11	V γ 9V δ 2 T cell heterogeneity	57
1.12	Phenotypic characterisation of V γ 9V δ 2 T cells	57
1.12.1	CD27/CD45RA.....	59
1.12.2	Naïve V γ 9V δ 2 T cells	59
1.12.3	CD27/CD28.....	60
1.12.4	CD27/CD45RA/CD62L/CD16	61
1.13	Human $\gamma\delta$ T cells – A summary	62
1.14	Bisphosphonate-related osteonecrosis of the jaw (BRONJ).....	63
1.14.1	BRONJ - An undesirable side-effect	63
1.14.2	Phossy Jaw and BRONJ – A resurgence of an historical disease?.....	64
1.14.3	BRONJ Classification and nomenclature	64
1.14.4	Prevalence and Incidence.....	65
1.14.5	Clinical features of BRONJ	66

1.14.6	Unexposed BRONJ.....	66
1.14.7	Histological features.....	67
1.15	Clinical management of BRONJ	68
1.15.1	Prevention.....	68
1.15.2	Antimicrobials.....	68
1.15.3	Surgery	69
1.16	The therapeutic use of bisphosphonates	69
1.16.1	Chemistry.....	69
1.16.2	Medical Indications for use	70
1.16.3	Dose and route of drug administration	70
1.16.4	Post-menopausal osteoporosis.....	71
1.16.5	Adverse skeletal events in cancer patients	72
1.16.6	Other Indications.....	72
1.17	BRONJ - Aetiology and Theories of Pathogenesis	72
1.17.1	Anti-angiogenesis	72
1.17.2	Dysregulation of normal bone turnover	73
1.17.3	Actinomyces / Bacterial cause	73
1.17.4	Direct toxic effect on oral epithelial cells	74
1.17.5	Mucosal breach / Tooth extraction	75
1.17.6	Evidence for V γ 9V δ 2 T cell involvement in BRONJ	75
1.18	Study Hypothesis.....	78
1.19	Working hypothesis	78
1.20	Aim and objectives of thesis	79
Chapter 2	Materials and methods	81
2.1	Ethical approval.....	81
2.2	Collaborative unit.....	83

2.3	Recruitment of study subjects	83
2.3.1	Healthy volunteers	83
2.3.2	Infants undergoing corrective cardiac surgery	84
2.3.3	Bisphosphonate treated control patients	84
2.3.4	BRONJ patients	84
2.4	Tissue Preparation	85
2.4.1	Blood donor cones	85
2.4.2	Blood.....	85
2.4.3	Separation of PBMCs from peripheral venous blood	86
2.4.4	Thymus	86
2.4.5	Isolation of thymocytes from the neonatal thymus	86
2.4.6	Cell counting and viability assessment	87
2.4.7	Storage of leukocyte cone samples	87
2.5	Cell Culture.....	88
2.5.1	Proliferation assay	88
2.5.2	Extracellular staining.....	89
2.5.3	Intracellular staining.....	92
2.6	Flow Cytometry: Machine set up and calibration	93
2.6.1	Cell sorting.....	93
2.6.2	Conventional Flow Cytometry analysis	94
2.6.3	Gating Strategy.....	94
2.6.4	Gating strategy applied for cell sort.....	94
2.6.5	Analysis of differentiation pathways using Probability State Modelling (PSM) (GemStone™software).....	95
2.7	Microarray of V γ 9V δ 2 T cell subsets.....	96
2.7.1	Enrichment of V γ 9V δ 2 T cells	96

2.7.2	Magnetic column cell separation.....	96
2.7.3	Extracellular staining.....	97
2.7.4	Cell sorting of V γ 9V δ 2 T cells.....	98
2.7.5	RNA stabilisation post-sorting.....	98
2.7.6	RNA extraction.....	99
2.7.7	RNA Concentration and RNA Integrity Quality Control	100
2.7.8	RNA Integrity Number (RIN) Scores	100
2.7.9	Ambion Total Prep Kit.....	101
2.7.10	Production and purification of cDNA from RNA.....	101
2.7.11	Transcription of purified cRNA from purified cDNA	101
2.7.12	Human expression array of V γ 9V δ 2 T cell subsets	102
2.7.13	Gene Array analysis.....	102
2.7.14	Statistical analysis.....	102
2.7.15	Validation of gene array	103
Chapter 3	Investigating V γ 9V δ 2 T cell heterogeneity in healthy human volunteers.....	105
3.1	Introduction.....	105
3.2	Leukocyte cone-derived PBMCs show wide variability in V γ 9V δ 2 T cell percentage, phenotype and expansion potential.....	105
3.3	Fresh peripheral blood samples also show variability in V γ 9V δ 2 T cell percentage, phenotype and expansion potential.....	108
3.4	CD45RA fails to define distinct phenotypic populations of V γ 9V δ 2 T cells when used in combination with CD27	110
3.5	The use of different combinations of surface markers reveal significant confusion when phenotyping V γ 9V δ 2 T cells.	111

3.6	V γ 9V δ 2 T cells showed no significant variation with respect to age, gender, ethnicity, or place of birth.	113
3.7	Re-assessment of the “naïve” V γ 9V δ 2 T cell population	115
3.8	CCR7 expression is dependent on clone and staining conditions.	117
3.9	CD27, CD28 and CD16 are more consistent markers for defining distinct V γ 9V δ 2 T cell populations	119
3.10	The four non-naïve V γ 9V δ 2 subsets vary markedly in percentage between healthy individuals.....	122
3.11	V γ 9V δ 2 T cell subset distribution does not appear to be related to age .	123
3.12	Individual V γ 9V δ 2 T cell profiles can be clustered into six phenotypic “signature” groups.....	124
3.13	V γ 9V δ 2 T cell phenotypic “signatures” are widely spread across all age groups.....	128
3.14	V γ 9V δ 2 T cell phenotypic “signatures” do not appear to correlate with ethnicity, region of birth or the development status of country of birth	130
3.15	Malaria has no significant effect on V δ 2/CD3(%) but may lead to extreme V γ 9V δ 2 T cell phenotypic signatures.....	130
3.16	Summary; What is the nature of V γ 9V δ 2 T cell differentiation?	133
Chapter 4 Phenotypic and functional characterisation of newly defined V γ 9V δ 2 T cell subsets		
4.1	Introduction.....	136
4.2	Surface marker expression on V γ 9V δ 2 T cell subsets.....	136
4.2.1	The $\gamma\delta^{(N)}$ subset is characterised by high levels of CCR7 and CD62L expression.....	136

4.2.2	The $\gamma\delta^{(28+)}$ subset is characterised by high CCR2 and CCR5 expression.....	138
4.2.3	CXCR5, CCR9 and CLA are expressed at low levels on $V\gamma 9V\delta 2$ T cells.....	140
4.3	Assessment of cytokine secreting potential by $V\gamma 9V\delta 2$ T cell subsets ...	140
4.3.1	All $V\gamma 9V\delta 2$ T cell populations can secrete IFN- γ and TNF- α with low levels of IL-17A	142
4.3.2	Perforin is produced at higher levels in $\gamma\delta^{(16-)}$ and $\gamma\delta^{(16+)}$ subsets.	142
4.4	Proliferative potential	144
4.4.1	Increased phosphoantigen-induced proliferation is observed in $CD27^{(+)}$ subsets compared to $CD27^{(-)}$ populations	144
4.5	Gene microarray on newly-defined $V\gamma 9V\delta 2$ subsets	147
4.5.1	Initial microarray validation	150
4.5.2	Gene microarray analysis	150
4.5.3	The $\gamma\delta^{(28+)}$ and $\gamma\delta^{(16+)}$ $V\gamma 9V\delta 2$ T cell subsets show most distinct expression profiles	153
4.5.4	Further microarray analysis.....	154
4.5.5	Transition from $\gamma\delta^{(28+)}$ to $\gamma\delta^{(28-)}$ subsets coincides with transcriptional regulation of cytotoxic proteins.....	159
4.5.6	Genes associated with an IL-17 secreting phenotype are expressed in the $\gamma\delta^{(28+)}$ subset.....	162
4.5.7	CCR6 and CX3CR1 show opposing patterns of gene expression in $V\gamma 9V\delta 2$ T cell subsets	162
4.5.8	Adhesion and migration associated proteins increase across the four $V\gamma 9V\delta 2$ T cell subsets	163
4.5.9	Increase in KIR regulatory proteins in the $\gamma\delta^{(16+)}$ subset.....	166

4.6	Summary	166
Chapter 5	Probability state modelling of $\gamma\delta$ T cell differentiation	169
5.1	Introduction.....	169
5.2	Generating a probability state model (PSM) for human $V\gamma 9V\delta 2$ T cells .	170
5.3	The PSM suggests that the $\gamma\delta^{(28-)}$ and $\gamma\delta^{(16-)}$ subsets are not distinct, but instead represent transitional populations.....	172
5.4	$V\gamma 9V\delta 2$ T cells do not share the same differentiation pathway as $\alpha\beta$ T cells.....	174
5.5	Summary	176
Chapter 6	A comparison of $V\gamma 9V\delta 2$ T cells with $V\delta 1^{(+)}$ T cells	178
6.1	Introduction.....	178
6.2	The $CD27^{(Hi)}$ $CD11a^{(Lo)}$ “naïve” subset is significantly higher for $V\delta 1^{(+)}$ T cells compared to $V\gamma 9V\delta 2$ T cells.....	178
6.3	$CD27/CD45RA$ identifies distinct subsets of $V\delta 1^{(+)}$ T cells.	180
6.4	$CD28/CD27/CD16$ also identify distinct $V\delta 1^{(+)}$ T cell subsets.	181
6.5	Preliminary surface marker analysis of $V\delta 1^{(+)}$ T cells	184
6.6	Summary	187
Chapter 7	Preliminary analysis of $\gamma\delta$ T cells in the human neonatal thymus.....	189
7.1	Introduction.....	189
7.2	$V\delta 1^{(+)}$ T cells are more prevalent in the neonatal thymus than $V\gamma 9V\delta 2$ T cells.....	189
7.3	$CD27/CD45RA$ expression on $V\delta 2^{(+)}$ T cells in the neonatal thymus.....	191
7.4	$CD28/CD27$ analysis of $V\gamma 9V\delta 2$ T cells in the neonatal thymus	193

7.5	CCR7/CD62L analysis of V γ 9V δ 2 T cells in the neonatal thymus.	193
7.6	A novel population of cells exist in the neonatal thymus.....	196
7.7	CD27 and CD11a define two V γ 9V δ 2 T cell thymic populations.....	196
7.8	Summary	199
Chapter 8	$\gamma\delta$ T cell changes in bisphosphonate-related osteonecrosis of the jaw (BRONJ).....	202
8.1	Introduction.....	202
8.2	BRONJ patient cohort.....	202
8.3	Control groups.....	204
8.4	BRONJ disease and treatment.....	206
8.5	Pain and quality of life related issues in BRONJ.....	206
8.6	V γ 9V δ 2 T cells are significantly depleted in BRONJ patients.	209
8.7	V δ 1 ⁽⁺⁾ T cells show no evidence of depletion in BRONJ patients compared to all other control groups.	211
8.8	No evidence for a predominating V γ 9V δ 2 T cell phenotype in BRONJ patients	212
8.9	Summary	216
Chapter 9	Discussion	218
9.1	CD45RA is not a reliable marker for accurate representation of V γ 9V δ 2 T cells.....	219
9.2	V γ 9V δ 2 T cells are better identified using CD28, CD27, and CD16.....	221
9.3	Significant individual-to-individual variation in the proportions of the four newly-defined V γ 9V δ 2 T cell subsets identifies at least six signature profiles.....	223
9.4	The $\gamma\delta$ ⁽²⁸⁺⁾ cell subset may retain the potential to develop into IL-17-secreting V γ 9V δ 2 T cells.....	224

9.5 Mutually exclusive CCR6 and CX3CR1 expression in V γ 9V δ 2 T cells identify an important differentiation stage in their functional biology	226
9.6 The $\gamma\delta^{(28+)}$ cell subset has a distinct chemokine receptor expression profile.....	227
9.7 KIR proteins are expressed at high levels in the $\gamma\delta^{(16+)}$ subset	229
9.8 Phenotypic subsets remain stable over time and suggest a homeostatic mechanism of control.....	231
9.9 A model for V γ 9V δ 2 T cell differentiation	232
9.10 CD27 and CD11a represent the most reliable naïve cell markers	235
9.11 Naïve cell surface markers do not predominate in the thymus.	236
9.12 Higher frequency of the [CD27 ^(Hi) CD11a ^(Lo)] subset in the V δ 1 ⁽⁺⁾ T cell population compared to V γ 9V δ 2 T cells may reflect differences in $\gamma\delta$ T cell development.	240
9.13 Depletion of V γ 9V δ 2 T cells in the peripheral blood is characteristic of patients on long-term bisphosphonates including BRONJ	241
9.14 Limitations of experimental data	243
9.14.1 Proliferation assay	243
9.14.2 Cytokine production	244
9.14.3 Age vs. Tissue (Thymus)	245
9.14.4 Critical appraisal of PSM.....	246
9.15 Future work	248
References.....	251
Chapter 10 Appendices.....	269
10.1 Ethics - Favourable opinion	269
10.2 Patient information sheets	273

10.3 Data collection sheets	278
10.3.1 Healthy volunteers	278
10.3.2 BRONJ group.....	279
10.3.3 Control groups	280
10.4 Gene microarray- All differentially expressed genes.	281
10.4.1 All differentially expressed genes in $\gamma\delta^{(28+)}$ v. $\gamma\delta^{(28-)}$	281
10.4.2 Differentially expressed genes in $\gamma\delta^{(28-)}$ vs. $\gamma\delta^{(16-)}$	281
10.4.3 Differentially expressed genes in $\gamma\delta^{(16-)}$ v. $\gamma\delta^{(16+)}$	282
10.4.4 Differentially expressed genes in $\gamma\delta^{(28+)}$ v. $\gamma\delta^{(16-)}$	283
10.4.5 Differentially expressed genes in $\gamma\delta^{(28+)}$ v. $\gamma\delta^{(16+)}$	286
10.4.6 Differentially expressed genes in $\gamma\delta^{(28+)}$ v. Others (grouped)	290
10.4.7 Differentially expressed genes in $\gamma\delta^{(28-)}$ vs. Others (grouped).	291
10.4.8 Differentially expressed genes in $\gamma\delta^{(16-)}$ vs. Others (grouped).	292
10.4.9 Differentially expressed genes in $\gamma\delta^{(16+)}$ vs. Others (grouped).	292

List of Figures

Figure 1.1 Major cell populations of the Immune System.	39
Figure 1.2 $\gamma\delta$ T cell mechanisms can mediate local immunoregulation.....	47
Figure 1.3 Functional plasticity of $V\gamma 9V\delta 2$ T cells.	49
Figure 1.4 Hypothesised role for $V\gamma 9V\delta 2$ T cells in the pathogenesis of Bisphosphonate-related osteonecrosis of the jaw.....	77
Figure 2.1 Schematic of the ethical approval process.....	82
Figure 3.1 Variation in $V\gamma 9V\delta 2$ T cell number, phenotype and functional potential in blood cones.	107
Figure 3.2 $V\gamma 9V\delta 2$ T cell variability in healthy human volunteer peripheral blood samples.	109
Figure 3.3 CD45RA is a poor discriminator of distinct $V\gamma 9V\delta 2$ T cell subsets.	110
Figure 3.4 Use of different $V\gamma 9V\delta 2$ T cell phenotypic strategies leads to a range of estimates for each population subset.....	112
Figure 3.5 Effect of age and gender on $V\delta 2/CD3(\%)$ in peripheral blood.	114
Figure 3.6 Variation in $V\delta 2/CD3(\%)$ in peripheral blood shown by ethnicity, region of birth and by country of birth development status.....	116
Figure 3.7 “Naïve” $V\gamma 9V\delta 2$ T cell subset estimates show large variation depending on phenotyping strategy.	117
Figure 3.8 CCR7 expression on $V\gamma 9V\delta 2$ and $\alpha\beta$ T cells varies depending on clone and staining conditions.....	118
Figure 3.9 Phenotypic analysis of $V\gamma 9V\delta 2$ T cells showing distinct phenotypic subsets	120
Figure 3.10 Proposed $V\gamma 9V\delta 2$ T cell phenotypic characterisation as defined by CD11a, CD28, CD27, and CD16.	121
Figure 3.11 $V\gamma 9V\delta 2$ T cell phenotypic subset distribution showing the four major non-naïve subsets.....	123

Figure 3.12 $V\gamma 9V\delta 2$ T cell subsets show little evidence of accumulating with increasing age.....	125
Figure 3.13 Criteria for phenotypic signature groupings of $V\gamma 9V\delta 2$ T cells. ...	126
Figure 3.14 $V\gamma 9V\delta 2$ T cell subsets cluster into six “phenotypic signatures”. ...	127
Figure 3.15 Distribution of phenotypic signatures in healthy volunteers.	129
Figure 3.16 Distribution of $V\gamma 9V\delta 2$ T cell phenotypic signatures by ethnicity, region of birth and by developmental status of country of birth.....	131
Figure 3.17 Effect of previous malaria infection on $V\gamma 9V\delta 2$ T cell percentage and phenotypic signature.....	132
Figure 3.18 Proposed models of $V\gamma 9V\delta 2$ T cell differentiation.	134
Figure 4.1 Expression levels of various surface markers on $V\gamma 9V\delta 2$ T cell subsets.	137
Figure 4.2 Expression levels of various chemokine receptors and homing markers on $V\gamma 9V\delta 2$ T cell subsets.	139
Figure 4.3 Cytokine potential of $V\gamma 9V\delta 2$ T cell subsets.....	141
Figure 4.4 Cytokine and Perforin-secreting potential in non-naïve $V\gamma 9V\delta 2$ T cell subsets.	143
Figure 4.5 $CD27^{(+)}$ $V\gamma 9V\delta 2$ T cell subsets show high proliferative potential...	145
Figure 4.6 $CD27^{(+)}$ cells show the highest proliferation following phosphoantigen stimulation	146
Figure 4.7 Enrichment, sorting and processing of $V\gamma 9V\delta 2$ subsets for gene microarray.....	148
Figure 4.8 Summary of healthy volunteer samples used for $V\gamma 9V\delta 2$ T cell subset purification.....	149
Figure 4.9 Initial validation of microarray	151
Figure 4.10 Schematic summary of gene microarray analysis strategy for $V\gamma 9V\delta 2$ T cell subsets.....	152
Figure 4.11 Total number of differentially expressed genes between $V\gamma 9V\delta 2$ T cell subsets.	153

Figure 4.12 Total number of differentially expressed genes between individual V γ 9V δ 2 T cell subsets and the other populations grouped together.	155
Figure 4.13 Differentially expressed genes with immune function in $\gamma\delta^{(28+)}$ T cells compared to the other three subsets grouped together	156
Figure 4.14 Differentially expressed genes in CD28 ⁽⁻⁾ CD27 ⁽⁻⁾ CD16 ⁽⁻⁾ V δ 2 T cells.	157
Figure 4.15 Differentially expressed genes with immune function in $\gamma\delta^{(16+)}$ T cells compared to the other three subsets grouped together	158
Figure 4.16 Granzyme B and Granzyme K expression for V γ 9V δ 2 T cell subsets.	160
Figure 4.17 Summary of expression levels of granzyme B and granzyme K on V γ 9V δ 2 T cell subsets.	161
Figure 4.18 CCR6 and CX3CR1 expression subdivides $\gamma\delta^{(28+)}$ V γ 9V δ 2 T cells into two further distinct subsets.....	164
Figure 4.19 Summary of expression levels of CCR6 and CX3CR1 on V γ 9V δ 2 T cell subsets.	165
Figure 5.1 Expression level assumptions for various markers used to generate a probability state model (PSM) for V γ 9V δ 2 T cell differentiation.....	171
Figure 5.2 Average probability state model for V γ 9V δ 2 T cell differentiation..	173
Figure 5.3 Probability state model for V γ 9V δ 2 ⁽⁺⁾ and V γ 9V δ 2 ⁽⁻⁾ T cells suggest a different sequence of differentiation.	175
Figure 6.1 “Naïve” [CD27 ^(Hi) CD11a ^(Lo)] V δ 1 ⁽⁺⁾ T cells are significantly more abundant than “naïve” V γ 9V δ 2 T cells.....	179
Figure 6.2 CD45RA expression is significantly increased on V δ 1 ⁽⁺⁾ T cells. ...	180
Figure 6.3 V γ 9V δ 2 and V δ 1 ⁽⁺⁾ T cells show different CD27/CD45RA profiles.	181
Figure 6.4 V δ 1 ⁽⁺⁾ and V γ 9V δ 2 T cells show different CD27/CD28/CD16 profiles.	182
Figure 6.5 V δ 1 ⁽⁺⁾ and V γ 9V δ 2 T cells show different CD27/CD28/CD16 subset distribution.....	183
Figure 6.6 CCR7, CD62L and β 7-Integrin expression levels in V δ 1 ⁽⁺⁾ T cells.	185

Figure 6.7 CCR2 and CCR5 expression levels on V δ 1 ⁽⁺⁾ T cells.....	186
Figure 7.1 V δ 1 ⁽⁺⁾ T cells are found at higher proportions in the neonatal thymus than V γ 9V δ 2 T cells.....	190
Figure 7.2 CD27/CD45RA expression on V δ 2 ⁽⁺⁾ T cells in the thymus.....	192
Figure 7.3 CD27/CD28 expression on V δ 2 ⁽⁺⁾ T cells in the thymus.....	194
Figure 7.4 A comparison of CCR7/CD62L expression on V δ 2 ⁽⁺⁾ T cells in the thymus.	195
Figure 7.5 CD27/CD11a expression on V δ 2 ⁽⁺⁾ T cells in the thymus.....	197
Figure 7.6 CD27 and CD11a define two distinct thymic V δ 2 ⁽⁺⁾ T cell subsets.	198
Figure 7.7 A comparison of surface marker expression on thymic V δ 2 ⁽⁺⁾ T cells.	200
Figure 8.1 V δ 2/CD3(%) depletion in BRONJ patients and in patients on long-term bisphosphonate therapy.	210
Figure 8.2 V δ 1 ⁽⁺⁾ T cells show no evidence of depletion in BRONJ patients and in patients on long-term bisphosphonate therapy.	211
Figure 8.3 Range of V γ 9V δ 2 T cell phenotypes in BRONJ patients.....	213
Figure 8.4 Range of V γ 9V δ 2 T cell phenotypes in osteoporotic patients taking intravenous bisphosphonates.	214
Figure 8.5 Range of V γ 9V δ 2 T cell phenotypes in osteoporotic patients taking oral bisphosphonates.....	215

List of Tables

Table 1.1 A summary of the primate studies investigating V γ 9V δ 2 T cell memory function.	50
Table 1.2 Variation in V δ 2/CD3(%) in published studies.	55
Table 1.3 Theoretical number of phenotypic subsets as the number of surface markers used increase.....	58
Table 1.4 Summary of the main published V γ 9V δ 2 T cell phenotypic systems.	58
Table 2.1 Table of antibodies used in thesis.	90
Table 2.2 Antibody panels used in thesis.....	91
Table 3.1 Summary table of V γ 9V δ 2 T cell subset size as defined by different phenotypic strategies.	113
Table 8.1 BRONJ cohort bisphosphonate details.	203
Table 8.2 Bisphosphonate control group details.	205
Table 8.3 BRONJ disease details and treatment summary.	207
Table 8.4 Pain and Quality of life issues in BRONJ patients.....	208

Abbreviations

$\alpha\beta$ T cell - Alpha beta T cell

$\gamma\delta$ T cell - Gamma delta T cell

AAOMS - American Association of Oral and Maxillofacial Surgery

AICD - Activation Induced Cell Death

APC - Antigen presenting cell

ARONJ - Antiresorptive agent-induced osteonecrosis of the jaw

β -ME - β -mercaptoethanol

BAONJ - Bisphosphonate-associated osteonecrosis of the Jaw

BON - Bisphosphonate osteonecrosis of the Jaw

BONJ - Bisphosphonate osteonecrosis of the Jaw

BRONJ - Bisphosphonate-related osteonecrosis of the Jaw

BTN3A - Butyrophilin-3A

CCR - Chemokine receptor ((C-C structure)

CD - Cluster of differentiation

CXCR - chemokine receptor (C-X-C structure)

DNA - Deoxyribonucleic acid

EPCR - Endothelial protein C receptor

FACS - Fluorescence-activated cell sorting

FBM - FACS buffer containing brefeldin and monensin

FBS - Fetal bovine serum

FDA - Food and Drug Administration

FMO - Fluorescence Minus One

FPPS - Farnesyl diphosphate synthase

FSC-A - Forward Scatter-Area

FSC-H - Forward Scatter-Height

$\gamma\delta$ T cell - Gamma delta T cell

$\gamma\delta^{(N)}$ - Naïve $\gamma\delta$ T cell

$\gamma\delta^{(CM)}$ - Central memory $\gamma\delta$ T cell

$\gamma\delta^{(TEM)}$ - Effector memory $\gamma\delta$ T cell

$\gamma\delta^{(EMRA)}$ - Terminally differentiated Effector Memory $\gamma\delta$ T cell (CD45RA⁽⁺⁾)

HIV - Human Immunodeficiency Virus

HMB-PP - 4-hydroxy-3-methyl-but-2-enyl pyrophosphate

IELs - Intraepithelial lymphocytes

IFN- γ - Interferon gamma

Ig - Immunoglobulin

IL - Interleukin

IPP - Isopentenyl pyrophosphate

MAC - Membrane attack complex

MICA - MHC class I polypeptide-related sequence A

MICB - MHC class I polypeptide-related sequence B

MHC - Major histocompatibility complex

MRONJ - Medication-related osteonecrosis of the jaw

NETs - Neutrophil extracellular traps

n-BP - Nitrogen-containing bisphosphonate

NK-cell - Natural killer cell

NKG2D receptor - Natural killer group 2, member D receptor

ORN - Osteoradionecrosis

PAMPs - Pathogen-associated molecular patterns

PBS - Phosphate buffered saline

PRR - Pattern recognition receptor

PSM - Probability state modelling

RIN - Ribonucleic acid Integrity Number

RNA - Ribonucleic acid

SSC-A - Side Scatter-Area

SSC-H - Side Scatter-Height

T_{CM} - Central memory T cell

T_{EMRA} - Terminally differentiated Effector Memory T cell (CD45RA⁽⁺⁾)

T_{APC-like} – Antigen presenting-like T cell

T_{H1-like} cell - Type 1-like T helper cell

T_{H2-like} cell - Type 2-like T helper cell

T_{H17-like} cell - T_{H17-like} T helper cell

T_{FH-like} cell - Follicular helper-like T cell

T_N - Naïve T cell

T_{TEM} - Effector memory T cell

TB - Tuberculosis

TCR - T cell receptor

TCR δ - T cell receptor δ chain

TLRs – Toll-like receptors

TNF- α - Tumour necrosis factor alpha

UK - United Kingdom

ULBP - UL16 binding protein

USA – United States of America

V δ 1 - Variant delta chain 1

V δ 2 - Variant delta chain 2

V γ 9V δ 2 - Variant gamma chain 9 Variant delta chain 2

V(D)J recombination - Variable, Diversity and Joining (gene segments)
recombination

VEGF - Vascular endothelial growth factor

vs. - versus

ZOL - Zoledronate

Chapter 1

Thesis Overview

Chapter 1 Thesis overview

The oral cavity presents a unique anatomical micro-environment in that it is the only site in the body where hard tissues (teeth) protrude through lining mucosa. This unusual anatomical environment coupled with the richly diverse bacterial biofilm that colonises the oral cavity soon after birth makes the mouth one of the most immunological dynamic regions of the body (Tlaskalová-Hogenová *et al.* 2004).

The innate and adaptive immune responses have evolved defensive mechanisms over a huge evolutionary period to protect the teeth, gingivae, mucosa and underlying bone from common infections that result in caries (tooth decay) and periodontal disease (gum disease). But despite these protective responses, there are a large number of oral diseases that manifest when the infective burden becomes overwhelming or when immunological responses become defective or inappropriate (Hamzaoui 2011, Fye *et al.* 1976).

In the last 10-12 years, Bisphosphonate-related osteonecrosis of the jaw (BRONJ) has emerged as one of the most enigmatic and difficult to treat conditions in the mouth. It is a chronic jaw disease that first presented as a surprising side-effect in a minority of patients on long-term bisphosphonate medication (Marx 2003). Bisphosphonates are a widely prescribed drug to prevent skeletal bone loss in the treatment of osteoporosis and cancer. However, the reason why BRONJ specifically targets the jawbones and why it only affects certain individuals is still unclear. BRONJ is typically characterised by exposed necrotic and infected jawbone that fails to heal and persists unpredictably for long periods of time (O'Ryan and Lo 2012). The condition can

progress and in severe cases lead to chronic infection, pain and jaw fracture which can severely affect the quality of life of patients (Miksad *et al.* 2011). Whilst many consider the condition to result from a disruption of normal bone turnover or due to the anti-angiogenic or toxic properties of the drug, others have postulated a bacterial aetiology (Allen and Burr 2009). However, it is somewhat surprising that to date an immunological cause has not been extensively investigated, and even more so given the widely accepted effects of bisphosphonates on the immune system. In particular, bisphosphonates are known to cause indirect activation of a specific unconventional immune cell known as the $\gamma\delta$ T cell. Thus, the initial aim of the study was to characterise $\gamma\delta$ T cell biology in the blood and tissues of BRONJ patients and to examine whether there was any evidence to support their role in this disease.

At this point, it became quickly apparent that there were a number of challenges in studying $\gamma\delta$ T cells in BRONJ. Firstly, the challenge of studying a relatively rare disease in a unit with no designated BRONJ clinic would make recruitment of enough patients difficult and obviously required involvement of an external collaborator to help in patient recruitment. To achieve this, the process of gaining ethical approval at multiple sites needed to be tackled, and a local collaboration with the Eastman Dental Hospital was established. Secondly, a further challenge in studying BRONJ as an immune-related condition was going to be the lack of tissue samples available to investigate the immune cells present in these lesions. This is due to the general treatment consensus currently within the UK that BRONJ should be managed conservatively with a focus on anti-infective and symptomatic management as opposed to surgical intervention and removal of necrotic tissue. Indeed, a simple, symptomatic and non-surgical management strategy is a prudent one in many of the cancer

patients with BRONJ, as they often suffer with a number of different co-morbidities as a direct result of their cancer therapy.

Due to these initial practical issues that would obviously delay direct assessment of BRONJ patients, the initial work of the thesis sets out to characterise $\gamma\delta$ T cells in the peripheral blood of healthy individuals to serve as an important baseline for further studies on the role of $\gamma\delta$ T cells in disease. Anonymised frozen human blood donor derived leukocyte cones were initially investigated due to their ease of availability. However, it quickly became apparent that the study of these cells was not straight forward due to the following initial observations:

- $V\gamma9V\delta2$ T cells varied markedly in their phenotypic profile as defined by the conventional phenotyping strategy of these cells that used the surface expression of CD27 and CD45RA; this describes four populations; Naïve T_N [CD27⁽⁺⁾CD45RA⁽⁺⁾], Central Memory T_{CM} [CD27⁽⁺⁾CD45RA⁽⁻⁾], Effector Memory T_{EM} [CD27⁽⁻⁾CD45RA⁽⁻⁾] and Terminally differentiated Effector Memory T_{EMRA} [CD27⁽⁻⁾CD45RA⁽⁺⁾].
- The system of phenotyping using this conventional system (CD27 and CD45RA) was problematic, first due to the wide range of expression levels of CD45RA, and second because this method did not seem to divide cells into four distinct populations as described in the literature.
- $V\gamma9V\delta2$ cells from different individuals responded differently following stimulation with phosphoantigen/bisphosphonates.
- The use of anonymised frozen blood samples was not helpful in elucidating the factors affecting $V\gamma9V\delta2$ T cell heterogeneity, as it was not possible to know the age, sex, ethnicity, infectious history etc. of the

samples. In addition, there were too many unknown variables associated with these samples including the significance of freeze-thaw cycles as well as the transportation, storage and age of each sample (Germann *et al.* 2013, Olson *et al.* 2011, Weinberg *et al.* 2009). These factors are known to effect levels of extracellular marker expression and functional responses leading to the conclusion that it was vital that fresh blood samples should be used in the study.

These initial observations along with the practical issues regarding the study of BRONJ, led to a reconsideration of the focus of the thesis. It was clear that the wide range of $\gamma\delta$ T cell phenotypes and functional activity, along with the difficulty in phenotyping cells, warranted further investigation using fresh healthy blood samples. It was also apparent that it would be important to establish a better understanding of $V\gamma9V\delta2$ T cell biology in healthy individuals before moving on to consider the significance of $V\gamma9V\delta2$ T cells in BRONJ when ethical approval was obtained.

In beginning to review the literature, it also became apparent that $V\gamma9V\delta2$ T cells were implicated in a range of diseases and had a range of different effector functions. $V\gamma9V\delta2$ T cells have properties of both innate and adaptive immune cells and can mount significant and rapid immune responses to the first signs of immune danger (Kistowska *et al.* 2008). In addition they have a multifunctional immune role in antigen presentation, cytotoxic responses to tumour cells, killing of activated macrophages, as well as in regulating wound healing (Pang *et al.* 2012, Havran 2000). $V\gamma9V\delta2$ T cells are also implicated in a number of systemic diseases including malaria and tuberculosis and are now also being targeted as a potential immunotherapy in certain cancers

(Kunzmann *et al.* 2012). It is therefore clear that an improved understanding of $\gamma\delta$ T cell biology will benefit the study of several human diseases.

This thesis begins by re-evaluating human $V\gamma 9V\delta 2$ T cells in healthy individuals in an attempt to reconcile the confusion that exists in the literature regarding their identification, and to fully document and assess the variability of this T cell population between individuals. The thesis suggests an improved methodology for the assessment of $V\gamma 9V\delta 2$ T cells, and explores the functional characteristics of the newly described $V\gamma 9V\delta 2$ T cell subsets.

Finally these findings will be applied to the chronic disease Bisphosphonate-related osteonecrosis of the jaw (BRONJ) in a small patient cohort to examine whether there is preliminary evidence to suggest that $V\gamma 9V\delta 2$ T cell could be implicated in this enigmatic condition.

Introduction

1.1 The Immune System

The human immune system has evolved over many years to protect the host against infection from pathogens (Danilova 2006). In general, the skin and mucous membranes of the body are extremely effective non-specific barriers to infection. However when these vital structures are breached, it is important that the immune system can then identify foreign pathogens from self tissues and to manage their clearance from the body.

However, as fast as the immune system adapts to combating these foreign pathogens, these same pathogens also adapt and evolve mechanisms to evade host defences (Martínez-Borra *et al.* 2012). Thus, there is a constant “arms race” between the mammalian immune system and the microbial world that has resulted in the immune system seen today.

1.1.1 The Innate Immune System

In basic terms, the human immune response can be subdivided into innate and adaptive processes that coordinate to effectively eliminate a foreign challenge. Innate immune responses are evolutionary conserved mechanisms shared by both simple and complex organisms and are commonly described as a non-specific, first line of defence against infection. They are typically mounted rapidly in response to common danger motifs found in viruses, bacteria, parasites etc. known as Pattern Associated Molecular Proteins (PAMPs). These are sensed by Pattern Recognition Receptors PRRs such as Toll-like receptors (TLRs) on host cells (Arancibia *et al.* 2007). The main processes under the umbrella of innate responses include:

- Skin and mucosal surface barrier function (Doran *et al.* 2013).
- The recruitment of innate immune cells such as neutrophils and macrophages to the site of infection (Foxman *et al.* 1997).
- Neutrophil functions, phagocytosis and release of anti-microbial hydrolytic enzymes and proteins. In addition neutrophils can produce extracellular Neutrophil Extracellular Traps (NETs) which are DNA structures that resemble a web to trap and lyse pathogens (Brinkmann *et al.* 2004).
- Complement protein activation cascade; this leads to the cytolysis of pathogens through the complement cascade that culminates in the formation of a membrane attack complex (MAC) (Daha 2010).
- Phagocytosis of foreign bodies within the tissues by cells such as macrophages, dendritic cells and neutrophils (Underhill and Goodridge 2012).
- The uptake, processing and presentation of antigens in preparation for initiation of adaptive immune responses (Jensen 2007).

Essentially, these non-specific immune processes attempt to keep an infection under control while more specific and targeted processes are being initiated.

1.1.2 The Adaptive Immune System

In contrast to the immediate and non-specific innate response, the adaptive immune response is very antigen specific and is targeted to specific invading pathogens. However, the generation of these responses can take several days to reach their maximum effect. The main cells that coordinate adaptive immune responses are T cells (largely CD4⁽⁺⁾ and CD8⁽⁺⁾ T cells). T cell receptor (TCR) and B cell receptor (which when secreted is referred to as antibody) diversity results from a process known as somatic recombination (V(D)J recombination)

as the cells develop. This random genetic recombination event generates a large number of unique receptors capable of recognising distinct foreign antigen, a feature that endows the adaptive immune response tremendous power to tackle a huge array of pathogens (Oltz 2001).

Unlike the B cell receptor/Immunoglobulin (Ig) that can recognise soluble antigen, the TCR can only recognise antigen that is presented by Major Histocompatibility Complex (MHC) molecules. MHC Class I molecules on the surface of antigen presenting cells (e.g. macrophages and dendritic cells) present antigen to CD8⁽⁺⁾ cytotoxic T cells, while MHC Class II molecules present antigen to CD4⁽⁺⁾ T-helper cells. Once activated by specific recognition of antigen through their antigen receptors, lymphocytes must undergo a phase of clonal expansion that takes several days. For this reason, effective adaptive responses do not take immediate effect, allowing a window of time in which pathogen expansion may cause disease. Nonetheless, once fully primed, the adaptive response can efficiently clear most infections.

Another important property of the adaptive immune system is the acquisition of immunological memory. It is now well-established that immune responses on re-exposure to the same antigen are more rapid and effective and can be deployed for many years after first exposure. Memory cells are thought to be generated as part of the clonal expansion process and retained within the B/T cell pool following the effective initial clearance of the primary infection. It is apparent that memory cells can persist for many years after the initial encounter of the antigen and probably without re-exposure to antigen during that period (Hudu *et al.* 2013).

In summary, both B and T cell responses coordinate to provide appropriate and measured primary immune responses through specific recognition of non-self antigen, while also being capable of quicker and better secondary “memory” responses if and when these antigens are encountered again. The major cell types of the immune system are shown in (Figure 1.1).

1.2 Human $\gamma\delta$ T cells

Gamma delta T cells ($\gamma\delta$ T cells) are unconventional T cells that typically constitute between 1-5% of lymphocytes in the peripheral blood of human adults (Parker *et al.* 1990). They are considered as the prototypic unconventional T cell because they; are predominantly tissue-located; respond to stressed tissues, and; do not require priming nor conventional MHC-based antigen presentation to facilitate activation (Fisch *et al.* 1992). They also have properties common to both the innate and adaptive immune systems and hence have been described as bridging both systems. As evidence of this, $\gamma\delta$ T cells can on the one hand respond rapidly to danger signals in tissues and display potent cytotoxic responses without the need for priming, while on the other hand also act as antigen presenting cells, provide B cell help, and even display evidence of genuine memory recall responses (Brandes *et al.* 2005, Maniar *et al.* 2010, Wu *et al.* 2009, Bansal *et al.* 2012, Worku *et al.* 2001b, Worku *et al.* 2001a).

In terms of evolution, it has been argued that $\gamma\delta$ T cells may be an older cell type than conventional $\text{TCR}\alpha\beta^{(+)}$ T cells, and may even be a vestige of more primitive immune cells that are now functionally redundant (Cooper and Alder 2006). However, the fact that $\gamma\delta$ T cells have been evolutionary conserved

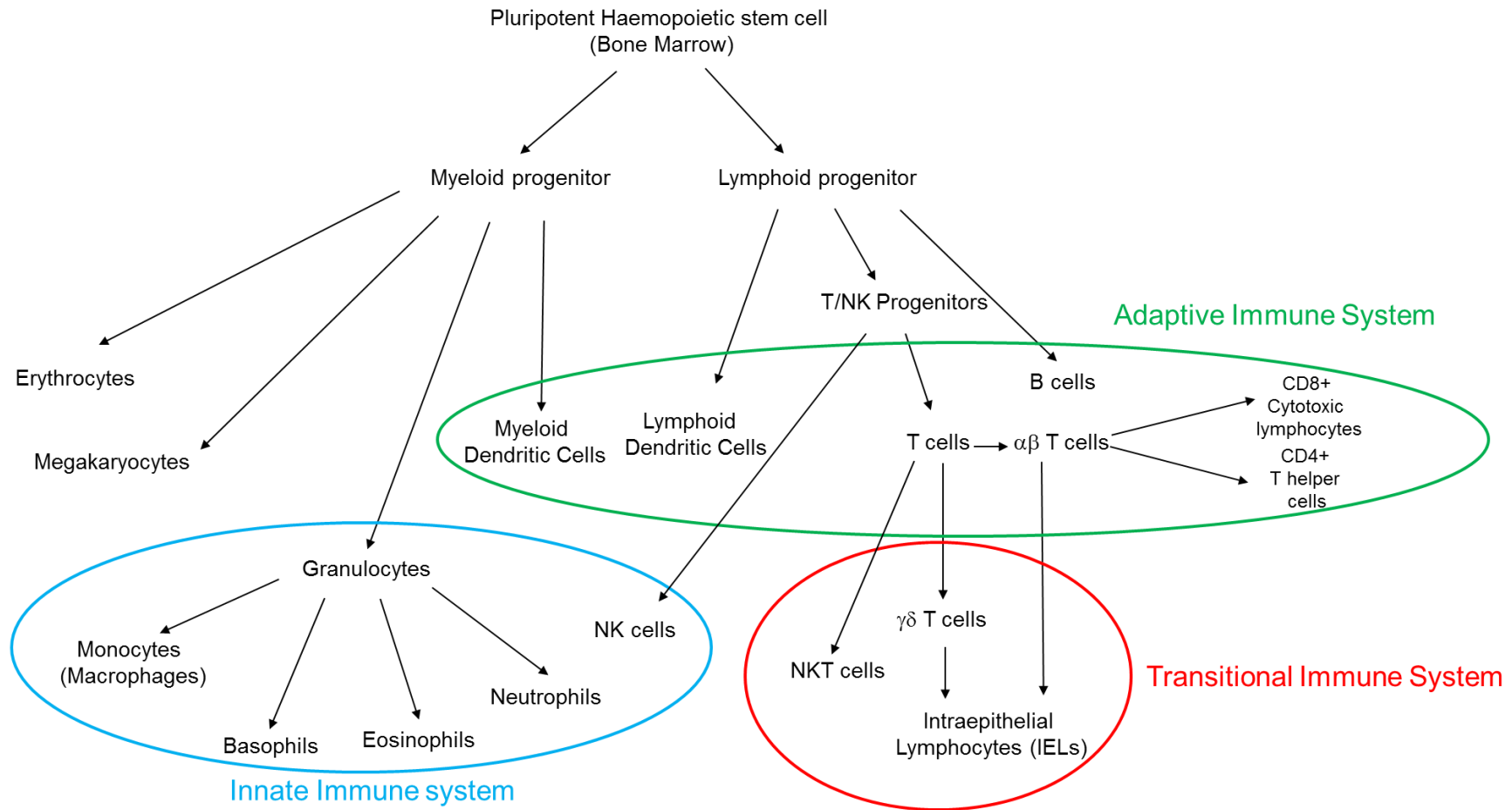


Figure 1.1 Major cell populations of the Immune System.

A diverse number of different immune cells with a variety of phenotypic characteristics develop from a common pluripotent haemopoietic stem cell in the bone marrow and together make up the innate, adaptive and transitional immune systems. Transitional immune cells exhibit characteristics of both the innate and adaptive systems and so do not fit neatly into either of the conventionally described innate or adaptive systems.

over many millions of years and in all jawed vertebrates alongside the more specific and targeted adaptive immune system perhaps reflects their importance to early and rapid immune responses against invading pathogens. Indeed, this is best demonstrated by the fact that these cells appear to play a vital role in immune responses to some of the most significant human infectious disease such as malaria and tuberculosis (TB) (Inoue *et al.* 2013, Kabelitz *et al.* 1990).

1.2.1 Human $\gamma\delta$ T cell subsets

Human $\gamma\delta$ T cells are generally divided into two major subsets based on the usage of the TCR δ chain, using either TCR δ variable region-1 (V δ 1 T cells) or TCR δ variable region-2 (V δ 2 T cells). V δ 1 and V δ 2 cells are found predominantly in different locations in the body, and are known to respond through their TCRs to different types of ligand. Because of these features V δ 1 and V δ 2 cells are thought to have significantly different functions, and are likely to be required in significantly different scenarios.

1.2.2 V δ 1 T cells

V δ 1⁽⁺⁾ T cells are the predominant tissue resident $\gamma\delta$ T cells and are found at much lower levels in the blood compared to V δ 2 T cells. Functionally they are thought to have a role in preventing opportunistic infiltration of commensal bacteria, and in tissue homeostasis and repair (Ismail *et al.* 2009). They have also been identified as having opposing roles in both promoting and preventing tissue inflammation (Holtmeier 2003), and are also thought to be key cells in maintaining adaptive tolerance towards self-antigen including food antigen in the intestine (Locke *et al.* 2006, Bhagat *et al.* 2008).

The antigen specificity and the mechanisms by which $V\delta 1^{(+)}$ T cells recognise antigen are still unclear (Kalyan and Kabelitz 2013). The greater diversity of receptor chains in $V\delta 1^{(+)}$ T cell in comparison to $V\delta 2$ T cells has led many to postulate that they recognise diverse antigens. Possible $V\delta 1^{(+)}$ T cell ligands include the stress-induced molecules MICA/MICB that are found on the surface of many tumour cells, and that bind to NKG2D. CD1c and endothelial protein C receptor (EPCR) are also putative ligands that perhaps present foreign antigen. However, the recognition and binding of the $V\delta 1$ TCR is not thought to be via the presented ligands. Instead, these molecules probably act as classic stress ligands that are up-regulated when tissues are infected or damaged (Willcox *et al.* 2012, Haig *et al.* 2011).

1.2.3 $V\delta 2$ T cells

$V\delta 2$ T cells are the predominant $\gamma\delta$ T cell subset in the blood (approximately 1-5% of total $CD3^{(+)}$ lymphocytes) and are almost exclusively co-expressed with a $TCR\gamma$ chain that uses variable region-9, so are commonly called $V\gamma 9V\delta 2$ T cells. They are unique to higher primates and have no direct equivalent in non-primate models, which makes their experimental study more difficult. In contrast to conventional $\alpha\beta$ T cells, $V\gamma 9V\delta 2$ T cells show limited receptor diversity by adulthood (McVay and Carding 1999). In addition, they also show more restricted diversity in comparison to $V\delta 1^{(+)}$ T cells.

$V\gamma 9V\delta 2$ T cells respond directly to non-proteinaceous, low-molecular weight compounds known as phosphoantigens, e.g. 1-Hydroxy-2-methyl-2-buten-4-yl 4-diphosphate (HMB-PP) and iso-pentyl pyrophosphate (IPP). HMB-PP is produced as an essential intermediate metabolite in the non-mevalonate

pathway of isoprenoid biosynthesis by many pathogenic bacteria. Eukaryote cells in contrast only produce isoprenoids via the mevalonate pathway and do not produce HMB-PP. However, IPP is generated by the mevalonate pathway and is often unregulated in situations of stress and infection, that then can potentially activate V γ 9V δ 2 T cells.

V γ 9V δ 2 T cells are thought to respond to phosphoantigen through the TCR in a MHC class II-independent mechanism i.e. without the need for conventional antigen presentation. Although, the exact mechanism of TCR recognition is still not fully understood, it is now thought to involve the widely expressed molecule butyrophilin-3 (BTN3A or CD277; a B7-like protein) that is found on the surface of a large range of cell types. Studies using activating and inhibitory antibodies to CD277 have suggested that binding of phosphoantigen to the intracellular region of a CD277 dimer induces an extracellular conformational change, that then permits binding of the V γ 9V δ 2 TCR (Harly *et al.* 2012). However, more work is required to confirm this.

Nitrogen-containing bisphosphonates like zoledronate and pamidronate are also believed to drive phosphoantigen production. They do this by inhibiting a key enzyme in the mevalonate pathway known as farnesyl pyrophosphate synthase (FPPS). This leads to increased intracellular accumulation of IPP (Roelofs *et al.* 2009). It is the intracellular accumulation of IPP in monocytes/dendritic cells that is believed to cause V γ 9V δ 2 T cell activation via a mechanism similar to that described above. In the absence of monocytes/CD14⁽⁺⁾ cells, bisphosphonates show reduced ability to activate V γ 9V δ 2 T cells, an observation that supports the requirement of antigen presenting cells in facilitating V γ 9V δ 2 T cell activation (Nussbaumer *et al.* 2013).

1.3 Development of human $\gamma\delta$ T cells

Our knowledge regarding human $\gamma\delta$ T cell development is to a large extent inferred from murine experiments, as direct experiments on human thymic tissue are obviously limited for ethical reasons. Despite these problems, there is evidence that rearrangement of the $\gamma\delta$ TCR can be detected as early as 8 weeks *in utero* in the human thymus and has also been reported at some extra-thymic sites including the fetal liver (McVay and Carding 1999). Initially, there is a relatively diverse repertoire of $\gamma\delta$ TCRs that populate the blood with a range of differing TCR chain pairings. However, as human development progresses after birth there is a significant shift to a more restricted $\gamma\delta$ TCR repertoire (McVay and Carding 1999). This is exemplified by a shift from a predominance of $V\delta 1^{(+)}$ T cells at birth to $V\gamma 9V\delta 2$ T cells becoming the major population during early years of development (Parker *et al.* 1990). This change in terms of chain dominance is also accompanied by a shift from cells expressing typical “naïve” markers such as CD45RA, to those of effector and memory characteristics (De Rosa *et al.* 2004). This early shift from a naïve to an effector phenotype and post-thymic expansion is in contrast to conventional $\alpha\beta$ T cells where differentiation to effector and memory phenotypes are only observed when these cells are activated in specific immune responses in the secondary lymphoid organs.

1.4 Function of $\gamma\delta$ T cells

The precise function of $\gamma\delta$ T cells in immune responses has been debated since the cells were first inadvertently identified during experimental characterisation of the $\alpha\beta$ TCR (Saito *et al.* 1984). Their functions and characteristics can be

sub-divided into four broad areas that include; unique responses to microbial infection; protective responses in young animals; immunosurveillance of cancer; and immunoregulation. These individual functions are explored in turn below.

1.4.1 Unique responses to microbial infection

Certain bacterial and parasitic infections in humans can have dramatic effects on $V\gamma9V\delta2$ T cells, which can expand to completely dominate the lymphocyte population in the blood (Kroca *et al.* 2000). Bacterial infections with *Listeria monocytogenes* and *Mycobacterium tuberculosis* as well as parasitic infections like malaria and toxoplasmosis have all been reported to have potent effects on $V\gamma9V\delta2$ T cells via low-molecular weight phosphoantigens that are produced by these pathogens (Munk *et al.* 1990, Perera *et al.* 1994, Scalise *et al.* 1992).

1.4.2 Protective response in young animals

Immune responses in the first few weeks of life very much depend on inherited maternal immunoglobulins either acquired passively from the mother or alternatively via the breast-milk. At this stage of life, the immune system is under-developed and is unable to make the complex and coordinated responses seen in mature adults. As an example of this, $\alpha\beta$ T cells have been shown to be deficient in both cytokine production and cytotoxic and helper responses, and this coupled with sub-optimal antigen processing leaves their responses underdeveloped compared to those seen in later life (Seghaye *et al.* 1998, Burchett *et al.* 1992).

By contrast, $V\gamma9V\delta2$ T cell expansion in the young is rapid and sees a dynamic shift from a “naïve” to a memory/effector-like phenotype (De Rosa *et al.* 2004). This ability to mount early $\gamma\delta$ T cell effector responses has led to the proposition

that $\gamma\delta$ T cells are an important cell population in early life before acquired immune responses have had time to develop. It seems that it is not only in young humans that $\gamma\delta$ T cells are disproportionately active compared to $\alpha\beta$ T cells, as this same pattern seems to be repeated in all vertebrates that have been studied to date (Hayday *et al.* 2000).

1.4.3 Immunosurveillance of cancer

$\gamma\delta$ T cells have also been implicated in cancer immunosurveillance in that they are capable of sensing “stress/danger” signals on tumour cells. In addition, transformed eukaryote cells often have disrupted metabolic processes and often produce high levels of IPP. Because of this, $V\gamma9V\delta2$ T cells have a central role in sensing, as well as mounting cytotoxic responses to, a range of cancer cell types (Kabelitz 2008). As further evidence of an important anti-tumour role, murine knockout models that lack $\gamma\delta$ T cells often display an increased risk of tumour development (Girardi *et al.* 2001).

The anti-tumour effector function of $V\gamma9V\delta2$ T cells has initiated a plethora of research into developing immunotherapies to boost the $V\gamma9V\delta2$ T cell response as a cancer immunotherapy for certain solid tumours (e.g. prostate and breast cancer) as well as B cell lymphomas (Dieli *et al.* 2007, Wilhelm *et al.* 2003, Bennouna *et al.* 2008). The success of these clinical trials has been mixed with the therapy only effective in a certain “responder” cohort of patients. The use of $V\gamma9V\delta2$ T cells as a cancer immunotherapy will be further discussed, later in the introduction.

1.4.4 Immunoregulation

Although the predominant tissue subset of human $\gamma\delta$ T cells bears the V δ 1 TCR, it is also evident that V γ 9V δ 2 T cells be found in the tissues during disease (McCarthy *et al.* 2013). Whilst many have questioned the functional significance of these $\gamma\delta$ T cells, it is becoming clear that they may play an important role in controlling pathological immune dysregulation by exerting their effects on immune cells locally at tissue sites. As an example of this, a recent study considered the effects of complete absence of skin resident $\gamma\delta$ T cell intra-epithelial lymphocytes (IELs) in a $\gamma\delta$ T cell “knockout” mouse model. The animals in this study showed spontaneous chronic dermatitis (local inflammation) in comparison to wild type mice (Girardi *et al.* 2001). The authors of this study concluded that tissue resident $\gamma\delta$ T cell subsets could have a significant role in controlling $\alpha\beta$ T cell mediated inflammation. Indeed, there are now several further pieces of experimental evidence to support the immunoregulatory control that $\gamma\delta$ T cells exert on $\alpha\beta$ T cells and the immune dysregulation that results in their absence (Mombaerts *et al.* 1993, D'haese *et al.* 2010, D'Souza *et al.* 1997, Mukasa *et al.* 1995). Clearly the dual properties (pro and anti-inflammatory effects) that $\gamma\delta$ T cells possess are key to regulating immune responses. Figure 1.2 illustrates some of the mechanisms by which $\gamma\delta$ T cells are thought to exert their immunoregulatory effects (Jameson *et al.* 2002, Vincent *et al.* 1996, Tramonti *et al.* 2006, Kapp *et al.* 2004, Hsieh *et al.* 1996, King *et al.* 1999).

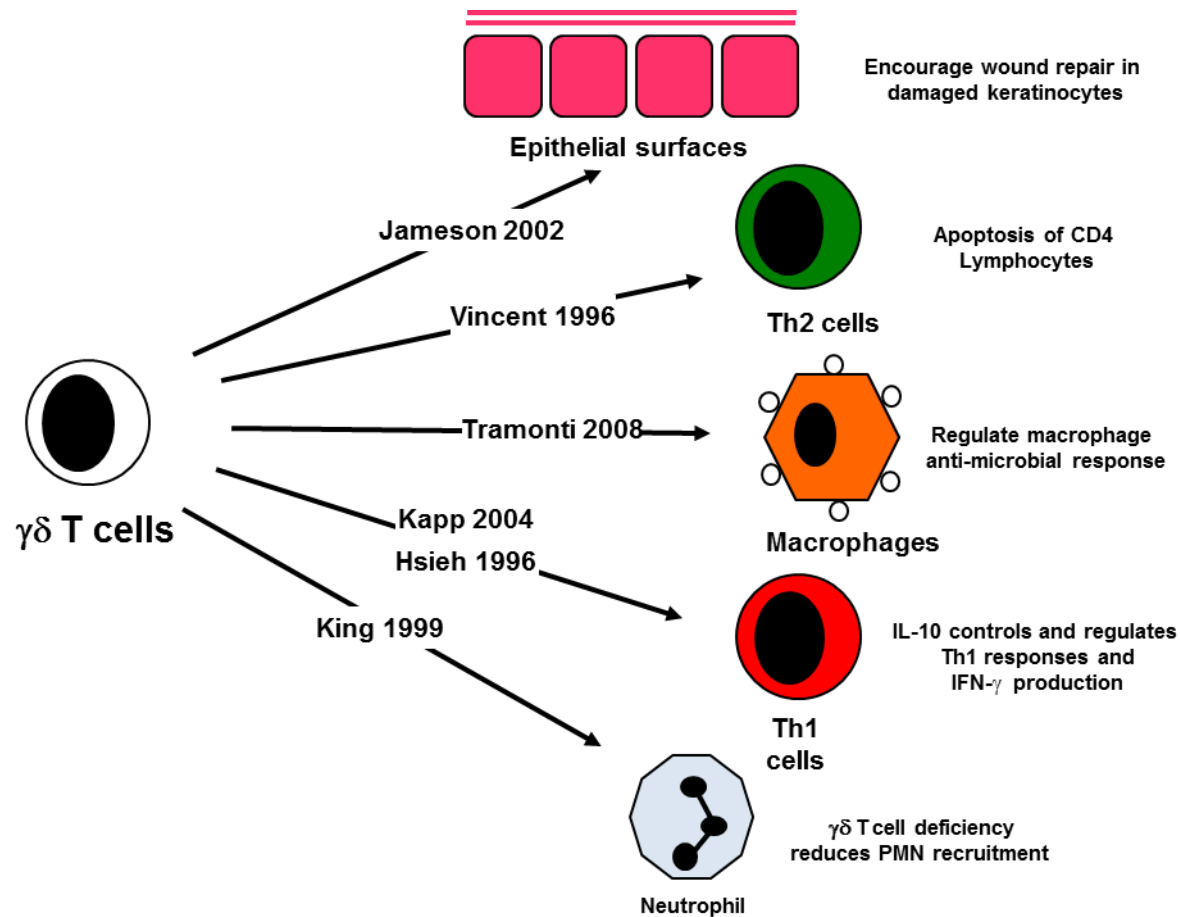


Figure 1.2 $\gamma\delta$ T cell mechanisms can mediate local immunoregulation.

$\gamma\delta$ T cells can exert immunoregulation by their various effector mechanisms. An overview of the experimental evidence is summarised above. $\gamma\delta$ T cells can encourage wound repair, induce CD4 cell apoptosis, regulate macrophage responses, and control T_H1 and cytokine responses as well as reducing neutrophil recruitment. The various published studies highlighting each of these immunoregulatory functions are indicated in the text.

1.5 Functional plasticity of V γ 9V δ 2 T cells

On the whole, the default V γ 9V δ 2 T cell cytokine profile seems to resemble that of a T_H1 response in $\alpha\beta$ T cells; namely the production of IFN- γ and TNF- α . This ability appears to be acquired by the majority of V γ 9V δ 2 T cells quickly after birth (De Rosa *et al.* 2004). However, it is unclear whether the cytokine milieu during initial T cell activation has any bearing on the cytokines produced by these same cells in subsequent immune responses (Manetti *et al.* 1993). Despite the prevalence of this T_H1-like phenotype of human V γ 9V δ 2 T cells from the peripheral blood, it has been shown *in vitro* that a wide range of phenotypic and functional states can be generated following phosphoantigen activation in the presence of various priming cytokine conditions (Pang *et al.* 2012). This functional plasticity is arguably greater than that seen for $\alpha\beta$ T cells. A summary of the conditions required to induce these distinct phenotypes *in vitro* is summarised in Figure 1.3 (Wesch *et al.* 2001, Caccamo *et al.* 2011a, Bansal *et al.* 2012, Brandes *et al.* 2005, Casetti *et al.* 2009). Interestingly, this remarkable plasticity of human V γ 9V δ 2 T cells is in complete contrast to murine $\gamma\delta$ T cells which seem to polarise and commit early in development to a particular cytokine profile (Ribot *et al.* 2009).

1.6 $\gamma\delta$ T cells and memory responses

One of the traits of the adaptive immune system is the ability to generate memory cells that provide faster and better immune responses on re-exposure to a particular antigen. V γ 9V δ 2 T cells have been postulated to show some evidence of memory in both human and primate experimental models

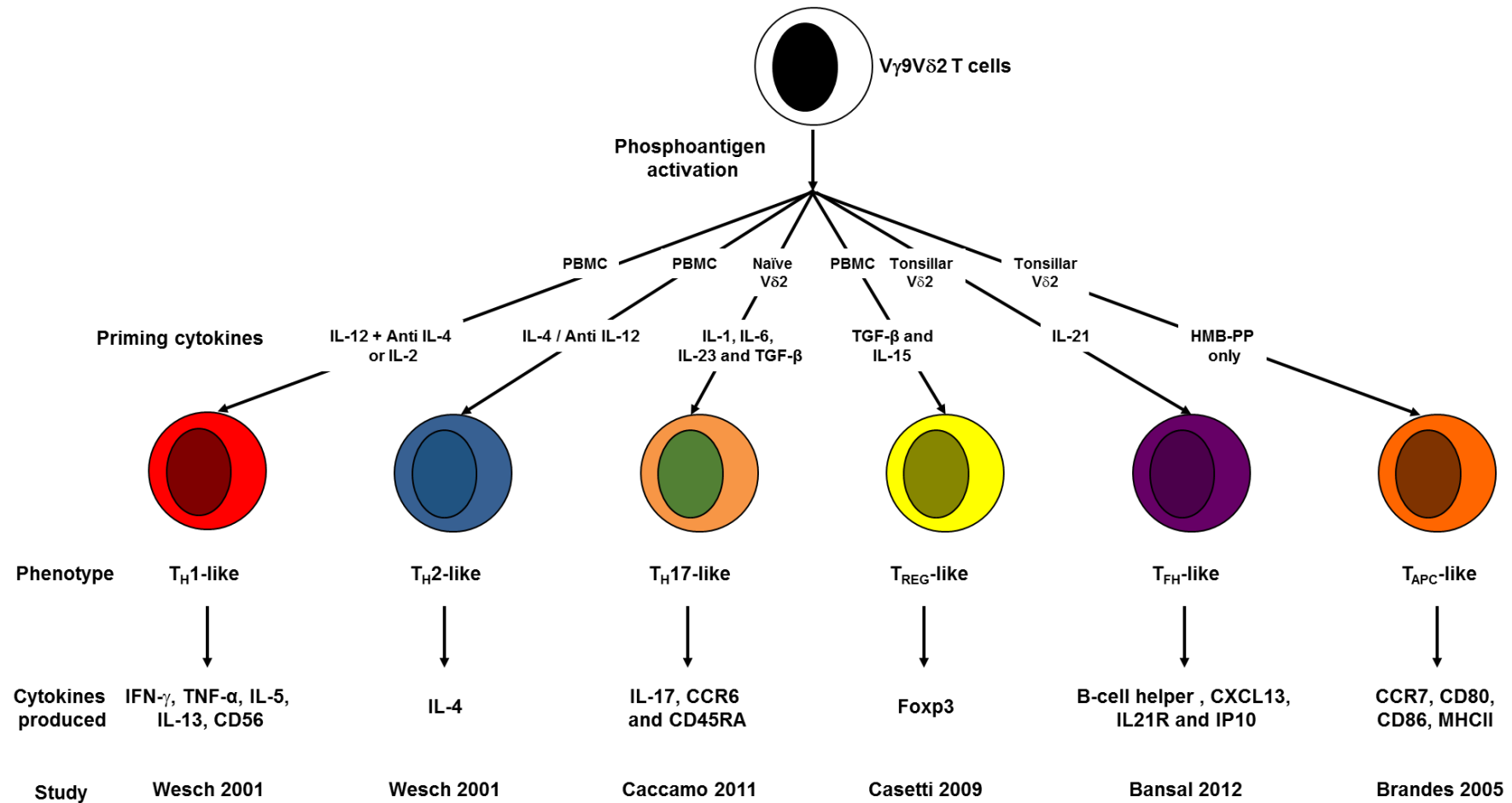


Figure 1.3 Functional plasticity of V γ 9V δ 2 T cells.

V γ 9V δ 2 T cells exhibit extensive plasticity following phosphoantigen stimulation in the presence of certain combinations of priming cytokines. The studies demonstrating this plastic function are indicated for each of the six described effector subsets as well as the characteristic cytokine production/extracellular marker expression associated with each phenotypic population.

(Abate *et al.* 2005, Cendron *et al.* 2007, Ryan-Payseur *et al.* 2012, Shen *et al.* 2002, Shao *et al.* 2009, Worku *et al.* 2001a) (Table 1.1).

Study Author	Model (Disease/Infectious agent)	Primary response	Effector responses	Proliferative Responses on re-exposure	Memory recall (Y/N)
Abate 2005	Human (Smallpox/Vaccinia)	Previously immunised (Not known)	IFN- γ	Increased proliferation.	Y
Cendron 2006	Rhesus macaques (TB)	V γ 9 proliferation with Th1 cytokine response	Reduced Th1 cytokine response – IFN- γ , TNF- α , IL-2 and IL-6	Reduced proliferation up to 4 months on re-exposure.	N
Shen 2002	Rhesus macaques (TB/BCG)	Absolute V δ 2 T cell expansion	Not reported	2-9 times increased expansion in absolute V δ 2 T cell number compared to primary infection. Recall expansion.	Y
Shao 2009	Rhesus macaques (Vaccinia virus, MPV)	V δ 2 expansion	IFN- γ	4 fold increases in absolute V δ 2 T cell number (re-expansion response). Re-expansion only.	N
Shao 2009	Rhesus macaques (Vaccinia virus/cidofovir, MPV)	Little or no primary expansion of V δ 2 population.	IFN- γ	Up to 40 fold absolute expansion in absolute V δ 2 T cells number compared to baseline. Recall expansion.	Y
Ryan-Payseur 2012	Rhesus macaques (Listeriosis, attenuated Listeria monocytogenes)	Low level expansion of V δ 2 cells	IL-17, IFN- γ , IL-4, TNF- α and Perforin. Cytotoxicity against monocyte derived DCs	V γ 9V δ 2 T cell increase from 50 cells/ μ l up to 15,000 cells/ μ l within a week after secondary inoculation. Recall expansion.	Y
Worku 2001	Human (In-vitro) (Canarypox/Live recombinant Canary pox virus).	Unknown Previously immunised	IFN- γ	Increased V δ 2 proliferation in subjects immunised with Canarypox vaccine.	Y

Table 1.1 A summary of the primate studies investigating V γ 9V δ 2 T cell memory function.

For each study, the primate model is indicated along with infectious agent/vaccine and the memory effector responses measured. MPV is Monkeypox vaccine, BCG is Bacille Calmette-Guérin and TB is Tuberculosis.

Whilst many of these studies present evidence to demonstrate memory properties in terms of a greater magnitude of response on re-exposure, others indicate that phosphoantigen priming may actually induce V γ 9V δ 2 T cell anergy (Cendron *et al.* 2007). Indeed, there is some evidence to suggest that V γ 9V δ 2 T cells are particularly sensitive to repeated stimulation by phosphoantigen and are prone to activation induced cell death (AICD) (Gan *et al.* 2001).

However, as V γ 9V δ 2 T cells are not activated in the same manner as conventional $\alpha\beta$ T cells the use of the term “memory” to describe certain types of V γ 9V δ 2 T cells is perhaps misplaced. Alternatively, these changes in functionality may be short-term and solely based on changes in expression of co-receptors/co-stimulatory molecules. This may render V γ 9V δ 2 T cells more responsive on experimental re-challenge for a short period after initial stimulation, thus appearing as if a memory response had occurred.

1.7 Differentiation pathway of V γ 9V δ 2 T cells

V γ 9V δ 2 T cell differentiation describes the progression of “naïve” V γ 9V δ 2 T cells that are generated in the thymus to the more mature phenotypes seen in the secondary lymphoid organs and tissues. There is very little experimental evidence for a definitive differentiation pathway. Nonetheless, it has been suggested that V γ 9V δ 2 T cells follow a linear pathway of progression in sequential, non-reversible stages that are best defined by the surface expression of CD27 and CD45RA; passing through; Naive (T_N) [CD27⁽⁺⁾CD45RA⁽⁺⁾] → Central memory (T_{CM}) [CD27⁽⁺⁾CD45RA⁽⁻⁾] → Effector memory (T_{EM}) [CD27⁽⁻⁾CD45RA⁽⁻⁾] → Effector Memory CD45RA⁽⁺⁾ or Terminally differentiated Effector Memory (T_{EMRA}) – [CD27⁽⁻⁾CD45RA⁽⁺⁾]. Evidence for this

differentiation pathway was presented by Dieli and co-workers (Dieli *et al.* 2003b) using a 12-day *in vitro* experimental cell culture model whereby individual sorted T_N , T_{CM} , and T_{EM} cell populations were stimulated in culture by phosphoantigen (IPP). This paper showed that T_N cells could be differentiated into T_{CM} cells and T_{CM} cells into T_{EM} cells, thus suggesting that a linear differentiation pathway exists. The generation of T_{EMRA} was suggested to occur *in vivo* in response to an inflammatory tissue environment. However, apart from this paper there is very little other evidence to show that these cells differentiate in a similar way to conventional $\alpha\beta$ T cells which clearly follow a $T_N \rightarrow T_{CM} \rightarrow T_{EM} \rightarrow T_{EMRA}$ pathway (Hintzen *et al.* 1993, Hamann *et al.* 1997, Okada *et al.* 2008, Inokuma *et al.* 2013). In summary, the differentiation of $V\gamma 9V\delta 2$ T cells has been poorly studied and has not been conclusively determined.

1.8 $\gamma\delta$ T cell homeostasis

Although T cell numbers fluctuate following infection and immune challenge, in general their numbers are maintained at a relatively constant level throughout life (Almeida *et al.* 2005). The majority of studies investigating $\gamma\delta$ T cells in health and disease have tended to observe percentages and phenotypes on a single occasion, making it difficult to follow how these characteristics change over time. However, one study did follow nine healthy volunteers for a period of 14 years and concluded that on average there was a reduction of 0.1% in the proportion of $V\gamma 9V\delta 2$ T cells (as a proportion of total lymphocytes) every year after the age of twenty. However, this was an average figure with some individuals experiencing a slight increase (+0.06%/year) but with others experiencing a significant depletion with time (-0.42%/year) (Caccamo *et al.* 2006). This same study also investigated whether there was any evidence for

phenotypic changes as a result of aging. On the whole, phenotypes remained relatively stable throughout life and particularly in females. However, this same study did report age related changes in males with an increase in the T_{CM} [CD27⁽⁺⁾CD45RA⁽⁻⁾] population and a depletion of T_{EM} [CD27⁽⁻⁾CD45RA⁽⁻⁾] and T_{EMRA} [CD27⁽⁻⁾CD45RA⁽⁺⁾] cells from the peripheral circulation with increasing age. Importantly, there was no real evidence to support a linear differentiation pathway from $T_N \rightarrow T_{CM} \rightarrow T_{EM} \rightarrow T_{EMRA}$ over time, as the latter subsets did not significantly accumulate over the 14-year period of study.

1.9 Role of the thymus

Current thinking suggests that the thymus undergoes involution and reduction in size at around the age of 20, and that its functional output after this point is very much reduced. However, a recent study postulated that the thymus continues to produce “naïve cells” well into adult life and that females maintain a higher proportion of recent thymic emigrants (RTEs) and maintain a better thymic function with increasing age compared to males (Pido-Lopez *et al.* 2001). It is clear from patients thymectomised after birth that the thymus is not absolutely essential for a fully functioning immune system and that the early seeding of cells from the thymus into the peripheral pool must also provide some “stem-like” properties especially in the memory pool.

1.10 Variation in $\gamma\delta$ T cell number

In general, the percentage of $\gamma\delta$ T cells in the peripheral blood of adults is relatively stable between 1 and 5% (Parker *et al.* 1990). This level is reached early in adult life following earlier dynamic changes due to V γ 9V δ 2 T cell post-thymic expansion. Peak levels seem to occur between the ages of 10-20 years

with mean levels rising to as high as 15-20% of total CD3⁽⁺⁾ lymphocytes (Parker *et al.* 1990, Caccamo *et al.* 2006). Following the dynamic variation seen during these early years, $\gamma\delta$ T cell levels then seem to plateau. The factors affecting $\gamma\delta$ T cells levels in the blood have been associated with a range of factors including age, sex, ethnicity/race, genetics, place of birth, infectious history, environmental exposure and certain diseases (see Table 1.2). However it is extremely difficult to elucidate the true reasons for observed differences, as these factors are obviously intimately linked.

1.10.1 Age

There is a steady increase in the absolute and relative numbers of V γ 9V δ 2 T cells found in the peripheral blood in the first 10 years of life which seems to be independent of thymic V γ 9V δ 2 T cell production (Parker *et al.* 1990). This expansion results in the V γ 9V δ 2 T cell subset becoming the predominant $\gamma\delta$ T cell population representing > 75% of all $\gamma\delta$ T cells in adult peripheral blood. The extra-thymic expansion is thought to be as a result of repeated environmental challenges, but perhaps may instead represent normal maturation.

1.10.2 Gender

While some reports suggest relative percentages of V γ 9V δ 2 T cells to be higher in adult females (Caccamo *et al.* 2006), others have suggested that the reverse is true with higher levels also being reported in males (Michishita *et al.* 2011). Caccamo *et al.* also suggested that the gender differences were only seen after the age of 20 years and reported that aging differences seemed more marked in males with less age-related depletion in females.

Study (Year)	Country of Study	Population	N	Mean Vδ2/CD3 (%)+/- SD (if known) Age range (years)	Male N (Vδ2/CD3 %)	Female N (Vδ2/CD3%)	Significant difference between male and female (p-value)	Other findings/ conclusions
Ishizawa 1993	Japan	Healthy volunteers	150	3.8 +/- 2.5 (Range 0.6-16.1%) 20-69	Data unknown		NS p>0.05	Significant Decrease in Vδ2/CD3% with age
Esin 1996	Sweden	Healthy volunteers (Sweden)	24	4.2% (Median)	Data not shown			Proportion of individuals with >10% Vδ2/CD3 ^(*) 0/24 (0%)
		Healthy volunteers (Japan)	35	4.5% (Median)				Proportion of individuals with >10% Vδ2/CD3 ^(*) 6/35 (17.1%)
		Healthy volunteers (Turkey)	26	9.3% (Median)				Proportion of individuals with >10% Vδ2/CD3 ^(*) 12/26 (46.2%)
		Healthy volunteers (Asian-Non Japanese)	14	9.2% (Median)				Proportion of individuals with >10% Vδ2/CD3 ^(*) 5/14 (35.7%)
Hviid 2000	Denmark /Nigeria	Healthy child donors (Ghana-Africa)	77	10% Age - Data not shown	Data not shown			TCR γδ is twice as high in African adults (Ghana) cf. European adult controls (Denmark). Vδ1 ^(*) 5 times higher (Ghana) cf Denmark donors.
		European adult donors (Denmark)	10	Vδ2/CD3 (%) Approximately 3.5-4% Age - Data not shown				
		Healthy adult donors (Ghana)	8	Vδ2/CD3 (%) Approximately 9% Age - Data not shown				
Argentati 2002	Italy	Healthy volunteers	40	3.4 19-50	Data not shown			Reduced number and altered cytokine profile due to ageing
			33	1.7 60-90				
			31	1.2 100-103				
Caccamo 2006	Italy	Healthy Volunteers	64	3.5% 2-15	24 (3.2)	20 (3.7)	NS	Gender and phenotypic difference in Vγ9Vδ2 reported.
			127	3.0% 20-30	60 (2.6)	67 (3.5)	p<0.05, F>M	
			98	1.5% 30-60	51 (0.9)	47 (2.5)	p<0.05, F>M	
Cairo 2010	USA	Healthy volunteers Caucasian	33	3.71 +/- 4.37 26-64	19	14	Data not shown	Importance of using age and race matched controls in clinical studies is highlighted with regard to γδ T cells.
		Healthy volunteers (African American)	32	1.18 +/- 2.14 19-63	19	13		
Michishita 2011	Japan	Healthy volunteers	84	Data not shown 20-69	42	42	P=0.007 M>F	Importance of using age and sex matched controls in clinical studies is highlighted with regard to γδ T cells.
			120	2.45 20-79	Data not shown			
			31	4.9 20-29				
			36	4.09 30-39				
			25	3.45 40-49				
			16	2.95 50-59				
			12	1.98 60-69				
			31	1.2 100-103				

Table 1.2 Variation in Vδ2/CD3(%) in published studies.

The variation in Vδ2/CD3(%) is shown depending on gender, age, ethnicity and country of study population. The age range (years), gender distribution and Vδ2/CD3(%) is shown for each study.

1.10.3 Ethnicity/race and environmental exposure

Ethnicity/race and environmental exposure are also factors suggested as having an impact on V γ 9V δ 2 T cell number. Once again, these are difficult factors to unravel in terms of determining the causative factor.

As an example of this, a Swedish study (Esin *et al.* 1996) found a significantly higher percentage of V γ 9V δ 2 T cells in Turkish (9.3%) and Asian (non-Japanese) (9.2%) healthy volunteers compared to those who were Swedish (4.2%) or Japanese (4.5%). The study concluded that these differences could be due to either genetic or environmental factors (Esin *et al.* 1996). In general, $\gamma\delta$ T cell levels seen in the hygiene-conscious Westernised populations are lower compared to other parts of the world. Therefore, the “cleaner” environment of the Western world seems to impact on the immunological development and probably the phenotype of V γ 9V δ 2 T cells (Romagnani 2004).

As V γ 9V δ 2 T cells are clearly reactive to environmental challenge, particularly early in life, it is possible that early exposure or significant disease exposure (e.g. malaria) can affect $\gamma\delta$ T cell number. This is exemplified in studies of $\gamma\delta$ T cells in West African populations. One of these, that compared Ghanaian and Danish populations, showed $\gamma\delta$ T cells to be around twice the level in healthy individuals from Ghana (\approx 9%) compared to the Danish population (\approx 3.5-4%) (Hviid *et al.* 2000). Interestingly however, the predominant population was the V δ 1 population and not V γ 9V δ 2 T cells as typically found in white Caucasian populations (Esin *et al.* 1996). However, it is obviously difficult to tease out the relative impact that genes compared to environment have on these

unconventional T cells particularly when sampling from a heterogeneous population who have a different environmental history and genetic background.

1.11 V γ 9V δ 2 T cell heterogeneity

Recent studies have clearly highlighted the remarkable functional plasticity of V γ 9V δ 2 T cells at least *in vitro*. They have also questioned whether the use of a system of identification designed for conventional T cells (i.e. using CD27 and CD45RA) is appropriate for $\gamma\delta$ T cells. For these reasons several groups have tried to establish an improved methodology for cataloguing V γ 9V δ 2 T cells heterogeneity. These systems typically use between two and four markers in combination to divide the total V γ 9V δ 2 T cell population cells into four or five subsets based on whether these extracellular markers are present or absent. The increased use of multi-colour flow cytometry now means that 10-12 extracellular markers are being routinely used to analyse cell phenotypes. Whilst this allows the analysis of many different combinations of markers, it does make the elucidation of their relationship difficult, particularly when two-dimensional flow cytometry plots are used. The use of multiple marker combinations potentially leads to a huge number of theoretical subsets that increases exponentially with additional markers (Table 1.3). Thus great care needs to be taken when designing new identification strategies.

1.12 Phenotypic characterisation of V γ 9V δ 2 T cells

The characterisation of human V γ 9V δ 2 T cells has utilised several combinations of markers, that include; CD45RA, CD45RO, CD27, CD28, CD16, CD56, CD11a, CCR7 and CD62L. This has led to different groups characterising V γ 9V δ 2 T cells in terms of their favoured markers (Table 1.4) with little attempt

Number of extracellular markers	Number of mathematically possible phenotypic groups
2	4
3	7
4	15
5	31
6	63
8	255
10	1023
12	4095
15	32767

Table 1.3 Theoretical number of phenotypic subsets as the number of surface markers used increase.

Theoretically possible number of phenotypic groups based on the number of potential combinations of different numbers of extracellular markers. Phenotypic group combinations are based on each marker having only two levels of expression i.e. assuming the surface marker is expressed or not.

Study	Phenotypic descriptor				
	T _N	T _{CM} T _{Early CM}	T _{CM27-} T _{Early CM27-}	T _{EM} T _{EM Intermediate}	T _{EMRA} T _{EMRA Late}
Dieli <i>et al.</i> 2005	CD27 ⁽⁺⁾ CD45RA ⁽⁺⁾	CD27 ⁽⁺⁾ CD45RA ⁽⁻⁾		CD27 ⁽⁻⁾ CD45RA ⁽⁻⁾	CD27 ⁽⁻⁾ CD45RA ⁽⁺⁾
Puan <i>et al.</i> 2009		CD27 ⁽⁺⁾ CD28 ⁽⁺⁾	CD28 ⁽⁺⁾ CD27 ⁽⁻⁾	CD27 ⁽⁺⁾ CD28 ⁽⁻⁾	CD27 ⁽⁻⁾ CD28 ⁽⁻⁾
DeRosa <i>et al.</i> 2004	CD27 ^(Bright) CD45RO ⁽⁺⁾ CD11a ^(dim)				
Morita <i>et al.</i> 2012		CD27 ⁽⁺⁾ CD28 ⁽⁺⁾	CD28 ⁽⁺⁾ CD27 ⁽⁻⁾	CD27 ⁽⁺⁾ CD28 ⁽⁻⁾	CD27 ⁽⁻⁾ CD28 ⁽⁻⁾ CD45RA ⁽⁺⁾
Angelini <i>et al.</i> 2004	CD27 ⁽⁺⁾ CD45RA ⁽⁺⁾ CD62L ⁽⁺⁾ CD16 ⁽⁻⁾	CD27 ⁽⁺⁾ CD45RA ⁽⁻⁾ CD62L ⁽⁺⁾ CD16 ⁽⁻⁾		CD27 ⁽⁻⁾ CD45RA ⁽⁻⁾ CD62L ⁽⁻⁾ CD16 ⁽⁻⁾	CD27 ⁽⁻⁾ CD45RA ⁽⁺⁾ CD62L ⁽⁻⁾ CD16 ⁽⁺⁾
Yokobori 2009 Teixeira <i>et al.</i> 2014	CCR7 ⁽⁺⁾ CD45RA ⁽⁺⁾	CCR7 ⁽⁺⁾ CD45RA ⁽⁻⁾		CCR7 ⁽⁻⁾ CD45RA ⁽⁻⁾	CCR7 ⁽⁻⁾ CD45RA ⁽⁺⁾

Table 1.4 Summary of the main published V γ 9V δ 2 T cell phenotypic systems.

The published classification systems used to describe V γ 9V δ 2 T cell subsets with a variety of different extracellular markers are shown. The year and author of each study is indicated along with the surface markers used to define each of the various sub-populations. V γ 9V δ 2 T cell subsets are described as; Naïve (T_N), Central memory (T_{CM}), Central memory CD27⁽⁻⁾ (T_{CM27-}), Effector memory (T_{EM}) and Terminally differentiated Effector Memory CD45RA⁽⁺⁾ (T_{EMRA}).

to reconcile how their subsets correspond to other studies. Indeed, a definitive methodology has yet to emerge.

1.12.1 CD27/CD45RA

As mentioned previously, the most common method of characterising V γ 9V δ 2 T cells in the literature is to use CD27 and CD45RA. This gives four populations; T_N [CD27⁽⁺⁾CD45RA⁽⁺⁾], T_{CM} [CD27⁽⁺⁾CD45RA⁽⁻⁾], T_{EM} [CD27⁽⁻⁾CD45RA⁽⁻⁾] and T_{EMRA} [CD27⁽⁻⁾CD45RA⁽⁺⁾] (Dieli *et al.* 2003a). This landmark paper described the T_N and T_{CM} populations as having lymph node homing potential but lacking immediate effector function, whilst the T_{EM} and T_{EMRA} populations express markers facilitating homing to inflammatory tissues and display immediate effector function. This paper also implied a sequential linear pattern of differentiation [T_N→ T_{CM}→ T_{EM}→ T_{EMRA}], with T_N (21.4%) cells in the lymph nodes, T_{CM} (52.1%) and T_{EM} (26.5%) cells largely “patrolling the blood” and T_{EMRA} cells present at inflammatory sites.

1.12.2 Naïve V γ 9V δ 2 T cells

A continued area of debate concerns the size and phenotype of a “naïve” V γ 9V δ 2 T cell population. Whilst CD27 and CD45RA are good markers at defining “naïve” cells in the $\alpha\beta$ T cell world, many consider that their use in describing “naïve” V γ 9V δ 2 T cells grossly overestimates this subset (De Rosa *et al.* 2004). Whilst the Dieli study estimates the “naïve” subset at about 21% of peripheral blood V γ 9V δ 2 T cells (Dieli *et al.* 2003b), this is in stark contrast to other groups who have found only very low levels of “naïve” V γ 9V δ 2 T cells when alternative combinations of markers are used (De Rosa *et al.* 2004, Morita *et al.* 2007). For example, the DeRosa study favours the use of CD27 with

CD11a; CD27^(Bright) CD11a^(Dull) being the phenotype used in combination with either CD45RA⁽⁺⁾ or CD45RO⁽⁻⁾ to identify “naïve” cells. By contrast, the aforementioned Dieli study also found that both T_N (75%) and T_{CM} (63%) V γ 9V δ 2 T cells express CCR7. This would suggest that the majority of these subsets retain the ability to recirculate through secondary lymphoid organs in a similar way to naïve conventional $\alpha\beta$ T cells. However, these levels of CCR7 expression were not observed in other studies with a general consensus that <25% of V γ 9V δ 2 T cells express CCR7 compared to around 80% of conventional $\alpha\beta$ T cells (Morita *et al.* 2007, Brandes *et al.* 2003). If the more conservative estimates of CCR7 expression are correct, then it means that far less V γ 9V δ 2 T cells retain the ability to recirculate through lymph nodes. The MHC-independent mode of antigen recognition used by V γ 9V δ 2 T cells to recognise phosphoantigen also raises the question as to why V γ 9V δ 2 T cells would need to recirculate through lymph nodes (Sallusto *et al.* 1999). Thus, the use of CCR7 as a reliable phenotypic marker must be considered with a note of caution.

1.12.3 CD27/CD28

A further system for the identification of V γ 9V δ 2 T cell subsets uses the co-stimulatory molecules CD27 and CD28 to divide cells into four subsets; Central Memory T_{CM} [CD28⁽⁺⁾CD27⁽⁺⁾], Central Memory CD27⁽⁻⁾ T_{CM27-} [CD27⁽⁻⁾ CD28⁽⁺⁾], Effector Memory T_{EM} [CD28⁽⁺⁾CD27⁽⁻⁾], and Terminally differentiated Effector Memory T_{EMRA} [CD28⁽⁻⁾CD27⁽⁻⁾] (Puan *et al.* 2009). The same terms i.e. T_{Naïve}, T_{CM}, T_{EM} and T_{EMRA} are used to describe the four subsets, which becomes slightly confusing as it is not clear how these populations relate to subsets which have the same phenotypic names but are defined based on different

surface markers (i.e. CD27 and CD45RA). In particular, whilst Dieli describes a T_{EM} population as CD27⁽⁻⁾CD45RA⁽⁻⁾, Puan uses CD27⁽⁺⁾CD28⁽⁻⁾, which is clearly inconsistent with regard to CD27 expression (Puan *et al.* 2009, Dieli *et al.* 2003b). In addition, the use of T_{EMRA} to describe the [CD28⁽⁻⁾CD27⁽⁻⁾] subset by Puan *et al* is odd, as it makes no reference to CD45RA expression despite the “RA” of TEMRA referring to CD45RA, and thus seems to assume that this population will be CD45RA⁽⁺⁾.

1.12.4 CD27/CD45RA/CD62L/CD16

A final system of identification for V γ 9V δ 2 T cells uses four markers (CD27, CD45RA, CD62L and CD16) (Angelini *et al.* 2004). This system is really a modification of Dieli’s original methodology as it uses CD62L and CD16 in combination with the markers CD27 and CD45RA to describe four subsets; Naïve T_N [CD27⁽⁺⁾ CD45RA⁽⁺⁾ CD62L⁽⁺⁾ CD16⁽⁻⁾]; Central Memory T_{CM} [CD27⁽⁺⁾ CD45RA⁽⁻⁾CD62L⁽⁺⁾CD16⁽⁻⁾]; Effector Memory T_{EM} [CD27⁽⁻⁾ CD45RA⁽⁻⁾ CD62L⁽⁻⁾ CD16⁽⁻⁾] and Terminally differentiated Effector Memory RA⁽⁺⁾ T_{EMRA} [CD27⁽⁻⁾ CD45RA⁽⁺⁾ CD62L⁽⁺⁾ CD16⁽⁺⁾]. The additional use of markers here does give some indication as to how multiple markers are related, but clearly ignores the CD27⁽⁺⁾ CD62L⁽⁻⁾ population (which is clearly visible in the paper) as well as the CD27⁽⁻⁾CD62L⁽⁻⁾CD16⁽⁻⁾CD45RA⁽⁺⁾ population in the analysis. Therefore, this phenotyping system does not characterise all V γ 9V δ 2 T cells and demonstrates how the addition of further markers often leads to small subsets and an unmanageable number of populations for practical purposes.

1.13 Human $\gamma\delta$ T cells – A summary

Human $\gamma\delta$ T cells are an enigmatic and under-studied component of the immune system. They demonstrate rapid innate-like responses without the need for prior priming in secondary lymphoid organs, yet possess a rearranged TCR and possible memory characteristics which are hallmarks of adaptive cells. They display a range of functions from direct anti-microbial activity through to immunoregulation, and appear to be important at certain times (i.e. in young animals) and in some locations (i.e. epithelial tissues). Recent work has highlighted the considerable heterogeneity of both $V\delta 1^{(+)}$ and $V\gamma 9V\delta 2$ T cell populations, and particularly for $V\gamma 9V\delta 2$ T cells has demonstrated remarkable plasticity of function *in vitro*. Finally, there is ever-increasing interest in utilising and boosting $\gamma\delta$ T cell function in the clinic, and a growing appreciation that these cells may have a central role in several immunopathologies. This introduction will now consider these roles, in particular the hypothesis that $V\gamma 9V\delta 2$ T cells may be a key component of the chronic disease known as BRONJ (Bisphosphonate-related osteonecrosis of the jaw).

1.14 Bisphosphonate-related osteonecrosis of the jaw (BRONJ)

A central hypothesis to this work is the view that $V\gamma 9V\delta 2$ T cells are a central component of Bisphosphonate-Related Osteonecrosis of the Jaw (BRONJ). This next section will review the disease and outline reasons for implicating $V\gamma 9V\delta 2$ T cells as a possible disease component.

1.14.1 BRONJ - An undesirable side-effect

Bisphosphonates were first licensed for therapeutic use in the early 1990s for treatment of hypercalcaemia and in the mid-1990s for osteoporosis (Agency 2011). In addition, bisphosphonates were also licensed for use in the prevention of adverse skeletal events, a recognised side effect of some malignancies, in particular multiple myeloma and breast cancer (Terpos *et al.* 2009). Despite their clear beneficial therapeutic role in preventing bone loss, an inadvertent side-effect of the drug was first described in a case series in 2003 (Marx 2003). This initial publication highlighted an apparent association between patients taking bisphosphonates and osteonecrosis of the jaw. It also led to the FDA issuing a patient safety notice for the drug the following year (2004) as more cases of BRONJ were diagnosed in patients taking bisphosphonate medication. Indeed, since this initial description there have been numerous case reports and case series describing the condition (Ruggiero *et al.* 2004, Sarathy *et al.* 2005, Merigo *et al.* 2005, Ficarra *et al.* 2005, Bonacina *et al.* 2011, Nicolatou-Galitis *et al.* 2011). Several theories have been proposed to explain the condition but to date there is no consensus as to its pathogenesis (Allen and Burr 2009).

1.14.2 Phossy Jaw and BRONJ – A resurgence of an historical disease?

There have been parallels drawn between BRONJ and an historical disease known as “Phossy jaw” observed in match-making factory workers in the 19th century. These workers were exposed to white/yellow phosphorus as part of the “strike anywhere” match-making process. Workers directly involved in match production at this time developed necrotic jaw lesions similar to those since observed in BRONJ (Hellstein and Marek 2004). It is now thought that phosphorous match-making compounds with similarities to therapeutic bisphosphonates were inhaled into the lungs of factory workers and were subsequently incorporated into bone. These observations have led many in the field to conclude that the pathophysiology of the historical disease, phossy jaw is likely to be the same as BRONJ (Marx 2008).

1.14.3 BRONJ Classification and nomenclature

A number of different terms are used to describe the disease driven mainly by semantic preferences by leaders in the field. These include;

- Bisphosphonate-related osteonecrosis of the Jaw (BRONJ)
- Bisphosphonate osteonecrosis of the Jaw (BON/BONJ)
- Bisphosphonate-associated osteonecrosis of the Jaw (BAONJ).
- Antiresorptive agent-induced osteonecrosis of the jaw (ARONJ)
- Medication-related osteonecrosis of the jaw (MRONJ)

The latter term (MRONJ) has arisen as a cover-all to describe osteonecrosis arising in patients on different forms of medication including bisphosphonates, RANKL inhibitors, as well as Vascular Endothelial Growth Factor (VEGF) pathway modifiers. However it is still unclear whether the underlying

pathologies caused by different treatments are similar. For the purposes of consistency in this thesis, BRONJ will be used throughout to refer to patients who have osteonecrosis with a history of bisphosphonate intake.

1.14.4 Prevalence and Incidence

Prevalence and incidence of new diseases can be difficult to determine particularly when pathogenesis is poorly understood. Risk of osteonecrosis appears to be related to cumulative exposure to bisphosphonates with a median range of exposure from 4-120 months (Zervas *et al.* 2006), but typically occurring between 18 and 39 months (Durie *et al.* 2005, Bamias *et al.* 2005). The incidence of osteonecrosis in patients on intravenous bisphosphonate therapy ranges from 0.9%-18.3% (Stumpe *et al.* 2009, Zervas *et al.* 2006, Aragon-Ching *et al.* 2009) with generally higher incidence in multiple myeloma patients compared to breast cancer and prostate cancer patients (Wang *et al.* 2007). A recent meta-analysis has suggested that the mean cumulative incidence is 6.1% (Migliorati *et al.* 2010) but this may represent an over estimation of the true incidence, with the majority of studies suggesting the true figure to be in the range of 1-3% (Wang *et al.* 2007, Badros *et al.* 2006, Hoff *et al.* 2008, Stumpe *et al.* 2009, Tosi *et al.* 2006, Pozzi *et al.* 2007). By contrast, the incidence of osteonecrosis in patients on oral bisphosphonates is extremely low with an estimated incidence of only 0.06% (Mavrokokki *et al.* 2007).

1.14.5 Clinical features of BRONJ

Bisphosphonate-related osteonecrosis of the jaw is characterised by the following features;

- Current or previous exposure to bisphosphonate medication.
- Exposed necrotic bone in the maxillofacial region persisting for at least eight weeks.
- No previous exposure to head and neck radiotherapy.

These essential disease characteristics were identified by an expert committee of The American Association of Oral Maxillofacial Surgery (AAOMS) in a paper in 2007 (AAOMS 2007). The committee also highlighted the potential for misdiagnosis, with similar diseases in this group of patients including; alveolar osteitis (dry-socket), osteomyelitis, osteoradionecrosis, caries, periodontitis and sinusitis.

1.14.6 Unexposed BRONJ

More recently, exposure of necrotic bone has been questioned as a necessary clinical sign in BRONJ diagnosis with reports of pain, bone enlargement, and gingival swelling in the absence of evidence of oral mucosal breach (Patel *et al.* 2012, Junquera and Gallego 2008, Fedele *et al.* 2010). This suggests that bisphosphonates may cause osteonecrosis without the need for a mucosal breach in the form of an extraction socket or through a periodontal pocket. It also raises doubt as to the importance of oral bacteria in initiating the disease (Marx 1983). These observations give further credence to theories of pathogenesis initiated within the bone, soft tissues or perhaps initiated by immunological changes.

1.14.7 Histological features

Whilst the clinical presentation of BRONJ is similar to osteomyelitis and osteoradionecrosis (ORN), the histological descriptions of BRONJ differ subtly but significantly from these similar conditions (Hansen *et al.* 2006b). In osteoradionecrosis, the necrotic areas of bone are avascular, which is in line with the proposed pathogenesis of the condition in which the jaw vasculature is obliterated by direct radiotherapeutic damage (Chrcanovic *et al.* 2010). Interestingly, there are some reports of increased osteoclast numbers in osteonecrotic lesions of BRONJ patients (Kuroshima *et al.* 2012, Hansen *et al.* 2006a). This observation is slightly counter-intuitive as bisphosphonates are thought to work by causing osteoclast apoptosis. Another histological feature of BRONJ is the colonisation of lesions with the *Actinomyces* species of bacteria (Biasotto *et al.* 2006, Bisdas *et al.* 2008, Hansen *et al.* 2007, Hansen *et al.* 2006b, Lazarovici *et al.* 2009, Lugassy *et al.* 2004). The presence of *Actinomyces* species in chronically exposed lesions may however be a result of colonisation of normal host oral bacteria. It is therefore unclear whether these bacterial species are causative agents or simply innocent bystanders in the disease process. Finally, the dominant cell types in the mixed inflammatory cell infiltrate in BRONJ lesions are neutrophils and plasma cells (Hansen *et al.* 2007). However, a recent research abstract has also highlighted an increased mononuclear cell infiltrate in BRONJ specimens and 4-5 fold higher levels of $\gamma\delta$ T cells localised to the gingival tissue of BRONJ specimens (Mawardi H (2013)). Indeed, $\gamma\delta$ T cells have also been previously found in chronically infected oral tissues as a result of chronic dental infection (Sol *et al.* 1998, McCutcheon *et al.* 2004).

1.15 Clinical management of BRONJ

There is no consensus as to the best methods to treat the condition although most emphasis today is on prevention and ensuring good oral health and oral hygiene practices prior to starting the medication. There is also an increased dental awareness of the potential of osteonecrosis development in patients on bisphosphonates and the risks posed by extraction and/or oral surgery. It is hoped that this heightened understanding may lead to a reduction in the number of BRONJ cases over time (Saldanha *et al.* 2012). The broad treatment strategies of BRONJ are explored below.

1.15.1 Prevention

Patients are encouraged to undergo pre-dental screening to ensure optimal oral health before embarking upon bisphosphonate medication particularly in those on the intravenous and more potent forms of the drug. Caries and periodontitis are the two most common causes of oral infection and are the two principle diseases of tooth loss. Promoting dental disease prevention through oral health advice, oral hygiene instruction, fluoride delivery and encouraging regular dental maintenance has clear benefits in terms of reducing the requirement for interventional dentistry and need for extraction (Krimmel *et al.* 2013).

1.15.2 Antimicrobials

The control of infection is one of the most important management principles in patients with BRONJ with antimicrobial preparations available as local mouth rinses or as a systemic medication. The choice of antimicrobial preparation is dependent on disease stage, with systemic antibiotics reserved for use where there are overt clinical signs of infection and antimicrobial mouth rinses for

treatment of all patients with exposed lesions. Indeed it is considered that antimicrobials are important in managing infections resulting secondarily as a result of mucosal exposure that occurs in BRONJ and not as a primary treatment agent. However the efficacy of antimicrobials in changing the bacterial profile has been questioned by one recent study that found little change in the microbial profile in BRONJ patients treated with antimicrobials compared to those who had not received this therapy (Ji *et al.* 2012).

1.15.3 Surgery

Surgical resection has been reported in some maxillofacial units to be a highly effective modality of BRONJ treatment with low recurrence rates of 3.1% and 9.4% at 3 and 6 months respectively (Bedogni *et al.* 2011). However, aggressive resection and curettage has also been shown to lead to further osteonecrosis, which has led to a move away from interventional surgical treatment of BRONJ lesions (Khan *et al.* 2008, McLeod *et al.* 2011). However, particularly when there are large regions of necrotic jawbone, there is a need to surgically remove sequestrae in order to manage infection and improve quality of life. Nonetheless, the consensus now favours a more conservative approach to BRONJ lesion management (McLeod *et al.* 2011, Khan *et al.* 2008).

1.16 The therapeutic use of bisphosphonates

1.16.1 Chemistry

Bisphosphonates are synthetic pyrophosphate analogues that exist in two main structural forms based on the presence or absence of nitrogen within the compound. Nitrogen-containing bisphosphonates are the group most highly associated with jaw osteonecrosis and are more potent osteoclast inhibitors

compared with non-nitrogen containing bisphosphonates (Rogers *et al.* 2000). Non-nitrogen containing bisphosphonates function by inducing osteoclast apoptosis by interfering with normal ATP metabolism (Roelofs *et al.* 2010). By contrast, nitrogen-containing bisphosphonates work by inhibiting farnesyl pyrophosphate synthase (FPPS), an enzyme critical to the mevalonate pathway of isoprenoid synthesis. The inhibition of this key enzyme subsequently leads to the inhibition of several downstream proteins and ultimately to the apoptosis of osteoclasts (Roelofs *et al.* 2010).

1.16.2 Medical Indications for use

The first clinical use of bisphosphonates was described in the late 1960s and early 1970s with the first use of etidronate to treat *myositis ossificans* and Paget's disease (Bassett *et al.* 1969, Smith *et al.* 1973, Altman *et al.* 1973). Etidronate and clodronate continued to be used in the 1970s and into the 1980s at which time more bisphosphonate compounds were developed, and in particular the more potent anti-resorptive nitrogen-containing bisphosphonates. Over the past 20 years nitrogen-containing bisphosphonates have been approved for medical use with FDA approvals granted for Pamidronate in 1991, Alendronate in 1995 and Zoledronate in 2002. These drugs were licensed as a medical therapy to treat a variety of conditions including osteoporosis, Paget's disease, multiple myeloma and the osteolytic skeletal effects of malignancy.

1.16.3 Dose and route of drug administration

For osteoporosis, alendronate is the first line treatment either prescribed at an oral dose of 10mg/day or 70mg/week. Alternatively risedronate is an alternative oral preparation prescribed at 5mg/day or 35mg/week. The intravenous dose for zoledronate is prescribed as a 5mg annual infusion. For the treatment of

hypercalcaemia of malignancy, Paget's disease and the osteolytic effects of malignancy, zoledronate is prescribed as a dose of 4mg and pamidronate at 60-90mg every 3-4 weeks by slow intravenous infusion. The drug is also available as a once yearly 5mg intravenous dose as an alternative to oral preparations for osteoporosis.

A single intravenous dose of the nitrogen containing bisphosphonate, zoledronate does not persist in the circulation for very long following a single administration. The pharmacokinetics of zoledronate shows that by 24 hours, 40% of the drug has been excreted in the urine and that the plasma concentration is only 1% of the post-administrative peak concentration. The remainder is sequestered into the bone around the whole skeleton (Reid *et al.* 2002). Zoledronate is then slowly leached back into the circulation over time although the dynamics of release is poorly understood. The half-life of zoledronate in plasma is thought to be around 167 hours (Reid *et al.* 2002).

1.16.4 Post-menopausal osteoporosis

Post-menopausal changes in oestrogen and progesterone levels are linked to a reduction in bone mineral density in females (Worley 1981). Bisphosphonates have clear benefits in terms of reducing adverse skeletal-related events in the elderly and have been shown to significantly improve morbidity without significantly affecting mortality rates (Mhaskar *et al.* 2010). Bisphosphonates are generally prescribed orally at a low dose for treatment of osteoporosis. However, intravenous bisphosphonates (typically zoledronate and pamidronate) are now also licensed and prescribed in once/twice yearly doses to patients intolerant to the oral form of the drug.

1.16.5 Adverse skeletal events in cancer patients

Multiple myeloma, prostate, breast and lung cancers are among the malignant diseases characterised by diffuse or more generalised bone resorption due to increased osteoclast activity. Reduced bone mass can lead to increased rates of fractures in this patient group which can have significant effects on quality of life and on morbidity and mortality rates (Diamond *et al.* 2011). There is a clear beneficial effect of bisphosphonates in reducing skeletal related-events in cancer. In contrast to osteoporotic doses, these drugs are typically delivered intravenously on a monthly basis at higher cumulative doses.

1.16.6 Other Indications

Less commonly, bisphosphonates are used to treat other osteolytic conditions where a reduction in bone remodelling is of benefit. These conditions include Paget's disease, giant cell lesions of the jaw, osteogenesis imperfecta, fibrous dysplasia, Gaucher's disease and osteomyelitis (Landesberg *et al.* 2009).

1.17 BRONJ - Aetiology and Theories of Pathogenesis

The cause of BRONJ remains poorly understood with numerous proposed theories of pathogenesis, none of which fully explain the clinical and histopathological manifestations of the condition.

1.17.1 Anti-angiogenesis

The two major clinical forms of osteonecrosis are avascular necrosis of the hip and osteoradionecrosis (Allen and Burr 2009, Malizos *et al.* 2007, Chrcanovic *et al.* 2010). It would therefore follow that disruption of the vascular supply might also be important in the pathogenesis of BRONJ. Bisphosphonates have been shown to be anti-angiogenic in *in vitro* studies by inhibiting vascular endothelial

growth factor (VEGF) (Wood *et al.* 2002, Wypij *et al.* 2008). However, one interesting study into the effect of bisphosphonates in a dog model failed to show a disruption of the bone vasculature despite the observation of loss of osteocytes within their lacunae (Allen and Burr 2008).

1.17.2 Dysregulation of normal bone turnover

As normal bone turnover in healthy adults sees the tight coupling of bone resorption with bone deposition, a drug that causes osteoclast inhibition/apoptosis would be expected to affect this process. However, although the uncoupling of this system and the resultant bone remodelling suppression might explain the osteonecrosis, it does not obviously explain why the condition is localised to the jaw. One proposed explanation for this may be due to the high turnover rate of jawbone in comparison to other extra-oral sites (Han *et al.* 1997, Garetto *et al.* 1995). As an example of this, the turnover rate in the jawbone is twenty-times faster compared to iliac crest bone. In further support of this theory, patients who were prescribed parathyroid hormone (a medication that simulates bone remodelling) in small clinical studies showed evidence of BRONJ healing (Harper and Fung 2007). However as these patients received this therapy alongside surgical and antimicrobial therapy it is difficult to be certain that the beneficial effects were directly due to the parathyroid hormone therapy.

1.17.3 *Actinomyces* / Bacterial cause

The search to explain the localisation of osteonecrosis to the jaws of patients who take bisphosphonates has led many to suggest a bacterial cause. The oral cavity is colonised by a huge number of bacteria with over 700 species identified (Aas *et al.* 2005). The large number of bacteria in the oral cavity

means that the identification of a causative species/strain is difficult as bacterial colonisation is present in both health and disease. However, one particular species of *Actinomyces* bacteria (*Actinomyces israelii*) has been described in a large number of BRONJ lesions (Hansen *et al.* 2007). These bacteria have also been identified as causing necrotic lesions in the head and neck region of humans (Actinomycosis) and a similar condition (lumpy-jaw) affecting cattle (Antiabong *et al.* 2013). Interestingly, these bacteria also have the ability to cause periodontal bone resorption as evident in mono-infection of the bacteria in a rat model (Garant 1976). Importantly, the *Actinomyces* species of bacteria produce HMB-PP bacteria and so have potential to also activate V γ 9V δ 2 T cells locally in jaw-associated tissues.

1.17.4 Direct toxic effect on oral epithelial cells

Bisphosphonates are rapidly sequestered by bone following therapeutic administration of the drug with much of the drug being taken up and stored in the bone matrix reservoir (Khan *et al.* 1997, Kimmel 2007). It is postulated that bisphosphonates are retained in the bone matrix and are released into the local microenvironment during periods of bone remodelling. This might suggest that the local release of bisphosphonates, perhaps following extraction and/or surgery may have toxic effects on oral epithelial cells in the jaw and may explain the exposed necrotic bone found in BRONJ. Studies have shown that a range of bisphosphonates affect proliferation of oral, renal, gastro-intestinal and cervical cells in a dose dependent manner (Landesberg *et al.* 2011). Indeed, mouse oral epithelial cells (Landesberg *et al.* 2008) and primary human osteoblasts (Marolt *et al.* 2011) showed dose-dependent inhibitory effects on cell viability, proliferation and wound healing after pamidronate treatment.

1.17.5 Mucosal breach / Tooth extraction

Dental tooth extraction or oral surgery is thought to precipitate osteonecrosis in patients taking bisphosphonates with evidence that supports this as a significant risk factor (Odds ratio=16.4) (Kyrgidis *et al.* 2008). However, it is also apparent that previous dental extraction or oral surgery is not an absolute pre-requisite for the development of BRONJ (Patel *et al.* 2012, Kyrgidis *et al.* 2008). Indeed, denture wear has also been shown to increase risk of development of BRONJ with an odds ratio of 4.9 in breast cancer patients (Kyrgidis *et al.* 2008).

1.17.6 Evidence for V γ 9V δ 2 T cell involvement in BRONJ

There is only limited published evidence (Kalyan *et al.* 2013, Mawardi H 2013) to suggest a role for V γ 9V δ 2 T cells in the pathogenesis of BRONJ, despite the well-established effects that bisphosphonate medications have on the activation of these unconventional T cells (Thiébaud *et al.* 1997). However, one recent study showed a correlation between intake of nitrogen-containing bisphosphonates (n-BP) (these patients included some with BRONJ) and low levels of V γ 9V δ 2 T cells in the peripheral blood. This observation was in contrast to age-matched osteoporotic patients that had not yet started bisphosphonate therapy and who showed no evidence of V γ 9V δ 2 T cell depletion (Kalyan *et al.* 2013).

The mechanistic implications of this study are several. These data could simply imply that long-term bisphosphonate use leads to an activation induced depletion of V γ 9V δ 2 T cells that may or may not recover after withdrawal of treatment. This could have obvious implications beyond BRONJ, as

bisphosphonates plus interleukin-2 are a promising approach to treat several cancers in early stage clinical trials. In terms of BRONJ pathogenesis, a scenario could be envisaged in which depletion of V γ 9V δ 2 T cells may lead to a disruption of immunoregulation resulting in active immune-driven disease (Hypothesis #1, Figure 1.4). V γ 9V δ 2 T cells are thought to display certain immunoregulatory function in certain circumstances, which could fit with this hypothesis. This may also explain the delay observed between starting bisphosphonate therapy and the onset of the clinical manifestations of disease, and the association of BRONJ with dental surgery, in which post-extraction mucosal healing may be affected by the absence of V γ 9V δ 2 T cells.

An alternative interpretation of a bisphosphonate-induced depletion of V γ 9V δ 2 T cells from the peripheral blood could be that these cells have left the blood and entered the tissues. Indeed, a recent research abstract suggested that these are increased numbers of $\gamma\delta$ T cells in the mononuclear cell infiltrates from BRONJ lesions when compared with similar lesion infiltrates from non-bisphosphonate associated necrosis (Mawardi H 2013). This abstract further suggested that a combination of oral bacteria, bisphosphonates and local cytokine could activate $\gamma\delta$ T cells to display direct cytotoxic effector function against gingival fibroblasts (Hypothesis #2, Figure 1.4). Extending this idea further, it is conceivable that the bisphosphonate-mediated activation of V γ 9V δ 2 T cells in jaw tissue could be affected in a range of ways by the presence or absence of various cytokines, and importantly, specific species of oral bacteria. For example, V γ 9V δ 2 T cells that are specifically activated to secrete certain cytokines such as interleukin-17, may affect the on-going differentiation of monocytes to macrophages or tissue dendritic cells, diverting them to

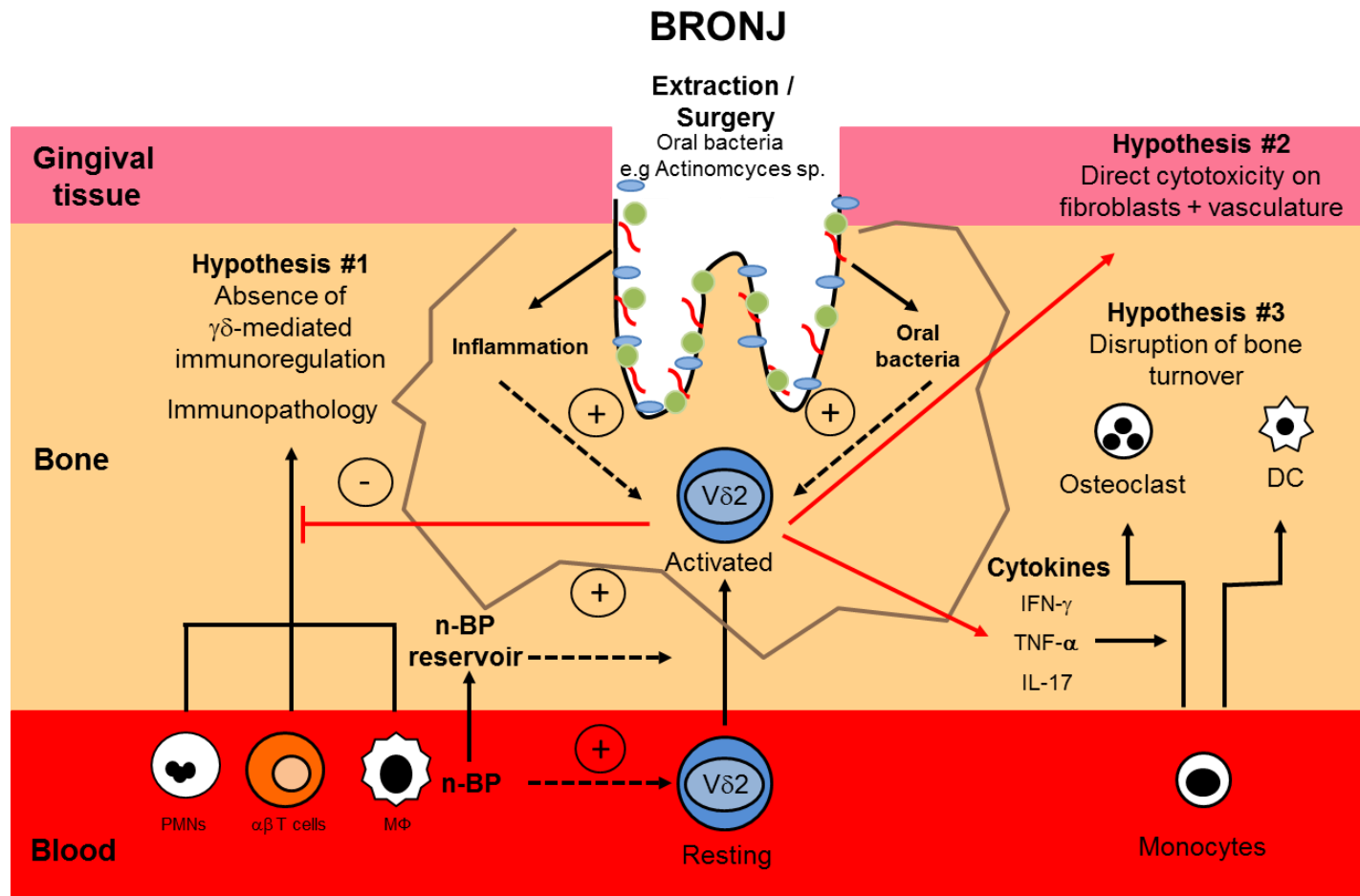


Figure 1.4 Hypothesised role for V γ 9V δ 2 T cells in the pathogenesis of Bisphosphonate-related osteonecrosis of the jaw.

Activation of V γ 9V δ 2 T cells by bisphosphonates in the presence of inflammation and oral bacteria in the jaws is proposed to cause BRONJ by a number of potential mechanisms including; (1) loss of immunoregulation through depletion of V γ 9V δ 2 T cells in the local tissues (Hypothesis #1), (2) direct cytotoxicity to fibroblasts and endothelial cells (Hypothesis #2) and (3) regulating osteoclast activity through local cytokine release (Hypothesis #3). Cell abbreviations are PMNs – Polymorphonuclear Neutrophils, M ϕ - Macrophages and DCs – Dendritic cells. (+) symbolises activation and (-) symbolises inhibition.

alternative fates, such as osteoclasts. This may disrupt the balance of bone remodelling in the jaw leading to osteonecrosis (Hypothesis #3, Figure 1.4).

1.18 Study Hypothesis

The general hypothesis that underpins this study is that; Bisphosphonate-mediated activation of V γ 9V δ 2 T cells, in combination with oral bacteria, and located in the jaw tissue, is a central component of the pathogenesis that underpins Bisphosphonate-related osteonecrosis of the jaw. The key ideas incorporated in this hypothesis are illustrated in Figure 1.4.

1.19 Working hypothesis

As detailed in the thesis overview section of the introduction, there were several logistical issues that significantly delayed the recruitment of patients into the study. While these issues were being dealt with, it was decided that an initial characterisation of V γ 9V δ 2 T cells from the peripheral blood of healthy individuals would be an important step to establish a suitable baseline for the study. However, as described in the initial sections of this first chapter, these initial investigations revealed some surprising findings. These observations led us to quickly establish some further working hypotheses, which are as follows;

1. That healthy individuals are heterogeneous for V γ 9V δ 2 T cell phenotype and function, that has direct implications for V γ 9V δ 2 T cells cell based-therapies.
2. That an individual's V γ 9V δ 2 T cells profile is stable over time with minimal differentiation between V γ 9V δ 2 T cell subsets.
3. That the definition of "naïve" and memory subsets needs to be re-considered with respect to V γ 9V δ 2 T cells.

1.20 Aim and objectives of thesis

The aims and objectives of the thesis, as described in the following results sections, are as follows;

1. To extensively characterise the degree of heterogeneity in the phenotype of V γ 9V δ 2 T cells in a large sample of healthy individuals.
2. To assess the functional potential of V γ 9V δ 2 T cells from individuals with significantly different V γ 9V δ 2 T cell profiles.
3. To compare and contrast V γ 9V δ 2 T cells with V δ 1⁽⁺⁾ $\gamma\delta$ T cells, using information generated in aim-1 and aim-2.
4. To initially characterise the phenotype of V γ 9V δ 2 T cells from fresh human neonatal thymus, to establish the phenotype of a “naïve” V γ 9V δ 2 T cell subset.
5. To use information generated in aims 1-4 to make initial observations on the status of V γ 9V δ 2 T cells in a small cohort of BRONJ patients.

Chapter 2

Materials and Methods

Chapter 2 Materials and methods

2.1 Ethical approval

Four separate research ethical approvals cover the tissue sample use in this study:

- Immunoregulation at the mucosal barrier (P/03/122) –East London and City REC - Healthy Blood samples (Existing ethical approval in place for recruitment of healthy volunteers).
- Inflammation and Immunity in diseases involving the digestive system in children and adults (P/01/023) - East London and City REC – Healthy blood samples. (Existing ethical approval in place for recruitment of youngest healthy volunteers).
- Thymus Transplantation for Complete DiGeorge Syndrome (06-MI-13(B)) Thymus Study ethics – Paediatric thymic organs were obtained under an existing ethical approval.
- BRONJ and the Immune System (13/LO/0548) – East London and City REC - Healthy Blood samples, BRONJ Blood samples and Osteoporotic patient samples are covered in this ethic approval.

Details of the process of applying for ethical approval (BRONJ and the Immune System) are outlined in the flow chart below (Figure 2.1). The Health Research Authority (HRA) oversees clinical research within the NHS. This body ensures ethical review and monitoring of all health research involving patients in England.

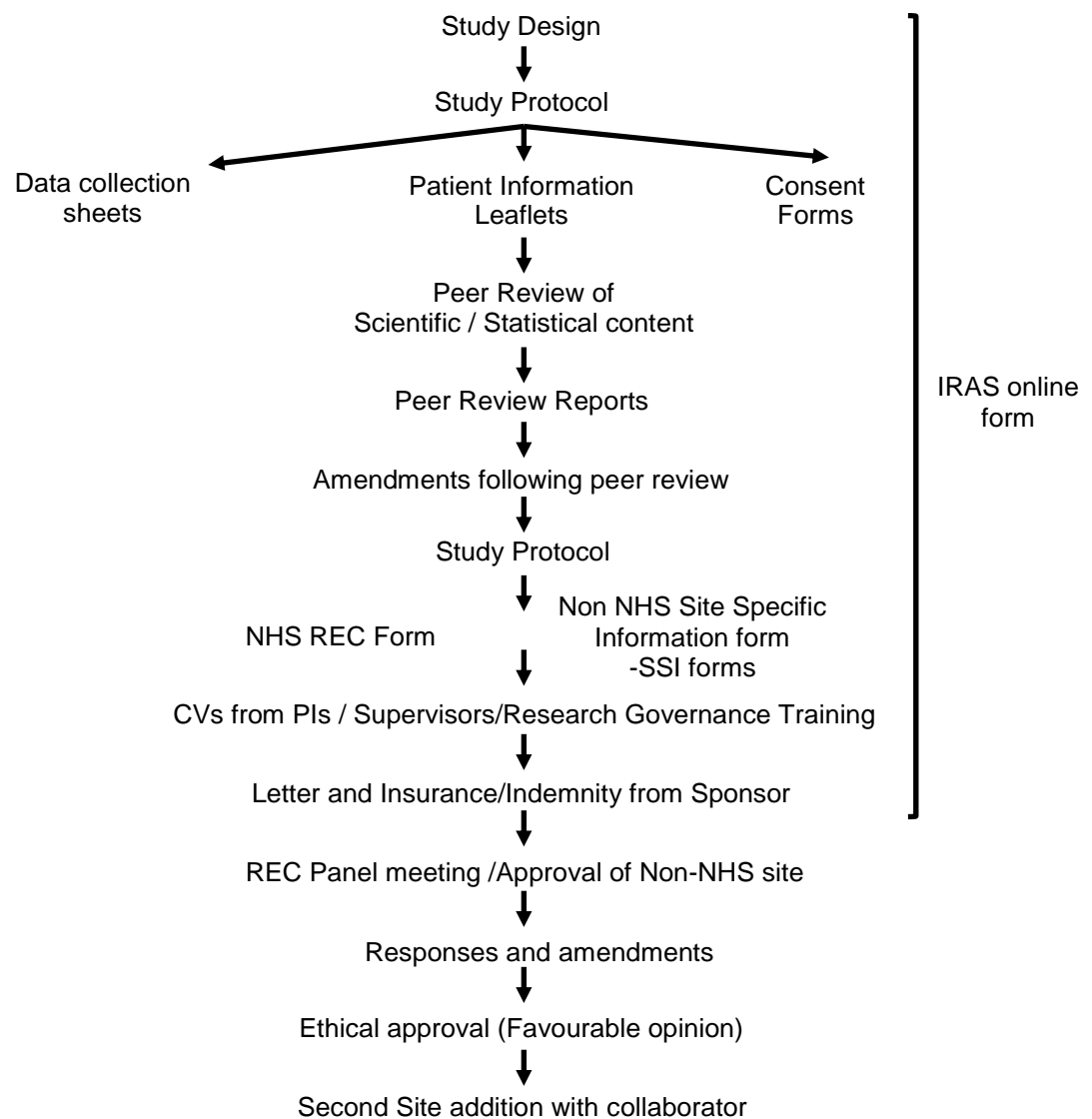


Figure 2.1 Schematic of the ethical approval process.

Overview of the stages involved in obtaining ethical approval for research involving healthy volunteers and NHS patients. Initially the research methodology and study design were formulated with justification for patient involvement in the research study. Following internal peer review, all documents (shown above) were sent for approval by the City and East research ethics committee (REC). A favourable opinion for the study at Barts Health NHS Trust and the Blizard Institute (QMUL) was then granted. A subsequent amendment was then added to the application by addition of another research site to facilitate sample collection at a second site (University College London Hospitals NHS Foundation Trust).

Therefore the process of obtaining ethical approval required an application to this regulatory body for permissions to work with clinical samples and data relating to patients. While this was an essential process it also provided valuable training in research design as it involved careful planning of the

research project. In particular, it involved considering how patients are approached and recruited, the necessary clinical samples/patient information required, planning the laboratory experiments and ensuring overall that the project was carried out ethically (Appendices 10.1-10.3).

2.2 Collaborative unit

A collaborative agreement was reached with the Eastman Dental Hospital for recruitment of BRONJ patients. A further amendment to the ethics application was obtained to add Eastman Dental Institute as a secondary research site to the project ethics approval (University College London Hospitals Foundation Trust).

2.3 Recruitment of study subjects

2.3.1 Healthy volunteers

A total of 63 healthy volunteers were predominantly recruited from staff and postgraduate students at the Blizard Institute (Queen Mary University of London) and from the Dental Institute (Barts Health NHS Trust). Two of the youngest individuals in the study were recruited as patients from Barts Health NHS Trust. Healthy volunteers ranged in age from 3-69 years with a median age of 33 years (31 males, 32 females). Informed consent was obtained from each subject and peripheral venous blood (up to 50ml) was collected along with relevant demographic and health information (see data collection sheets - Appendix 10.3).

2.3.2 Infants undergoing corrective cardiac surgery

A total of 8 children who were undergoing surgery for correction of congenital heart defects at Great Ormond Street Hospital were enrolled in the study. Parents of children undergoing these operations were asked for permission to analyse thymic tissue removed during the normal course of corrective cardiac operations. Children's ages ranged from 4 days–35 months (Males=4, Females = 4) with a median age of 11.5 months.

2.3.3 Bisphosphonate treated control patients

Osteoporotic patients were recruited from patients attending the outpatient Rheumatology Clinic at Mile End Hospital (Barts Health NHS Trust). A total of 10 patients treated with either oral or intravenous bisphosphonates were recruited as a BRONJ control group. This group was subdivided into;

- 5 patients on intravenous bisphosphonates (Zoledronate and Pamidronate), aged from 44-81 years with a median age of 76.5 years. (4 females and 1 male).
- 5 patients on oral bisphosphonates (Aledronic acid), aged from 56-79 with a median age of 72 years (4 females, 1 male).

Informed consent was obtained from each patient and peripheral venous blood (up to 50ml) was collected along with relevant demographic and health information (see data collection sheets - Appendix 10.3).

2.3.4 BRONJ patients

BRONJ patients were recruited from patients attending Oral and Maxillofacial Surgery and Oral Medicine clinics at both The Royal London Dental Institute (Barts Health NHS Trust) and The Eastman Dental Institute (University College

London Hospitals NHS Foundation Trust). Patients ranged from 46-88 years with a median age of 58.5 years (6 females and 2 males). Informed consent was obtained from each patient and peripheral venous blood (up to 50ml) was collected from each patient along with relevant demographic and clinical/health information (see data collection sheets Appendix 10.3).

2.4 Tissue Preparation

2.4.1 Blood donor cones

Six 15ml blood samples were obtained initially in the form of anonymised “leukocyte cone” samples from the National Blood Transfusion Service. Cones are provided as a concentrated cell sample from an original 600ml blood sample. The contents of the leukocyte cone were initially transferred to a 50ml centrifuge tube and 40mls of sterile PBS was used to wash the cone and maximise the cell yield into the collecting tube. Following this, peripheral blood mononuclear cells (PBMCs) were extracted in the same way as subsequently described for fresh blood samples.

2.4.2 Blood

Peripheral venous blood was collected from volunteers and patients following informed consent in accordance with the ethical approvals outlined above. Blood samples were collected in 10ml BD Vacutainer® sodium heparin tubes (Becton Dickinson (BD), UK) ready for PBMC extraction. All samples were processed on the same day of venepuncture and were analysed and used fresh. No samples were frozen or cryopreserved prior to analysis.

2.4.3 Separation of PBMCs from peripheral venous blood

Peripheral blood was diluted 1:1 in sterile Phosphate Buffered Saline (PBS) and then gently layered on Ficoll-Paque (GE Healthcare, Amersham, UK). Up to 20ml of diluted blood was layered onto 15ml Ficoll-Paque at room temperature (18°C) in 50ml tubes. PBMCs were separated by density gradient centrifugation at 1500rpm (400xg) for 35 minutes (brake off) (Thermo Scientific™, USA) at room temperature (18°C). The plasma layer was removed before carefully pipetting off the buffy coat interface containing mononuclear cells. This layer was then washed in FACS buffer (2% FBS (Gibco, Life Technologies, UK) in Sterile PBS and 1mM EDTA (Life Technologies) and pelleted by centrifugation (400xg – 10 minutes) prior to counting.

2.4.4 Thymus

Human thymic organs were obtained from The Institute of Child Health (Great Ormond Street Hospital for Children NHS Foundation Trust), and stored in complete media containing; RPMI 1640 (Invitrogen, Life Technologies, UK), 10% Heat-inactivated FBS (Gibco, Life Technologies), 10mM HEPES buffer, 50µg/ml Streptomycin (Life Technologies), 50U/ml Penicillin (Life Technologies). Samples were then transferred cold with the aid of an ice pack in an organ transport cool bag to The Blizard Institute (Queen Mary University of London).

2.4.5 Isolation of thymocytes from the neonatal thymus

The thymic organs were then weighed, re-immersed in complete media and whole organs were left overnight at 4°C before processing the following day. Thymic organs were processed in a sterile laminar flow cabinet keeping the

tissue moist with complete media wherever possible throughout all stages of preparation. The fat and connective tissue were removed from the thymus using sterile forceps and scissors and cut into small cubes in a sterile petri dish. The tissue and complete culture media was then transferred to a 200ml beaker and placed on a stirrer at room temperature for 30 minutes. The supernatant (thymocyte fraction 1) was filtered using a 100 μ m cell strainer and then stored on ice. The remaining tissue was then placed on a sterile steel mesh and mechanically disrupted with the use of a sterile syringe plunger over a beaker using complete media. This second supernatant (thymocyte fraction 2) was then pooled with thymocyte fraction 1 making up the total extracted thymocyte sample ready for flow cytometric analysis.

2.4.6 Cell counting and viability assessment

PBMCs and thymocytes were enumerated using Trypan Blue exclusion. Samples were diluted in 0.4% Trypan Blue (Sigma-Aldrich, Poole, UK) and counted using an improved Neubauer haemocytometer. Mononuclear live cells were counted and blue dead cells excluded to determine cell number. Typical yields were approximately 1×10^6 cells per 1ml of peripheral venous blood.

2.4.7 Storage of leukocyte cone samples

Due to the large number of cells obtained in each leukocyte cone sample, cells were initially frozen down in 10% DMSO (Sigma-Aldrich) and 90% Human AB serum (Sigma-Aldrich). Cells were aliquotted in 2ml cryovials (Fisher Scientific, UK) at a 25 million cells/ml concentration and frozen slowly at -80°C a rate of -1°C per minute in an isopropyl alcohol gradient freezing device. Samples were subsequently used as required by rapid thawing of individual samples in a 37°C water bath before washing of cells in complete media to remove the

cryopreserving DMSO. Cells were then recounted and viability assessed by Trypan blue (Sigma-Aldrich) cell exclusion, which was previously described (Section 2.4.6).

2.5 Cell Culture

PBMCs were cultured in complete media in 96-well round-bottomed plates (VWR) at a final concentration of 2×10^6 /ml at 37°C and 5% CO₂.

- HMB-PP 1nM (Sigma-Aldrich) + recombinant human Interleukin-2 (rhIL-2) 100U/ml (PeproTech, Rocky Hill, NJ, USA) – Proliferation assays (5 days).
- Zoledronate 1 μ M (Novartis pharma, Basel, Switzerland) + IL-2 (rhIL-2) 100U/ml (PeproTech) (7 days).

2.5.1 Proliferation assay

A single cell suspension of PBMCs was prepared and washed twice in sterile PBS (warmed to room temperature) to remove any serum. PBMCs were then resuspended at 4×10^6 /ml (twice the final culture concentration). A 10 μ M solution of cell proliferation dye eFluor® 670 (eBioscience, UK) in PBS (pre-warmed to room temperature) was mixed 1:1 with the cell suspension whilst vortexing (i.e. cells were labelled at a final concentration of 5 μ M). The cells were incubated for 10 minutes at 37°C in the dark. After incubation the labelling was stopped by the addition of 5 volumes of complete media (RPMI 1640 + 10%FBS (Gibco, Life Technologies) + Pen.Strep (Life Technologies).) and incubated on ice for a further 5 minutes. The cells were then washed three times in complete media before culturing for 5 days in the presence of 1nM HMB-PP and IL-2 (100U/ml).

Baseline flow cytometry data (at day 0) was obtained by acquiring PBMCs on the flow cytometer BD FACSCanto™ II (Becton Dickinson-BD) to ensure even loading of cells and a fluorescent intensity reference to compare cultured cells at 5 days. After 5 days, the cultured cells were extracellularly stained and analysed on the flow cytometer BD FACSCanto™ II. Percentage of proliferating cells at 5 days was calculated as the percentage of cells below the fluorescent loading peak using FlowJo (Version 8.8.7)(Tree Star).

2.5.2 Extracellular staining

Peripheral blood mononuclear cells (Typically 5×10^6) were stained and incubated in 100 μ l total FACS buffer (Sterile PBS containing 2% FBS (Gibco, Life Technologies) / 1mM EDTA) in 5ml polystyrene Falcon Tubes (Becton Dickinson) using directly conjugated monoclonal antibodies (mAbs) to extracellular markers (Tables 2.1). The antibody panels used in experiments are summarised in Table 2.2 with isotype and FMO staining controls used when appropriate. Staining was carried out for 30 minutes at 4°C (on ice) in the dark using manufacturers suggested dilutions of monoclonal antibodies (mAbs). Cells were subsequently washed in FACS Buffer and pelleted by centrifugation at 350xg and resuspended in a final volume 500 μ l of FACS buffer. Cells were then acquired on the flow cytometer (BD FACSCanto™ II). In order to detect the maximum number of V γ 9V δ 2 T cells within a mixed PBMC population it was necessary to acquire almost the entire 500 μ l sample.

Supplier	Marker	Antigen	Clone	Fluorophore	Cat. No.
BioLegend	Variant of TCR δ chain	V δ 2	B6	FITC	331406
Thermo Scientific	Variant of TCR δ chain	V δ 1	TS8.2	FITC	TCR2730
BioLegend	A chain of the CD3/TCR	CD3 ϵ	HIT3a	APC	300312
BioLegend	Co-stimulatory receptor	CD27	O323	Pacific Blue	302822
BioLegend	Type I transmembrane protein	CD45RA	HI100	APC-Cy7	304128
BioLegend	Co-stimulatory receptor	CD28	CD28.2	PE Cy-7	302926
BioLegend	Transmembrane adhesion molecule	CD11a	HI111	PE	301208
BD Bioscience	Fc-receptor	CD16	3G8	V500	561394
BioLegend	Transmembrane glycoprotein	CD56	HCD56	PerCPCy5.5	318322
BioLegend	Lymph node homing receptor	CCR7	G043H7	APC	357203
BioLegend	Lymph node homing marker	CD62L	DREG-56	PerCP/Cy-5.5	304823
BioLegend	Chemokine Receptor	CCR2	K036C2	PerCP/Cy-5.5	357203
BioLegend	Chemokine Receptor	CCR9	L053E8	APC	358907
BioLegend	Chemokine Receptor	CCR5	HEK/1/85a	PerCP/Cy-5.5	313715
BioLegend	Chemokine Receptor	CXCR5	J252D4	APC	356907
BioLegend	Chemokine Receptor	CX3CR1	K0124E1	PE	355703
BioLegend	Chemokine Receptor	CCR6	G034E3	PerCP/Cy-5.5	353405
eBioscience	Serine protease	Granzyme B	GB11	PE	12-8899-41
eBioscience	Serine protease	Granzyme K	G3H69	PerCP-eFluor 710	46-8897-41
BioLegend	Skin/mucosa-homing receptor	CLA	HECA-452	APC	130-098-573
BioLegend	Ig superfamily of receptors	β 7-Integrin	FIB-27	PerCP/Cy-5.5	121008
BioLegend	Pro-inflammatory cytokine	IFN- γ	4S.B3	APC	502512
eBioscience	Pro-inflammatory cytokine	TNF- α	MAb11	PerCP/Cy-5.5	45-7349-41
BioLegend	Pro-inflammatory cytokine	IL-17	BL168	PerCP/Cy-5.5	512314
eBioscience	Cytotoxic protein	Perforin	dG9	APC	17-9994-41
BioLegend	Isotype Control	Mouse IgG1, κ Isotype	MOPC-21	APC	400119
BioLegend	Isotype Control	Mouse IgG1, κ Isotype	MOPC-21	PerCPCy5.5	400149
Miltenyi	TCR $\gamma\delta$	Anti-TCR $\gamma\delta$ -Biotin,	11F2	Biotin	130-050-701
Miltenyi	Biotin	Biotin	NA	Biotin	120-000-900

Table 2.1 Table of antibodies used in thesis.

Antibody type, clone, fluorophore and supplier details are shown for each antibody. Antibodies used were all anti-human and were used as indicated in manufacturer's guidelines. Fluorophores are as follows; APC is Allophycocyanin, APC-Cy7 is allophycocyanin+cyanine dye Cy7, FITC is Fluorescein isothiocyanate, PE is Phycoerythrin, PECy7 is Phycoerythrin and Cyanine dye (Cy7), PerCP is Peridinin Chlorophyll protein, PerCPCy5,5 is Peridinin Chlorophyll protein and Cyanine dye 5.5 and V500 is Violet excitable dye 500.

A

Fluorophore	FITC	FITC	APC	APC	APC	Pacific Blue	APCCy7	PECy7	PE	PerCpCy5.5	V500	PerCpCy5.5	PerCpCy5.5	PE	PerCP-eFluor 710
Conjugated marker	Vδ2	Vδ1	CD3	IFN-γ	Perforin	CD27	CD45RA	CD28	CD11a	CD56	CD16	IL-17A	TNF-α	Granzyme B	Granzyme K
Vδ2 Standard panel	✓		✓			✓	✓	✓	✓	✓	✓				
Vδ1 Standard panel		✓	✓			✓	✓	✓	✓	✓	✓				
Vδ2 IC panel 1	✓			✓		✓	✓	✓	✓		✓	✓			
Vδ2 IC panel 2	✓				✓	✓	✓	✓	✓		✓		✓		
Vδ2 IC panel 3	✓		✓			✓		✓			✓			✓	✓

B

Fluorophore	FITC	FITC	APC	APC	APC	PE	PerCpCy5.5	APC	Pacific Blue	APCCy7	PECy7	PE	PerCpCy5.5	PerCpCy5.5	PerCpCy5.5	V500
Conjugated marker	Vδ2	Vδ1	CCR9	CCR7	CXCR5	CX3CR1	CCR6	CD3	CD27	CD45RA	CD28	CD11a	CCR2	CD62L	CCR5	CD16
Vδ2 Chemokine panel 1	✓			✓					✓	✓	✓	✓		✓		✓
Vδ2 Chemokine panel 2	✓				✓				✓	✓	✓	✓			✓	✓
Vδ2 Chemokine panel 3	✓		✓						✓	✓	✓	✓	✓			✓
Vδ2 Chemokine panel 4	✓					✓	✓	✓	✓		✓					✓
Vδ1 Chemokine panel 1		✓		✓					✓	✓	✓	✓		✓		✓
Vδ1 Chemokine panel 2		✓			✓				✓	✓	✓	✓			✓	✓
Vδ1 Chemokine panel 3		✓	✓						✓	✓	✓	✓	✓			✓

Table 2.2 Antibody panels used in thesis.

Table A and B show the combinations of directly conjugated markers used in flow cytometry staining of Vδ1 and Vδ2 T cells. Table A shows the standard extracellular and intracellular panels used with chemokine panels shown in B. Full fluorophore descriptions are as follows; Fluorophores are as follows; APC is Allophycocyanin, APC-Cy7 is allophycocyanin+cyanine dye(Cy7) , FITC is Fluorescein isothiocyanate, PE is Phycoerythrin, PECy7 is Phycoerythrin + Cyanine dye (Cy7), PerCPCy5,5 is Peridinin Chlorophyll protein+Cyanine dye(5.5) and V500 is Violet excitable dye 500, PerCP-eFluor 710 is Peridinin Chlorophyll protein + eFluor® 710.

2.5.3 Intracellular staining

Cell stimulation, surface staining, permeabilisation and intracellular staining were carried using protocols currently in use in the Blizzard Institute and recommended by manufacturers of the reagents (BioLegend, UK) and eBioscience, Hatfield, UK).

PBMCs (5×10^6 cells) were re-suspended in 1ml of complete media stimulated with PMA (50ng/ml) and Ionomycin (1 μ g/ml) in a 5ml polystyrene Falcon Tube (Becton Dickinson - BD) for 4 hours in an incubator (37°C and 5% CO₂). Cells were vortexed every 30 minutes throughout this 4-hour period to prevent settling of cells. After 2 hours incubation, 10 μ g/ml Brefeldin A (eBioscience) and 2 μ m Monensin (GolgiStop: Becton Dickinson) were added to the mixture and left for a further 2 hours. Cell were then washed in 2ml FACS buffer containing 3 μ g/ml **B**refeldin A (eBioscience) and 2 μ M **M**onensin (eBioscience) (**FBM**). Extracellular staining was then carried out at 4°C (on ice) for 30 minutes in FBM as per protocol outlined in section 2.3.3. Following extracellular staining, cells were again washed in FBM and centrifugation at 400xg. Following removal of supernatant, the pellet was vortexed to dissociate the pellet and then fixed for 20 minutes in the dark with 250 μ l of Fixation-Permeabilisation solution containing 4% Paraformaldehyde (BD). Vortexing was carried out throughout the addition of the fixating solution to avoid clumping. Cells were then washed twice in 250 μ l Wash/Perm Buffer™ (BD). The fixed and permeabilised cells were then resuspended in 100 μ l of Perm/Wash™ (BD) containing intracellular fluorochrome-cojugated anti-cytokine antibody (IFN- γ , IL-17A, TNF- α and Perforin) as well as appropriate isotype controls. Antibodies were incubated on ice (4°C) for 30 minutes in the dark. Cells were finally washed again in 500 μ l

Wash/Perm Buffer™ (BD) and pelleted before finally being resuspended in FACS buffer and analysed on a BD FACSCanto™ II.

2.6 Flow Cytometry: Machine set up and calibration

Analysis of the staining of cell surface markers and intracellular molecules was carried out using the BD FACSCanto™ II flow cytometer. Measurement parameters and spectral overlap between adjacent fluorophores were set up using single stained compensation beads as recommended by the manufacturer (BD™ CompBeads Anti-Mouse Ig,κ microparticles and BD™Comp Beads Negative control) for each antibody used in the experiments. PBMCs from each sample were used to set appropriate voltages for forward scatter (FSC) and side scatter (SSC) to determine the gating of the lymphocyte population according to size and granularity. Compensation was performed prior to running the samples by use of the automated compensation matrix on the BD FACS Diva software and checked and corrected manually as necessary.

2.6.1 Cell sorting

Cell sorting was carried out on the BD FACSAria™ II (Becton Dickinson – BD). The machine was set up as described for the BD FACSCanto™ II and cell populations sorted into 12 x 75mm falcon polypropylene collection tubes containing 1ml of RPMI 1640 (Invitrogen, Life Technologies) culture media and 20% FBS (Life Technologies) were used to collect the sorted cell populations. Media containing Fetal Bovine Serum (FBS) was used to increase overall cell viability of sorted cells.

2.6.2 Conventional Flow Cytometry analysis

FlowJo (Version 8.8.7)(Tree Star) software was used to analyse all flow cytometry data with conventional 2-dimensional plots. Pre-compensated .fcs data files were imported into the FlowJo programme from the flow cytometer BD FACSCanto™ II.

2.6.3 Gating Strategy

Lymphocytes were first gated based on FSC-A/SSC-A plots by size (FSC-A) size and granularity (SSC-A). Doublet discrimination was carried out to ensure only analysis of single cells was carried out by gating out doublets on Forward Scatter-Height vs. Area as well as Side Scatter-Height vs. Area plots i.e. (FSC-H v FSC-A) and (SSC-H v SSC-A). Subsequently CD3 v V δ 2 plots were generated to allow gating of V δ 2⁽⁺⁾CD3⁽⁺⁾ cells as well as V δ 2⁽⁻⁾CD3⁽⁺⁾ and TCR $\gamma\delta$ ⁽⁻⁾CD3⁽⁻⁾ populations. Following this, a range of extracellular and chemokine markers were assessed on V δ 2⁽⁺⁾CD3⁽⁺⁾ T cells. Where appropriate, relevant isotype controls, fluorescence minus one (FMO) controls or reference population controls were used to determine gating of populations.

2.6.4 Gating strategy applied for cell sort

In order to sort the four populations, lymphocytes were first identified and gated based on size (FSC-A) and granularity (SSC-A) as previously described. Following elimination of doublet cells (doublet discrimination), V δ 2⁽⁺⁾CD3⁽⁺⁾ T cells were identified and subsequently gated using CD27 and CD28 extracellular markers. CD27⁽⁻⁾CD28⁽⁻⁾ cells were then further divided into CD16⁽⁺⁾ and CD16⁽⁻⁾ populations. The four cell subsets were sorted at > 90% purity.

2.6.5 Analysis of differentiation pathways using Probability State Modelling (PSM) (GemStone™software)

Probability state modelling (PSM) using GemStone™ software was applied to V γ 9V δ 2 T cells using a range of different extracellular markers in an attempt to model the differentiation pathway and identify the major population subsets. PSM was used as an unbiased system of displaying correlated multi-colour flow cytometric markers and modelling the cell differentiation pathway. This modelling system (PSM) was used alongside conventional 2-dimensional analysis plots as it removed subjective user-defined gating to identify key cell subsets and their likely differentiation pathway. PSM was used to integrate extracellular marker parameters on a common “progression” axis (i.e. a single plot) and the strength of the model was determined by use of a goodness of fit reduced chi-square (RCS) test. The GemStone™ programme allowed visualisation assessing the relationship and transition of markers.

Cell differentiation was modelled using a set of known rules/assumptions about directional change in marker expression as cells differentiate from a presumed early “naïve” phenotype along a pathway to a final terminally differentiated population. PSM involved generating and integrating single parameter progression plots also known as Q functions and modelling these correlated measurements along a cumulative probability axis. The cumulative probability (x-axis) was used as a surrogate measure of time/differentiation and a proposed cellular differentiation pathway generated from combined single progression plots.

2.7 Microarray of V γ 9V δ 2 T cell subsets

2.7.1 Enrichment of V γ 9V δ 2 T cells

- **Preparation of PBMCs**

V γ 9V δ 2 T cells were enriched by magnetic bead column separation (Miltenyi Biotec, Germany) in order to facilitate more time efficient cell sorting. PBMCs were extracted from peripheral venous blood and counted to determine cell number and viability using trypan blue exclusion as described (section 2.4.6). Baseline phenotyping of whole PBMCs was carried out using the standard V δ 2 panel (Table 2.2) of extracellular markers so that subsequent magnetic enrichment efficiency could be established.

A biotin conjugated TCR $\gamma\delta$ antibody (Miltenyi) was then added to the PBMCs at 10 μ l/10x10⁶ cells in 100 μ l of MACs buffer (Miltenyi) at 4°C for 10 minutes in the dark. Frequent vortexing of cells was carried out to ensure maximal antibody binding. Following cell washing in MACS buffer (Miltenyi) and pelleting at 300xg for 5 minutes, anti-biotin microbeads (Miltenyi) were added at (20 μ l/10x10⁶ cells) for a further 15 minutes at 4°C. The cells were then washed and pelleted (300xg/5 minutes) before resuspension of up to 10x10⁶ cells in 500 μ l of MACS buffer (Miltenyi).

2.7.2 Magnetic column cell separation

A cell separation column (LS Column – MACS Miltenyi Biotec) was placed in a VarioMACS™ Separator (MACS Miltenyi Biotec) to create a high-gradient magnetic field within the separation column. The column was first prepared by pre-rinsing with 3ml of MACS buffer (Miltenyi) before transferring the previously prepared cell suspension to the LS column.

The unlabelled flow through containing the non- $\gamma\delta$ T cell component was collected in a falcon collection tube. Three further washes were carried out with the column within the magnetic field by adding 1ml of MACS buffer through the column to ensure all non- $\gamma\delta$ T cells were washed through and to increase the purity of the enrichment process. The unlabelled fraction containing non- $\gamma\delta$ T cells was discarded and the column subsequently removed from the magnetic field and placed on a fresh falcon collection tube.

The positively selected $\gamma\delta$ T cell fraction retained within the column was then flushed into the new collection tube by plunging 5mls of MACS buffer through the column outside the magnetic field. Cells were then pelleted by centrifugation at 300xg for 5 minutes. The supernatant was discarded and FACS buffer added to concentrate cells at approximately 50×10^6 /ml in preparation for cell sorting.

2.7.3 Extracellular staining

The enriched $\gamma\delta$ T cell fraction was stained with the following antibody cocktail in preparation for cell sorting (see antibody Table 2.1) for details of directly conjugated antibodies.

- CD3 - APC
- V δ 2 - FITC
- CD27 - Pacific Blue
- CD28 - PeCy7
- CD16 - V500
- CD56 - PerCPCy5.5
- CD45RA - APCCy7

Enriched $\gamma\delta$ T cells were stained for 30 minutes as described previously. Following staining, the cells were washed and the cells were resuspended in FACS buffer to a final concentration of approximately 50×10^6 /ml in preparation for cell sorting. Enriched and stained $\gamma\delta$ T cells were kept on ice on transfer to the cell sorter.

2.7.4 Cell sorting of V γ 9V δ 2 T cells

Enriched $\gamma\delta$ T cells were sorted using the BD FACSAria™ II cell sorter (Becton Dickinson) in order to collect the following four V γ 9V δ 2 T population subsets:

- Subset 1. $\gamma\delta^{(28+)} [CD28^{(+)}CD27^{(+)}$
- Subset 2. $\gamma\delta^{(28-)} [CD28^{(-)}CD27^{(+)}$
- Subset 3. $\gamma\delta^{(16-)} [CD28^{(-)}CD27^{(-)}CD16^{(-)}$
- Subset 4. $\gamma\delta^{(16+)} [CD28^{(-)}CD27^{(-)}CD16^{(+)}$

The enriched $\gamma\delta$ T cell fraction was first vortexed to re-suspend the settled cells and then loaded onto the sorter by inserting the falcon tube into the tube holder. Four 12 x 75 mm falcon polypropylene collection tubes containing 1ml of RPMI 1640 culture media and 20% FBS (Life Technologies) were used to collect the sorted cell populations. Media containing FBS was used to increase overall cell viability of sorted cells.

2.7.5 RNA stabilisation post-sorting

Following sorting, cells were first re-suspended in their polypropylene collection tubes and transferred to polystyrene tubes in order to pellet cells by centrifugation at 300xg/5 minutes. Finally, 300 μ l of RNeasy Protect (Qiagen, UK)

was added to pelleted cells in 1ml RNase free Eppendorf tubes in order to stabilise RNA prior to storage at -80°C.

2.7.6 RNA extraction

The RNA was then extracted according to recommended protocols using the RNeasy Micro Kit (Qiagen) which are briefly outlined. Stored frozen sorted populations were thawed and centrifuged at 5000xg for 5 minutes. After careful removal of the supernatant, the pellets were loosened, by flicking the 1ml eppendorff tubes and 350µl of lysis Buffer RLT containing 1% β-mercaptoethanol (β-ME) was added to each sample. β-mercaptoethanol was added to reduce and prevent RNA degradation during the process).

Briefly, the pellet was rigorously resuspended by vortexing for one minute to facilitate homogenization of the sample. Following this, 350µl of 70% ethanol was added to the homogenized sample and mixed well by pipetting. Each sample was then transferred to an RNeasy MinElute spin column and centrifuged for 15 seconds at 8000xg. The flow through was discarded. 350µl of Buffer RW1 was then added to the RNeasy MinElute spin column and again centrifuged for 15 seconds at 8000xg to wash the spin column membrane. The flow-through was again discarded. Next, 10µl of DNase I stock solution was added to 70µl of incubation mix and mixed by gentle inversion. This mixture was added directly onto the RNeasy MinElute spin column membrane and left for 15 minutes at room temperature (20 degrees). Once again the spin column was washed by adding 350µl of Buffer RW1 and again centrifuged for 15 seconds at 8000xg. The flow through was once again discarded. The RNeasy Min Elute spin column was then placed on a new collection tube and 500µl of

ethanol diluted Buffer RPE was added to the spin column. This was centrifuged at 8000xg for 15s to wash the spin column. 500µl of 80% ethanol was added to the column and centrifuged for 2 minutes and the supernatant discarded. The column was then transferred to a new collection tube and centrifuged at full speed with cap off to evaporate the column. Finally, 14µl of RNase-free water was added to the centre of the spin column and placed over a fresh collection tube. After centrifugation for one minute the RNA was eluted in the collection tube and the RNA samples were stored at -80°C until quality and quantity assessments of the samples were made. RNA samples were then transferred on ice to the genome centre for microarray analysis. The final stages of the microarray process of cell subsets is outlined in 2.7.8-2.7.11 and was carried out by staff at the Genome Centre core facility in Charterhouse Square, London (QMUL).

2.7.7 RNA Concentration and RNA Integrity Quality Control

The *NanoDrop* TM8000 Spectrophotometer was used to measure the absorbance of the sample to determine the following ratios:

- 260nm/280nm (measure of the purity of RNA).
- 260nm/230nm (secondary measure of RNA purity and is usually in the range of 2.0-2.2).

2.7.8 RNA Integrity Number (RIN) Scores

The quality of the RNA was further monitored using the RIN score, an objective measurement obtained to assess RNA quality and is independent of the actual quantity of RNA in the sample. RIN scores were determined using a bioanalyser (Agilent) and scored (1-10). All RIN scores were >7 and

determined to be of good quality/integrity. Briefly the RNA sample was deposited into an RNA Nano LabChip before inserting the chip into the Bioanalyser (Agilent). The bioanalyser then created an electrophoretic trace of the sample, which is converted to a numeric score based on RNA quality.

2.7.9 Ambion Total Prep Kit

The Ambion WT expression kit® (Life Technologies) was used to generate cRNA from a starting RNA sample. The technique involved firstly the production and purification of cDNA from RNA by reverse transcription. This was then followed by *in vitro* transcription to generate multiple copies of cRNA from cDNA ready for array hybridisation.

2.7.10 Production and purification of cDNA from RNA

RNA samples were made up to 11µl with RNase free water and 9µl of Reverse Transcription Master Mix was added and incubated at 42°C for 3 hours. Following this the second complimentary strand of cDNA was generated by adding 80µl of Second Strand Master mix and incubated for a further 2 hours at 16°C. The cDNA was then purified by adding cDNA binding buffer and then running the mixture through a cDNA filter cartridge. The cartridge was washed to remove primers, RNA, enzymes and salts within each sample to prevent interference in the later process of *in vitro* transcription. The cDNA was finally obtained in 20µL Nuclease-free Water at 55°C.

2.7.11 Transcription of purified cRNA from purified cDNA

Firstly, 7.5µl of *In Vitro* Transcription reaction Master Mix (IVT Master Mix) was added to each cDNA sample and mixed at 37°C for 6 hours to construct the cRNA. 75µl of nuclease free water was then added to each sample.

Purification of the cRNA was carried out by pipetting a mixture of 350µl cRNA of binding buffer and 250µl of 100% ethanol to the initial cRNA samples. This was then filtered through a cRNA Filter cartridge and washed again with 650µl of each buffer. The final purified cRNA sample was then eluted at 55°C in 200µl of nuclease-free water.

2.7.12 Human expression array of V γ 9V δ 2 T cell subsets

The human expression array (HumanHT-12 v4 Expression BeadChip array) (Illumina) was used to carry out the gene microarray, analysing each of the four subsets in triplicate. This allowed determination of the transcriptome of over 47,000 characterised genes and splice variant probes in the analysed populations.

2.7.13 Gene Array analysis

The data from the array was exported into Genome Studio (Illumina) to allow analysis of differential gene expression between populations. In general the differential expression threshold was assessed using a fold difference of >2 and $p < 0.05$ (Bonferroni corrected). Each of the four V γ 9V δ 2 T cell subsets was compared against the others in a systematic way to highlight transcriptome differences between populations. Validation of the sorted populations analysed in the transcriptome array was confirmed by flow cytometry.

2.7.14 Statistical analysis

All graphs and statistical data were generated using GraphPad Prism and individual tests and statistics are described in individual results sections. Genome Studio (Illumina) was used to analyse differential transcriptome gene

expression. Threshold for differential gene expression was set at a fold difference of > 2 and a p-value < 0.05 (Bonferroni corrected).

2.7.15 Validation of gene array

Initial validation of the sorted populations involved comparing the level of gene expression determined by the microarray to the surface markers used to initially sort the $V\gamma 9V\delta 2$ T cell subsets (i.e. CD27, CD28 and CD16). Following this, validation of four further differentially expressed genes (CX3CR1, CCR6, Granzyme B and Granzyme K) determined by the microarray (at least 2-fold different and $p < 0.05$ between $V\gamma 9V\delta 2$ T cell subsets) was carried out by flow cytometry to confirm the differential expression at the protein level.

Chapter 3

Investigating V γ 9V δ 2 T cell heterogeneity in healthy human volunteers

Chapter 3 Investigating V γ 9V δ 2 T cell heterogeneity in healthy human volunteers

3.1 Introduction

The first results chapter describes the process of surface marker re-evaluation in the initial characterisation of V γ 9V δ 2 T cells in human healthy volunteers. The initial experiments detail some of the challenges encountered when V γ 9V δ 2 T cells were analysed using the most popular method of phenotyping with CD27 and CD45RA, as well as issues surrounding the source of blood sample used for the investigations. The process of surface marker evaluation is then described leading to a conclusion as to an improved set of surface markers that best characterise V γ 9V δ 2 T cell populations. This in turn revealed V γ 9V δ 2 T cell “person-profiles” at the level of the individual. Finally, the effect of age, gender, infection history, ethnicity, and region of birth is considered in terms of V γ 9V δ 2 T cell number and phenotype in the peripheral blood.

3.2 Leukocyte cone-derived PBMCs show wide variability in V γ 9V δ 2 T cell percentage, phenotype and expansion potential

In order to investigate a potential role for $\gamma\delta$ T cells, and in particular the V γ 9V δ 2 T cell subtype, in BRONJ, it was important to establish baseline characteristics for these cells in a number of healthy individuals. In the first instance, it was decided to characterise the percentage, phenotype and expansion potential of V γ 9V δ 2 T cells in six PBMC samples obtained from anonymised blood bank derived leukocyte cones. These were used, as they were a readily available

source of large blood volumes from healthy individuals and therefore allowed for analysis of a large number of cells.

Analysis of six healthy cone samples revealed there to be a significant variation in percentage of V γ 9V δ 2 T cells relative to the total number of CD3⁽⁺⁾ lymphocytes, ranging from 0.5% to 12.8% (Figure 3.1A). In addition, there was a wide variation in V γ 9V δ 2 T cell proliferative capacity when PBMCs were stimulated with zoledronate (1 μ M) and IL-2 (100U/ml) over seven days. Whilst certain samples showed high V γ 9V δ 2 T cell expansion relative to total CD3⁽⁺⁾ cells after 7-day culture (up to 17.7-fold), by contrast others seemed to show much lower expansion; as low as 1.4-fold (Figures 3.1B and 3.1C).

The initial CD27/CD45RA phenotypic characterisation of these cells also seemed to be challenging as the use of these particular cell surface markers did not seem to divide V γ 9V δ 2 T cells into distinct populations (Figure 3.1D). There was additionally a concern regarding the lack of information as to the identity and details of the blood donor samples. There was no information on the age of the sample, as well as no indication regarding the transport time and conditions, which could potentially be long and varied. Finally, the use of frozen aliquots of banked samples added another variable to the analysis, as it is well established that expression of surface markers can be significantly affected by freeze/thaw cycles. In summary, we concluded that the use of fresh healthy blood samples would be advantageous in all further experiments.

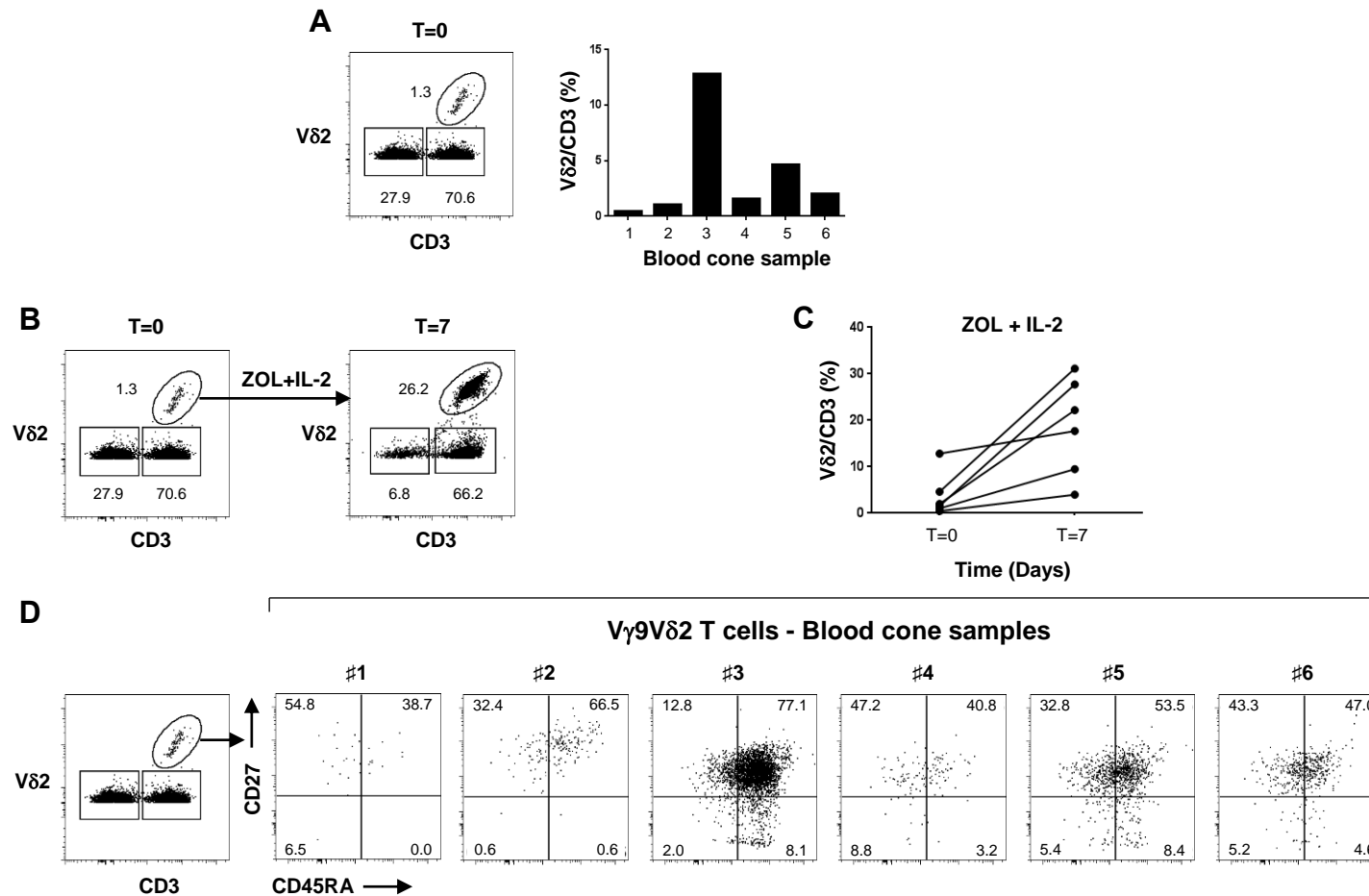


Figure 3.1 Variation in V γ 9Vδ2 T cell number, phenotype and functional potential in blood cones.

Blood cones from six anonymous human individuals show variation in; (A) Baseline Vδ2/CD3(%); (A-left panel) shows typical baseline PBMC staining with Vδ2 and CD3. (A-right panel) shows the variation in baseline Vδ2/CD3(%) for each of the six blood cone samples (1-6). (B) Example of typical flow cytometry dot plot at baseline (T=0) and at 7 days (T=7) following *in vitro* PBMC culture with zoledronate (ZOL) (1 μ M) + interleukin-2 (IL-2). (C) Variation in Vδ2/CD3(%) from (T=0) to (T=7) (relative expansion) in six different cone samples following 7-day ZOL + IL-2 culture. (D) Flow cytometry profiles (dot plots) of V γ 9Vδ2 T cells from the six cone samples stained with antibodies to the surface markers CD27 and CD45RA.

3.3 Fresh peripheral blood samples also show variability in V γ 9V δ 2 T cell percentage, phenotype and expansion potential

The analysis of fresh peripheral blood from the first six healthy volunteers also showed a great degree of variation in both the V δ 2/CD3(%) (range 1.1%-21.6%) and expansion capacity (range 2.2-60.9-fold change) following 7-day culture with zoledronate (1 μ M) and IL-2 (100U/ml) (Figure 3.2 A,B and C). In addition, a range of CD27/CD45RA phenotypes was again seen with fresh samples, including individuals with a predominantly CD27⁽⁺⁾ phenotype (mainly CD27⁽⁺⁾CD45RA⁽⁻⁾) (individual #1) to others who seemed to have a predominance of CD27⁽⁻⁾ effector populations and express a terminally differentiated effector phenotype [CD27⁽⁻⁾CD45RA⁽⁺⁾] (individuals #5 and #6) (Figure 3.2D).

These initial results from both frozen blood cone samples, and a small number of fresh blood samples suggested that a considerable amount of V γ 9V δ 2 T cell heterogeneity existed in the normal healthy population that was related to neither experimental technique nor sample processing. In addition, there was clearly a spectrum of normal healthy phenotypes in the peripheral blood that warranted further investigation and characterisation.

Having observed significant variability in these twelve initial blood samples, it was apparent that there was a need to describe this phenotypic variability in a greater number of healthy volunteers. Therefore a total of 63 fresh healthy volunteer samples were phenotyped in order to better understand this observed V γ 9V δ 2 T cell heterogeneity.

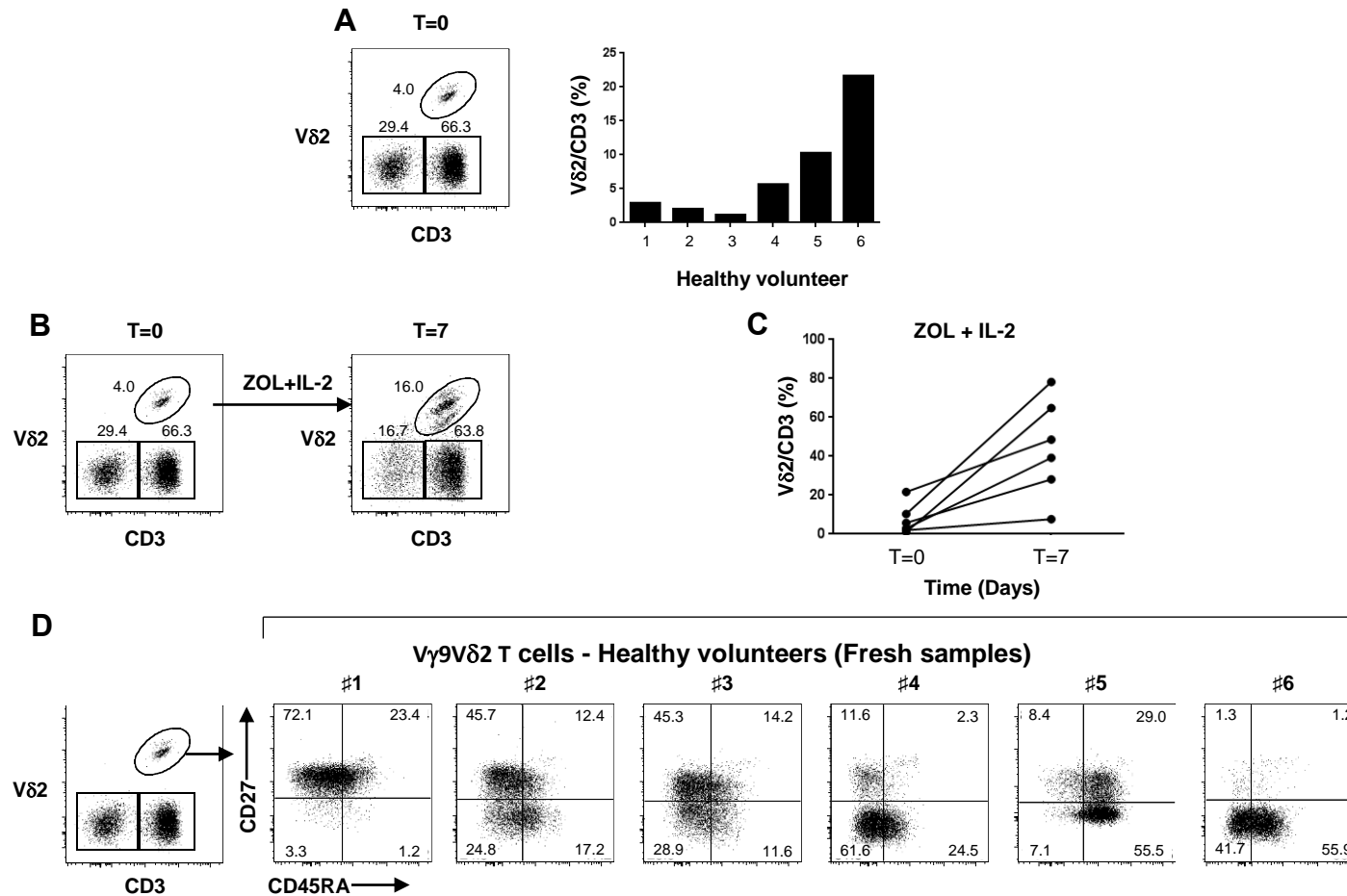


Figure 3.2 V γ 9V δ 2 T cell variability in healthy human volunteer peripheral blood samples.

Six freshly processed healthy volunteer peripheral blood samples show variation in (A) Baseline V δ 2/CD3(%); (A-left panel) shows example of typical baseline PBMC staining with V δ 2 and CD3 surface antibody markers. (A-right panel) shows variation in baseline V δ 2/CD3(%) for each of the six blood samples (1-6). (B) Example of typical flow cytometry dot plot at baseline (T=0) and at 7 days (T=7) following *in vitro* PBMC culture with zoledronate (ZOL) (1 μ M) + interleukin-2 (IL-2). (C) Variation in V δ 2/CD3(%) from (T=0) to (T=7) (relative expansion) following 7-day ZOL + IL-2 culture in six fresh healthy peripheral blood volunteer samples. (D) Flow cytometry profiles (dot plots) of V γ 9V δ 2 cells from six different individuals stained with antibodies to the surface markers CD27 and CD45RA.

3.4 CD45RA fails to define distinct phenotypic populations of $V\gamma 9V\delta 2$ T cells when used in combination with CD27

Having evaluated fresh peripheral blood samples from 63 healthy human volunteers (see later sections for details of these volunteers), it became apparent that CD45RA surface expression on $V\gamma 9V\delta 2$ T cells ranged widely (from 5.2% to 84.5%) and this was particularly obvious on $CD27^{(+)}$ cells. This consistently made the determination of $T_N [CD27^{(+)CD45RA^{(+)}]$ and $T_{CM} [CD27^{(+)CD45RA^{(-)}}]$ populations difficult (Figure 3.3). The use of CD27 and CD45RA consistently failed to divide $V\gamma 9V\delta 2$ T cells into the four conventionally-described phenotypic populations; $T_N [CD27^{(+)CD45RA^{(+)}]$, $T_{CM} [CD27^{(+)CD45RA^{(-)}}]$, $T_{EM} [CD27^{(-)CD45RA^{(-)}}]$ and $T_{EMRA} [CD27^{(-)CD45RA^{(+)}]$.

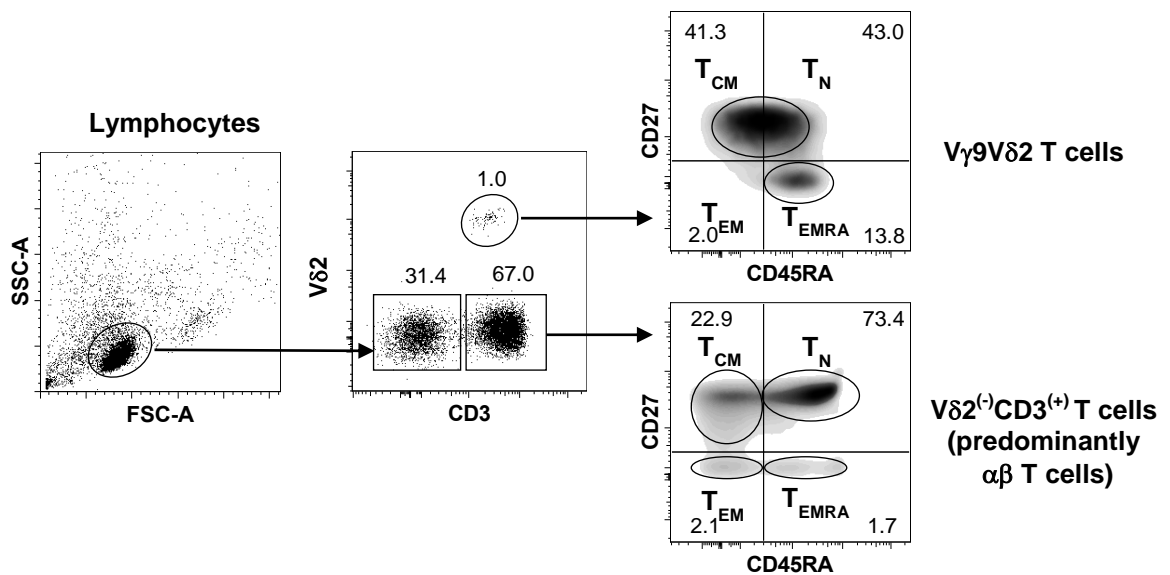


Figure 3.3 CD45RA is a poor discriminator of distinct $V\gamma 9V\delta 2$ T cell subsets.

A representative set of flow cytometry profiles (dot plots and density plots) from a single healthy individual peripheral blood sample showing gating strategy and expression of surface markers CD27 and CD45RA on $V\gamma 9V\delta 2$ T cell subsets (Top) and $V\delta 2^{(-)CD3^{(+)}}$ populations (predominantly $\alpha\beta$ T cells) (Bottom). Density plots are used to demonstrate the predominant cell populations. The percentage of cells in each quadrant/gate is indicated. $V\gamma 9V\delta 2$ T cell populations indicated are; $T_N [CD27^{(+)CD45RA^{(+)}]$, $T_{CM} [CD27^{(+)CD45RA^{(-)}}]$, $T_{EM} [CD27^{(-)CD45RA^{(-)}}]$ and $T_{EMRA} [CD27^{(-)CD45RA^{(+)}]$.

This was in direct contrast to the expression of these markers on CD3⁽⁺⁾ non-V γ 9V δ 2 T cells (most of which would be $\alpha\beta$ T cells) (Figure 3.3). The fact that both V γ 9V δ 2⁽⁺⁾ and non-V γ 9V δ 2⁽⁺⁾ T cells could be stained within the same PBMC sample indicated that the difference in CD45RA expression was a real effect and not related to differences in flow cytometry staining procedure. In moving forward, it was decided that phenotypic characterisation of V γ 9V δ 2 T cells with CD45RA was not robust, and that an alternative method of identifying these cells was required.

3.5 The use of different combinations of surface markers reveal significant confusion when phenotyping V γ 9V δ 2 T cells.

Figure 3.4 shows a single V γ 9V δ 2 T cell peripheral blood sample stained for multiple surface markers (CD27, CD45RA, CD28, CD11a, CD16, CCR7 and CD62L). This allowed us to display V γ 9V δ 2 T cells using methods described in the literature. This figure highlights the confusion that exists within the literature (Dieli *et al.* 2003b, De Rosa *et al.* 2004, Angelini *et al.* 2004, Puan *et al.* 2009, Yokobori *et al.* 2009) in both the use of different marker combinations and the nomenclature used to describe populations. For example, when defining the “naïve” population (T_N) as [CD27⁽⁺⁾CD45RA⁽⁺⁾] (Dieli *et al.* 2003b), it represented 27.3% of total V γ 9V δ 2 T cells, whilst if [CD27^(Hi) and CD11a^(Lo)] (De Rosa *et al.* 2004) was used, it was only 4.6%. Similarly, the T_{EM} was \approx 3.7% when defined as [CD27⁽⁻⁾CD45RA⁽⁻⁾] but much higher (\approx 18.7%) when [CD27⁽⁺⁾CD28⁽⁻⁾] was used (Table 3.1).

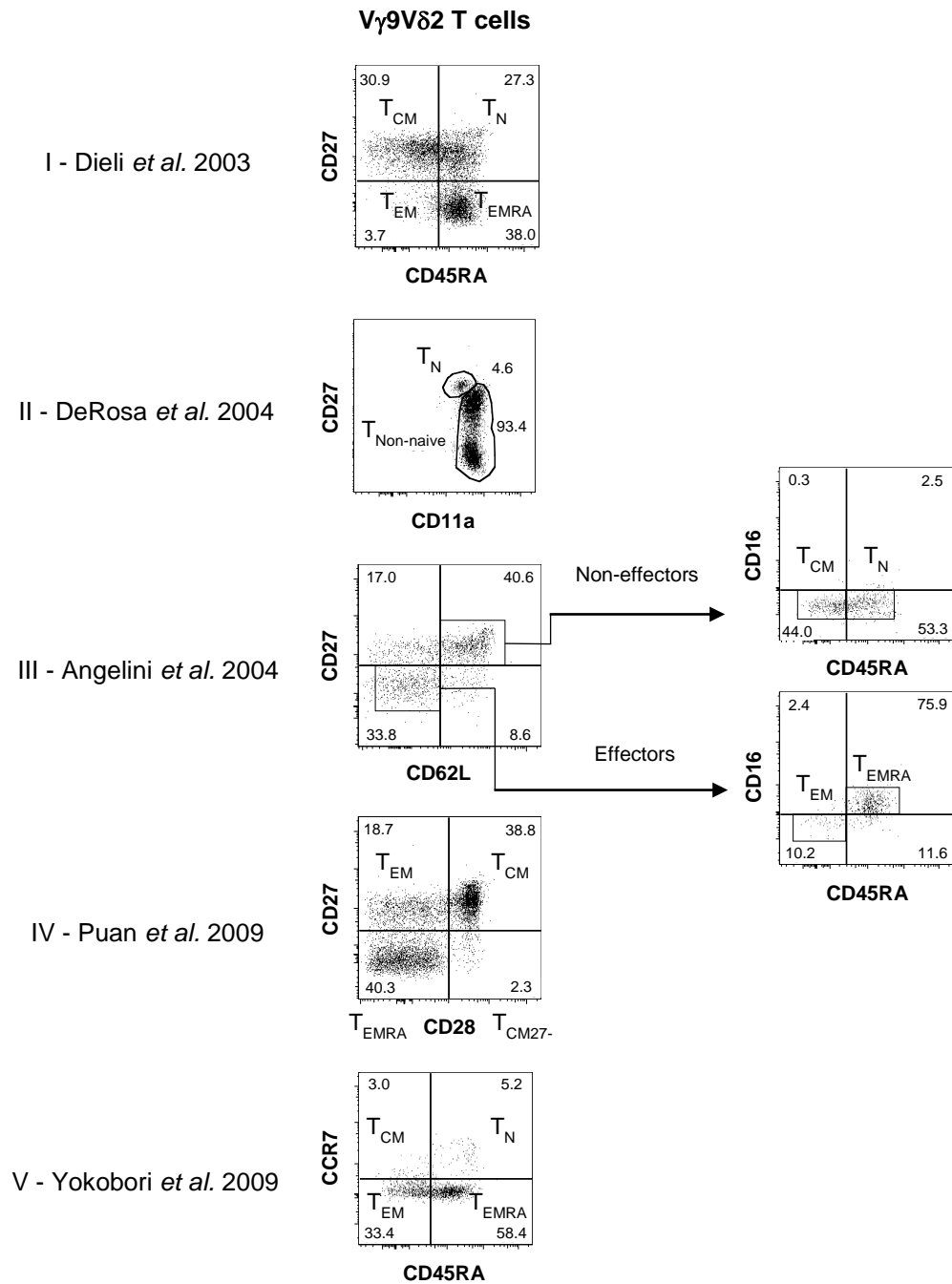


Figure 3.4 Use of different V γ 9V δ 2 T cell phenotypic strategies leads to a range of estimates for each population subset.

Flow cytometry dot plots showing differences in published V γ 9V δ 2 T cell phenotypic subsets depending on phenotyping strategy. Surface marker staining of V γ 9V δ 2 T cells from a single PBMC healthy volunteer sample is shown and is phenotyped using various extracellular marker combinations; (I) CD27 v CD45RA, (II) CD27 v CD11a, (III) CD27 v CD62L (CD16 v CD45RA) (IV) CD27 v CD28 (V) CCR7 v CD45RA. The year and lead author of each phenotypic strategy is indicated. Subsets are described as; T_N (Naive), T_{CM} (Central Memory), T_{CM27(-)} (Central Memory CD27⁽⁻⁾) T_{EM} (Effector Memory) and T_{EMRA} (Terminally differentiated Effector Memory CD45RA⁽⁺⁾). Summary table showing the percentage of different V γ 9V δ 2 T cell subsets using the various phenotypic strategies is shown in Table 3.1.

	Phenotypic description				
	T _N	T _{CM}	T _{CM} (CD27 ⁻)	T _{EM}	T _{EMRA}
Dieli (CD27 v CD45RA)	27.3	30.9	NA	3.7	38.0
DeRosa (CD27 v CD11a)	4.6	93.4			
Angelini (CD27 v CD62L CD16 v CD45RA)	21.6	17.9	NA	3.4	25.7
Puan (CD27 v CD28)	NA	38.8	2.3	18.7	40.3
Yokobori (CCR7 v CD45RA)	5.2	3.0	-	33.4	58.4

Table 3.1 Summary table of V γ 9V δ 2 T cell subset size as defined by different phenotypic strategies.

V γ 9V δ 2 T cell subset percentages from Figure 3.4 are compared. Subsets are termed; T_N (“Naïve”), T_{CM} (Central Memory), T_{CM27⁻} (Central Memory CD27⁻), T_{EM} (Effector Memory) and T_{EMRA} (Terminally differentiated Effector Memory CD45RA⁺). These results highlight the problem that exists in describing V γ 9V δ 2 T cells with different marker combinations particularly when similar terms of nomenclature are used by different groups.

These results highlight the problem that exists in describing V γ 9V δ 2 T cells with different marker combinations particularly when similar terms of nomenclature are used by different groups, using different combinations of surface markers.

3.6 V γ 9V δ 2 T cells showed no significant variation with respect to age, gender, ethnicity, or place of birth.

Having characterised 63 healthy individuals using conventional methods, it was apparent that there was no obvious gender differences in V γ 9V δ 2 T cell percentage within the lymphocyte population with a median V δ 2/CD3(%) of 2.1% in 31 males (range 0.4-21.4%) and 2.2% in 32 females (range 0.3-21.9%) (Figure 3.5). In addition, although there did not seem to be any statistically significant differences due to ageing ($p = 0.06$), the overall trend showed a slow downward decline in V γ 9V δ 2 T cell percentage with age, which approached significance when the youngest and oldest groupings were compared ($p = 0.07$) (Figure 3.5B).

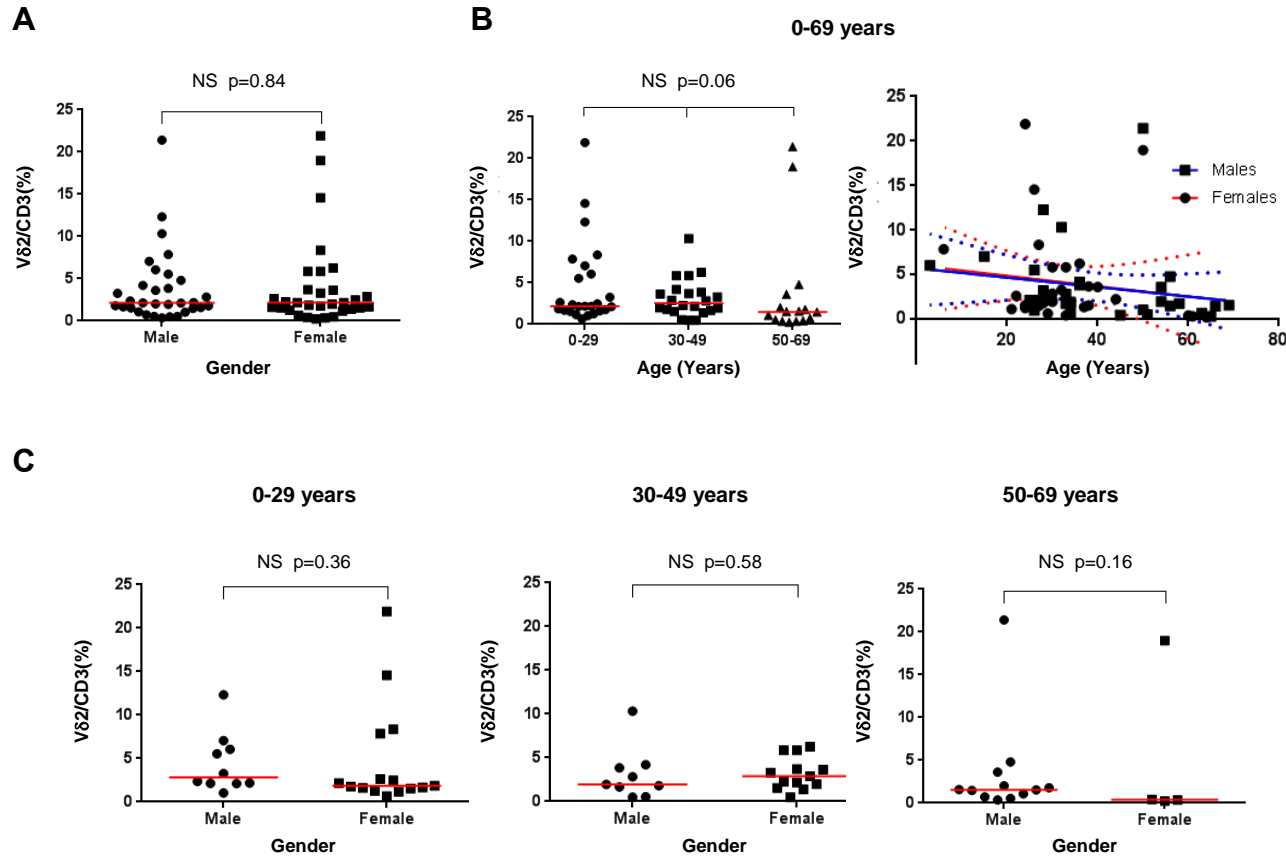


Figure 3.5 Effect of age and gender on V δ 2/CD3(%) in peripheral blood.

Peripheral V γ 9V δ 2 T cells are expressed as a percentage of total CD3⁽⁺⁾ lymphocytes comparing; (A) Males (M) vs. Females (F) (M=31, F=32, N=63) with age range 3-69 years. (B) Peripheral V δ 2/CD3(%) in all healthy individuals aged 3-69 years showing linear regression lines with 95% confidence interval bands indicated as dashed lines for males (blue) and females (red) respectively. V δ 2/CD3(%) is also shown by age sub-groups (C) 0-29 years (Male=10, Female=16), 30-49 years (Male=9, Female=12) and 50-69 years (Male=12, Female=4) comparing differences in V δ 2/CD3(%) in age groups. All data points are shown with red lines representing median V δ 2/CD3(%). Statistical differences were assessed using the Mann-Whitney U test with p-values indicated in (A and C) and Kruskal-Wallis one-way ANOVA with multiple comparison post-hoc testing (Bonferroni corrected) in B.

Although this summarises the general trend, it must be noted that two 50 year old healthy volunteers had a $V\delta 2/CD3(\%)$ of $> 20\%$ and highlighted that high percentages of $V\gamma 9V\delta 2$ T cells can be found in the peripheral blood well into adulthood.

Finally, healthy volunteers were then grouped by ethnicity, and region of birth to investigate whether these factors had any influence on $V\delta 2/CD3(\%)$. However, no significant differences were observed (Figure 3.6). Similarly, no significant differences were found if the developmental index of country of birth was considered in relation to $V\delta 2/CD3(\%)$ ($p = 0.18$).

3.7 Re-assessment of the “naïve” $V\gamma 9V\delta 2$ T cell population

In general, it was apparent that in moving away from the use of CD45RA as a marker, a “naïve” population of $V\gamma 9V\delta 2$ T cells appeared to be very small (consistently $< 5\%$) when other combinations of typical “naïve” markers were used i.e. CD11a, CCR7 and CD62L (Figure 3.7).

For example when $[CD27^{(Hi)}CD11a^{(Lo)}]$ was used to describe “naïve” cells the median percentage was 0.8% (range 0.1-14.0%). Other combinations of typical “naïve” markers including $[CCR7^{(+)} CD62L^{(+)}]$ as well as a combination of $[CD27^{(Hi)}CCR7^{(+)}CD62L^{(+)}CD11a^{(Lo)}]$ also seemed to confirm the small size of a “naïve” population, with median estimates of 1.9% and 0.6% respectively. It was therefore clear that the “naïve” population of $V\gamma 9V\delta 2$ T cells makes up a very small proportion of total $V\gamma 9V\delta 2$ T cells in the peripheral blood, when methods that do not use CD45RA are considered. A method using CD45RA gives a T_N cell estimate of 23.4% (range 1.2-52.6%).

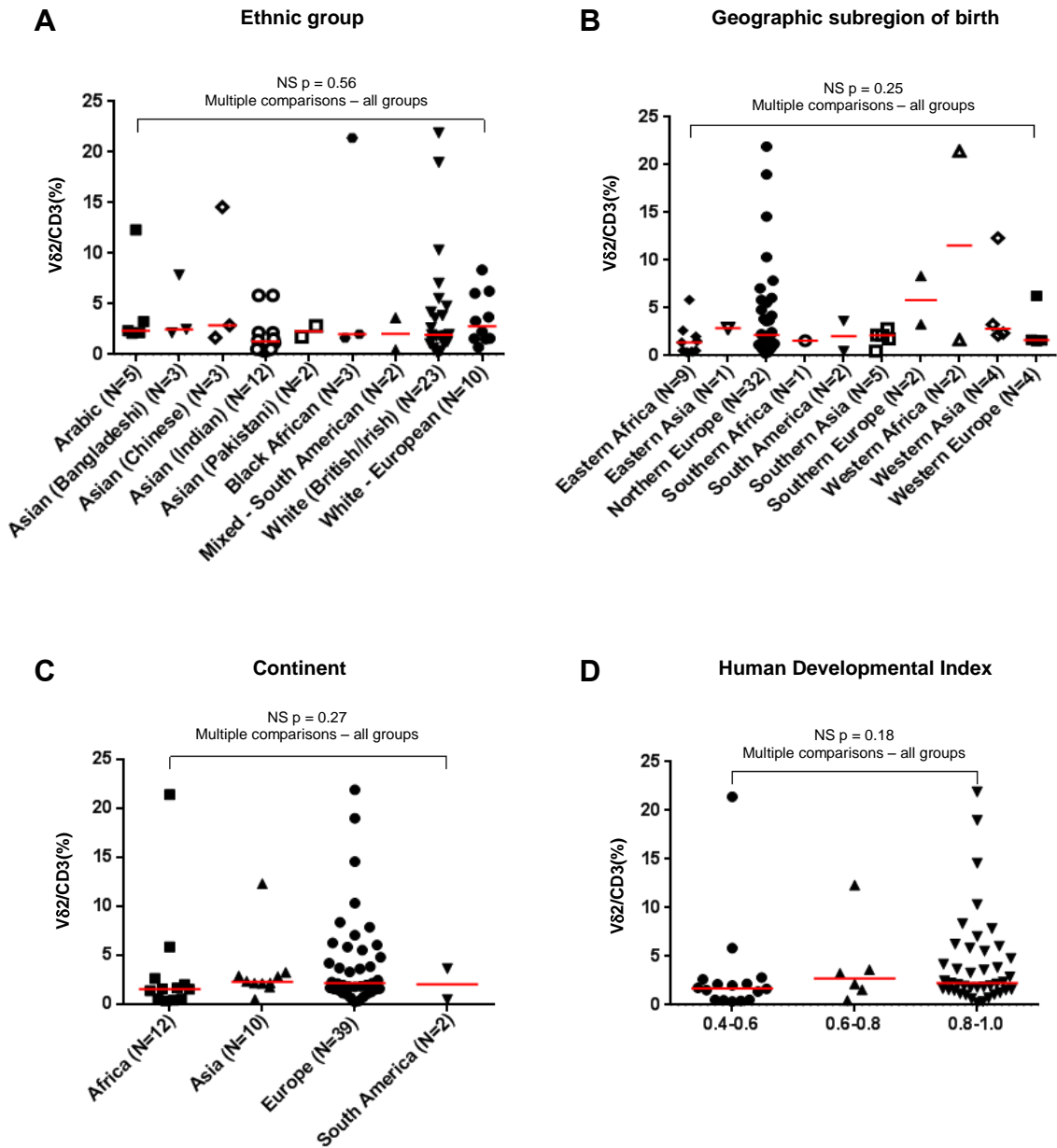


Figure 3.6 Variation in $V\delta 2/CD3(\%)$ in peripheral blood shown by ethnicity, region of birth and by country of birth development status.

$V\delta 2/CD3(\%)$ is shown in all sampled healthy individuals ($N=63$) by (A) Ethnic group (B) Geographic sub-region of birth (C) Continent of birth and (D) Human Development Index (HDI). Ethnic groupings in A are based on Office for National Statistics (ONS) ethnic groupings used for UK census data. Regions stated in B are as per scheme derived from the United Nations Statistics Division (UNSD) of sub-regions of the world. Human Development index (HDI) is a United Nations composite index of life expectancy, education and income HDI score (Low 0.4-0.6), Medium (0.6-0.8) and High (0.8-1.0). Red bars represent median $V\delta 2/CD3(\%)$ with statistical differences assessed using Kruskal-Wallis test (ANOVA) and multiple comparison post-hoc testing (A-D) with Bonferroni correction (p -values < 0.05 were considered significant).

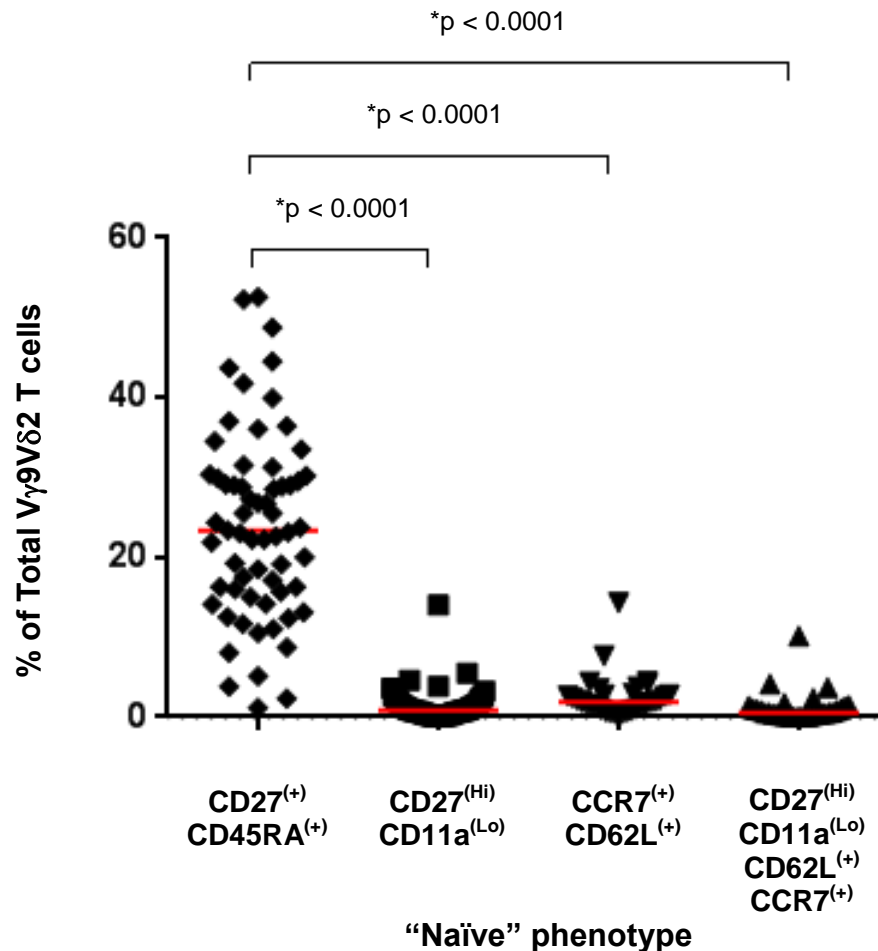


Figure 3.7 “Naïve” V γ 9V δ 2 T cell subset estimates show large variation depending on phenotyping strategy.

(A) Scatter plot showing the range of estimates of the “naïve” subset by use of four different marker combinations. CD27⁽⁺⁾CD45RA⁽⁺⁾ (N=63), CD27^(Hi)CD11a^(Lo) (N=63), CCR7⁽⁺⁾CD62L⁽⁺⁾ (N=31) and a combination of all markers CD27^(Hi)CD11a^(Lo)CD62L⁽⁺⁾CCR7⁽⁺⁾ (N=31). Red lines represent median V δ 2/CD3(%) with statistical differences assessed using Kruskal-Wallis test (ANOVA) and multiple comparison post-hoc testing with Bonferroni correction. p-values are indicated, with p < 0.05 considered significant.

3.8 CCR7 expression is dependent on clone and staining conditions.

CCR7 seemed to show a great variation in expression on V γ 9V δ 2 T cells and this appeared to depend on the clone of antibody used as well as the staining conditions. Figure 3.8 shows an example of this variation in a single healthy peripheral blood sample (CCR7 $\alpha\beta$ T cell staining shown as a positive control).

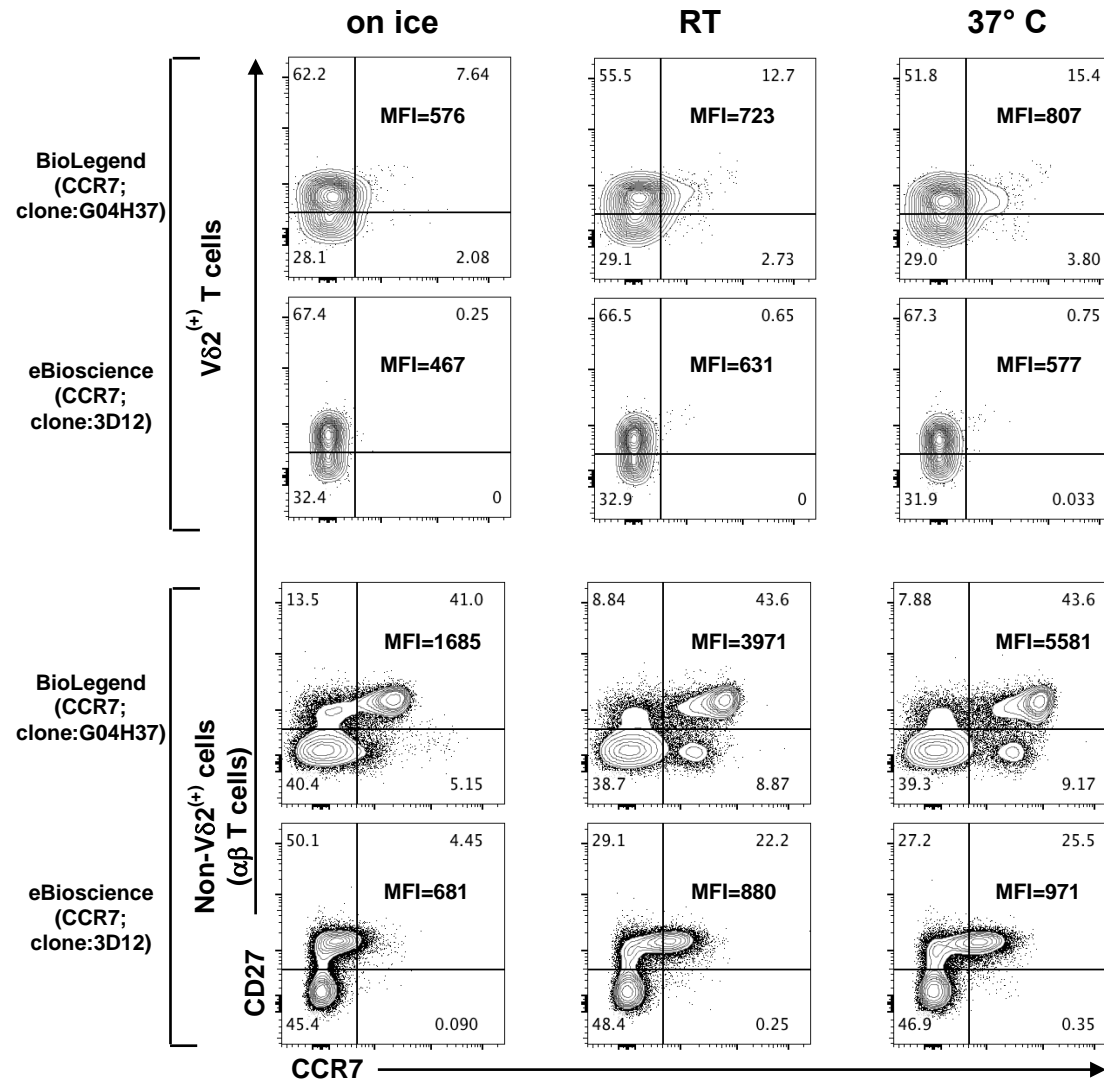


Figure 3.8 CCR7 expression on V γ 9V δ 2 and $\alpha\beta$ T cells varies depending on clone and staining conditions.

V γ 9V δ 2 and $\alpha\beta$ T cells from a single representative peripheral blood sample showing the variation in CCR7 expression depending on clone of antibody and staining conditions. Two different antibody clones (BioLegend (clone G04H37) and eBioscience (clone 3D12)) are shown under three different staining conditions; ice, room temperature (RT) and at 37°C. Flow cytometry contour plots are shown with the percentage of cells in each gate indicated. Median fluorescent intensity (MFI) of CCR7⁽⁺⁾ events is indicated for each clone under the three staining conditions.

Similarly, the median fluorescent intensity of CCR7 positive events seemed to be greater when staining at 37°C (MFI=807) compared to on ice (MFI=576). The clone of antibody used also seemed to effect the detection of CCR7 expression on V γ 9V δ 2 T cells with much higher levels found using G04H37 (BioLegend) compared to the 3D12 clone (eBioscience). As an example of this, at 37°C the percentage of CCR7⁽⁺⁾ cells was 19.2% with G04H37 (BioLegend) compared to only 0.8% with 3D12 (eBioscience). The variation of CCR7 expression on V γ 9V δ 2 T cells therefore led to concerns in the use of this marker for characterising the “naïve” cell population. In addition the reported instability of CD62L also suggested this to be an unsuitable marker for predictable characterisation (De Rosa et al. 2004). Consequently CD27 and CD11a were considered to be the most reliable markers to use in the characterising of the small “naïve” V γ 9V δ 2 T cell population.

3.9 CD27, CD28 and CD16 are more consistent markers for defining distinct V γ 9V δ 2 T cell populations

In order to establish the most appropriate markers to phenotype V γ 9V δ 2 T cells, all 63 healthy individuals were stained with a range of commonly used markers including CD27, CD45RA, CD28, CD11a, CD16 and CD56 (Dieli *et al.* 2003b, De Rosa *et al.* 2004, Angelini *et al.* 2004, Puan *et al.* 2009, Yokobori *et al.* 2009). Following extensive analysis, it was apparent that the combined use of CD27 and CD28 consistently divided non-naïve V γ 9V δ 2 T cells into three clear distinct populations; [CD28⁽⁺⁾CD27⁽⁺⁾], [CD28⁽⁻⁾CD27⁽⁺⁾] and [CD28⁽⁻⁾CD27⁽⁻⁾] (Figure 3.9 and 3.10).

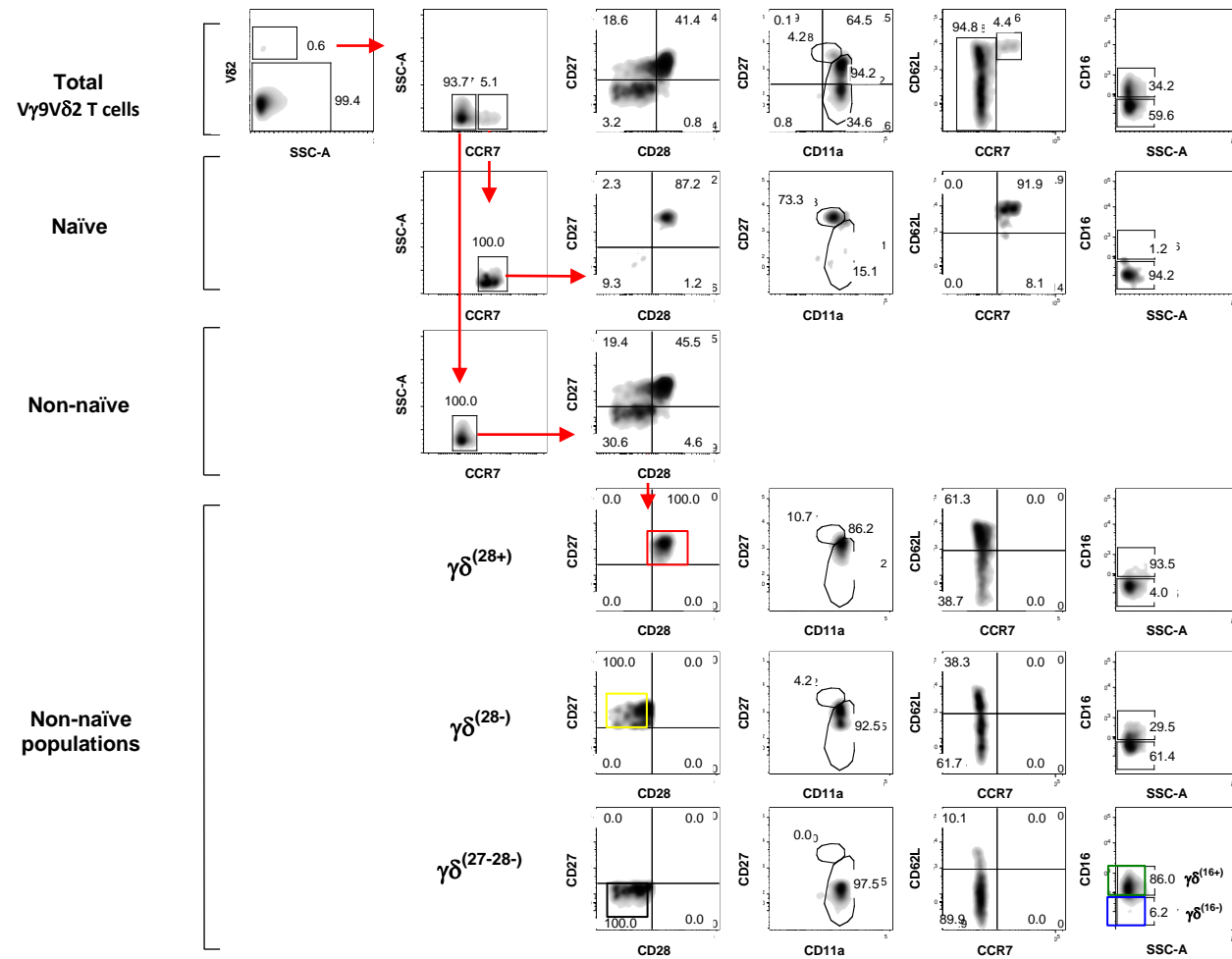


Figure 3.9 Phenotypic analysis of V γ 9V δ 2 T cells showing distinct phenotypic subsets

Flow cytometry density plots showing the predominant V γ 9V δ 2 T cell subsets in the peripheral blood of a single healthy human donor using; CD27, CD11a, CCR7, CD28, CD62L and CD16. The figure shows an individual with all the major V γ 9V δ 2 T cell phenotypic populations. Populations are initially subdivided into “Naïve” and “Non-naïve” V γ 9V δ 2 T cell populations. Naïve V γ 9V δ 2 T cells are characterised as; [CCR7⁽⁺⁾, CD27^(Hi), CD28⁽⁺⁾, CD11a^(Lo) and CD62L⁽⁺⁾]. “Non-naïve cells” are subsequently subdivided into four groups based on CD27, CD28 and CD16 expression to give four further phenotypic populations; $\gamma\delta^{(28+)}$ [CD28⁽⁺⁾CD27⁽⁺⁾] (red box), $\gamma\delta^{(28-)}$ [CD28⁽⁻⁾CD27⁽⁺⁾] (yellow box), $\gamma\delta^{(16-)}$ [CD28⁽⁻⁾CD27⁽⁻⁾CD16⁽⁻⁾] (Blue box) and $\gamma\delta^{(16+)}$ [CD28⁽⁻⁾CD27⁽⁻⁾CD16⁽⁺⁾] (green box).

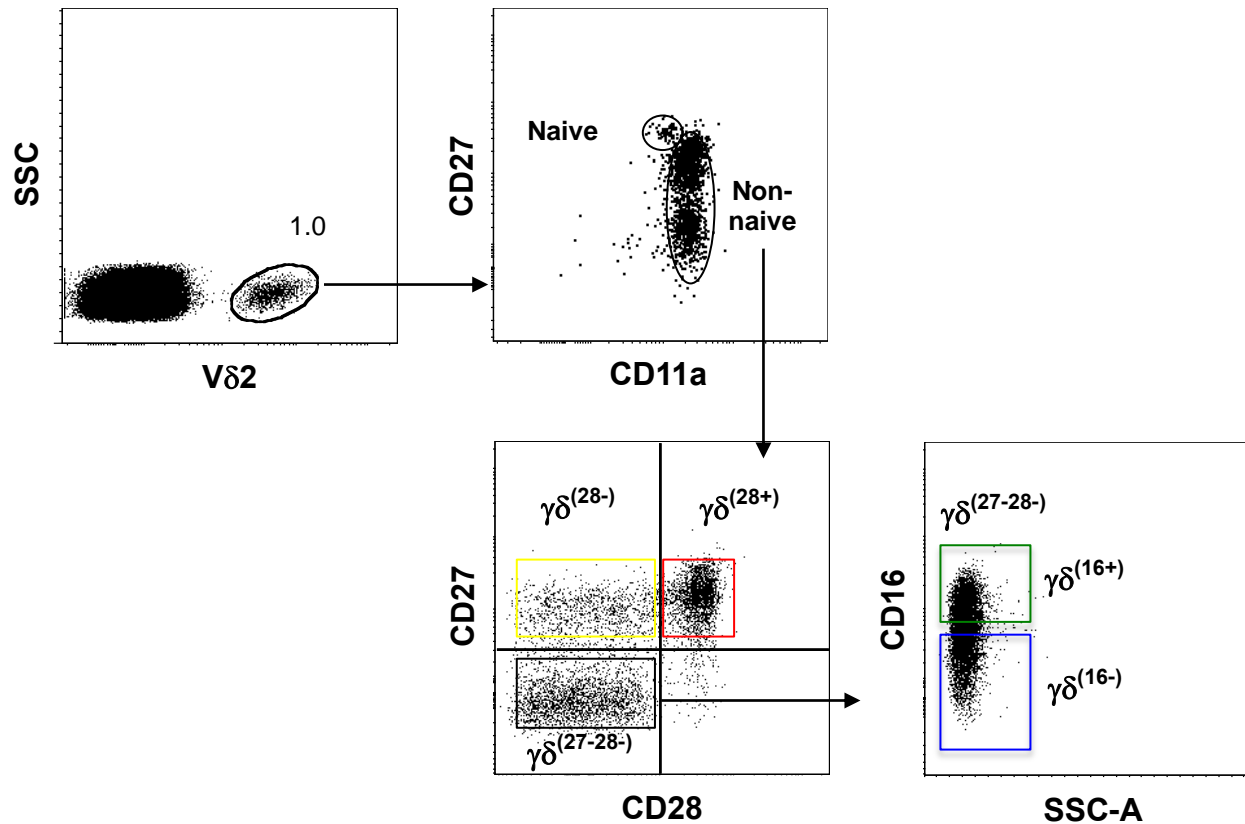


Figure 3.10 Proposed $V\gamma 9V\delta 2$ T cell phenotypic characterisation as defined by CD11a, CD28, CD27, and CD16.

Phenotypically distinct $V\gamma 9V\delta 2$ T cell subsets as identified using CD11a, CD28, CD27 and CD16. A small naïve cell subset is defined as $CD27^{(Hi)}CD11a^{(Lo)}$ with the majority of $V\gamma 9V\delta 2$ T cells being non-naïve ($CD11a^{(Hi)}$). This non-naïve subset can then be divided into four major phenotypic subsets and will be subsequently referred to as; $\gamma\delta^{(28+)} [CD28^{(+)}CD27^{(+)}]$ (red box), and $\gamma\delta^{(28-)} [CD28^{(-)}CD27^{(+)}]$ (yellow box), $\gamma\delta^{(16-)} [CD28^{(-)}CD27^{(-)}CD16^{(-)}]$ (blue box) and $\gamma\delta^{(16+)} [CD28^{(-)}CD27^{(-)}CD16^{(+)}]$ (green box).

A [CD28⁽⁺⁾CD27⁽⁻⁾] population was rarely seen, and when present seemed to form part of a “tail” from the [CD28⁽⁺⁾CD27⁽⁺⁾] population, and so was not thought to represent a significant V γ 9V δ 2 T cell population. It also appeared that V γ 9V δ 2 T cells appeared to be transitioning from the [CD28⁽⁺⁾CD27⁽⁺⁾] to the [CD28⁽⁻⁾CD27⁽⁻⁾] population via a [CD28⁽⁻⁾CD27⁽⁺⁾] intermediate.

Thus, having concluded that CD27 and CD28 were useful markers to use, it was then decided to also use CD16 as a late effector marker to further subdivide the [CD28⁽⁻⁾CD27⁽⁻⁾] population into two further sub-populations, as CD16 expression seemed to increase in expression across the [CD28⁽⁻⁾CD27⁽⁺⁾] to [CD28⁽⁻⁾CD27⁽⁻⁾] subsets (Figure 3.9).

3.10 The four non-naïve V γ 9V δ 2 subsets vary markedly in percentage between healthy individuals.

In looking at the percentage of each of our newly-defined V γ 9V δ 2 T cell subsets in healthy volunteers, it was apparent that there was huge variability in the proportions of these non-naïve subsets across the 63 individuals (Figure 3.11). The $\gamma\delta^{(28+)}$ population ranged from (0.6-89.6%) with a median percentage of 55.9%, the $\gamma\delta^{(28-)}$ population ranged from (0.5-51.1%) with a median percentage of 20.8%, the $\gamma\delta^{(16-)}$ population ranged from (0.4-44.6%) with a median percentage of 4.5% and finally the $\gamma\delta^{(16+)}$ population ranged from (0.1-88.7%) with a median percentage of 3.8%. Clearly there is not a typical “normal” healthy phenotype and individuals ranged from those with an almost complete predominance of the $\gamma\delta^{(28+)}$ subset to those with a predominance of the $\gamma\delta^{(16+)}$ population with a spectrum of profiles in between.

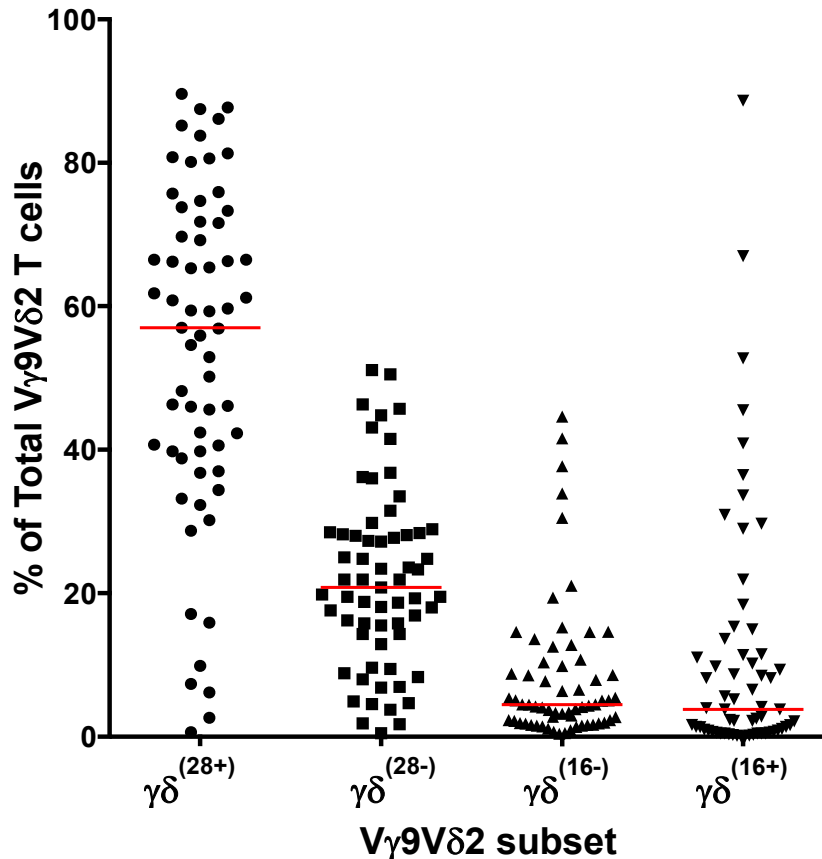


Figure 3.11 V γ 9V δ 2 T cell phenotypic subset distribution showing the four major non-naïve subsets.

Peripheral blood mononuclear cells (PBMCs) were stained with CD28, CD27 and CD16 and the relative percentage of each of the newly-defined non-naïve V γ 9V δ 2 T cell subsets determined. Individual data points for all 63 healthy volunteers are shown with median values indicated. V γ 9V δ 2 subsets; $\gamma\delta^{(28+)}$ [CD28⁽⁺⁾ CD27⁽⁺⁾], $\gamma\delta^{(28-)}$ [CD28⁽⁻⁾ CD27⁽⁺⁾], $\gamma\delta^{(16-)}$ [CD28⁽⁻⁾ CD27⁽⁻⁾ CD16⁽⁻⁾] and $\gamma\delta^{(16+)}$ [CD28⁽⁻⁾ CD27⁽⁻⁾ CD16⁽⁺⁾].

3.11 V γ 9V δ 2 T cell subset distribution does not appear to be related to age

In observing the spectrum of V γ 9V δ 2 T cell phenotypes in healthy volunteers, it might be reasonably postulated that a certain subset might accumulate in the peripheral blood as a consequence of ageing and cumulative increase in antigen and infection experience. Thus, the distribution of the main V γ 9V δ 2 T cell subsets was assessed across three different age ranges (0-29 years),

(30-49 years) and (50-69 years) to determine whether there were any significant changes due to ageing (Figure 3.12). No significant changes were observed in the $\gamma\delta^{(N)}$, $\gamma\delta^{(28+)}$, $\gamma\delta^{(16-)}$ or $\gamma\delta^{(16+)}$ subsets across the three age ranges with the only exception being decrease in the $\gamma\delta^{(28-)}$ subset between the youngest age group (0-29 years) and the oldest group (50-69 years) ($p= 0.005$). Thus, there was little evidence to support the hypothesis that a certain V γ 9V δ 2 T cell subset accumulated with increasing age.

3.12 Individual V γ 9V δ 2 T cell profiles can be clustered into six phenotypic “signature” groups

Previous literature has mainly described V γ 9V δ 2 T cells from a single “representative” individual with little consideration of how this phenotype varied between individuals. Having observed considerable variability in the expression of each our newly-defined V γ 9V δ 2 T cell subsets, it became apparent that individuals could be grouped into distinct clusters based on the relative proportions of each V γ 9V δ 2 T cell subset in their peripheral blood.

The apparent spectrum of V γ 9V δ 2 T cell “phenotypic signatures” seen across the normal healthy population ranged from those with a $\gamma\delta^{(28+)}$ biased phenotype to those with an almost exclusive $\gamma\delta^{(16+)}$ phenotype. It was therefore possible to group the 63 individuals into six “phenotypic signature” clusters, which were established based on criteria outlined in Figure 3.13 and illustrated in Figure 3.14.

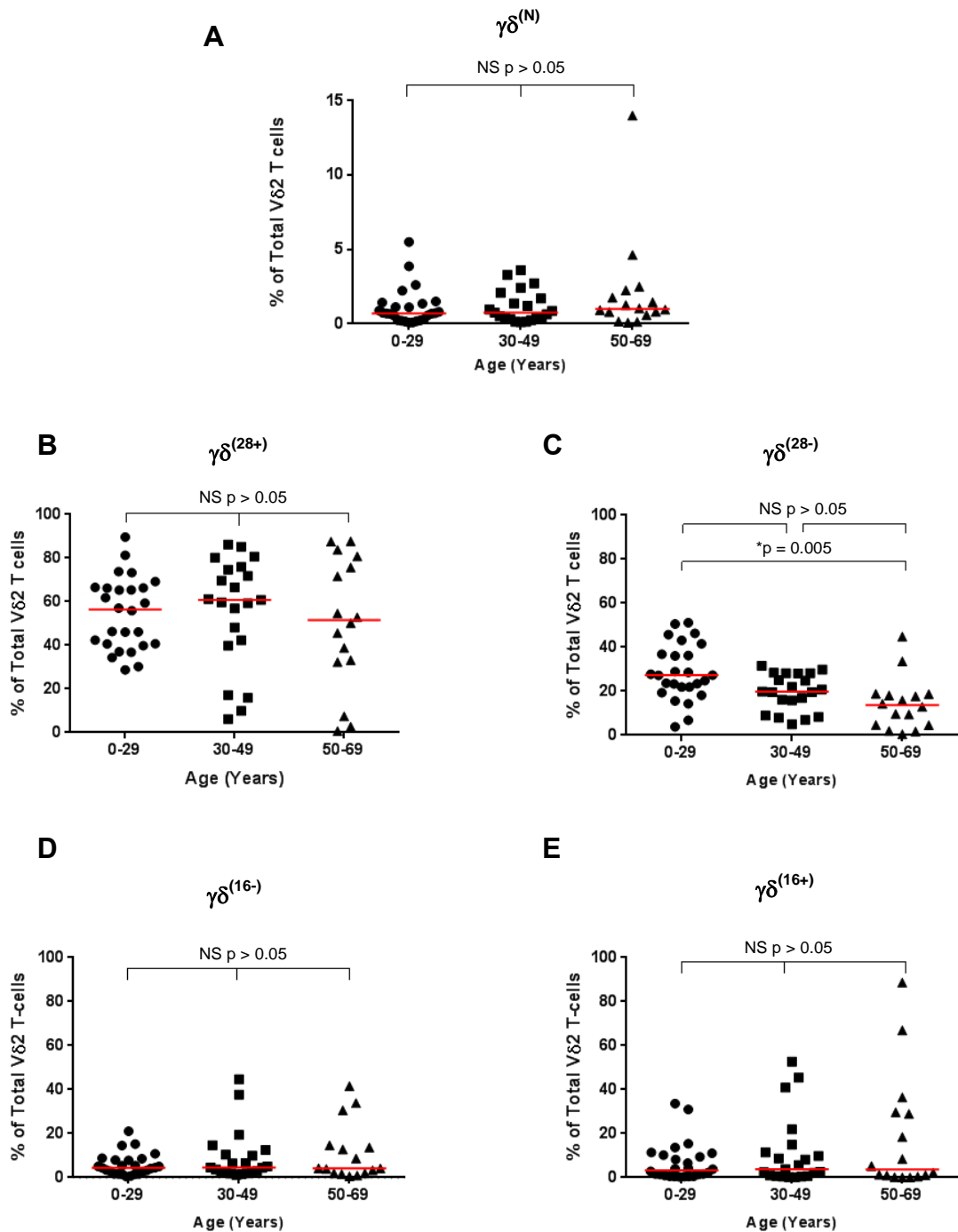


Figure 3.12 $V\gamma 9V\delta 2$ T cell subsets show little evidence of accumulating with increasing age.

Healthy volunteers were grouped into three age groups; 0-29 years (Male=10, Female=16), 30-49 years (Male=9, Female=12,) 50-69 years (Male=12, Female=4) and examined for changes in $V\gamma 9V\delta 2$ T cell subsets over time. $V\gamma 9V\delta 2$ T cell subsets are defined as (A) $\gamma\delta^{(N)}$ [$CD27^{(Hi)}CD11a^{(Lo)}$], (B) $\gamma\delta^{(28+)}$ [$CD28^{(+)}CD27^{(+)}$], (C) $\gamma\delta^{(28-)}$ [$CD28^{(-)}CD27^{(+)}$], (D) $\gamma\delta^{(16-)}$ [$CD28^{(-)}CD27^{(-)}CD16^{(-)}$] and (E) $\gamma\delta^{(16+)}$ [$CD28^{(-)}CD27^{(-)}CD16^{(+)}$]. Red bars represent median values with statistical differences assessed using Kruskal-Wallis one-way ANOVA and multiple comparison post-hoc testing Bonferroni correction. p-values < 0.05 were considered significant.

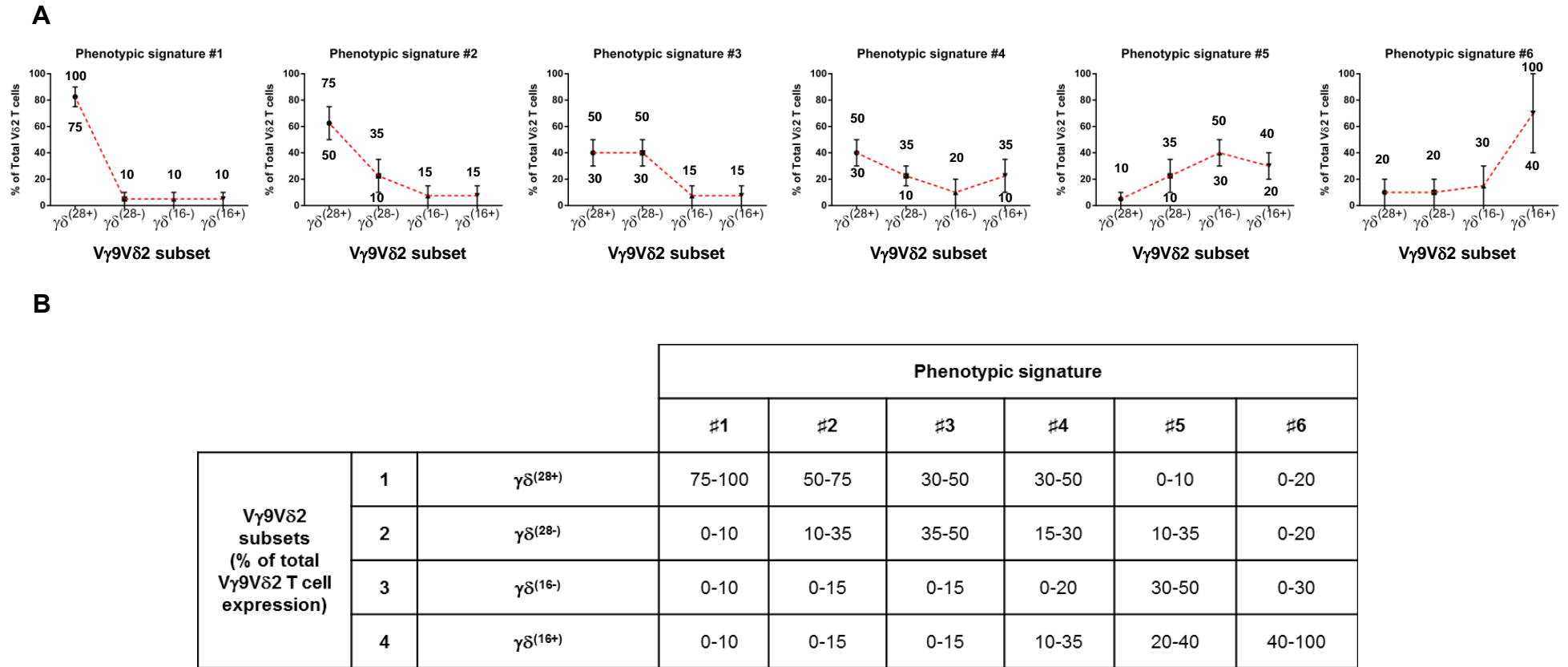


Figure 3.13 Criteria for phenotypic signature groupings of V γ 9V δ 2 T cells.

Graphs show the relative proportions of the four newly-defined V γ 9V δ 2 T cell subsets based on CD28, CD27 and CD16 expression in each of six phenotypic signature groups (#1-6). V γ 9V δ 2 T cell subsets are defined as $\gamma\delta^{(28+)}$ [CD28⁽⁺⁾CD27⁽⁺⁾], $\gamma\delta^{(28-)}$ [CD28⁽⁻⁾CD27⁽⁺⁾], $\gamma\delta^{(16-)}$ [CD28⁽⁻⁾CD27⁽⁻⁾CD16⁽⁻⁾] and $\gamma\delta^{(16+)}$ [CD28⁽⁻⁾CD27⁽⁻⁾CD16⁽⁺⁾]. Graphs show the range of each V γ 9V δ 2 T cell subsets in each signature group with the dotted red line bisecting these proposed ranges and showing a pictorial representation of each phenotypic signature (1-6). The approximate percentage of each V γ 9V δ 2 T cell subset in each phenotypic signature group is shown in the table below (B). Grouping criteria were established based on apparent clustering of similar profiles.

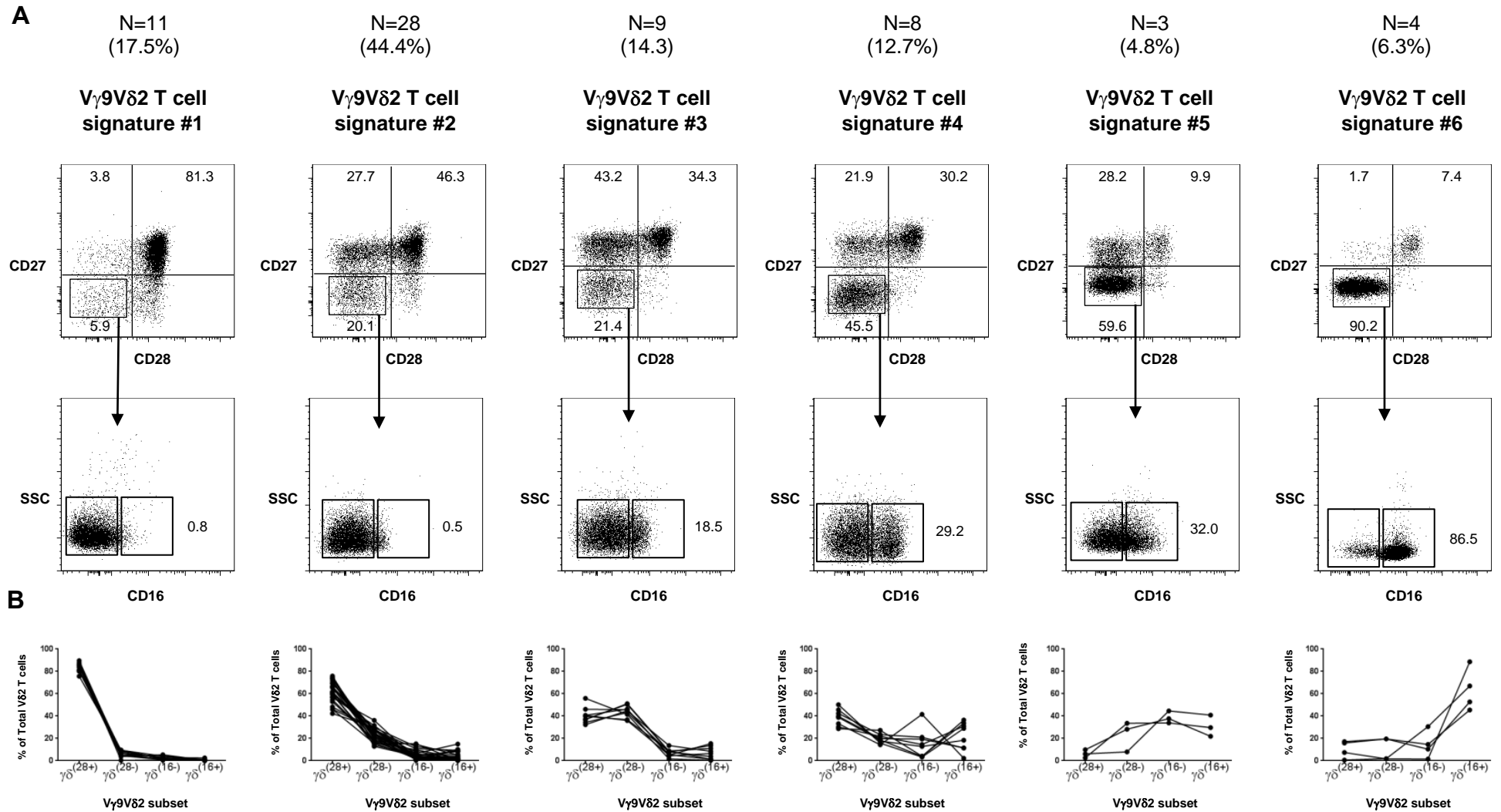


Figure 3.14 V γ 9V δ 2 T cell subsets cluster into six “phenotypic signatures”.

(A) Representative dot plots show the relative percentage of each subset based on CD28, CD27 and CD16 in each phenotypic signature (1-6). (B) Six phenotypic signatures were established based on clustering of similar phenotypic profiles and based on the relative proportions of each V γ 9V δ 2 T cell subset. Criteria for groupings are outlined in Figure 3.13.

The most commonly observed phenotypic signature in 44.4% of individuals (28/63) was signature #2, characterised by a predominance of both $\gamma\delta^{(28+)}$ and $\gamma\delta^{(28-)}$ cells (Figure 3.14/3.15A). Individuals in this profile group had 50-75% of the $\gamma\delta^{(28+)}$ subset and 10-35% in the $\gamma\delta^{(28-)}$ subset with < 20% of $\gamma\delta^{(16-)}$ and $\gamma\delta^{(16+)}$ cells. The next most commonly seen cluster was phenotypic signature #1, observed in 17.5% (11/63) of healthy volunteers and characterised by a predominance of $\gamma\delta^{(28+)}$ cells (> 75%). Signatures #3 and #4 were observed in 10-15% of the healthy volunteer group with signatures #5 and #6 being the least commonly observed at around 5% of the cohort (Figure 3.14/3.15A).

3.13 V γ 9V δ 2 T cell phenotypic “signatures” are widely spread across all age groups.

The correlation between the six newly-defined phenotypic signatures and the age of individuals in the cohort was next examined to see whether there was evidence that certain signatures were gained with increasing age. The graph in Figure 3.15B plots the six signatures against age and shows that there are no obvious correlations for age distribution and any of the signature groups ($p>0.05$). This supports the previous observation that a certain V γ 9V δ 2 T cell phenotype is not gained as individuals get older. This in turn suggests that increasing cumulative infectious exposure is also not a factor defining V γ 9V δ 2 T cell phenotype. Indeed, in looking at the signature groups (indicated in parentheses) of the five oldest volunteers aged 63-69 years (1,2,1,3,6) and the five youngest volunteers aged 3-24 years (2,2,2,2,3) there were no obvious differences between these age extremes (Figure 3.15C).

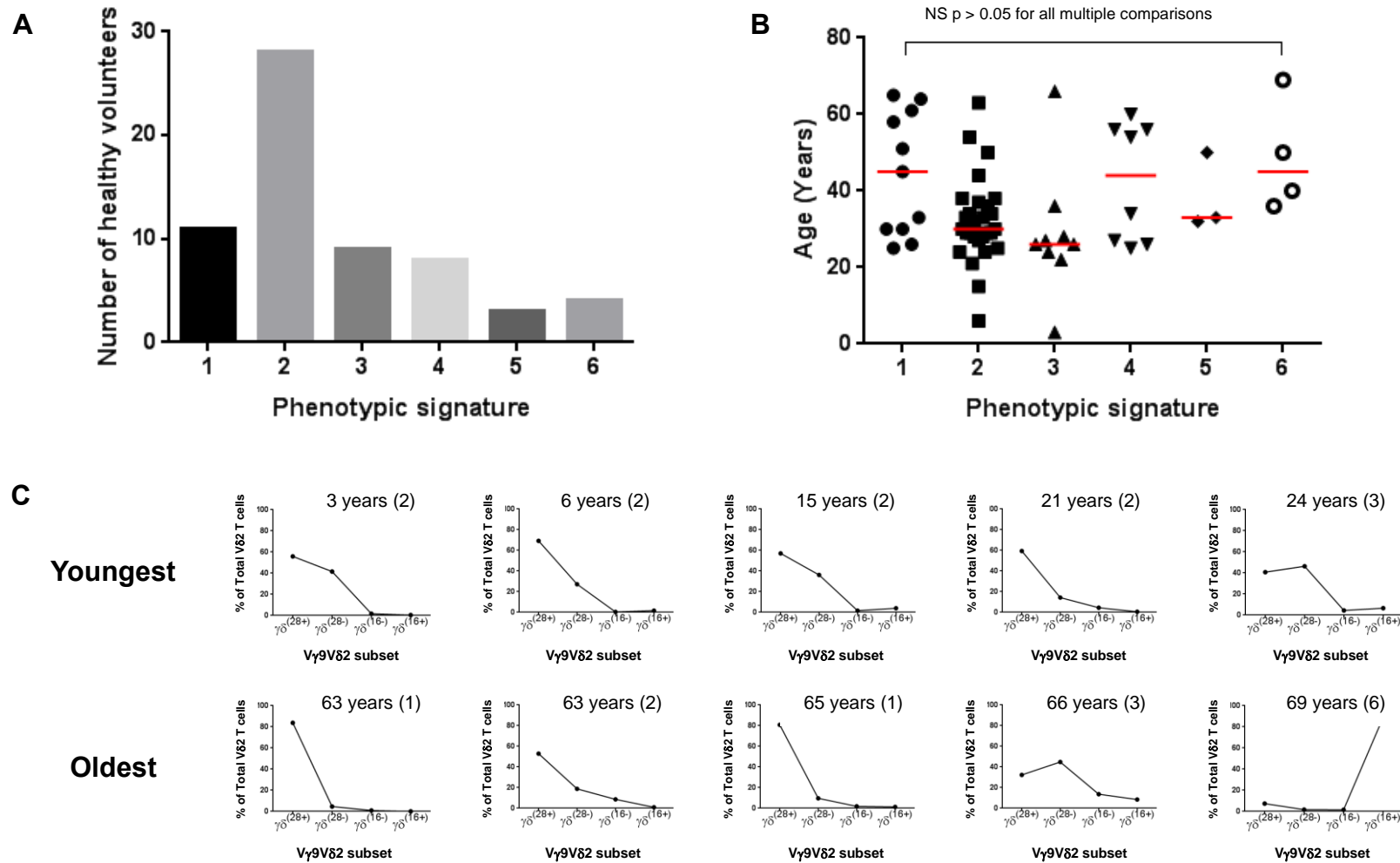


Figure 3.15 Distribution of phenotypic signatures in healthy volunteers.

(A) Distribution of phenotypic signatures of all 63 healthy volunteers (B) Distribution of age (years) for the six phenotypic signatures with median values indicated (red). Statistical differences were assessed using ANOVA Kruskal-Wallis non-parametric testing and multiple-comparison post-hoc testing using Bonferroni correction $p < 0.05$. (C) Phenotypic signatures of five youngest and the five oldest healthy volunteers with phenotypic signature group (1-6) indicated for each individual.

3.14 V γ 9V δ 2 T cell phenotypic “signatures” do not appear to correlate with ethnicity, region of birth or the development status of country of birth

Having assigned each individual to a particular phenotypic signature, the correlation between these signatures and ethnicity, sub-region/continent of birth, and the developmental status of country of birth, was then assessed. There was no phenotypic signature that predominated in individuals of a particular ethnicity, sub-region or continent of birth (Figure 3.16). Nor did these signature groupings seem to relate to the developmental status of country of birth. However one interesting observation was that all three of the most extreme phenotypes (signature #6) were born and spent their early life in the continent of Africa, raising the question whether a particular early environmental exposure to specific antigen or infections might have a permanent effect on an individual's V γ 9V δ 2 T cell phenotype.

3.15 Malaria has no significant effect on V δ 2/CD3(%) but may lead to extreme V γ 9V δ 2 T cell phenotypic signatures

In five of the healthy volunteer cohort, a history of malaria exposure was reported in early life (< 5 years old in all cases). Therefore, in order to examine the influence of this specific infection, the V δ 2/CD3(%) and the phenotypic signature were examined in each of these individuals to investigate whether there could be an association between exposure to malaria and changes in V γ 9V δ 2 T cells in the peripheral blood. Figure 3.17 shows that V δ 2/CD3(%) did not seem to be significantly affected by previous malaria infection with a median

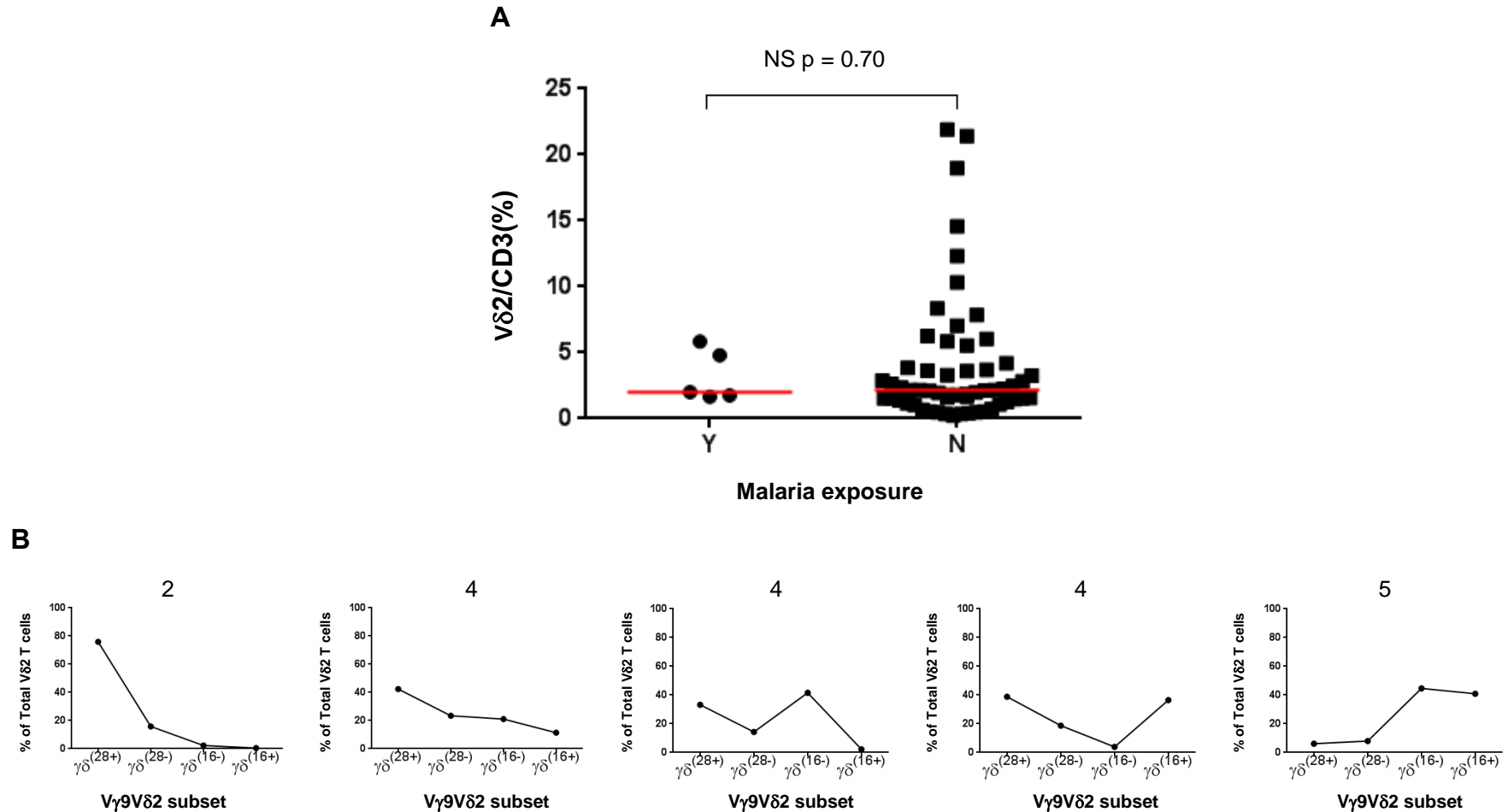


Figure 3.17 Effect of previous malaria infection on V γ 9V δ 2 T cell percentage and phenotypic signature.

A comparison of healthy volunteers, with and without a previous history of malaria infection. (A) Graph comparing V δ 2/CD3(%) in healthy volunteers with and without a previous history of malaria exposure is shown. Statistical differences were assessed using the Mann–Whitney U test with p-values indicated (Y=Yes, N=No). (B) Phenotypic profiles of the 5 healthy volunteers with a previous history of malaria infection are shown, with phenotypic signature groups indicated above each of these 5 individuals.

percentage of 2.0% in the malaria sub-group compared to 2.2% in unaffected healthy controls ($p = 0.70$). However the phenotypic signatures of the group with a past history of malaria infection seemed to contain a number of the more extreme phenotypes (2,4,4,4 and 5) and perhaps suggested that this specific infection might permanently increase the percentage of certain $V\gamma 9V\delta 2$ T cell subsets in the peripheral blood over a longer period of time.

3.16 Summary; What is the nature of $V\gamma 9V\delta 2$ T cell differentiation?

The data described in this chapter have argued that the commonly-used methods of phenotyping $V\gamma 9V\delta 2$ T cells are sub-optimal. Furthermore, the literature has under-represented the degree to which the phenotype of $V\gamma 9V\delta 2$ T cells differs between individuals. Here, we re-assess the phenotype of these cells using CD28, CD27 and CD16, proposing a method of identification which recognises four subsets; $\gamma\delta^{(28+)} [CD28^{(+)}CD27^{(+)}$], $\gamma\delta^{(28-)} [CD28^{(-)}CD27^{(+)}$], $\gamma\delta^{(16-)} [CD28^{(-)}CD27^{(-)}CD16^{(-)}$] and $\gamma\delta^{(16+)} [CD28^{(-)}CD27^{(-)}CD16^{(+)}$]. Interestingly, the relative proportions of these subsets allow individuals to be placed in a number of clusters or phenotypic signatures. These signatures differ significantly from one another, and importantly do not correlate with age, gender, ethnicity, or country of birth. Finally, the data pose interesting questions as to the nature of $V\gamma 9V\delta 2$ T cell differentiation; Do $V\gamma 9V\delta 2$ T cells move through the various CD28/CD27/CD16-defined subsets in a linear manner, or are the phenotypic signatures that they define stable over time, or even determined by genetic inheritance and or developmental history. These ideas are summarised in Figure 3.18.

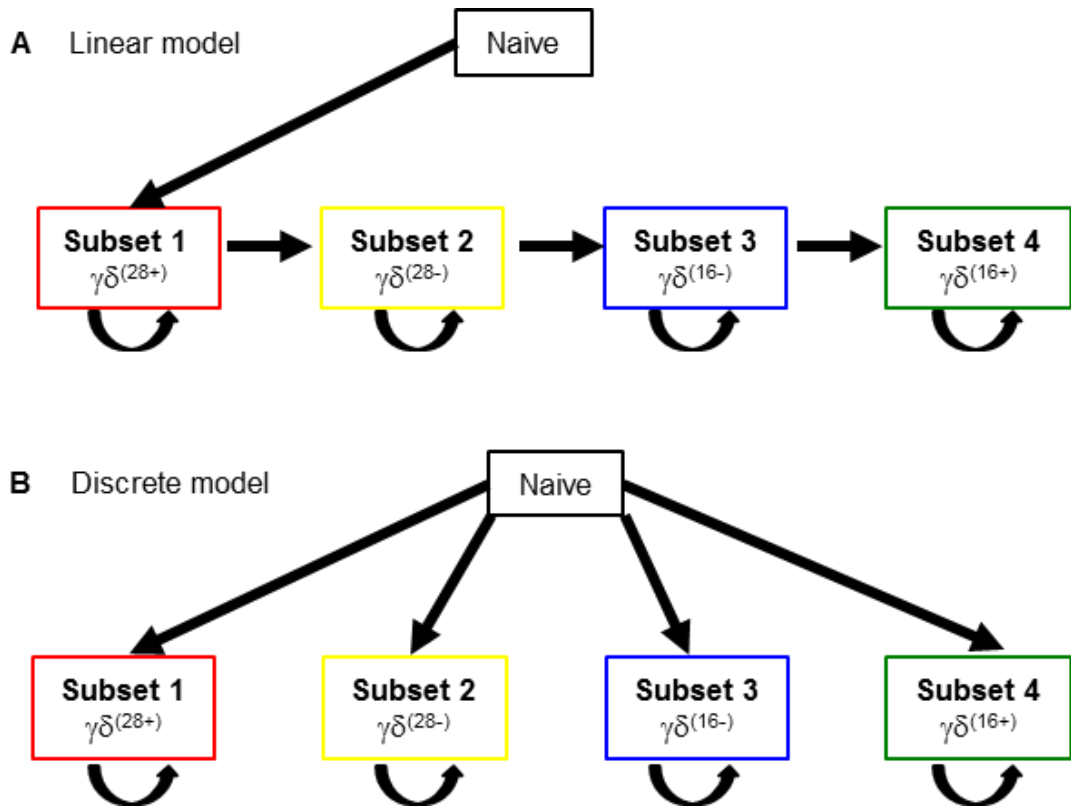


Figure 3.18 Proposed models of V γ 9V δ 2 T cell differentiation.

Model A shows a linear pattern of differentiation where cells move along a sequential pathway from “Naïve” to other phenotypes. Model B describes an alternative model that implies that each individual subset arises from a common naïve progenitor or stem-like cell. Homeostatic mechanisms from a stem-like progenitor subset may be involved in replenishing depleted subsets after infectious challenge, or alternatively the thymus may have a continued role in topping up subsets despite gradual age-related involution.

Chapter 4

Phenotypic and functional characterisation of newly defined $V\gamma 9V\delta 2$ T cell subsets

Chapter 4 Phenotypic and functional characterisation of newly defined V γ 9V δ 2 T cell subsets

4.1 Introduction

Having proposed a revised system of V γ 9V δ 2 T cell classification based on CD11a, CD28, CD27 and CD16, it was important to further characterise the five distinct V γ 9V δ 2 T cell subsets; [$\gamma\delta^{(N)}$; $\gamma\delta^{(28+)}$; $\gamma\delta^{(28-)}$; $\gamma\delta^{(16-)}$ and $\gamma\delta^{(16+)}$] in order to establish their properties and functional potential. This chapter describes this analysis, which assesses the expression of a range of common extracellular markers, cytokine secretion and proliferative potential. Finally a gene microarray was performed on four of the five subsets to reveal further differences between these populations.

4.2 Surface marker expression on V γ 9V δ 2 T cell subsets

4.2.1 The $\gamma\delta^{(N)}$ subset is characterised by high levels of CCR7 and CD62L expression

The small “naïve” V γ 9V δ 2 T cell subset $\gamma\delta^{(N)}$, defined as [CD27^(Hi)CD11a^(Lo)] was characterised using a number of other common markers. Figure 4.1 shows that the $\gamma\delta^{(N)}$ population also commonly expresses CCR7 (median percentage of subset positive for CCR7 being 69.1%) and CD62L (median percentage of subset positive for CD62L being 85.7%). By contrast, the percentage of the non-naïve V γ 9V δ 2 T cell populations expressing CCR7 was low (typically <10%), with CCR7 being surprisingly poorly expressed by $\gamma\delta^{(28+)}$ and $\gamma\delta^{(28-)}$ subsets (Figure 4.1A).

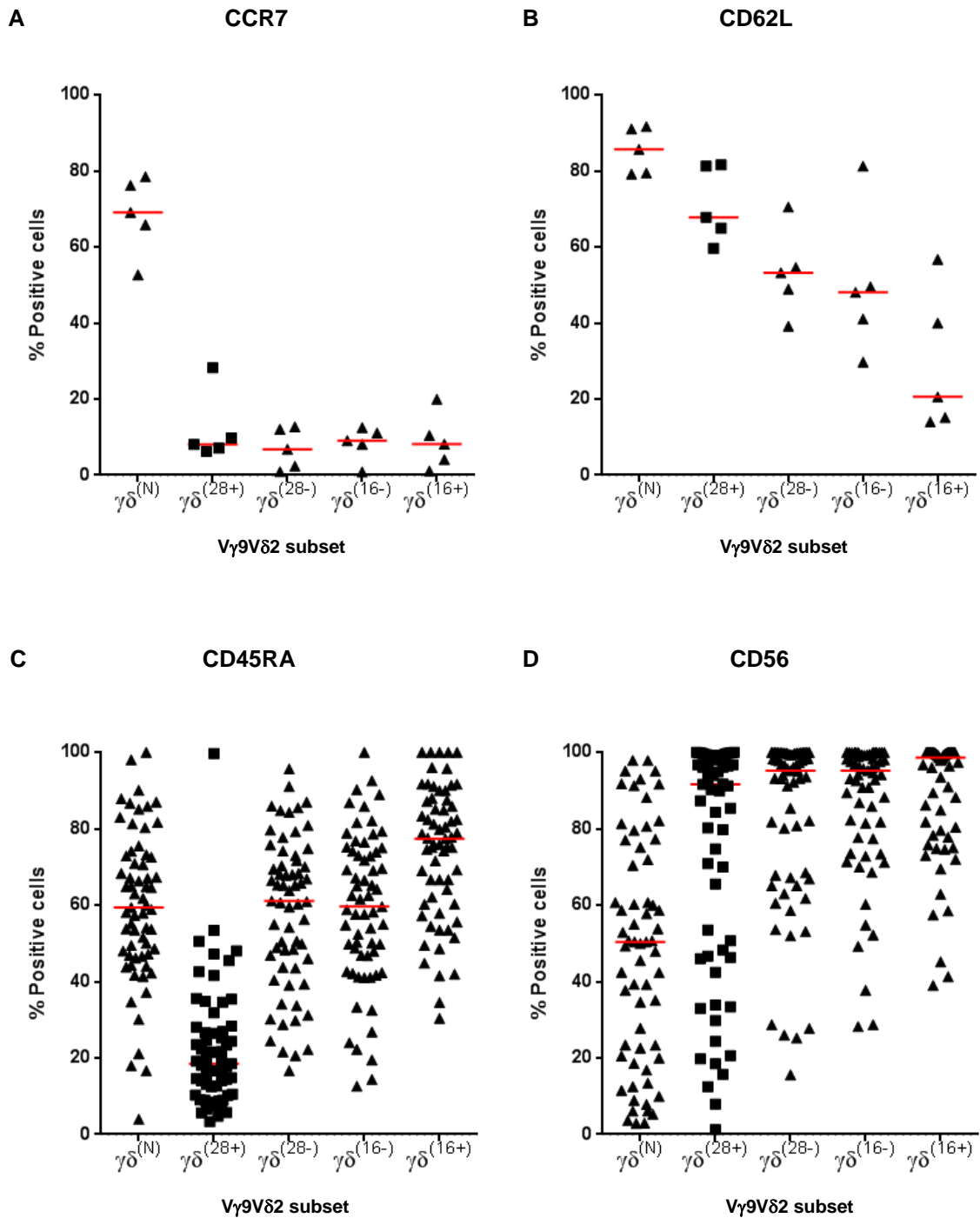


Figure 4.1 Expression levels of various surface markers on V γ 9V δ 2 T cell subsets.

Extracellular surface marker expression is shown for (A) CCR7, (B) CD62L, (C) CD45RA and (D) CD56 on V γ 9V δ 2 T cell subsets. For each marker, individual data points are shown indicating percentage of positive cells in each subset with median values indicated as a red bar. V γ 9V δ 2 T cell subsets are defined as; $\gamma\delta^{(N)}$ [CD27^(Hi)CD11a^(Lo)], $\gamma\delta^{(28+)}$ [CD28⁽⁺⁾CD27⁽⁺⁾], $\gamma\delta^{(28-)}$ [CD28⁽⁻⁾CD27⁽⁺⁾], $\gamma\delta^{(16-)}$ [CD28⁽⁻⁾CD27⁽⁻⁾CD16⁽⁻⁾] and $\gamma\delta^{(16+)}$ [CD28⁽⁻⁾CD27⁽⁻⁾CD16⁽⁺⁾].

The percentage of cells positive for CD62L expression decreased across the populations from high levels in the $\gamma\delta^{(N)}$ subset to low levels in the $\gamma\delta^{(16+)}$ population (Figure 4.1B). The $\gamma\delta^{(N)}$ population also commonly expresses CD45RA (median percentage of subset positive for CD45RA being 59.4%) although the range of expression of this marker is large (4-100%), and similar in magnitude and distribution to the $\gamma\delta^{(28-)}$ and $\gamma\delta^{(16-)}$ populations (Figure 4.1C). The wide range of expression of CD45RA on the $\gamma\delta^{(N)}$ population adds further weight to the argument that CD45RA is a variable and unreliable naïve cell marker for V γ 9V δ 2 T cells (Figure 4.1C).

The cytotoxic marker CD56 was expressed by the vast majority of non-naïve subsets (typically > 80%) but was only expressed by around 50% of the $\gamma\delta^{(N)}$ population. This suggests that perhaps all of the non-naïve cell populations have cytotoxic potential in contrast to the memory and effector populations observed for conventional $\alpha\beta$ T cells.

4.2.2 The $\gamma\delta^{(28+)}$ subset is characterised by high CCR2 and CCR5 expression

The $\gamma\delta^{(28+)}$ population appears to be the most different non-naïve V γ 9V δ 2 T cell subset in terms of surface markers. $\gamma\delta^{(28+)}$ cells showed a significantly lower median percentage of CD45RA expression (18.5%) compared to $\gamma\delta^{(28-)}$ cells (61.1%), $\gamma\delta^{(16-)}$ cells (59.6%) and $\gamma\delta^{(16+)}$ cells (77.4%) ($p < 0.05$) (Figure 4.1). In addition, $\gamma\delta^{(28+)}$ cells also displayed a high median percentage expression of both CCR2 (66.9%) and CCR5 (94.2%) with significantly higher levels compared to all other subsets ($p < 0.05$) (Figure 4.2).

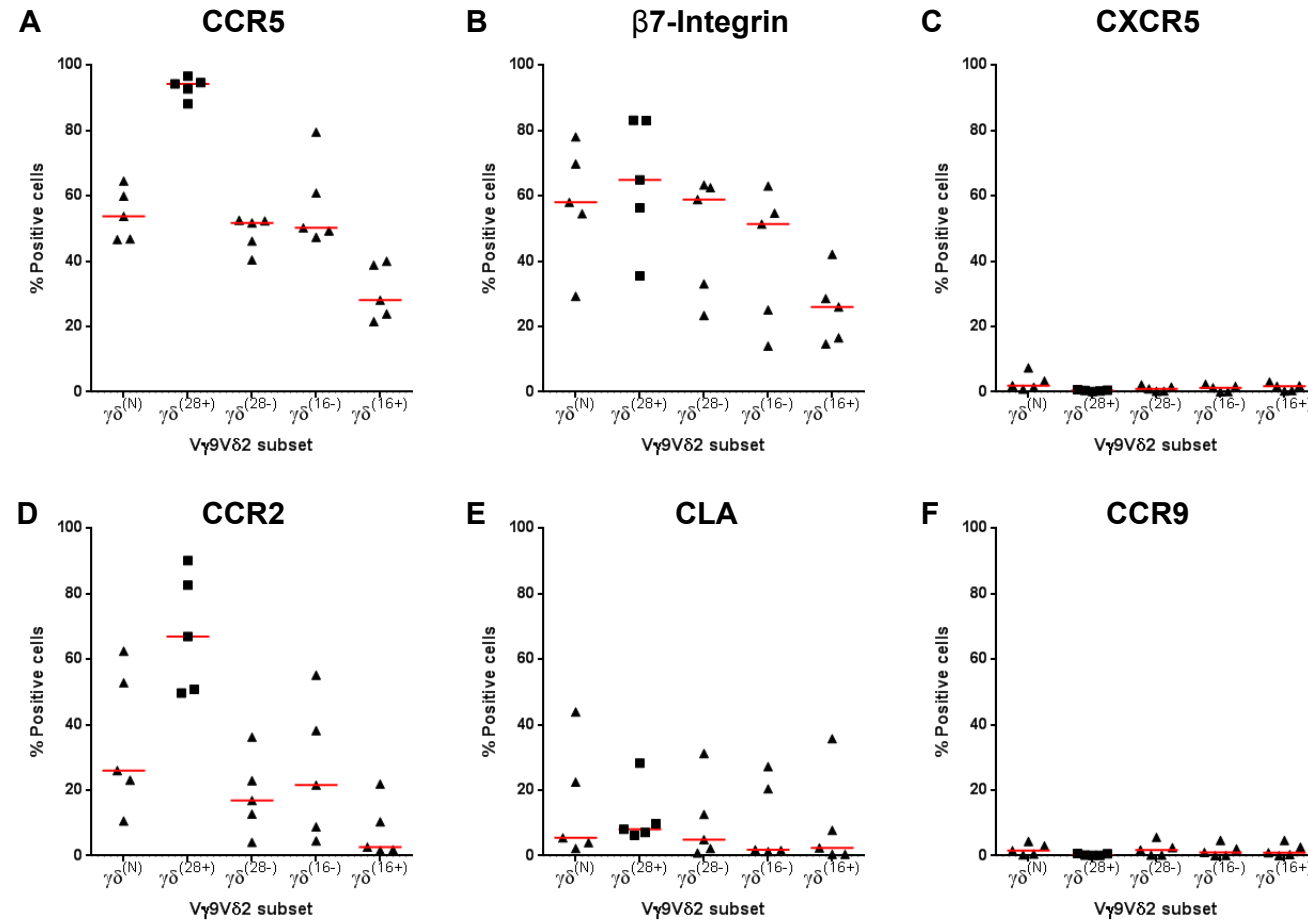


Figure 4.2 Expression levels of various chemokine receptors and homing markers on V γ 9V δ 2 T cell subsets.

Surface marker staining is shown for (A) CCR5, (B) β 7-Integrin, (C) CXCR5, (D) CCR2, (E) Cutaneous lymphocyte antigen (CLA) and (F) CCR9 on V γ 9V δ 2 subsets. For each marker, individual data points are shown indicating percentage of positive cells in each subset with median values indicated as a red bar. V γ 9V δ 2 subsets are defined as; $\gamma\delta^{(N)}$ [CD27^(Hi)CD11a^(Lo)], $\gamma\delta^{(28+)}$ [CD28⁽⁺⁾CD27⁽⁺⁾], $\gamma\delta^{(28-)}$ [CD28⁽⁻⁾CD27⁽⁺⁾], $\gamma\delta^{(16-)}$ [CD28⁽⁻⁾CD27⁽⁻⁾CD16⁽⁻⁾] and $\gamma\delta^{(16+)}$ [CD28⁽⁻⁾CD27⁽⁻⁾CD16⁽⁺⁾].

This same population also expressed the highest median percentage of the $\beta 7$ -integrin marker (67.8%). In summary, it appears that $\gamma\delta^{(28+)}$ cells represents a particularly distinct population with many different surface markers in comparison to the other $V\gamma 9V\delta 2$ T cell subsets.

4.2.3 CXCR5, CCR9 and CLA are expressed at low levels on $V\gamma 9V\delta 2$ T cells

Characterisation of $V\gamma 9V\delta 2$ T cells with CXCR5, CCR9 and CLA showed there to be low levels of surface expression of these markers and with no obvious differences between subsets ($p > 0.05$) (Figure 4.2).

4.3 Assessment of cytokine secreting potential by $V\gamma 9V\delta 2$ T cell subsets

Having characterised some common surface markers on the newly-defined $V\gamma 9V\delta 2$ T cell subsets, the cytokine-secreting potential of these populations was then established by investigating the production of IFN- γ , TNF- α , and IL-17A following 4-hour stimulation with PMA and ionomycin. In addition, the potential of subsets to produce the cytotoxic protein, Perforin was also determined using the same method. The small number of cells in the $\gamma\delta^{(N)}$ population meant that it was not possible to characterise the secreting-potential of this subset, and therefore this subset (that also has a $CD28^{(+)CD27^{(+)}$ expression pattern) was included together with the $\gamma\delta^{(28+)}$ subset. A typical example from a single individual healthy volunteer is shown in Figure 4.3 showing the cytokine secreting potential of each subset for IFN- γ , TNF- α and IL-17A as well as for Perforin.

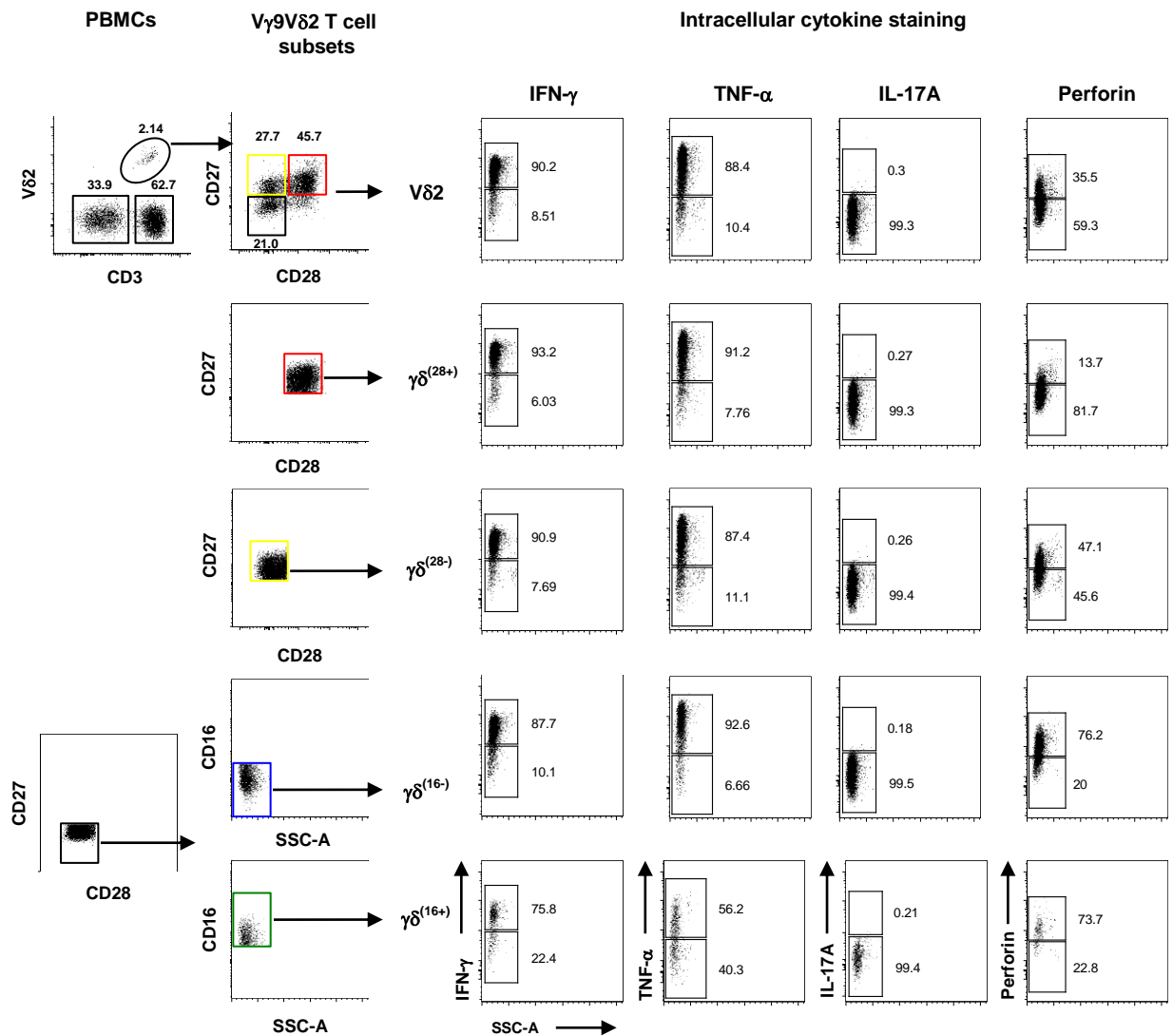


Figure 4.3 Cytokine potential of V γ 9V δ 2 T cell subsets.

Representative plots from a single healthy individual are shown. PBMCs were stimulated with PMA and Ionomycin for 3 hours, blocked with Brefeldin/Monensin and then fixed and permeabilised before staining for intracellular cytokines; Interferon- γ (IFN- γ), Tumour Necrosis Factor- α (TNF- α) and Interleukin-17A (IL-17A). Cell secreting potential for the intracellular cytotoxic protein, perforin is also shown (far right). Flow cytometry dot-plots show percentage of cells positive and negative for each cytokine in total V γ 9V δ 2 cells and in constitutive subsets. V γ 9V δ 2 subsets are defined as; $\gamma\delta^{(28+)}$ [CD28⁽⁺⁾CD27⁽⁺⁾] (red box), $\gamma\delta^{(28-)}$ [CD28⁽⁻⁾CD27⁽⁺⁾] (yellow box), $\gamma\delta^{(16-)}$ [CD28⁽⁻⁾CD27⁽⁻⁾CD16⁽⁻⁾] (blue box) and $\gamma\delta^{(16+)}$ [CD28⁽⁻⁾CD27⁽⁻⁾CD16⁽⁺⁾] (green box).

4.3.1 All V γ 9V δ 2 T cell populations can secrete IFN- γ and TNF- α with low levels of IL-17A

Intracellular cytokine staining revealed that the majority of the V γ 9V δ 2 T cell subsets showed the capacity to secrete IFN- γ upon stimulation, with a high median percentage expression in all four non-naïve subsets (typically between 60-80%) (see Figure 4.4). Similarly, TNF- α was also readily produced by a high percentage of cells in all V γ 9V δ 2 T cell subsets. However, the percentage of TNF- α secreting cells in the $\gamma\delta^{(16+)}$ subset was significantly lower (median = 38.4%) in comparison to the $\gamma\delta^{(28+)}$ subset, which had a median expression percentage of 91.9% ($p = 0.002$). In addition, whilst not significantly different, $\gamma\delta^{(28-)}$ and $\gamma\delta^{(16-)}$ subsets also appeared to express TNF- α at much higher levels than the $\gamma\delta^{(16+)}$ subset. IL-17A was expressed at very low levels (< 5%) in all V γ 9V δ 2 T cell populations with no obvious differences between subsets ($p = 0.35$).

4.3.2 Perforin is produced at higher levels in $\gamma\delta^{(16-)}$ and $\gamma\delta^{(16+)}$ subsets

The ability of each V γ 9V δ 2 T cell subsets to make the cytotoxic protein Perforin was also assessed following PBMC stimulation. Results indicated in Figure 4.4 show a significantly higher percentage of cells expressing Perforin in the $\gamma\delta^{(16-)}$ and $\gamma\delta^{(16+)}$ V γ 9V δ 2 subsets ($p < 0.05$) with median percentage expression levels of 39.3% and 47.4% respectively compared to the $\gamma\delta^{(28+)}$ population (3.7%). This suggests that CD27 $^{(-)}$ populations [$\gamma\delta^{(16-)}$ and $\gamma\delta^{(16+)}$ subsets] have increased cytotoxic potential.

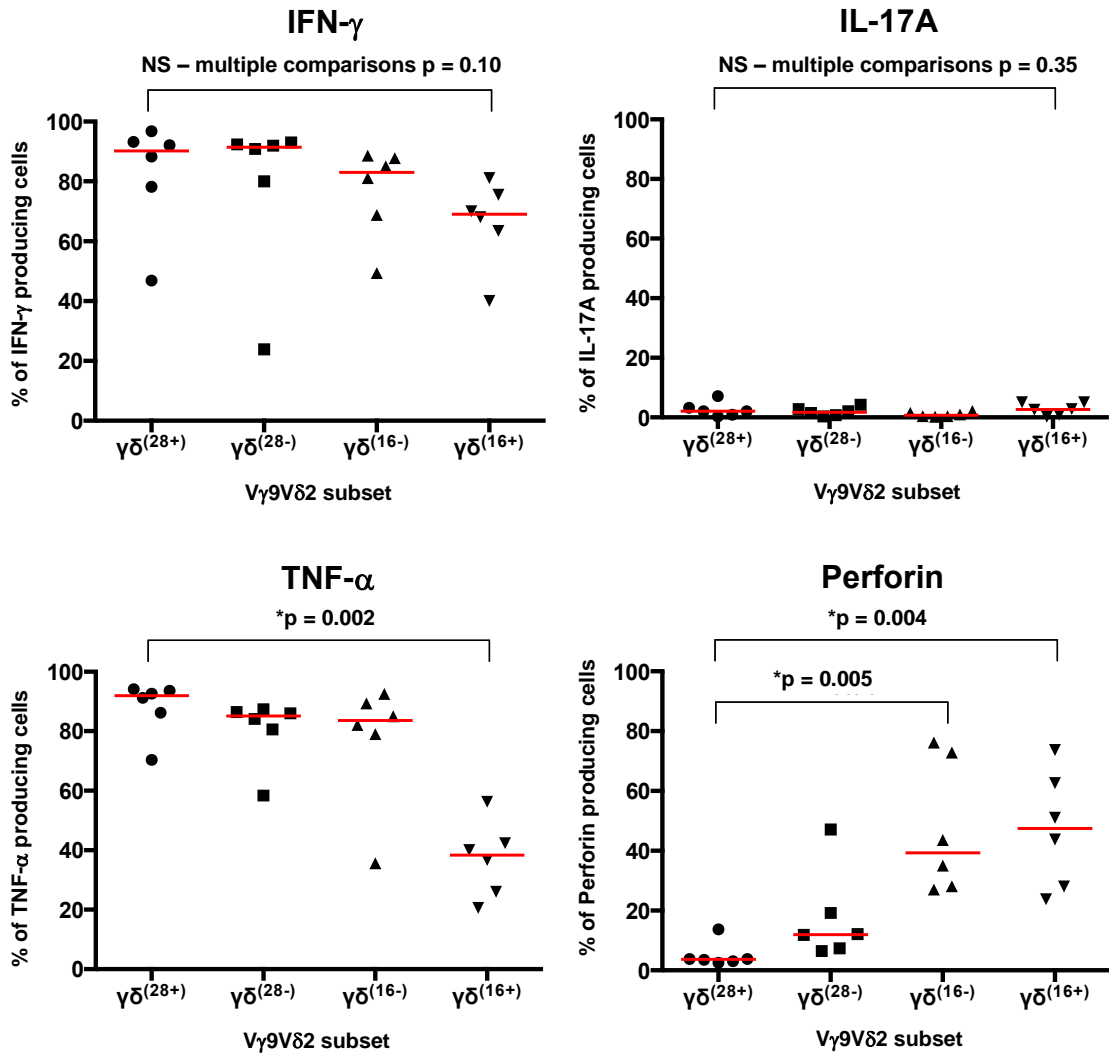


Figure 4.4 Cytokine and Perforin-secreting potential in non-naïve V γ 9V δ 2 T cell subsets.

Percentage of cells with cytokine-secreting potential (IFN- γ , IL-17A and TNF- α) is shown for each V γ 9V δ 2 T cell subset from six healthy peripheral blood PBMC samples. Cell-secreting potential for the intracellular cytotoxic protein, perforin is also shown (bottom right). V γ 9V δ 2 subsets are $\gamma\delta^{(28+)}$ [CD28⁽⁺⁾CD27⁽⁺⁾], $\gamma\delta^{(28-)}$ [CD28⁽⁻⁾CD27⁽⁺⁾], $\gamma\delta^{(16-)}$ [CD28⁽⁻⁾CD27⁽⁻⁾CD16⁽⁻⁾] and $\gamma\delta^{(16+)}$ [CD28⁽⁻⁾CD27⁽⁻⁾CD16⁽⁺⁾]. Red lines represent median values with statistical differences assessed using the Kruskal-Wallis one-way ANOVA test and multiple comparison post-hoc testing with Bonferroni correction (p -values < 0.05 were considered significant).

4.4 Proliferative potential

4.4.1 Increased phosphoantigen-induced proliferation is observed in CD27⁽⁺⁾ subsets compared to CD27⁽⁻⁾ populations

Proliferative potential was assessed in each of the four main V γ 9V δ 2 T cell subsets after 5 days of culture *in vitro* with HMB-PP (1nM) and IL-2 (100U/ml). Figure 4.5 shows a V γ 9V δ 2 T cell proliferation assay from a single representative individual. Histograms showing membrane incorporation of the eFluor 670 proliferation dye (eBioscience) in V γ 9V δ 2 T cells, as well as for the individual V γ 9V δ 2 subsets are shown at day-0 and subsequently at day-5. On day-5, 77.3% of the total V γ 9V δ 2 T cell population had proliferated in response to HMB-PP and IL-2, unlike the IL-2 only control, in which only 0.5% of the cells had divided. On further analysis of the proliferating populations, it was apparent that the CD27⁽⁺⁾ populations [$\gamma\delta^{(28+)}$ and $\gamma\delta^{(28-)}$ subsets] seemed to show a much higher proliferative capacity in comparison to those subsets not expressing CD27, with the percentage of cells with reduced levels of proliferative dye being 81.7% for the $\gamma\delta^{(28+)}$ subset, 82.1% for $\gamma\delta^{(28-)}$ cells, 15.8% for $\gamma\delta^{(16-)}$ cells, and 51.6% for the $\gamma\delta^{(16+)}$ population (Figure 4.5).

Having repeated the assay three times for two different healthy volunteers who had all four of the main V γ 9V δ 2 T cell subsets, a similar proliferation pattern seemed to emerge (Figure 4.6). Cells in the $\gamma\delta^{(16-)}$ subset at day-5 showed significantly less proliferation when compared to the $\gamma\delta^{(28+)}$ and $\gamma\delta^{(28-)}$ subsets (all $p < 0.05$). The $\gamma\delta^{(16+)}$ population also showed significantly less proliferation in healthy volunteer 2 compared to $\gamma\delta^{(28+)}$ and the $\gamma\delta^{(28-)}$ subsets ($p=0.003$ and $p=0.004$), but was not significantly different in healthy volunteer 1.

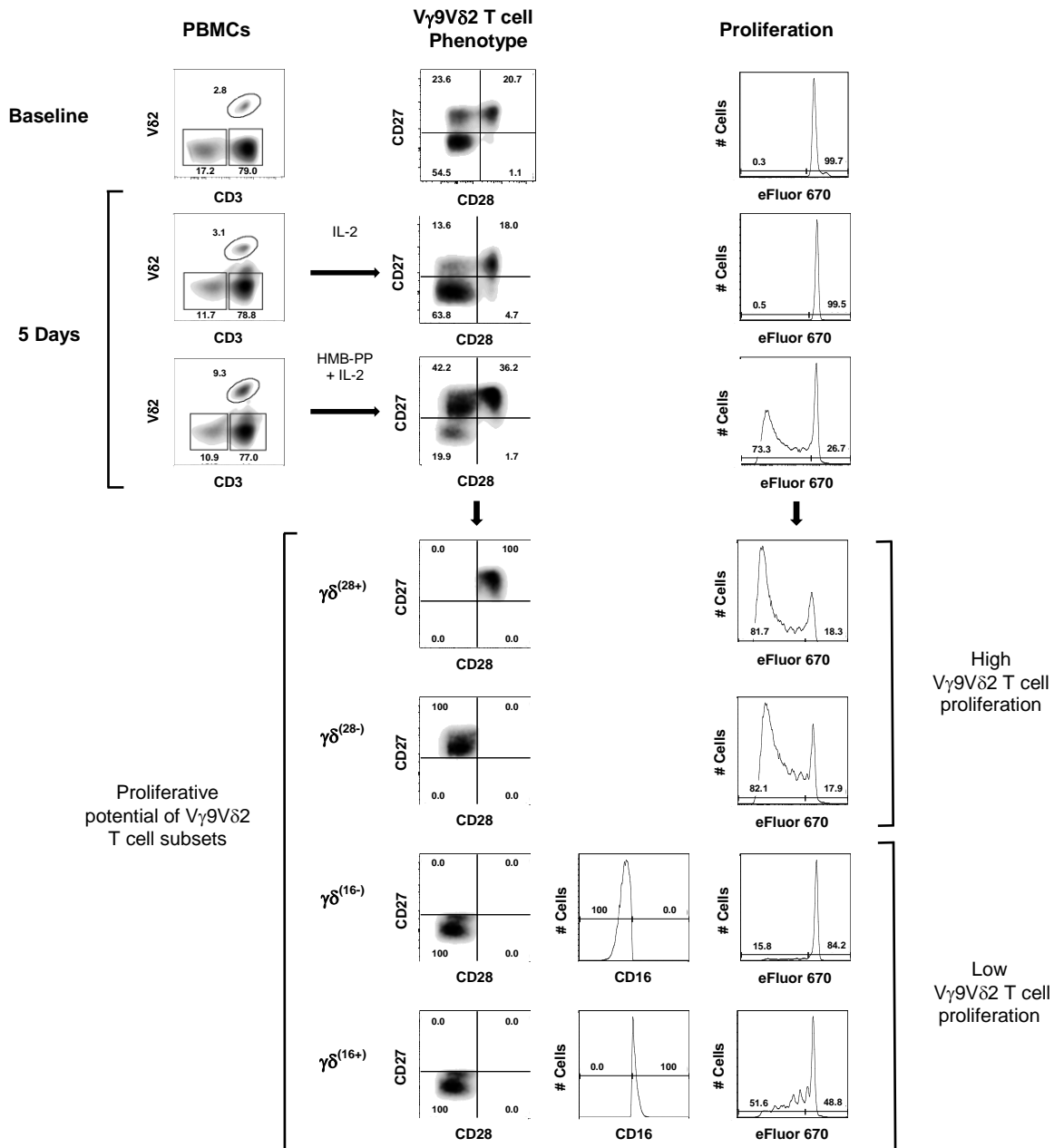


Figure 4.5 CD27⁽⁺⁾ V γ 9V δ 2 T cell subsets show high proliferative potential.

Representative plots are shown from a single healthy volunteer. PBMCs were initially loaded with eFluor 670 (eBioscience) and run to ensure even loading of cells at baseline. PBMCs were then cultured with HMB-PP (1nM) + IL-2 (100U/ml) over 5 days and then surface stained for V δ 2, CD3, CD27, CD28 and CD16 at the end of this period. Flow cytometry density plots show the gating of V γ 9V δ 2 subsets and histograms show eFluor670 expression and the percentage of non-proliferated and proliferated cells in each gated subset. V γ 9V δ 2 subsets are defined as; $\gamma\delta^{(28+)}$ [CD28⁽⁺⁾CD27⁽⁺⁾], $\gamma\delta^{(28-)}$ [CD28⁽⁻⁾CD27⁽⁺⁾], $\gamma\delta^{(16-)}$ [CD28⁽⁻⁾CD27⁽⁻⁾CD16⁽⁻⁾] and $\gamma\delta^{(16+)}$ [CD28⁽⁻⁾CD27⁽⁻⁾CD16⁽⁺⁾].

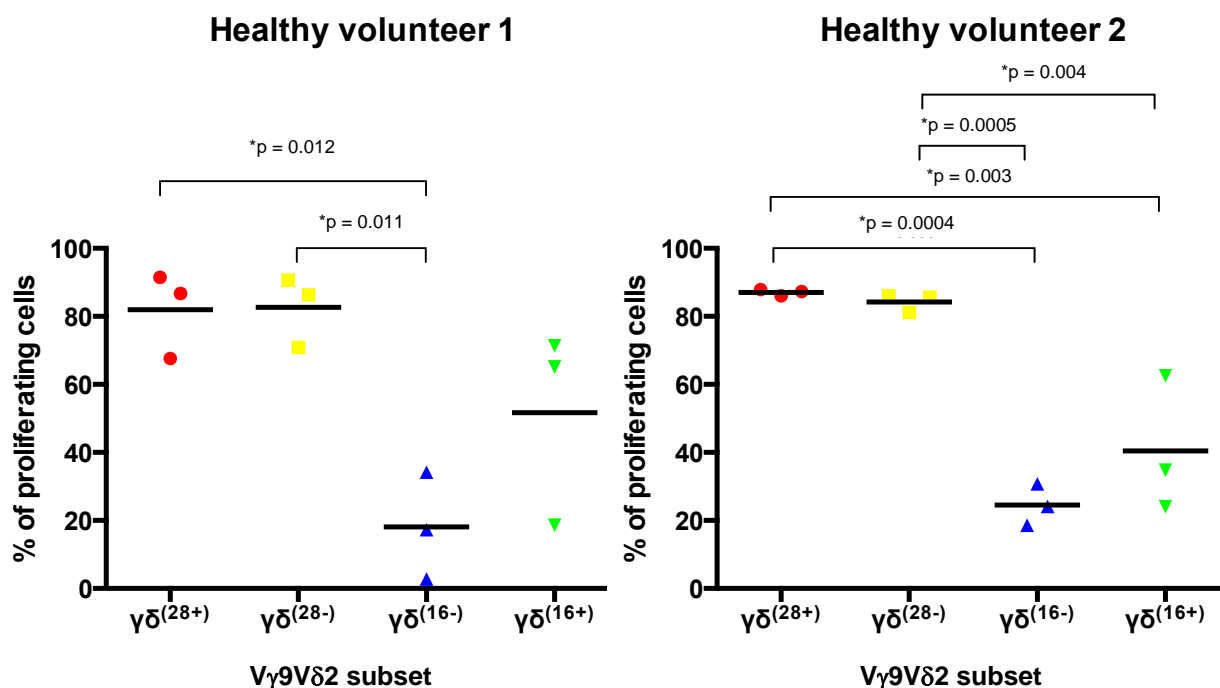


Figure 4.6 CD27⁽⁺⁾ cells show the highest proliferation following phosphoantigen stimulation

Graphs show percentage of proliferating cells in each V γ 9V δ 2 subset at 5-days following stimulation of PBMCs with HMB-PP (1nM) and IL-2 (100U/ml). Scatter graphs of two different healthy individuals performed in triplicate are shown (all data points are shown). Mean percentage of proliferating subsets are shown for each V γ 9V δ 2 subset. Significant differences were assessed using one-way ANOVA with Tukey's multiple comparison correction (p-values are stated). V δ 2 subsets are defined as; $\gamma\delta^{(28+)}$ [CD28⁽⁺⁾CD27⁽⁺⁾] (red), $\gamma\delta^{(28-)}$ [CD28⁽⁻⁾CD27⁽⁺⁾] (yellow), $\gamma\delta^{(16-)}$ [CD28⁽⁻⁾CD27⁽⁻⁾CD16⁽⁻⁾] (blue) and $\gamma\delta^{(16+)}$ [CD28⁽⁻⁾CD27⁽⁻⁾CD16⁽⁺⁾] (green).

In both volunteers the $\gamma\delta^{(16+)}$ subsets showed a higher median percentage expression compared to the $\gamma\delta^{(16-)}$ subset but this difference was not significant ($p > 0.05$). The results from these proliferation assays therefore suggests that the CD27 co-stimulatory molecule seems to be a key marker in identification of V γ 9V δ 2 cells capable of proliferation in response to HMB-PP and IL-2.

4.5 Gene microarray on newly-defined V γ 9V δ 2 subsets

At this point, having characterised the newly-defined V γ 9V δ 2 T cell subsets using a range of basic functional read-outs, it was decided to use a gene expression microarray to further assess these $\gamma\delta$ T cell populations. The four main subsets; $\gamma\delta^{(28+)}$, $\gamma\delta^{(28-)}$, $\gamma\delta^{(16-)}$ and $\gamma\delta^{(16+)}$ cells, were sorted to >90% purity. Due to its small size, the $\gamma\delta^{(N)}$ subset was included as part of the $\gamma\delta^{(28+)}$ subset. Figure 4.7 gives a summary overview of the sorting and processing of each V γ 9V δ 2 subset for gene microarray analysis.

Seven healthy individuals were used to purify three subset replicates for each of the four main V γ 9V δ 2 T cell subsets. In order to generate sufficient RNA for microarray analysis, a certain number of sorted cells ($\approx 10^6$) needed to be collected for each subset. Thus, it was necessary to use several different individuals from a range of phenotypic signatures to provide adequate yields. In addition, individuals with a high V δ 2/CD3(%) were chosen in order to maximise the number of sorted events to be collected for each subset (Figure 4.8).

Therefore having generated 12 RNA samples (each of the four subsets in triplicate) of sufficient quantity. RNA integrity was then determined using a bioanalyser and all samples had a RIN score of > 7.5 and were assessed to be of sufficient quality.

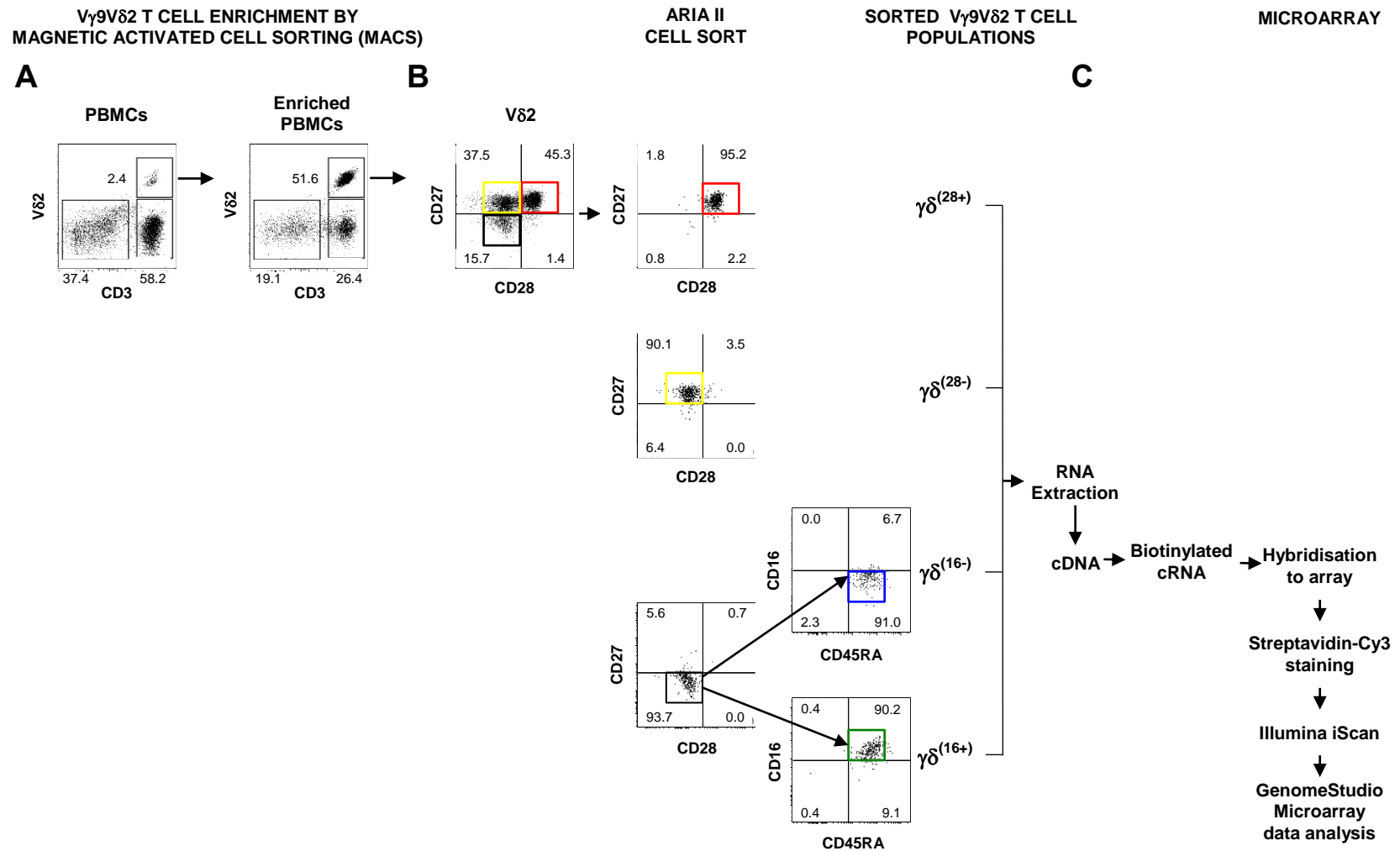


Figure 4.7 Enrichment, sorting and processing of V γ 9V δ 2 subsets for gene microarray.

Isolation of four subsets of V γ 9V δ 2 T cells by (A) Initial enriching PBMCs for V γ 9V δ 2 T cells by Magnetic Activated Cell Sorting (MACS) followed by (B) Fluorescence-activated cell sorting (FACS) using CD28, CD27 and CD16 extracellular markers to isolate four subsets; $\gamma\delta^{(28+)}$ [CD28⁽⁺⁾CD27⁽⁺⁾], $\gamma\delta^{(28-)}$ [CD28⁽⁻⁾CD27⁽⁺⁾], $\gamma\delta^{(16-)}$ [CD28⁽⁻⁾CD27⁽⁻⁾CD16⁽⁻⁾] and $\gamma\delta^{(16+)}$ [CD28⁽⁻⁾CD27⁽⁻⁾CD16⁽⁺⁾]. (C) Preparation of cRNA was carried out by RNA extraction followed by reverse transcription to generate cDNA samples. Finally the production of biotinylated cRNA samples for array hybridisation was generated and read on the iScan reader. Differential gene expression was determined using GenomeStudio software (Illumina).

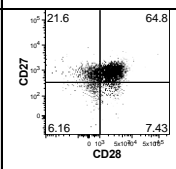
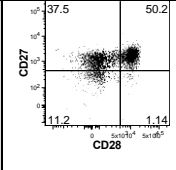
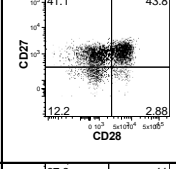
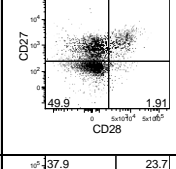
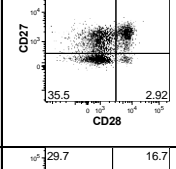
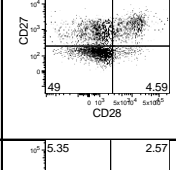
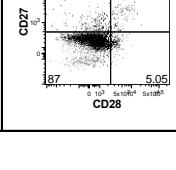
Donor	Age (Years)	Gender (Male/Female)	Ethnicity	V γ 9V δ 2 Phenotypic Signature	V δ 2/CD3(%)	V γ 9V δ 2 subset				CD27/CD28 profile
						$\gamma\delta^{(28+)}$	$\gamma\delta^{(28-)}$	$\gamma\delta^{(16-)}$	$\gamma\delta^{(16+)}$	
1	28	M	Arabic	2	12.3	•				
2	24	F	White British/Irish	3	21.9	•	•			
3	27	F	White European	3	8.4	•	•	•		
4	50	F	White British/Irish	5	19.0		•	•	•	
5	32	M	White British/Irish	5	14.6			•		
6	27	F	Chinese	4	10.3				•	
7	50	M	Black-African	6	21.4				•	

Figure 4.8 Summary of healthy volunteer samples used for V γ 9V δ 2 T cell subset purification.

Details of the healthy donors used to generate V γ 9V δ 2 T cell subsets for gene microarray analysis. Three separate sorted subsets were obtained for each V γ 9V δ 2 T cell subset. A range of donors with different phenotypic signatures was required in order to generate sufficient RNA for the array. Age, gender and ethnicity is shown along with V δ 2/CD3(%) and V γ 9V δ 2 T cell phenotypic signature (1-6). The subsets obtained from each individual are indicated along with their CD28/CD27 profile.

Following production of cDNA from RNA by reverse transcription, and subsequent production of cRNA as previously described in the material and methods, RNA was hybridised to the array overnight and finally stained with streptavidin Cy5 before being read on the illumina iScan (microarray scanner). Unfortunately, two of the $\gamma\delta^{(16-)}$ subsets failed to generate data for unknown experimental reasons and so the results presented for the $\gamma\delta^{(16-)}$ subset are from only a single sample.

4.5.1 Initial microarray validation

To initially validate the array data, the average expression signal was assessed for the three genes that were used to identify and sort the four $V\gamma9V\delta2$ subsets; *CD28*, *CD27* and *CD16*. Figure 4.9 shows that both *CD28* and *CD27* show gene expression levels from the array that directly correlate with the surface expression used to identify the subsets. Interestingly, *CD16* gene expression, whilst increasing across the four subsets and being highest in the $\gamma\delta^{(16+)}$ subset was not statistically significantly higher in the $\gamma\delta^{(16+)}$ subset than the $\gamma\delta^{(28+)}$, $\gamma\delta^{(28-)}$ or $\gamma\delta^{(16-)}$ subsets. However, taken together, the expression of *CD28*, *CD27* and *CD16* seemed to validate the microarray data.

4.5.2 Gene microarray analysis

Figure 4.10 shows a schematic outlining the approach to the gene microarray analysis for the 47,231 gene probes for each of the subsets. As shown in the figure, the initial analysis determined the number of differentially expressed genes (> 2 fold different and $p < 0.05$) between the four subsets, which is shown in Figure 4.11.

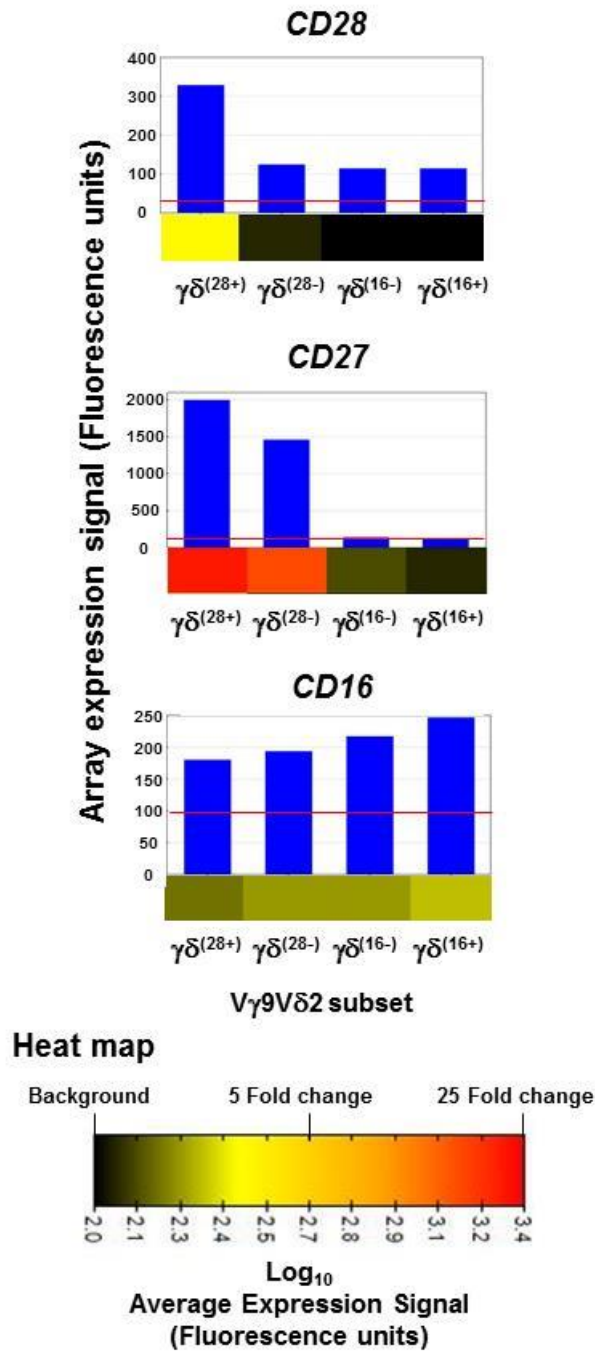


Figure 4.9 Initial validation of microarray

Assessment of mRNA expression levels for *CD28*, *CD27* and *CD16* determined by microarray analysis. Bar charts show the Average Signal Intensities (fluorescence units on linear scale) of analysed subsets relative to each other. Background levels are indicated by the red line (Average Signal Intensity = 100 fluorescence units). The heat-map shown below each graph indicate the relative difference in expression across all four subsets see log₁₀ scale (bottom) showing gene expression levels ranging from background level=2 (Log₁₀100) fluorescent units in black on a log scale to highest gene expression in red.

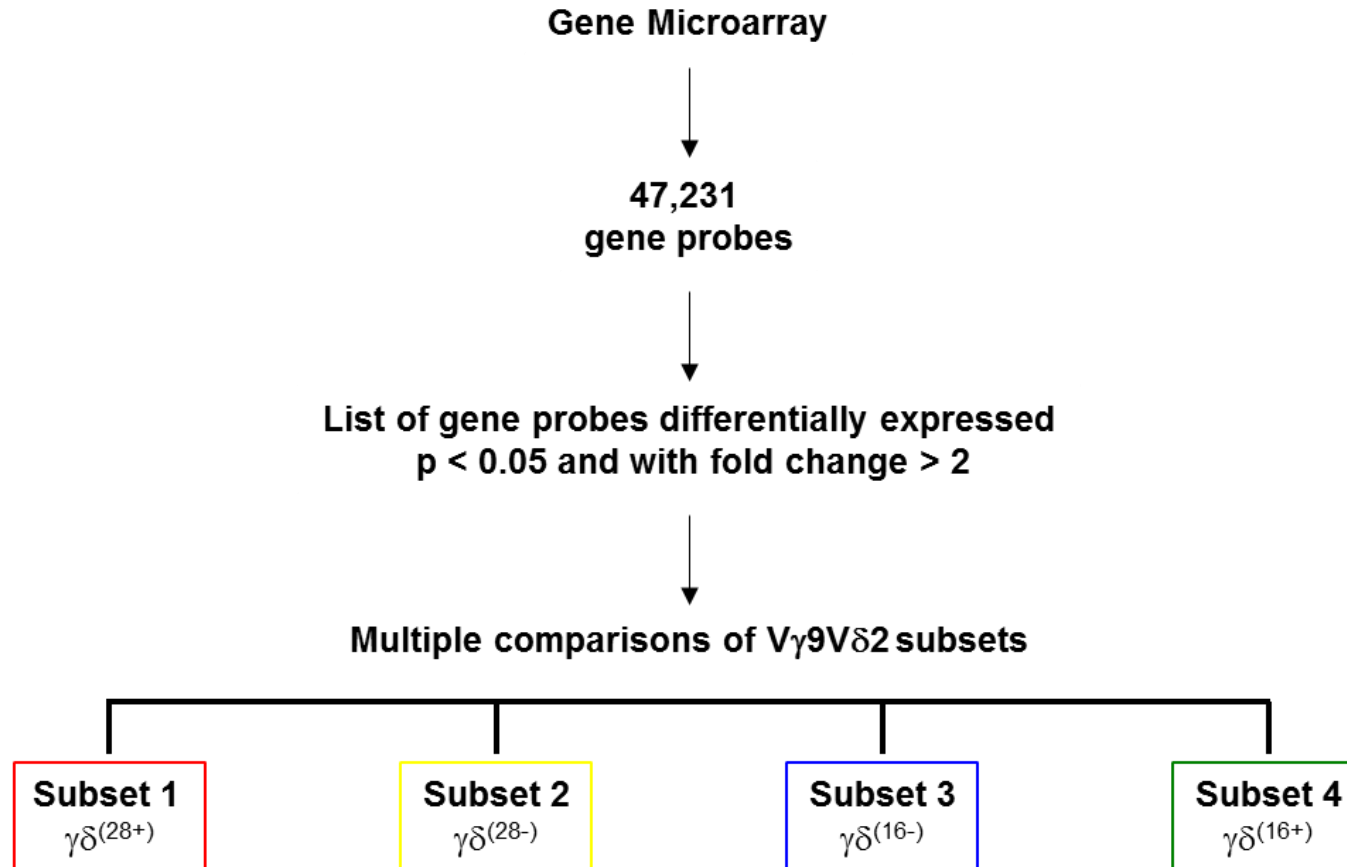


Figure 4.10 Schematic summary of gene microarray analysis strategy for V γ 9V δ 2 T cell subsets.

The gene microarray carried out analysed the transcriptome expression of the sorted RNA samples extracted from the four main V γ 9V δ 2 T cell subsets using 47,231 known gene probes. V γ 9V δ 2 T cell subsets were characterise as follows; $\gamma\delta^{(28+)}$ [CD28⁽⁺⁾CD27⁽⁺⁾] (red box), $\gamma\delta^{(28-)}$ [CD28⁽⁺⁾CD27⁽⁻⁾] (yellow box), $\gamma\delta^{(16-)}$ [CD28⁽⁻⁾CD27⁽⁻⁾CD16⁽⁻⁾] (blue box) and $\gamma\delta^{(16+)}$ [CD28⁽⁻⁾CD27⁽⁻⁾CD16⁽⁺⁾] (green box).

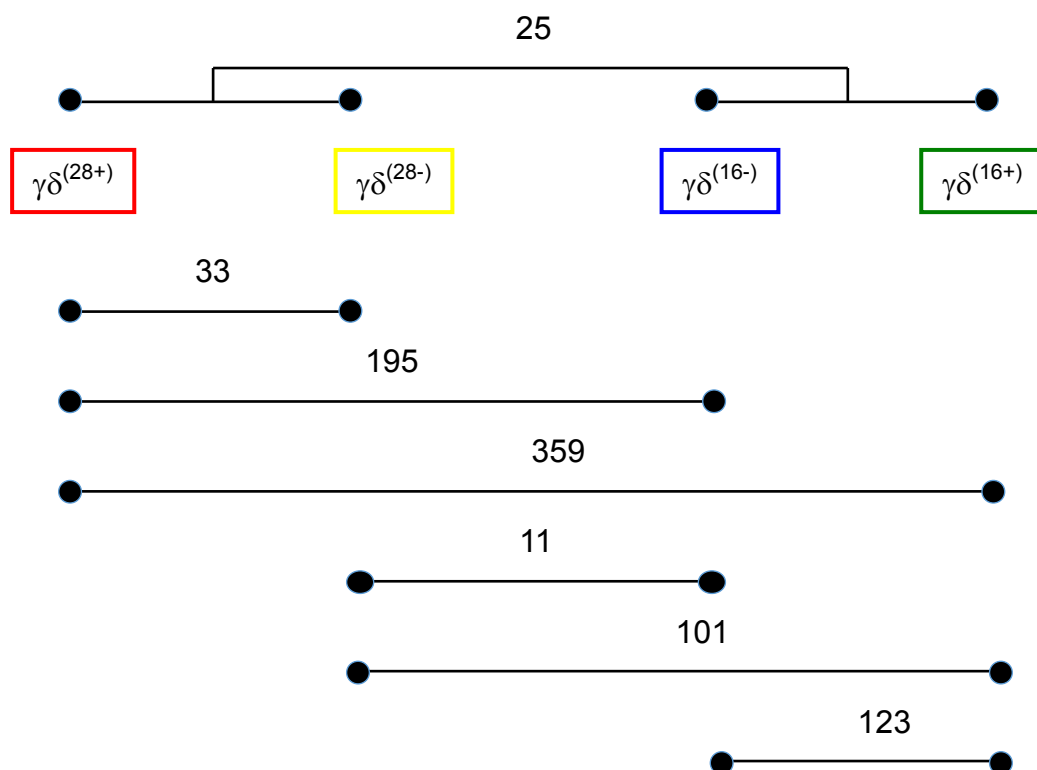


Figure 4.11 Total number of differentially expressed genes between V γ 9V δ 2 T cell subsets.

Schematic shows the total number of differentially expressed gene probes when different V γ 9V δ 2 T cell T cell subsets are compared. Differentially expressed genes are > 2 fold different in expression levels ($p < 0.05$) (Bonferroni corrected).

4.5.3 The $\gamma\delta^{(28+)}$ and $\gamma\delta^{(16+)}$ V γ 9V δ 2 T cell subsets show most distinct expression profiles

The most different subsets in terms of expression profile were the $\gamma\delta^{(28+)}$ and $\gamma\delta^{(16+)}$ populations (359 differences). This supports the view that they are located at either end of a differentiation pathway. Interestingly, if the four subsets are ordered by placing the most similar together and the most different apart, in terms of the number of differentially expressed genes between the subsets, this also support the hypothesis that V γ 9V δ 2 T cells differentiate sequentially from $\gamma\delta^{(28+)}$ to $\gamma\delta^{(28-)}$ to $\gamma\delta^{(16-)}$ and finally to $\gamma\delta^{(16+)}$. Following this line of reasoning, the most similar populations appear to be the $\gamma\delta^{(28-)}$ and $\gamma\delta^{(16-)}$

subsets. This could suggest that these are transitional populations that represent a bridge between the more distinct populations that are the $\gamma\delta^{(28+)}$ and $\gamma\delta^{(16+)}$ subsets.

This proposed sequence of differentiation is also supported when an alternative approach to differential analysis is taken i.e. when individual V γ 9V δ 2 T cell subsets are compared to remaining subsets grouped together as shown in Figure 4.12. This alternative method of differential analysis also supports the observation that $\gamma\delta^{(28+)}$ and $\gamma\delta^{(16+)}$ are the most distinct V γ 9V δ 2 T cell population subsets, with 81 differentially expressed genes in the $\gamma\delta^{(28+)}$ subset and 142 in the $\gamma\delta^{(16+)}$ subset compared to remaining grouped subsets. Again, the $\gamma\delta^{(28-)}$ and $\gamma\delta^{(16-)}$ subsets showed the least number of differentially expressed genes (0 and 6 differentially expressed genes respectively) compared to all other subsets grouped together, further supporting the proposition that they are transitional populations.

4.5.4 Further microarray analysis

Having identified the total number of differentially expressed genes between the four subsets, the list of genes was narrowed down to select those with obvious immune function. The full lists of immune-related differentially expressed genes are shown in figures 4.13 - 4.15 showing gene name/symbol, fold difference, p-value, heat-maps and gene function. No differentially expressed genes were observed when $\gamma\delta^{(28-)}$ cells were compared to other grouped subsets (Figure 4.12) and so differentially expressed immune-related gene comparisons are only shown for the $\gamma\delta^{(28+)}$, $\gamma\delta^{(16-)}$ and $\gamma\delta^{(28-)}$ subsets compared to the other grouped subsets.

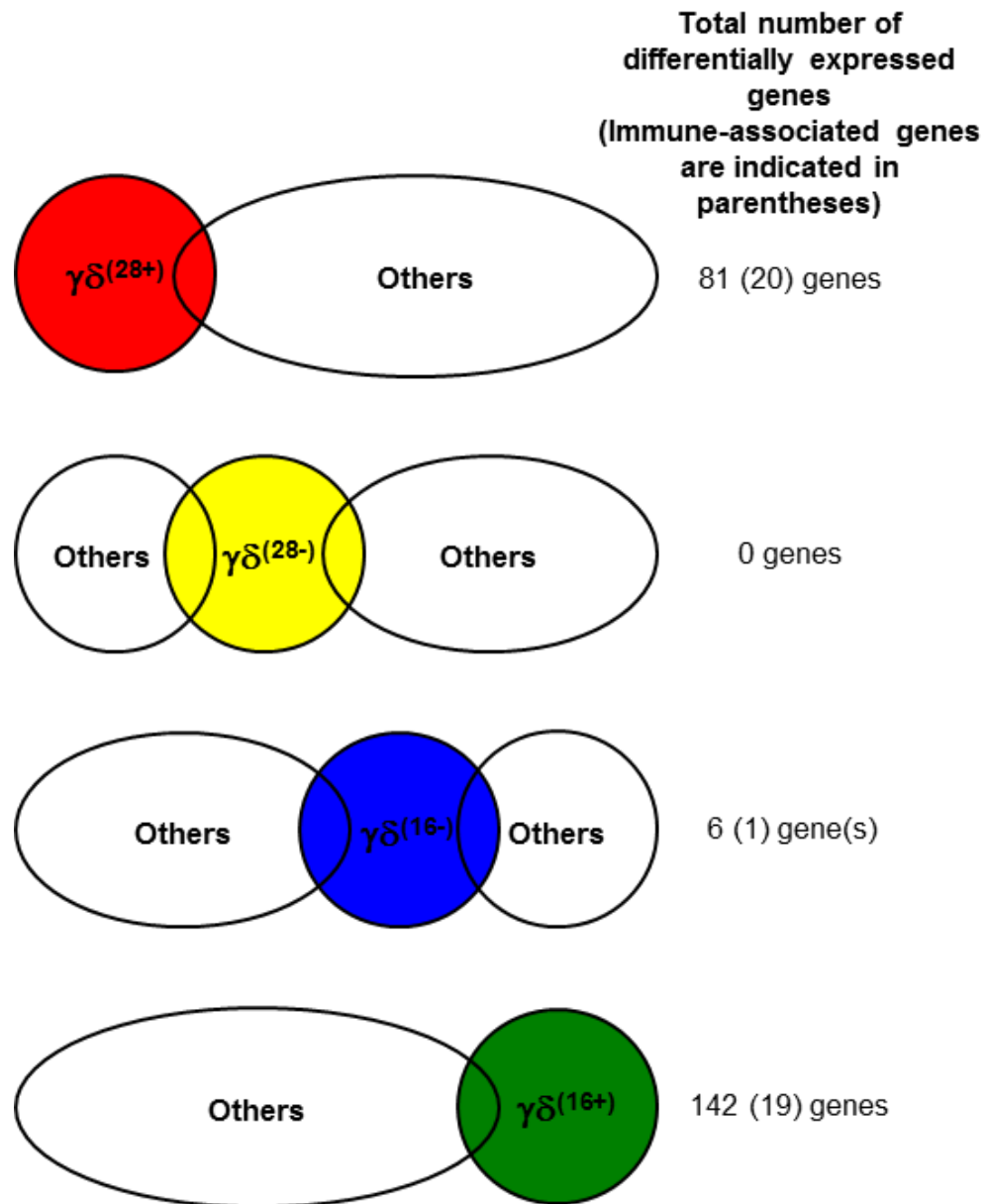
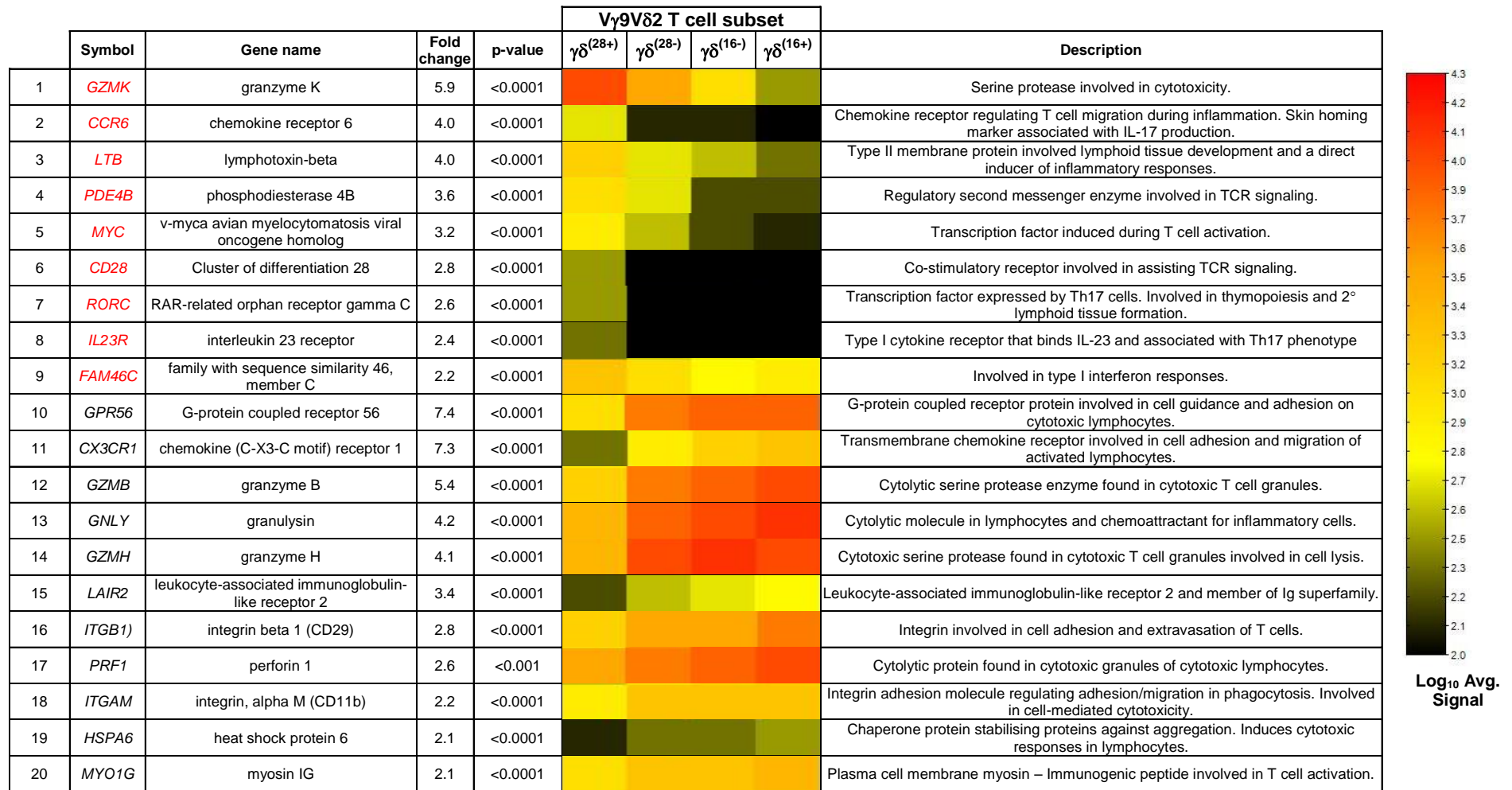


Figure 4.12 Total number of differentially expressed genes between individual V γ 9V δ 2 T cell subsets and the other populations grouped together.

Schematic shows the total number of differentially expressed gene probes when different V γ 9V δ 2 T cell subsets are compared against all other grouped V γ 9V δ 2 subsets. Differentially expressed genes are >2 fold different in expression levels ($p < 0.05$ – Bonferroni corrected). Genes with obvious immune function/links are indicated in parentheses and are a subset of the total number of differentially expressed genes.

$\gamma\delta^{(28+)}$ subset vs. [$\gamma\delta^{(28-)}$, $\gamma\delta^{(16-)}$ and $\gamma\delta^{(16+)}$] grouped subsets.



156

Figure 4.13 Differentially expressed genes with immune function in $\gamma\delta^{(28+)}$ T cells compared to the other three subsets grouped together

Table of genes indicates immune-related genes differentially expressed at > 2 fold difference ($p < 0.05$) in $\gamma\delta^{(28+)}$ cells compared to all non- $\gamma\delta^{(28+)}$ T cell subsets assessed as a group (others). The gene name, fold change, p-value, description of the gene, and heat map are indicated for each differentially expressed gene. The heat-maps indicate the relative difference in expression across populations showing gene expression levels ranging from background levels (black) to highest gene expression (red). Heat map scale values are \log_{10} transformed average signal intensities (fluorescence units). Gene symbols indicated in red are highest in the $\gamma\delta^{(28+)}$ subset with genes in black indicating genes significantly higher in the grouped non- $\gamma\delta^{(28+)}$ subsets.

$\gamma\delta^{(16-)}$ subset vs. [$\gamma\delta^{(28+)}$, $\gamma\delta^{(28-)}$ and $\gamma\delta^{(16+)}$] grouped subsets.

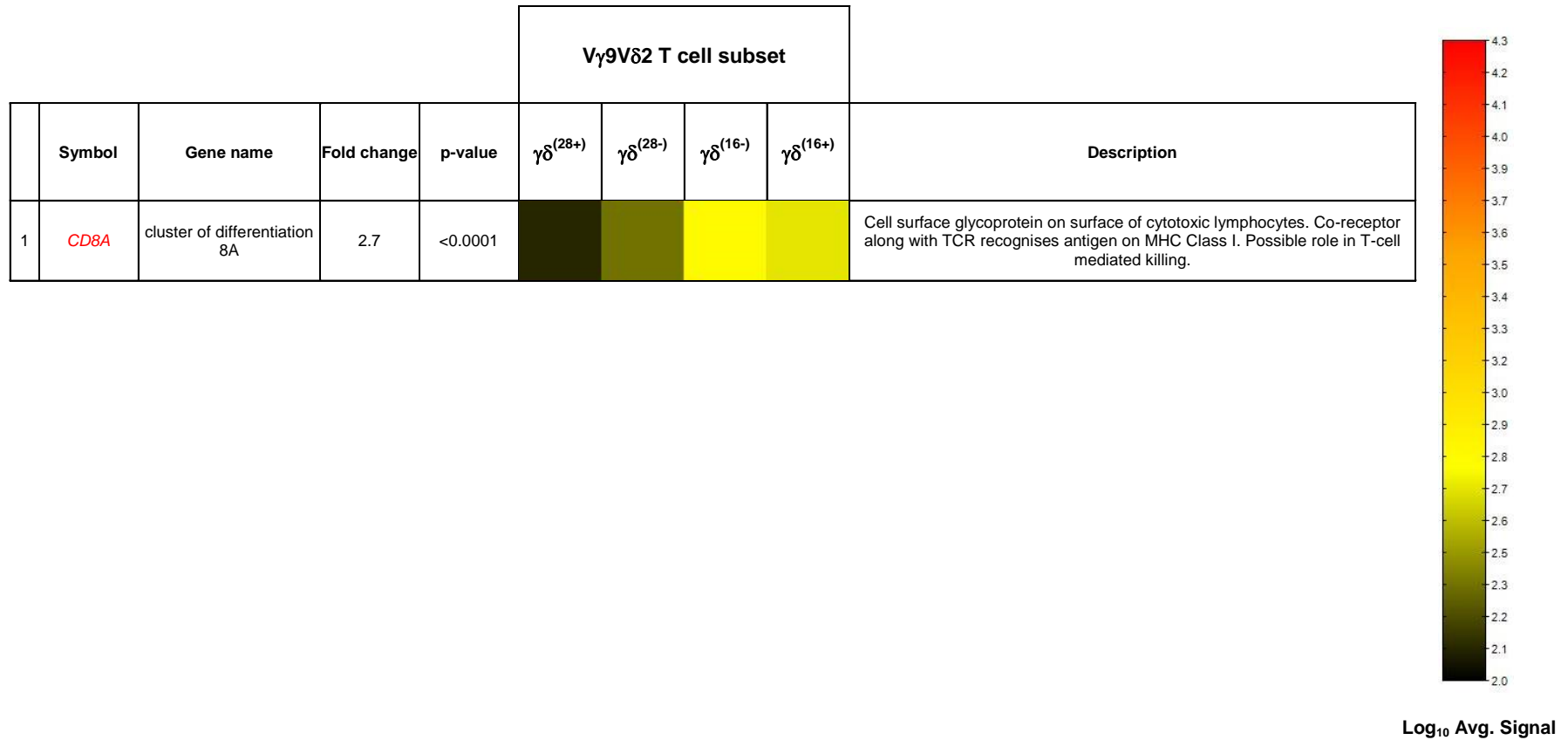


Figure 4.14 Differentially expressed genes in CD28⁽⁻⁾CD27⁽⁻⁾CD16⁽⁻⁾ V δ 2 T cells.

Table indicates the single immune-related gene differentially expressed at >2 fold difference ($p < 0.05$) in $\gamma\delta^{(16-)}$ cells compared to all non- $\gamma\delta^{(16-)}$ T cell subsets assessed as a group (others). The gene name, fold change, p-value, description of the gene, and heat map are indicated for the only immune-related differentially expressed gene. The heat-map indicates the relative difference in expression across populations showing gene expression levels ranging from background levels (black) to highest gene expression (red). Heat map scale values are \log_{10} transformed average signal intensities (fluorescence units). The gene symbol indicated in red is highest in the $\gamma\delta^{(16-)}$ subset.

$\gamma\delta^{(16+)}$ subset vs. [$\gamma\delta^{(28+)}$, $\gamma\delta^{(28-)}$, $\gamma\delta^{(16-)}$] grouped

	Symbol	Gene name	Fold change	p-value	$\gamma\delta$ T cell subset				Description
					$\gamma\delta^{(28+)}$	$\gamma\delta^{(28-)}$	$\gamma\delta^{(16-)}$	$\gamma\delta^{(16+)}$	
1	<i>CD3E</i>	CD3 epsilon chain	4.0	<0.0001	Yellow	Yellow	Yellow	Orange	Forms part of TCR. Involved in antigen recognition, T cell development and signalling.
2	<i>LSP1</i>	lymphocyte specific protein-1	2.6	<0.0001	Green	Green	Green	Yellow	Intracellular F-actin binding protein. Involved in trans-endothelial migration.
3	<i>KIR2DL3</i>	killer cell Ig-like receptor, two domains, long cytoplasmic tail, 3	2.6	<0.0001	Yellow	Orange	Yellow	Orange	Transmembrane regulatory glycoprotein and inhibitory receptor on the surface of cytotoxic lymphocytes preventing cell lysis.
4	<i>PACS1</i>	phosphofurin acidic cluster sorting protein 1	2.5	<0.0001	Green	Green	Green	Yellow	Coats proteins and controls localisation of trans-golgi network membrane proteins.
5	<i>KIR2DL4</i>	killer cell Ig-like receptor, two domains, long cytoplasmic tail, 4	2.4	0.0058	Yellow	Yellow	Yellow	Orange	Intracellularly expressed regulatory glycoprotein inside endosomes in cytotoxic lymphocytes regulating the immune response.
6	<i>ARHGEF1</i>	Rho guanine nucleotide exchange factor (GEF) 1	2.4	0.001	Yellow	Yellow	Yellow	Orange	Intracellular signalling molecule involved in cell mobility and migration and T_H2 cytokine responses and T cell signalling.
7	<i>FCAR</i>	Fc fragment of IgA receptor (CD89)	2.4	<0.0001	Yellow	Yellow	Yellow	Orange	Transmembrane glycoprotein on T cell surface involved in phagocytosis, cell-mediated cytotoxicity, and inflammatory mediator release.
8	<i>LY6E</i>	lymphocyte antigen 6 complex locus E	2.4	<0.0001	Orange	Orange	Orange	Red	Involved in signal transduction.
9	<i>BCL9L</i>	B-Cell CLL/lymphoma 9-like	2.3	<0.0001	Green	Green	Green	Yellow	Transcriptional regulator.
10	<i>SMAD7</i>	SMAD family member 7	2.2	0.0025	Green	Green	Yellow	Yellow	TGFB Type I receptor antagonist. Inhibits TGFB signaling.
11	<i>STXBP2</i>	syntaxin binding protein 2	2.1	<0.0001	Yellow	Yellow	Yellow	Orange	Protein involved in intracellular trafficking. Release of cytotoxic granules from cytotoxic cells.
12	<i>ITGB1</i>	integrin, beta 1 (CD29)	2.0	0.0185	Green	Yellow	Yellow	Yellow	Integrin involved in cell adhesion, recognition and facilitating extravasation of T cells.
13	<i>ABI3</i>	ABI gene family member 3	2.0	<0.0001	Yellow	Yellow	Yellow	Orange	Adaptor protein that inhibits tumour metastasis and reduces cell motility.
14	<i>CD27</i>	cluster of differentiation 27	12.4	0.0004	Orange	Orange	Black	Black	TNF-receptor (Co-stimulatory molecule) involved in TCR signalling and co-stimulation.
15	<i>CD160</i>	cluster of differentiation 160	3.4	0.0006	Orange	Orange	Yellow	Yellow	Cytotoxic activating receptor associated with cytotoxic T cells and cytotoxic effector activity.
16	<i>SIPA1</i>	signal-induced proliferation-associated protein 1	2.4	<0.0001	Orange	Orange	Orange	Orange	Involved in cell mobility and migration. Perinuclear mitogen induced GTPase activating protein (GAP). Reduces T cell adhesion to ICAM.
17	<i>HMHA1</i>	histocompatibility (minor) HA-1	2.2	<0.0001	Yellow	Yellow	Yellow	Yellow	Histocompatibility antigen involved in cytotoxic responses.
18	<i>SIRPG</i>	signal-regulatory protein gamma (CD172G)	2.1	<0.0001	Green	Green	Green	Black	Transmembrane glycoprotein and negative regulator of tyrosine kinase signalling processes
19	<i>IRF1</i>	interferon regulatory factor 1	2.1	<0.0001	Orange	Orange	Orange	Yellow	Regulatory transcription factor, induces cytotoxic function in T cells

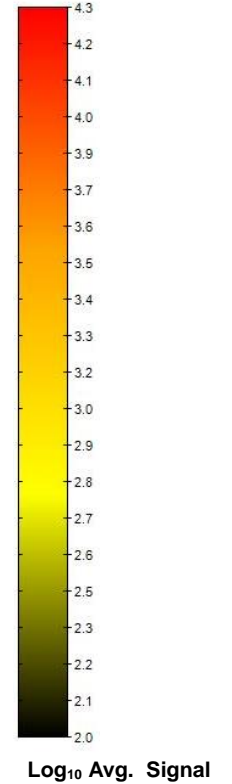


Figure 4.15 Differentially expressed genes with immune function in $\gamma\delta^{(16+)}$ T cells compared to the other three subsets grouped together

Table of genes indicates immune-related genes differentially expressed at > 2 fold difference ($p < 0.05$) in $\gamma\delta^{(16+)}$ cells compared to all non- $\gamma\delta^{(16+)}$ T cell subsets assessed as a group (others). The gene name, fold change, p-value, description of the gene, and heat map are indicated for each differentially expressed gene. The heat-maps indicate the relative difference in expression across populations showing gene expression levels ranging from background levels (black) to highest gene expression (red). Heat map scale values are \log_{10} transformed average signal intensities (fluorescence units). Gene symbols indicated in red are highest in the $\gamma\delta^{(16+)}$ subset with gene symbols in black indicating genes significantly higher in the grouped non- $\gamma\delta^{(16+)}$ subsets.

4.5.5 Transition from $\gamma\delta^{(28+)}$ to $\gamma\delta^{(28-)}$ subsets coincides with transcriptional regulation of cytotoxic proteins.

The expression of a number of cytotoxic proteins showed a significant upregulation in the three grouped CD28⁽⁻⁾ populations (the $\gamma\delta^{(28-)}$, $\gamma\delta^{(16-)}$ and $\gamma\delta^{(16+)}$ subsets), relative to the $\gamma\delta^{(28+)}$ subset ($p < 0.05$). These upregulated genes included; *GZMB* - Granzyme B (5.4-fold increased), *GZMH* - Granzyme H (4.1-fold increased) *GNLY* - Granulysin (4.2-fold increased), *GPR56* - G-protein coupled receptor 56 (7.4-fold increased) and *PRF1* - perforin (2.6-fold increased) (Figure 4.13). Thus, the transition from the $\gamma\delta^{(28+)}$ subset to the $\gamma\delta^{(28-)}$ i.e. the downregulation of CD28, appears to be the point at which many important cytotoxic genes increase their expression levels in V γ 9V δ 2 T cells. This may indicate a significant point in V γ 9V δ 2 T cell differentiation in which cells switch to a more cytotoxic phenotype.

One exception to this pattern of cytotoxic protein expression was seen in Granzyme K, which was significantly higher in $\gamma\delta^{(28+)}$ cells compared to CD28⁽⁻⁾ populations ($p < 0.0001$). Validation of the expression of Granzyme B and Granzyme K were carried out using flow cytometry (Figure 4.16 and 4.17). This showed an opposing pattern of expression in which a higher percentage of Granzyme B was observed in the CD28⁽⁻⁾ populations compared to $\gamma\delta^{(28+)}$ cells, which reached statistical significance when the $\gamma\delta^{(28+)}$ and $\gamma\delta^{(16-)}$ subsets were compared ($p=0.003$). By contrast, expression of Granzyme K was predominantly seen in the $\gamma\delta^{(28+)}$ subset, with significantly higher percentage of Granzyme K⁽⁺⁾ cells compared to the CD27⁽⁻⁾ subsets ($\gamma\delta^{(16-)}$ ($p=0.04$) and $\gamma\delta^{(16+)}$ ($p < 0.0001$)) as shown in figure 4.17.

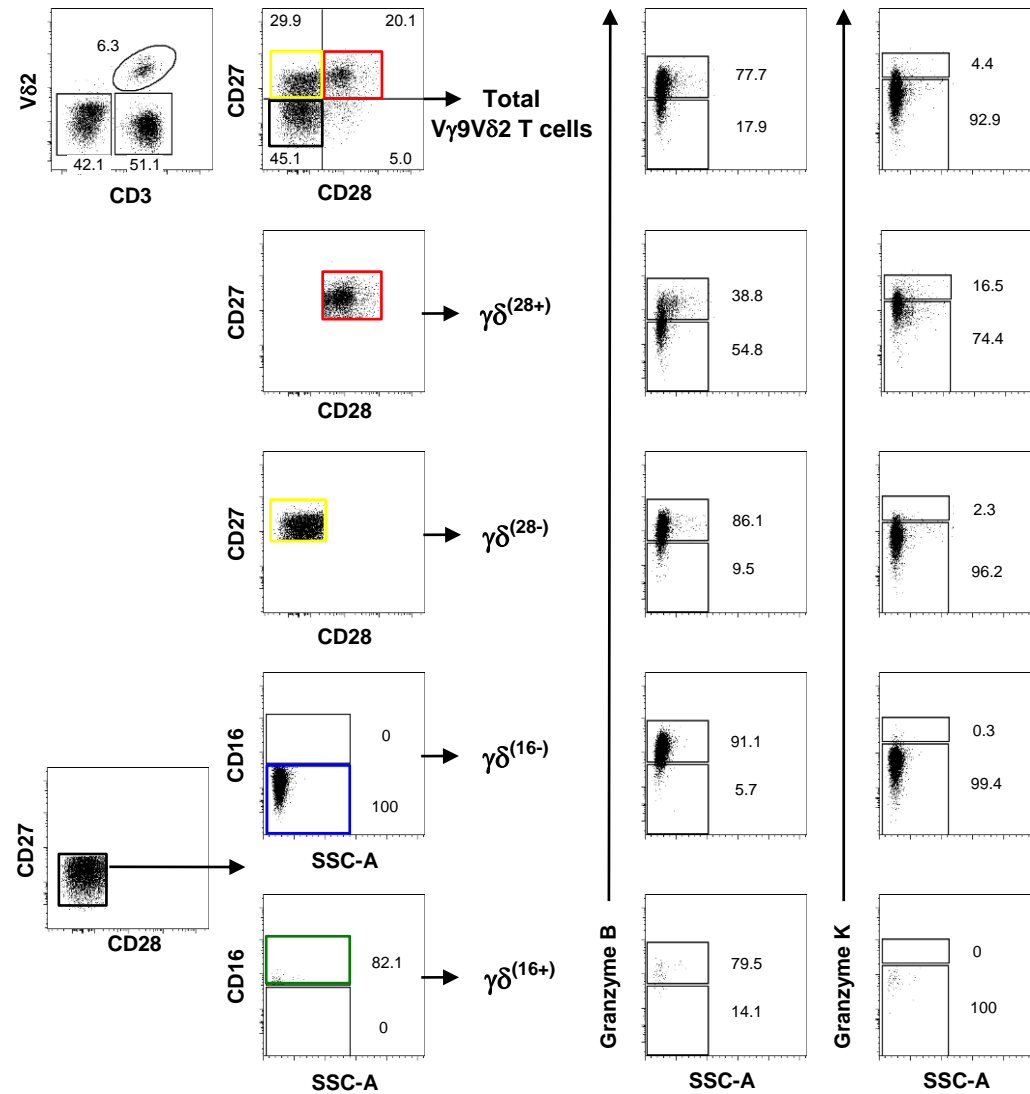


Figure 4.16 Granzyme B and Granzyme K expression for V γ 9V δ 2 T cell subsets.

Flow cytometry dot plots showing expression of Granzyme K and Granzyme B for V γ 9V δ 2 T cell subsets in a single representative sample. V γ 9V δ 2 T cell subsets are defined as; $\gamma\delta^{(28+)}$ [CD28⁽⁺⁾CD27⁽⁺⁾] (red box), $\gamma\delta^{(28-)}$ [CD28⁽⁻⁾CD27⁽⁺⁾] (yellow box), $\gamma\delta^{(16-)}$ [CD28⁽⁻⁾CD27⁽⁻⁾CD16⁽⁻⁾] (blue box) and $\gamma\delta^{(16+)}$ [CD27⁽⁻⁾CD28⁽⁻⁾CD16⁽⁺⁾] (green box).

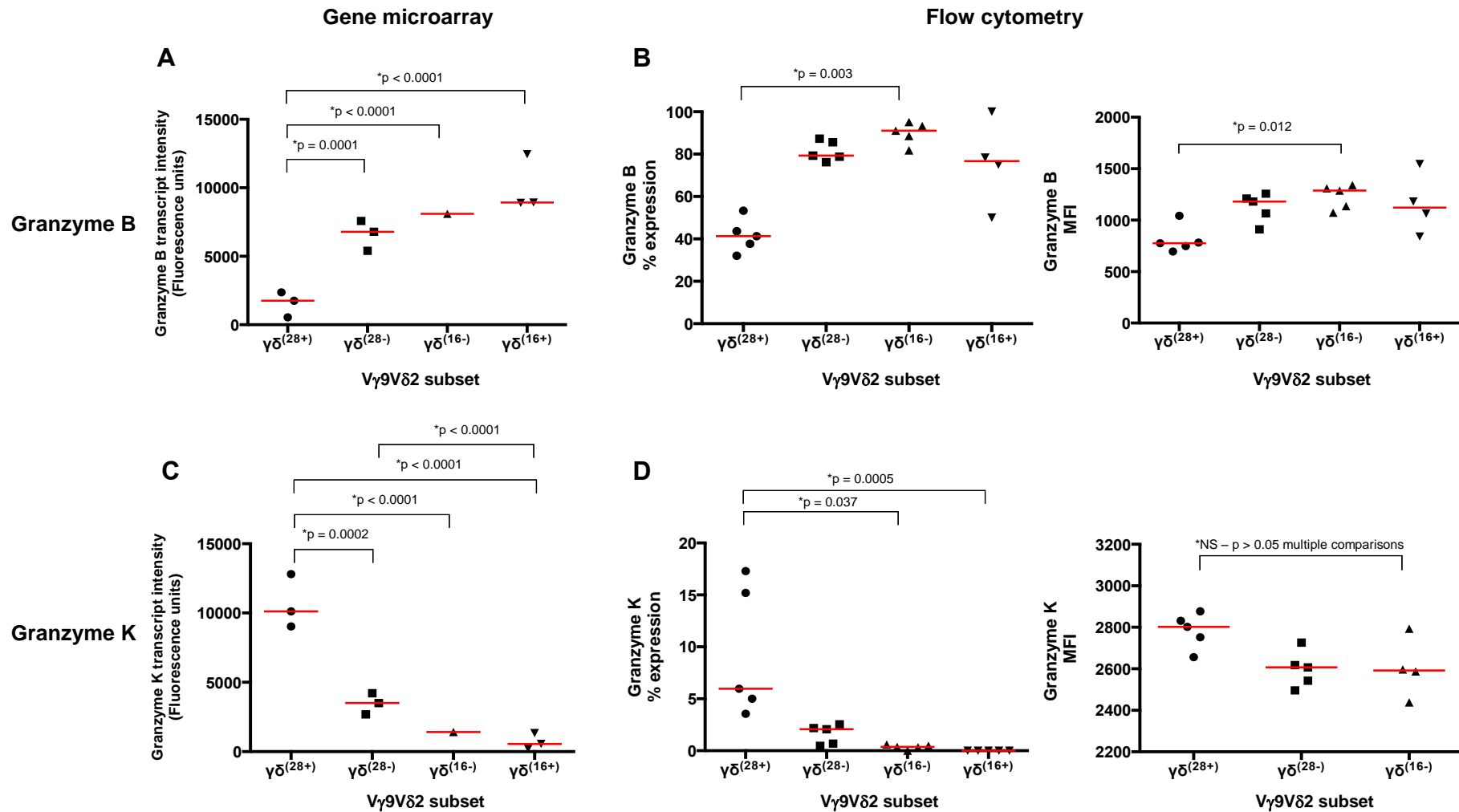


Figure 4.17 Summary of expression levels of granzyme B and granzyme K on V γ 9V δ 2 T cell subsets.

Microarray data for granzyme B and granzyme K are shown for V γ 9V δ 2 T cell subsets (A and C), with transcript intensities (fluorescence units) shown for each subset replicate. Flow cytometry data from five healthy individuals showing percentage of V γ 9V δ 2 T cell subset that express granzyme B or granzyme (B and D) and the median fluorescent intensities (MFIs) for positive cells. V γ 9V δ 2 T cell subsets are defined as; $\gamma\delta^{(28+)}$ [CD28⁽⁺⁾CD27⁽⁺⁾], $\gamma\delta^{(28-)}$ [CD28⁽⁻⁾CD27⁽⁺⁾], $\gamma\delta^{(16-)}$ [CD28⁽⁻⁾CD27⁽⁻⁾CD16⁽⁻⁾] and $\gamma\delta^{(16+)}$ [CD28⁽⁻⁾CD27⁽⁻⁾CD16⁽⁺⁾]. Median values are indicated in red.

4.5.6 Genes associated with an IL-17 secreting phenotype are expressed in the $\gamma\delta^{(28+)}$ subset

Chemokine (C-C Motif) Receptor 6 (*CCR6*), Interleukin-23 Receptor (*IL-23R*) and RAR-Related Orphan Receptor C (*RORC*) are associated with an IL-17 producing phenotype. Interestingly, the array data revealed that these genes are expressed at significantly higher levels in the $\gamma\delta^{(28+)}$ subset compared to the $CD28^{(-)}$ populations ($p < 0.0001$) (Figure 4.13). Following the downregulation of CD28, these IL17-associated genes demonstrated a complete loss of expression in the subsequent $\gamma\delta^{(28-)}$, $\gamma\delta^{(16-)}$ and $\gamma\delta^{(16+)}$ subsets, suggesting that the $\gamma\delta^{(28+)}$ population is the only subset with the transcriptional machinery to potentially produce IL17.

However, although the expression of these IL-17-associated genes might be necessary to produce this pro-inflammatory cytokine, they are clearly not sufficient, as there was little or no production of IL-17 in any of the $V\gamma9V\delta2$ T cell subsets when intracellular cytokine production was assessed (Figure 4.4). Nonetheless, future work will attempt to differentially generate IL-17-secreting $\gamma\delta$ T cells (something that heretofore has proved problematic), using this new valuable insight into which $\gamma\delta$ T cells may be capable of secreting this cytokine.

4.5.7 CCR6 and CX3CR1 show opposing patterns of gene expression in $V\gamma9V\delta2$ T cell subsets

The microarray data indicated that chemokine receptors *CCR6* and *CX3CR1* showed opposing patterns of expression when $\gamma\delta^{(28+)}$ cells were compared with the other $CD28^{(-)}$ populations (Figure 4.13). Whilst *CCR6* seemed to be exclusively expressed in the $\gamma\delta^{(28+)}$ subset, *CX3CR1* seems to be low in the

$\gamma\delta^{(28+)}$ subset and increase significantly in the $CD28^{(-)}$ subsets ($p < 0.0001$). Once again, the downregulation of CD28 seemed to represent a significant point in the transition of expression for these chemokine receptors. Thus, to validate the array data, flow cytometry was used to investigate the expression of *CCR6* and *CX3CR1* on the cell surface of all $V\gamma9V\delta2$ T cell subsets in 5 different healthy individuals (Figure 4.18 and Figure 4.19). As suggested by the array, *CCR6* was exclusively expressed on a significant proportion ($\approx 30-40\%$) of the $\gamma\delta^{(28+)}$ population and was absent from the three $CD28^{(-)}$ subsets. By contrast, *CX3CR1* was expressed predominantly in the $CD28^{(-)}$ subsets, but was also expressed by a significant proportion of the $\gamma\delta^{(28+)}$ subset (median=42.5%). Quite strikingly, the expression of *CCR6* and *CX3CR1* in the $\gamma\delta^{(28+)}$ subset was mutually exclusive, seeming to neatly divide the $\gamma\delta^{(28+)}$ subset into two distinct further subsets i.e. a $CCR6^{(+)}CX3CR1^{(-)}$ and a $CCR6^{(-)}CX3CR1^{(+)}$ subset. This suggests that within the $\gamma\delta^{(28+)}$ subset, there are two distinct subsets with a potentially important further transition between the two.

4.5.8 Adhesion and migration associated proteins increase across the four $V\gamma9V\delta2$ T cell subsets

Genes associated with a number of adhesion and migratory proteins also seem to show a consistent pattern of change across the four $V\gamma9V\delta2$ T cell subsets. G-protein coupled receptor 56 (*GPR56*), integrin alpha M (*ITGAM*), and integrin, beta 1 (*ITGB1*) all show significantly increased expression in the three $CD28^{(-)}$ subsets relative to $\gamma\delta^{(28+)}$ cells (Figures 4.13 and 4.15).

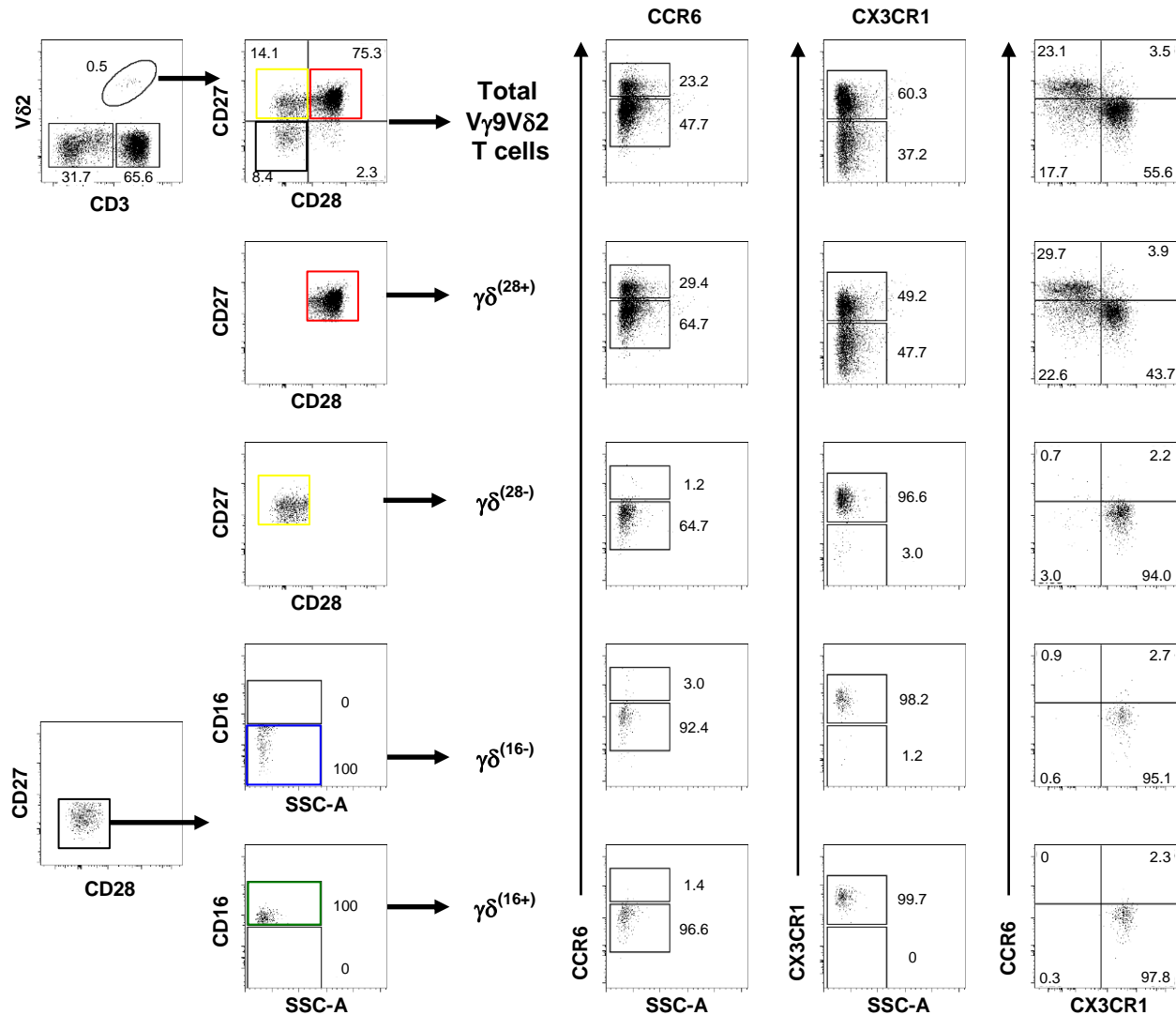


Figure 4.18 CCR6 and CX3CR1 expression subdivides $\gamma\delta^{(28+)}$ $V\gamma 9V\delta 2$ T cells into two further distinct subsets.

Flow cytometry dot plots showing expression of CCR6 and CX3CR1 on $V\gamma 9V\delta 2$ T cell subsets. CCR6/CX3CR1 bi-variate plots are also shown to show the relationship of both markers relative to each other on each $V\gamma 9V\delta 2$ subset. $V\gamma 9V\delta 2$ subsets are defined as; $\gamma\delta^{(28+)}$ [$CD28^{(+)CD27^{(+)}$] (red), $\gamma\delta^{(28-)}$ [$CD28^{(-)CD27^{(+)}$] (yellow box), $\gamma\delta^{(16-)}$ [$CD28^{(-)CD27^{(-)CD16^{(-)}}$] (blue box) and $\gamma\delta^{(16+)}$ [$CD28^{(-)CD27^{(-)CD16^{(+)}$] (green box).

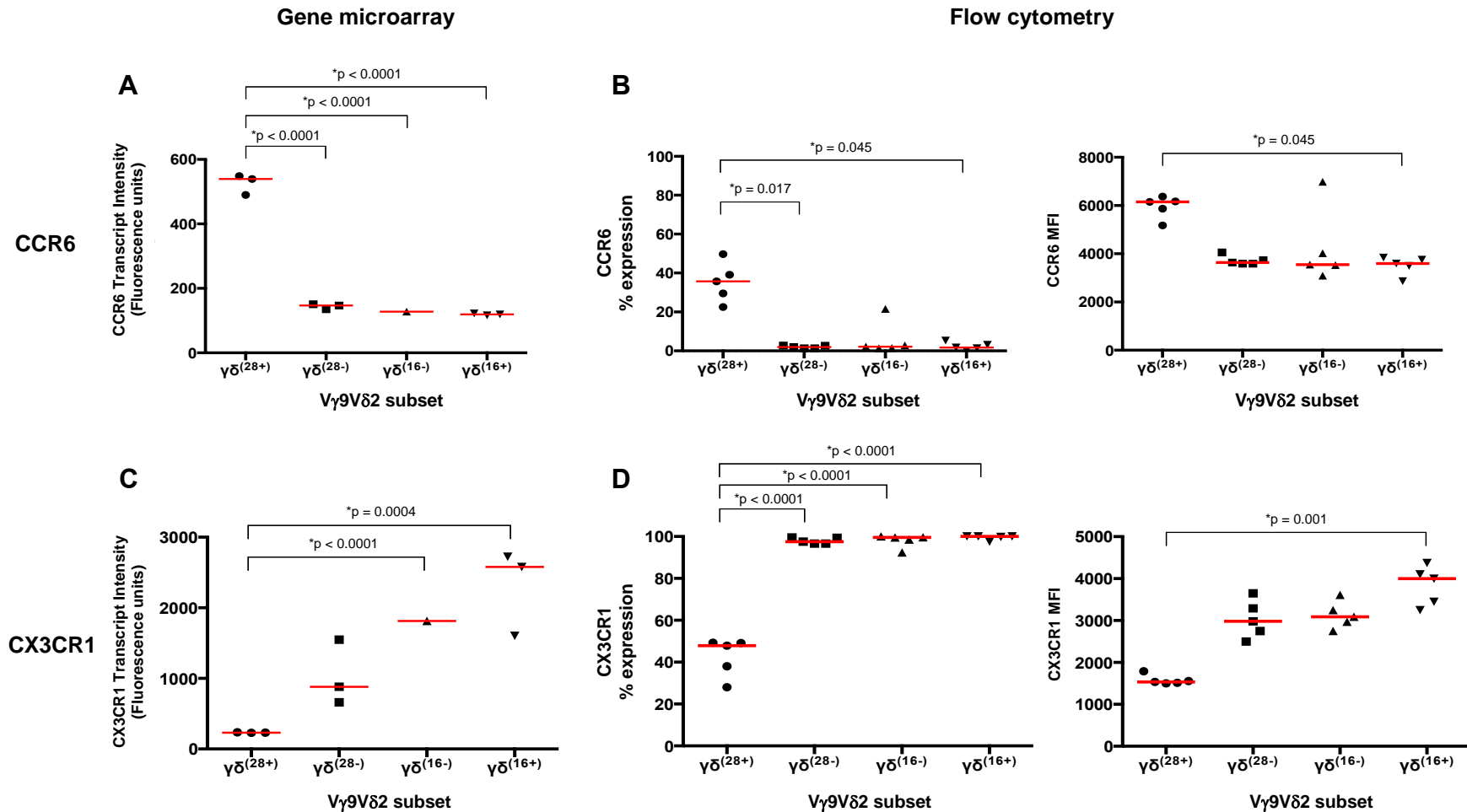


Figure 4.19 Summary of expression levels of CCR6 and CX3CR1 on Vγ9Vδ2 T cell subsets.

Microarray data for CCR6 and CX3CR1 are shown for Vγ9Vδ2 T cell subsets (A and C), with transcript intensities (fluorescence units) shown for each subset replicate. Flow cytometry data from five healthy individuals showing the percentage of each Vγ9Vδ2 T cell subset that express CCR6 or CX3CR1 (B and D) and the median fluorescent intensities (MFIs) for positive cells are shown. Vγ9Vδ2 T cell subsets are defined as; $\gamma\delta^{(28+)}$ [CD28⁽⁺⁾CD27⁽⁺⁾], $\gamma\delta^{(28-)}$ [CD28⁽⁻⁾CD27⁽⁺⁾], $\gamma\delta^{(16-)}$ [CD28⁽⁻⁾CD27⁽⁻⁾CD16⁽⁻⁾] and $\gamma\delta^{(16+)}$ [CD28⁽⁻⁾CD27⁽⁻⁾CD16⁽⁺⁾]. Median values are indicated in red.

Rho guanine nucleotide exchange factor 1 (*ARHGEF1*) and lymphocyte-specific protein 1 (*LSP1*) also demonstrate this same increase across the subsets, but are expressed significantly higher in the $\gamma\delta^{(16+)}$ subset compared to the three $CD16^{(-)}$ subsets (Figure 4.15). Overall there seems to be an increase in the expression of genes associated with adhesion and migration in $\gamma\delta^{(16+)}$ subsets compared to the $\gamma\delta^{(28+)}$ cells, suggesting an increased ability to home to tissues and sites of inflammation/infection.

4.5.9 Increase in KIR regulatory proteins in the $\gamma\delta^{(16+)}$ subset

Two of the Killer cell Ig-like Receptor regulatory genes (*KIR2DL3* and *KIR2DL4*) were both significantly differentially expressed in the $\gamma\delta^{(16+)}$ subset compared to all the three $CD16^{(-)}$ populations with respective fold difference and p-values of (fold change 2.6, $p < 0.001$) and (2.4 fold change, $p = 0.006$) (Figure 4.15). The surface expressed receptor *KIR2DL3* is as an inhibitory receptor thought to regulate cytotoxic T cell responses, with the related *KIR2DL4* receptor only expressed inside endosomes and conversely thought to be mildly pro-inflammatory in regulating pro-inflammatory cytokine release from cells (e.g. $IFN-\gamma$, $TNF-\alpha$ and $IL-1\beta$) (Rajagopalan and Long 2012).

4.6 Summary

In general, all $V\gamma9V\delta2$ T cell subsets produce $IFN-\gamma$ and $TNF-\alpha$, but not $IL-17$. The $\gamma\delta^{(28+)}$ and $\gamma\delta^{(28-)}$ subsets (i.e. the $CD27^{(+)}$ populations) demonstrated the highest proliferative potential. The $\gamma\delta^{(N)}$ subset, identified as $[CD27^{(Hi)}CD11a^{(Lo)}]$ expressed high levels of *CCR7* and *CD62L* but displayed a wide range of *CD45RA* expression. The $\gamma\delta^{(28+)}$ subset seemed to be the most distinct of all the populations, containing two further non-overlapping subsets, defined by

mutually exclusive expression of CCR6 and CX3CR1 (i.e. CCR6⁽⁺⁾CX3CR1⁽⁻⁾ and CCR6⁽⁻⁾CX3CR1⁽⁺⁾ subsets). $\gamma\delta^{(28+)}$ cells was also characterised by high levels of CCR2 and CCR5 surface expression, low CD45RA expression and interestingly high levels of *RORC*, *IL-23R* and *CCR6*, three genes associated with the secretion of IL-17. $\gamma\delta^{(16+)}$ cells also appeared to represent a distinct cytotoxic subset, expressing the highest levels of CD45RA, the lowest levels of CCR2 and CCR5 and the highest level of Perforin. $\gamma\delta^{(16+)}$ cells additionally showed the highest transcriptional levels of a number of cytotoxicity-associated genes including perforin, granzyme B, granzyme H and granulysin. $\gamma\delta^{(28-)}$ and $\gamma\delta^{(16-)}$ subsets appear to be much less distinct in terms of surface marker and gene expression, possibly representing transitional cell populations, with intermediate levels of gene expression between the predominant and more distinct $\gamma\delta^{(28+)}$ and $\gamma\delta^{(16+)}$ subsets.

Chapter 5

Probability state modelling of $\gamma\delta$ T cell differentiation

Chapter 5 Probability state modelling of $\gamma\delta$ T cell differentiation

5.1 Introduction

One of the main problems with multi-parameter flow cytometry data is the difficulty in understanding how multiple parameters relate to each other within a single sample. Whilst the identification of subsets is straightforward when using just two markers, it becomes extremely challenging when multiple markers are used.

Furthermore, there is a high degree of user subjectivity when setting gates and deciding which cells to investigate further. Thus, there exists a pressing need to remove these biases, and return to a more objective method of analysis. In relation to the work of this thesis, the hypothesis that V γ 9V δ 2 T cells differentiated through a series of stages, for example from $\gamma\delta^{(28+)}$ to $\gamma\delta^{(28-)}$ to $\gamma\delta^{(16-)}$ to $\gamma\delta^{(16+)}$, was difficult to test using conventional manual methods of FACS analysis, due to the multiple markers used, and the widely differing phenotypes of our cohort of healthy volunteers. Thus we used a relatively new analysis tool called Probability State Modelling (PSM), using the GemStone software from Verity Software House to assess our multiple datasets in as unbiased a manner as possible. This software allows all parameters to be visualised on a single plot, removing the subjectivity of user-defined gating, and allowing possible pathways of differentiation to be modelled objectively.

5.2 Generating a probability state model (PSM) for human V γ 9V δ 2 T cells

To generate a probability state model (PSM) for any system of cell differentiation a number of assumptions need to be made. First, it should be assumed that the various phenotypes that can be identified by flow cytometry represent stages along a pathway of differentiation. For V γ 9V δ 2 T cells based on the literature (Dieli *et al.* 2003b, Puan *et al.* 2009, De Rosa *et al.* 2004, Yokobori *et al.* 2009, Angelini *et al.* 2004) and our aforementioned studies, we would propose a differentiation pathway that started with the $\gamma\delta^{(28+)}$ subset and ended with the $\gamma\delta^{(16+)}$ subset with the $\gamma\delta^{(28-)}$ and $\gamma\delta^{(16-)}$ subsets placed tentatively in the middle. Additionally, for each of the markers considered in the model (i.e. V δ 2, CD3, CD28, CD27, CD16, CD45RA and CD11a.) a likely progression (e.g. start high, end low, or constant throughout etc.) should be inputted to guide generation of the model. The software then uses these assumptions to generate a model that represents the real expression values of the various cells in the samples run on the flow cytometer.

Figure 5.1 shows some of the expression level assumptions used to generate a model for V γ 9V δ 2 T cell differentiation. These include; CD27- 3-step down; CD28- 2-step down; CD16- 2-step up; CD45RA- 3-step, down followed by step-up; and CD11a- 2-step up. To generate an average PSM for V γ 9V δ 2 T cell differentiation we used 15 healthy volunteer samples. It was important to select individuals with all four subsets so that any relationships between these populations could be modelled. Thus, fifteen individuals with phenotypic signature profiles (2,3 and 4) were selected for modelling.

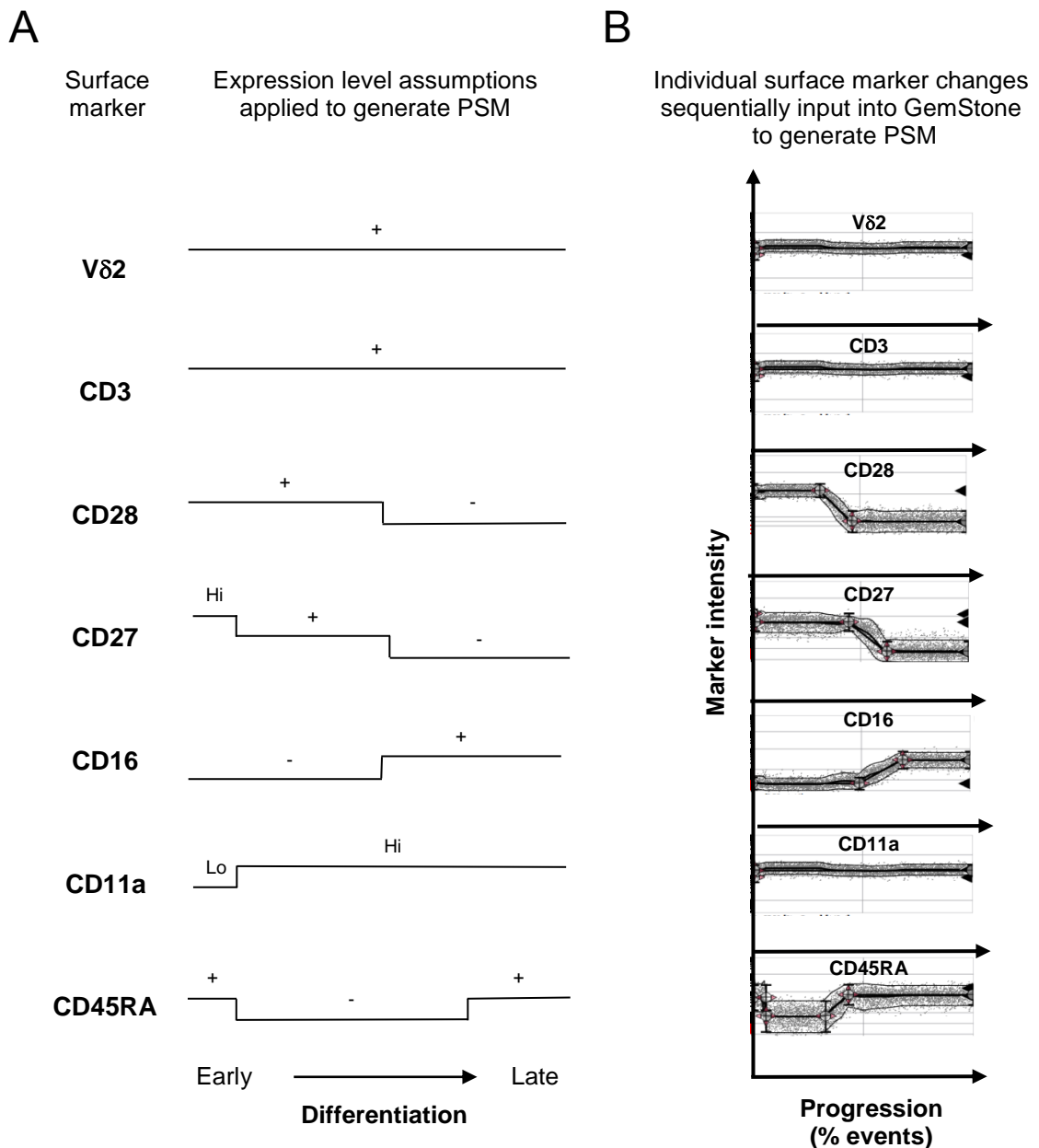


Figure 5.1 Expression level assumptions for various markers used to generate a probability state model (PSM) for V γ 9V δ 2 T cell differentiation.

(A) Shows the assumed changes in surface marker expression intensity used to generate a PSM for V γ 9V δ 2 T cell differentiation. (B) Shows an example of the surface marker intensity of sequential markers input into GemStone to generate the PSM model from the assumed changes indicated in (A).

Using the 15 samples, the GemStone software was able to generate an average PSM for V γ 9V δ 2 T cell differentiation. Essentially, the software uses the basic assumptions for the expression of the various markers to try to order the cells in a differentiation pathway. As an example, we used a simple “step-

down” rule for CD28 i.e. CD28 expression starts high and then at some point is downregulated. The software uses this rule to place cells with high CD28 at the start, with those with low CD28 placed at the end. It then sees whether the next rule for the next marker is compatible with the suggested order of cells, and so on. A model will only be generated if the cells can be ordered in a way that satisfies all the rules. Figure 5.2 shows the average PSM for the 15 selected samples. The relative intensity of each marker expression as cells progress along a proposed differentiation pathway is shown. “Control Definition Points” (CDPs) indicated by white diamonds show the average point at which a surface marker changes, with “d” indicating the distance (%) along the cumulative progression (i.e. % of events between the start and end of the transitional change on the cumulative progression axis) and r indicating the correlation coefficient for each statistically significant transitional change ($p < 0.01$). The thickness of each line represents the 95% confidence limits of relative intensity of each marker.

5.3 The PSM suggests that the $\gamma\delta^{(28-)}$ and $\gamma\delta^{(16-)}$ subsets are not distinct, but instead represent transitional populations

According to the PSM created for $V\gamma 9V\delta 2$ T cell differentiation (Figure 5.2) the initial $\gamma\delta^{(N)}$ subset is characterised as $[CD27^{(Hi)}, CD11a^{(Lo)}, CD45RA^{(+)}, CD28^{(+)}, CD16^{(-)}]$ and is only a small population making up $\approx 2\%$ of the total $V\gamma 9V\delta 2$ T cell pool. This population is followed by the $\gamma\delta^{(28+)}$ subset, representing over 50% of $V\gamma 9V\delta 2$ T cells and characterised as $[CD28^{(+)}CD27^{(+)}CD45RA^{(-)}CD16^{(-)}]$.

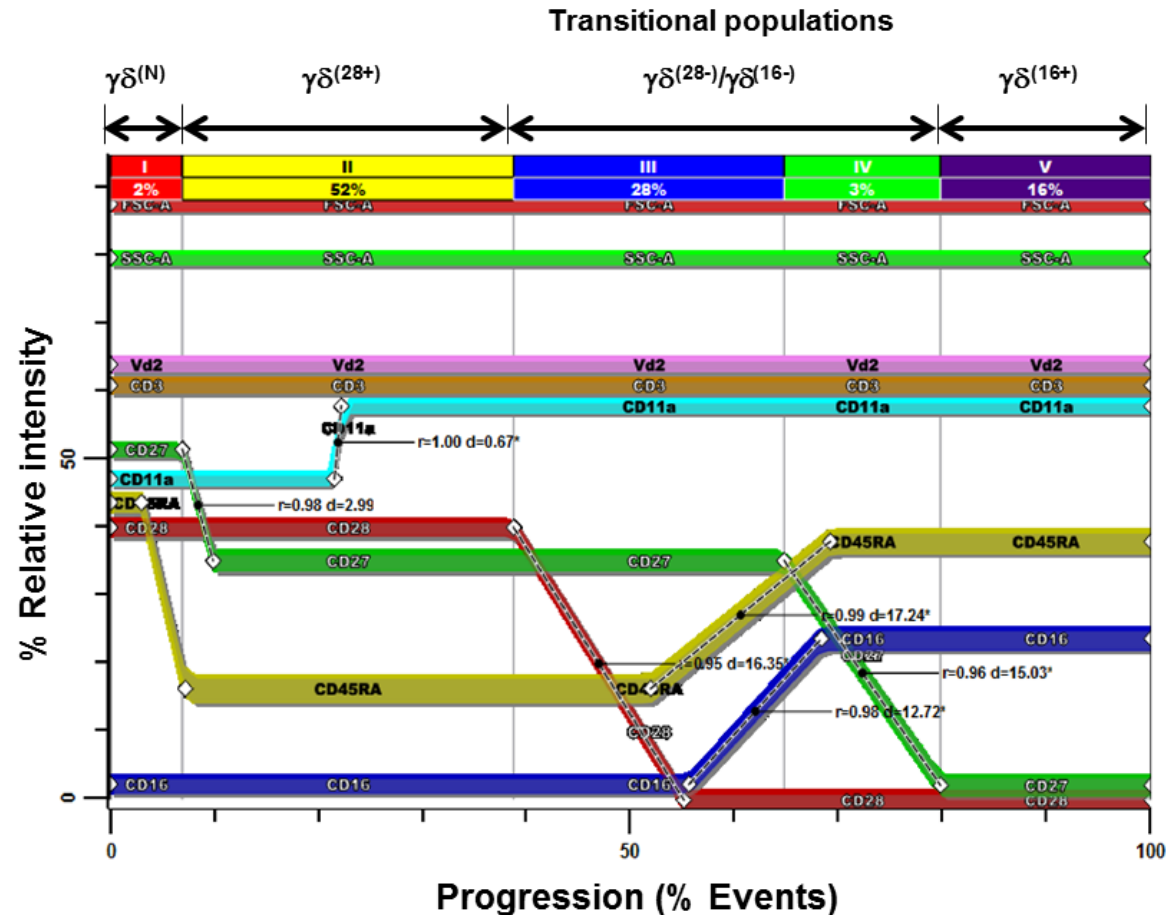


Figure 5.2 Average probability state model for V γ 9V δ 2 T cell differentiation.

An average probability state model derived from 15 healthy volunteers is shown for the markers (CD28, CD27, CD11a, CD16, and CD45RA) on V δ 2⁽⁺⁾CD3⁽⁺⁾ T cells. The relative intensity (%) of surface marker expression (y-axis) is indicated along a cumulative progression axis (x-axis), which acts as a surrogate measure of time. White diamonds indicate Control Definition Points (CDPs), which show the average position along the cumulative progression axis at which each marker expression changes. Dotted lines indicate the distance along the cumulative progression axis (d) between CDPs at the start and end of transitional change. Correlation coefficients (r-values) are indicated for each statistically significant CDP transitional change ($p < 0.01$). The thickness of each band in the progression plot is proportional to the 95% confidence limits.

The next transition involves the downregulation of CD28 which consistently occurs before CD27, and gives rise to the $\gamma\delta^{(28-)}$ subset [CD28⁽⁻⁾CD27⁽⁺⁾]. However, following downregulation of CD28 there is a period of dynamic marker change that involves upregulation of CD16 and CD45RA and downregulation of CD27. This somewhat blurs a boundary between the $\gamma\delta^{(28-)}$ and $\gamma\delta^{(16-)}$ subsets and suggests that cells with these features are undergoing a transitional phase in which 3 markers may change at about the same time. Finally, a stable end population emerges, the $\gamma\delta^{(16+)}$ subset [CD27⁽⁻⁾ CD28⁽⁻⁾CD16⁽⁺⁾CD45RA⁽⁺⁾].

5.4 V γ 9V δ 2 T cells do not share the same differentiation pathway as $\alpha\beta$ T cells.

Having constructed a PSM for V γ 9V δ 2 T cells that suggested a $\gamma\delta^{(28+)} \rightarrow \gamma\delta^{(28-)} / \gamma\delta^{(16-)} \rightarrow \gamma\delta^{(16+)}$ differentiation sequence, we next compared this model to one for $\alpha\beta$ T cells from the same individual. Figure 5.3 shows a comparison of PSMs from a single person for both V γ 9V δ 2 T cells and TCR $\gamma\delta^{(-)}$ CD3⁽⁺⁾ T cells (predominantly $\alpha\beta$ T cells).

This demonstrates that V γ 9V δ 2 T cells do not follow a similar differentiation pathway to conventional $\alpha\beta$ T cells. For example, for $\alpha\beta$ T cells, four distinct subsets are seen on a CD27/CD45RA plot with the PSM clearly predicting a CD27⁽⁺⁾CD45RA⁽⁺⁾ \rightarrow CD27⁽⁺⁾CD45RA⁽⁻⁾ \rightarrow CD27⁽⁻⁾CD45RA⁽⁻⁾ \rightarrow CD27⁽⁻⁾CD45RA⁽⁺⁾ differentiation pathway, as suggested by numerous studies (Okada *et al.* 2008, Libri *et al.* 2011, Di Mitri *et al.* 2011). However, despite a similar pathway being suggested in the literature for V γ 9V δ 2 T cells (Dieli *et al.* 2003b), the PSM predicts something quite different (Figure 5.3), confirming our initial view that the use of CD27 and CD45RA to describe V γ 9V δ 2 T cells was not appropriate.

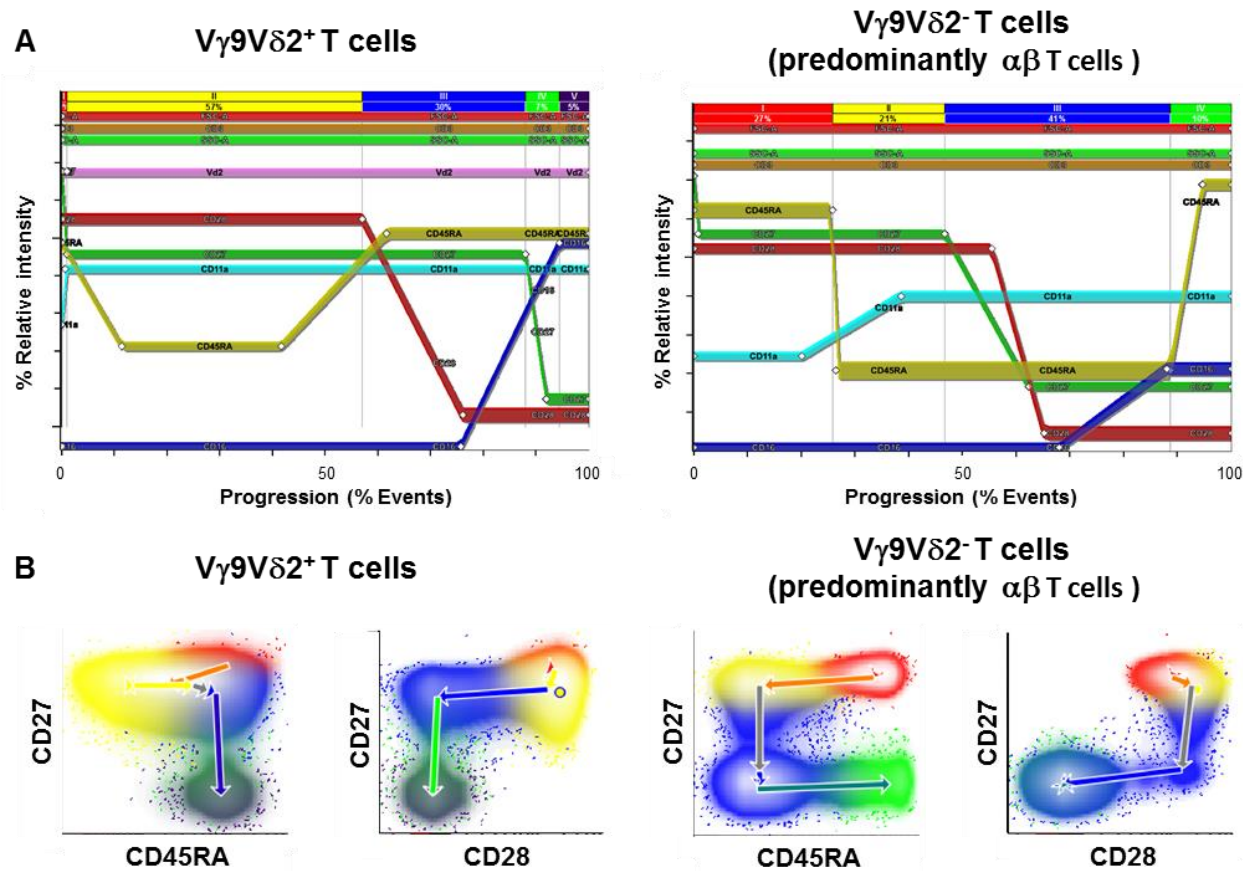


Figure 5.3 Probability state model for V γ 9V δ 2⁽⁺⁾ and V γ 9V δ 2⁽⁻⁾ T cells suggest a different sequence of differentiation.

(A) Probability State Modelling (PSM) progression plots are shown for V γ 9V δ 2⁽⁺⁾ and V γ 9V δ 2⁽⁻⁾ T cells (predominantly $\alpha\beta$ T cells), for a single healthy volunteer PBMC sample using surface markers (CD27, CD45RA, CD28, CD11a and CD16) on V δ 2⁽⁺⁾CD3⁽⁺⁾ T cells. White diamonds indicate control definition points (CDPs) at which each surface marker expression changes. The thickness of each band is proportional to the 95% confidence limits. Colour key for surface marker lines; Pink=V δ 2, Orange=CD3, Red=CD28, Yellow=CD45RA, Green=CD27, Light blue=CD11a, Dark blue=CD16, Light green =SSC-A and Light red FSC-A. Major subsets (I-IV/V) are indicated on top of each progression plot as modelled by PSM with percentage in each subset indicated below. (B) Two parameter density plot histograms (CD27 v CD45RA) and (CD27 v CD28) are shown for V γ 9V δ 2⁽⁺⁾ and V γ 9V δ 2⁽⁻⁾ T cells from the same individual with arrows indicating the proposed differentiation pathway.

This difference in proposed differentiation is also clearly evident. From the PSMs translated onto CD27/CD28 plots. A major difference here is the order of CD28 and CD27 downregulation, with CD28 preceding CD27 for V γ 9V δ 2 T cells, but CD27 preceding CD28 for $\alpha\beta$ T cells (Figure 5.3).

5.5 Summary

The use of probability state modelling allowed the relationship of multiple markers to be determined in V γ 9V δ 2 T cells. Overall, PSM confirmed the existence of two major V γ 9V δ 2 T cell populations; $\gamma\delta^{(28+)}$ and $\gamma\delta^{(16+)}$, at the possible start and end of a proposed differentiation process, with intermediate transitional populations $\gamma\delta^{(28-)}$ and $\gamma\delta^{(16-)}$ that perhaps should be considered as a single population, in between. Importantly, whilst PSM modelling confirms the much-published differentiation pathway of conventional $\alpha\beta$ T cells i.e. $CD27^{(+)}CD45RA^{(+)} \rightarrow CD27^{(+)}CD45RA^{(-)} \rightarrow CD27^{(-)}CD45RA^{(-)} \rightarrow CD27^{(-)}CD45RA^{(+)}$, it suggests that this is not appropriate for V γ 9V δ 2 T cells.

Chapter 6

A comparison of $V\gamma 9V\delta 2$ T cells with $V\delta 1^{(+)}$ T cells

Chapter 6 A comparison of V γ 9V δ 2 T cells with V δ 1⁽⁺⁾ T cells

6.1 Introduction

For V γ 9V δ 2 T cells, CD28, CD27 and CD16 were more appropriate markers for identifying distinct subsets compared to the much-used CD27 and CD45RA method. However, it was not clear whether this could also be applied to the less extensively studied V δ 1⁽⁺⁾ T cells. Indeed, relatively little is known (published) about the surface phenotype of these cells. Therefore, this chapter will investigate the surface markers on these cells and determine whether the newly-proposed system of V γ 9V δ 2 T cell identification is also appropriate for V δ 1⁽⁺⁾ T cells.

6.2 The CD27^(Hi) CD11a^(Lo) “naïve” subset is significantly higher for V δ 1⁽⁺⁾ T cells compared to V γ 9V δ 2 T cells

As was shown in Figure 3.9, the “naïve” subset for V γ 9V δ 2 T cells as defined as [CD27^(Hi) CD11a^(Lo)] is a very small population that is often absent or difficult to detect. However, it seems to constitute a significantly larger proportion of V δ 1 T cells with a median percentage of 35.9% (range 0.9-73.5%) compared to only 0.8% (0.1-14.0%) for V γ 9V δ 2 T cells (Figure 6.1). The majority of these “naïve” cells are CD45RA⁽⁺⁾ and overall CD45RA expression is significantly higher in V δ 1⁽⁺⁾ T cells (86.8%) compared to V γ 9V δ 2 T cells (median 34.3%) ($p < 0.0001$) (Figure 6.2).

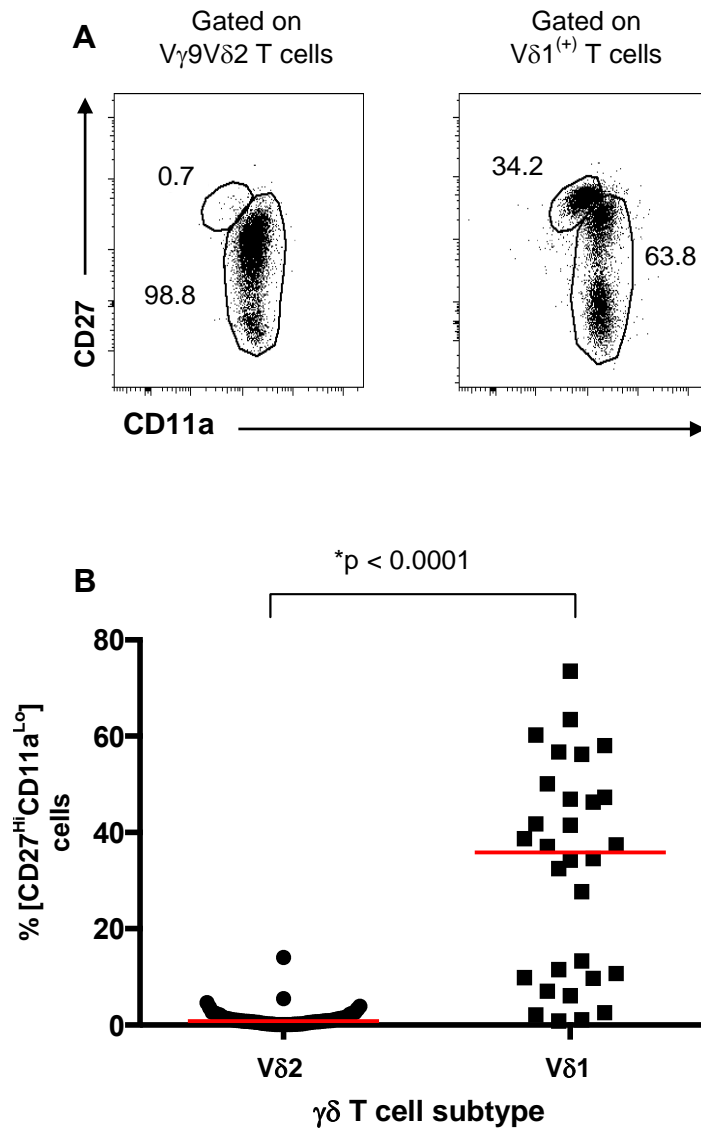


Figure 6.1 “Naïve” [CD27^(Hi) CD11a^(Lo)] Vδ1⁽⁺⁾ T cells are significantly more abundant than “naïve” Vγ9Vδ2 T cells.

(A) Representative dot plots comparing [CD27^(Hi)CD11a^(Lo)] naïve and CD11a^(Hi) non-naïve subsets of Vγ9Vδ2 T cells and Vδ1⁽⁺⁾ T cells in a single healthy individual. Percentage of each gated population is indicated. (B) Summary scatter plot comparing the percentage of total $\gamma\delta$ T cells expressing the naïve phenotype [CD27^(Hi)CD11a^(Lo)] in Vγ9Vδ2 T cells (N=63) and Vδ1⁽⁺⁾ T cells (N=30) from healthy volunteer peripheral blood samples. Median values are indicated as a red bar with statistical comparison conducted using a Mann-Whitney U test with p-value indicated.

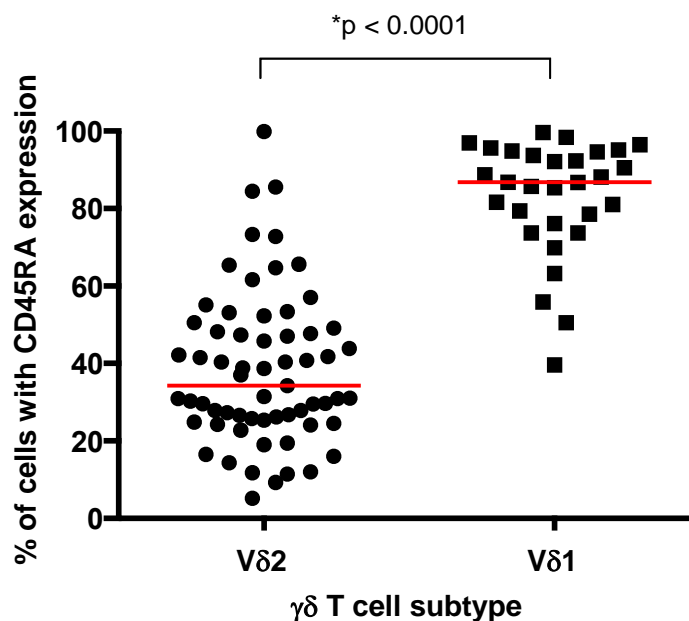


Figure 6.2 CD45RA expression is significantly increased on Vδ1⁽⁺⁾ T cells.

Summary scatter plot comparing the percentage of CD45RA expression in Vγ9Vδ2 (N=63) and Vδ1⁽⁺⁾ (N=30) T cells in healthy volunteer peripheral blood samples. Median values are indicated as a red bar with statistical differences compared using Mann-Whitney U test with p-value indicated.

6.3 CD27/CD45RA identifies distinct subsets of Vδ1⁽⁺⁾ T cells.

Figure 6.3 shows a comparison of Vγ9Vδ2 T cells, Vδ1⁽⁺⁾ and γδ⁽⁻⁾ CD3⁽⁺⁾ T cells stained with CD27 and CD45RA from a single healthy peripheral blood sample. This again highlights the difficulty of using CD27/CD45RA to identify distinct Vγ9Vδ2 T cell populations. However, as for αβ T cells, CD27/CD45RA does identify distinct subsets of Vδ1⁽⁺⁾ T cells. Indeed, CD45RA expression appears to dominate the Vδ1 subset, with CD27⁽⁺⁾CD45RA⁽⁺⁾ and CD27⁽⁻⁾CD45RA⁽⁺⁾ cells comprising the two major populations (Figure 6.3) in contrast to Vγ9Vδ2 T cells in which cells with a CD27⁽⁺⁾CD45RA⁽⁻⁾ phenotype often are the majority.

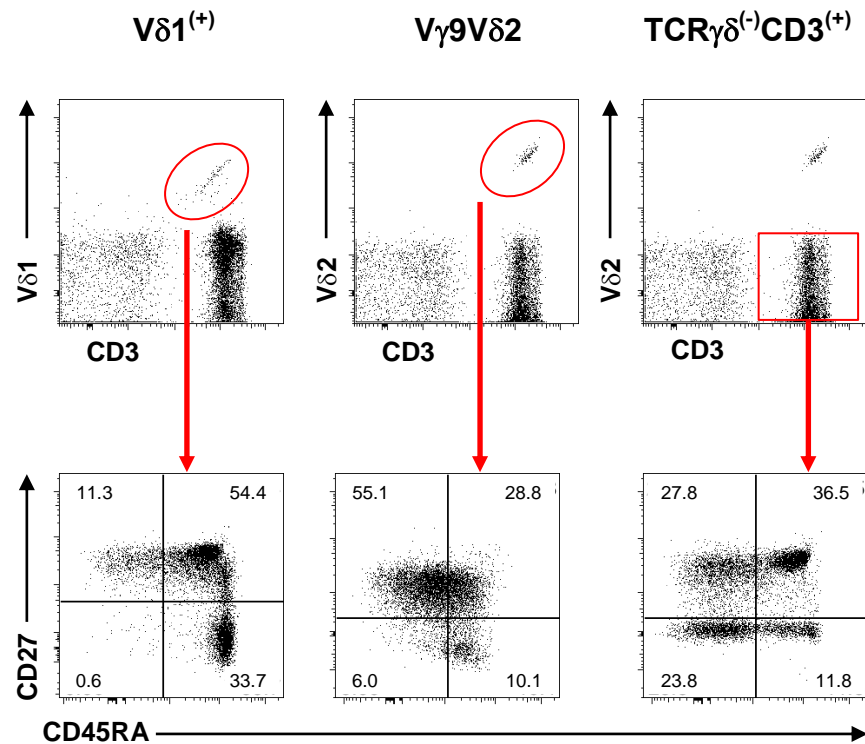


Figure 6.3 Vγ9Vδ2 and Vδ1⁽⁺⁾ T cells show different CD27/CD45RA profiles. (Dot plots show different CD27/CD45RA expression profiles for Vγ9Vδ2, Vδ1⁽⁺⁾ and non-δγ T cells from a single representative individual.

6.4 CD28/CD27/CD16 also identify distinct Vδ1⁽⁺⁾ T cell subsets.

Figure 6.4 and 6.5 illustrates the use of CD28, CD27 and CD16 to phenotype Vδ1⁽⁺⁾ T cells, in comparison with Vγ9Vδ2 T cells and TCR γδ⁽⁻⁾CD3⁽⁺⁾ (αβ) T cells. This methodology identifies distinct subsets for all T cell subtypes (Vδ1⁽⁺⁾, Vγ9Vδ2 and γδ⁽⁻⁾CD3⁽⁺⁾ T cells). This is a clear advantage over the CD27/CD45RA system as it allows comparison of populations in terms of the same surface markers. Three major non-naïve subsets are clearly distinguishable for both Vδ1⁽⁺⁾ and Vγ9Vδ2 T cells, these being; γδ⁽²⁸⁺⁾ cells [CD27⁽⁺⁾CD28⁽⁺⁾]; γδ⁽²⁸⁻⁾ cells [CD28⁽⁻⁾CD27⁽⁺⁾] and γδ⁽²⁷⁻²⁸⁻⁾ cells [CD28⁽⁻⁾CD27⁽⁻⁾]. By contrast, the γδ⁽⁻⁾CD3⁽⁺⁾ (αβ) T cells, whilst having similar [CD27⁽⁺⁾CD28⁽⁺⁾] and [CD27⁽⁻⁾CD28⁽⁻⁾] populations have a predominance of [CD27⁽⁻⁾CD28⁽⁺⁾] cells as opposed to the [CD27⁽⁺⁾CD28⁽⁻⁾] population seen for both γδ T cell subsets.

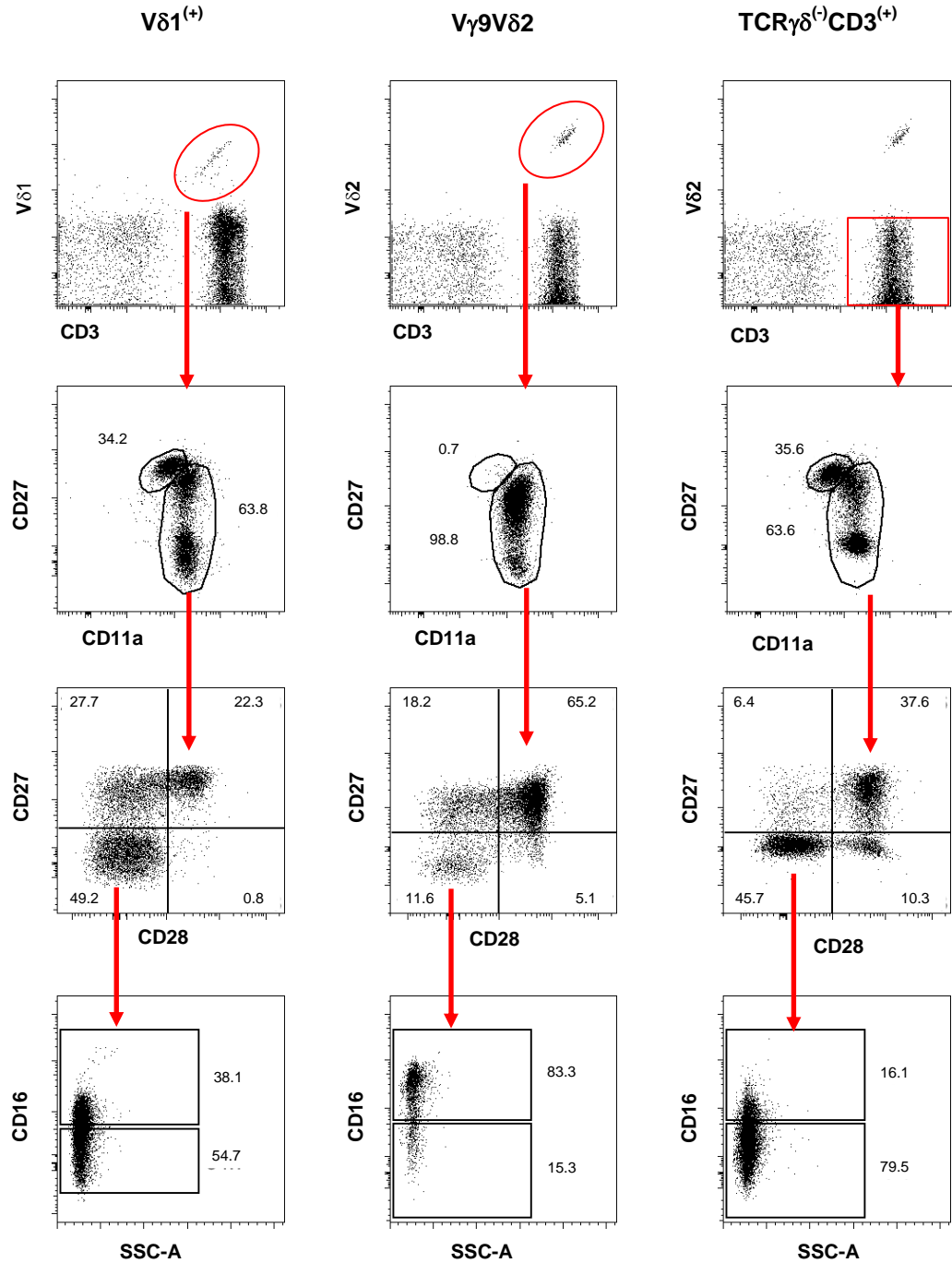


Figure 6.4 Vδ1⁽⁺⁾ and Vγ9Vδ2 T cells show different CD27/CD28/CD16 profiles.

Flow cytometry dot plots show CD27/CD11a/CD28/CD16 expression profiles on Vδ1⁽⁺⁾, Vγ9Vδ2 and non-γδ T cells in a single representative individual. CD27/CD28 plots are shown for non-naïve CD11a^(Hi) cells with CD16 expression shown for the CD27⁽⁻⁾CD28⁽⁻⁾ subset.

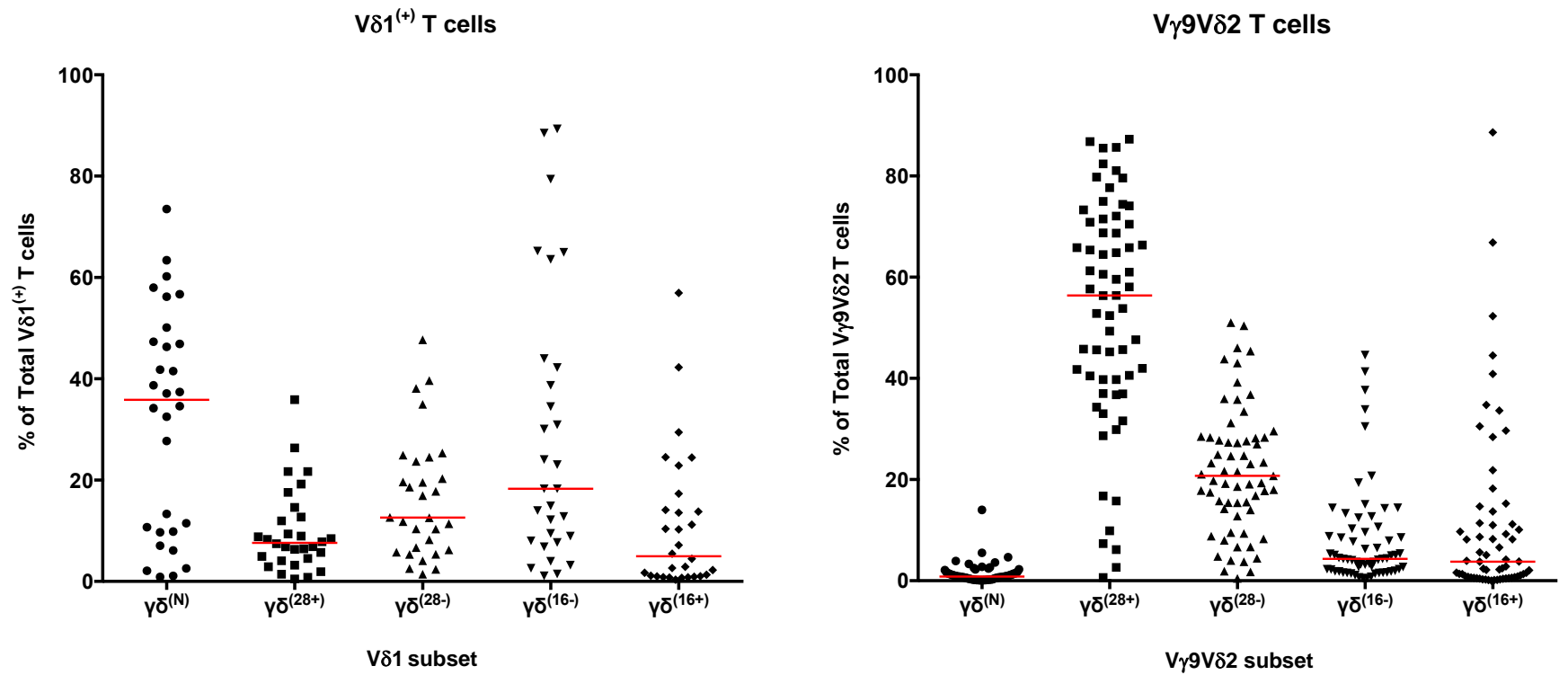


Figure 6.5 $V\delta 1^{(+)}$ and $V\gamma 9V\delta 2$ T cells show different $CD27/CD28/CD16$ subset distribution.

Summary scatter plots show the percentage of each $\gamma\delta$ subset in $V\delta 1^{(+)}$ ($n=30$) and in $V\gamma 9V\delta 2$ T cells ($n=63$) in healthy volunteer peripheral blood samples. Population median values are indicated as a red bar. $V\gamma 9V\delta 2$ subsets are defined as; $\gamma\delta^{(N)}$ [$CD27^{(Hi)}CD11a^{(Lo)}$], $\gamma\delta^{(28+)}$ [$CD28^{(+)}CD27^{(+)}$], $\gamma\delta^{(28-)}$ [$CD28^{(-)}CD27^{(+)}$], $\gamma\delta^{(16-)}$ [$CD28^{(-)}CD27^{(-)}CD16^{(-)}$] and $\gamma\delta^{(16+)}$ [$CD28^{(-)}CD27^{(-)}CD16^{(+)}$].

6.5 Preliminary surface marker analysis of V δ 1⁽⁺⁾ T cells

With it now clear that the CD28/CD27/CD16 methodology could also be used to identify distinct subsets of V δ 1⁽⁺⁾ T cells, this method was utilised to further characterise the surface phenotype of these cells, with reference and comparison to the previously analysed V γ 9V δ 2 T cells. Interestingly, surface CCR7, CD62L and β 7-Integrin levels were very similar on both the V δ 1⁽⁺⁾ and V γ 9V δ 2 T cell subsets (Figure 6.6). Indeed, none of the non-naïve subsets for either $\gamma\delta$ cell subtype expressed CCR7, with steadily decreasing levels of both CD62L and β 7-Integrin in a subset order $\gamma\delta^{(28+)} \rightarrow \gamma\delta^{(28-)} \rightarrow \gamma\delta^{(16-)} \rightarrow \gamma\delta^{(16+)}$. This suggests that for both V δ 1 and V δ 2 cells that homing to the secondary lymphoid organs is not an obvious priority.

The surface expression of CCR2 and CCR5 was also assessed on V δ 1⁽⁺⁾ T cells. Interestingly, V δ 1⁽⁺⁾ T cells did not express CCR2 on any of the non-naïve subsets (Figure 6.7). This was in stark contrast to V γ 9V δ 2 T cells, especially $\gamma\delta^{(28+)}$ V δ 2 T cells, in which \approx 60% of the cells expressed high CCR2 levels. CCR5 was also expressed at increased levels on V γ 9V δ 2 T cells in comparison to V δ 1⁽⁺⁾ T cells although the difference was not as dramatic as for CCR2 (Figure 6.7).

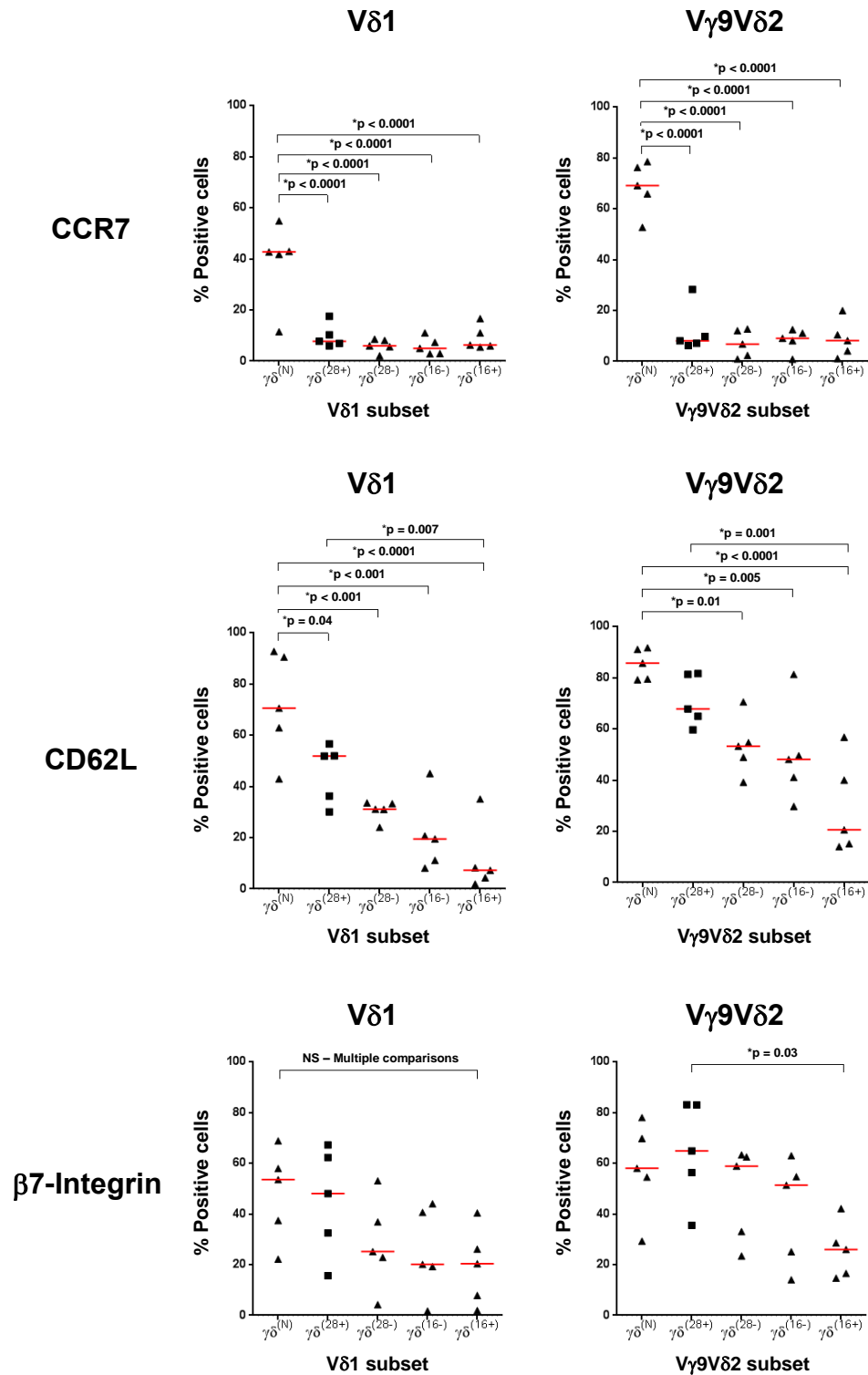


Figure 6.6 CCR7, CD62L and β7-Integrin expression levels in Vδ1⁽⁺⁾ T cells.

Scatter plots showing percentage of expression of CCR7, CD62L and β7-Integrin on Vδ1⁽⁺⁾ and Vγ9Vδ2 T cell subsets in healthy volunteer peripheral blood samples. $\gamma\delta$ T cell subsets are defined as; $\gamma\delta^{(N)}$ [CD27^(Hi)CD11a^(Lo)], $\gamma\delta^{(28+)}$ [CD27⁽⁺⁾CD28⁽⁺⁾], $\gamma\delta^{(28-)}$ [CD27⁽⁺⁾CD28⁽⁻⁾], $\gamma\delta^{(16-)}$ [CD27⁽⁻⁾CD28⁽⁻⁾CD16⁽⁻⁾] and $\gamma\delta^{(16+)}$ [CD27⁽⁻⁾CD28⁽⁻⁾CD16⁽⁺⁾]. Median values are indicated as a red bar. Statistical differences were assessed using ANOVA Kruskal-Wallis test with multiple comparison post-hoc testing with Bonferroni correction. p-values < 0.05 were considered significant.

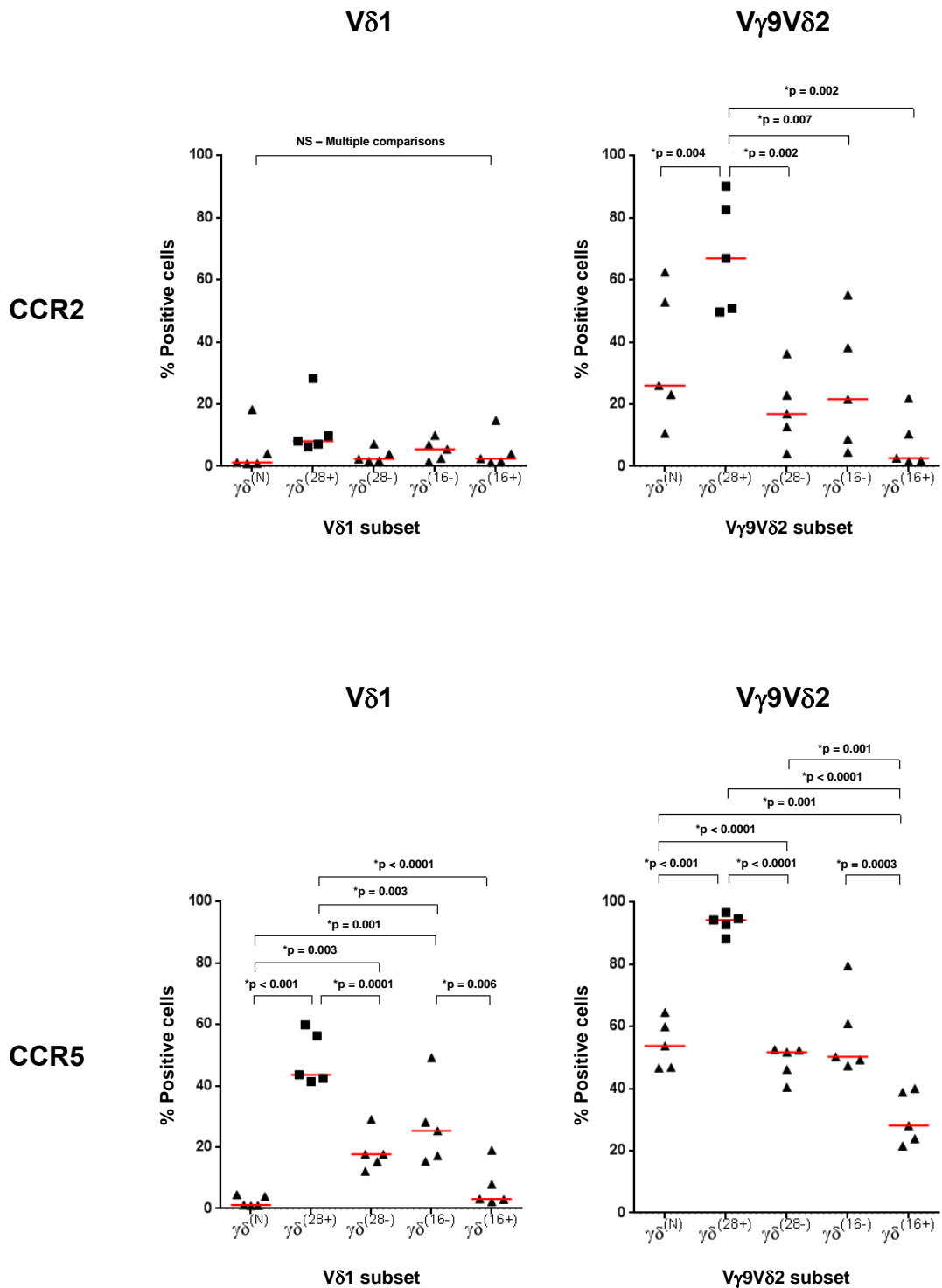


Figure 6.7 CCR2 and CCR5 expression levels on $V\delta 1^{(+)}$ T cells

Scatter plots showing percentage of expression of CCR2 and CCR5 on $V\delta 1^{(+)}$ and $V\gamma 9V\delta 2$ T cell subsets in healthy volunteer peripheral blood samples. $\gamma\delta$ T cell subsets are defined as; $\gamma\delta^{(N)}$ [CD27^(Hi)CD11a^(Lo)], $\gamma\delta^{(28+)}$ [CD27⁽⁺⁾CD28⁽⁺⁾], $\gamma\delta^{(27+)}$ [CD27⁽⁺⁾CD28⁽⁻⁾], $\gamma\delta^{(16-)}$ [CD27⁽⁻⁾CD28⁽⁻⁾CD16⁽⁻⁾] and $\gamma\delta^{(16+)}$ [CD27⁽⁻⁾CD28⁽⁻⁾CD16⁽⁺⁾]. Median values are indicated as a red bar. Statistical differences were assessed using ANOVA Kruskal-Wallis test with multiple comparison post-hoc testing with Bonferroni correction (p -values < 0.05 were considered significant).

6.6 Summary

This chapter outlined preliminary analysis of $V\delta 1^{(+)}$ T cells, with comparison to the previous investigations on $V\gamma 9V\delta 2$ T cells. Unlike for $V\gamma 9V\delta 2$ T cells CD27/CD45RA does identify clear subsets for $V\delta 1^{(+)}$ T cells, in a manner reminiscent of $\alpha\beta$ T cells. However, the proposed system of phenotyping cells using CD27/CD28 and CD16 does seem to offer an advantage in identifying clear populations that are directly comparable between $V\delta 1^{(+)}$ and $V\gamma 9V\delta 2$ T cell subsets.

Chapter 7

Preliminary analysis of $\gamma\delta$ T cells in the human neonatal thymus

Chapter 7 Preliminary analysis of $\gamma\delta$ T cells in the human neonatal thymus

7.1 Introduction

In phenotyping $V\gamma 9V\delta 2$ T cells from the adult peripheral blood it was apparent that defining a “naïve” population was problematic. Indeed, different phenotyping strategies lead to a wide range of estimates for the “naïve” $V\gamma 9V\delta 2$ T cell subset (Figure 3.7). In addition, there is much confusion in the literature as to the combination of markers to use to best describe the “naïve” $V\gamma 9V\delta 2$ T cell phenotype, with a range of different marker combinations used including combinations of; CD27, CD45RA, CD28, CD11a, CD62L and CCR7.

Therefore, in order to provide insight into the true nature of a “naïve” $V\gamma 9V\delta 2$ T cell phenotype, thymocytes were extracted from eight human neonatal thymus samples (see Figure 7.1A for details) and phenotyped using a panel of common “naïve” surface markers. Our rationale argued that the “naïve” phenotype would predominate in the thymus and would help inform us of the phenotype of these cells prior to antigen exposure.

7.2 $V\delta 1^{(+)}$ T cells are more prevalent in the neonatal thymus than $V\gamma 9V\delta 2$ T cells.

Initially, the percentage of $V\gamma 9V\delta 2$ and $V\delta 1^{(+)}$ T cells as a proportion of total $CD3^{(+)}$ T cells, was determined in the thymus samples and compared to the percentages of these cells in peripheral blood.

A

Thymus	Age (Days/Months)	Sex (M/F)	V δ 2/CD3(%)	V δ 1/CD3(%)
1	4d	M	0.03	0.51
2	20d	M	0.08	0.30
3	3m	F	0.06	0.33
4	7m	F	0.05	0.72
5	16m	M	0.12	0.62
6	17m	F	0.06	0.25
7	28m	F	0.12	0.75
8	35m	M	0.11	0.09

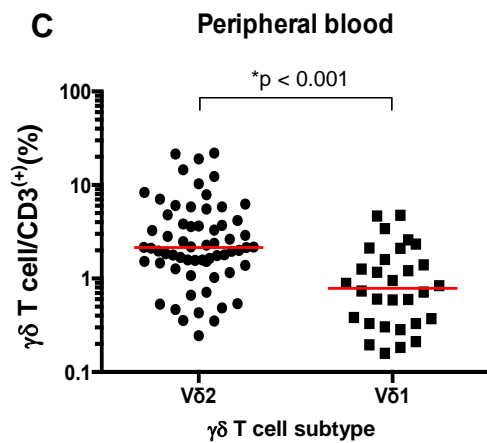
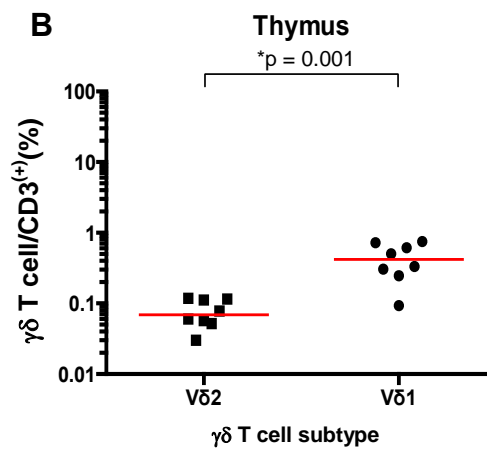


Figure 7.1 V δ 1⁽⁺⁾ T cells are found at higher proportions in the neonatal thymus than V γ 9V δ 2 T cells.

(A) Summary table of the eight thymuses analysed is shown indicating; age, gender, V δ 2/CD3(%) and V δ 1/CD3(%) for each sample. A comparison of $\gamma\delta$ T cell populations (V δ 2 vs.V δ 1⁽⁺⁾) expressed as a percentage of total CD3⁽⁺⁾ cells in (B) thymocytes obtained from neo-natal thymuses and (C) PBMCs from peripheral blood (Healthy volunteers). Median values are indicated in red. Data from thymocytes from neo-natal thymuses (n=8) is shown in comparison to levels in peripheral blood samples; V δ 2 (n=63) and V δ 1 (n=30).

Figure 7.1B shows that in the eight thymus samples, the median $V\delta 1/CD3(\%)$ was 0.42% which was significantly higher compared to the median $V\delta 2/CD3(\%)$ of 0.07% ($p = 0.001$). This relationship was reversed in peripheral blood samples where the median $V\delta 2/CD3(\%)$ of 2.2% was significantly higher than the median $V\delta 1/CD3(\%)$ of 0.8% ($p < 0.001$) (Figure 7.1C). This relationship was in accordance with the idea that $V\gamma 9V\delta 2$ T cells increase due to post-thymic expansion following antigen exposure.

7.3 CD27/CD45RA expression on $V\delta 2^{(+)}$ T cells in the neonatal thymus

After staining the eight thymus samples with a combination of markers (CD28, CD27, CD45RA, CD11a, CCR7, CD62L and CD16), we first assessed $V\gamma 9V\delta 2$ T cells for CD27/CD45RA expression. This method of analysis is commonly used in the literature (see previous chapters), and identifies “naïve” cells as $[CD27^{(+)CD45RA^{(+)}]$. If this staining combination represents a true “naïve” population, we would expect it to predominate in the thymus. However, figure 7.2A shows that in 6/8 thymus samples the $CD27^{(+)CD45RA^{(+)}$ subset was not the major population, with a median percentage of 27.4%. This value is somewhat similar to that observed for $CD27^{(+)CD45RA^{(+)}$ $V\gamma 9V\delta 2$ T cells in the peripheral blood; 23.4% (Figure 7.2B), suggesting that it is not enriched in the thymus samples. Indeed, the $CD27^{(+)CD45RA^{(-)}$ subset is generally the dominating population (in 6/8 samples). Interestingly, two of the three youngest samples (Age = 4 days and Age = 3 months) did show higher expression of CD45RA, although a further sample from a child aged 20 days did not.

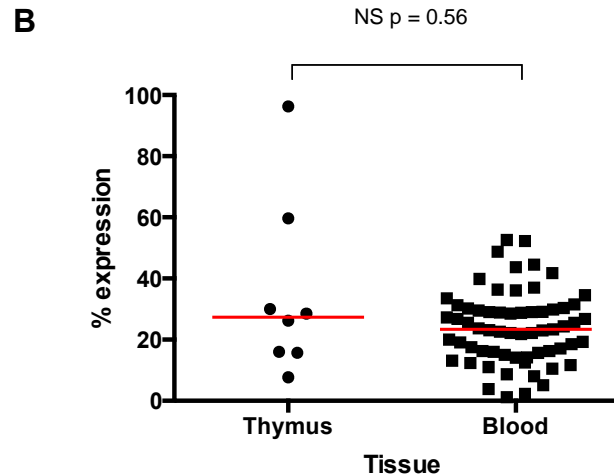
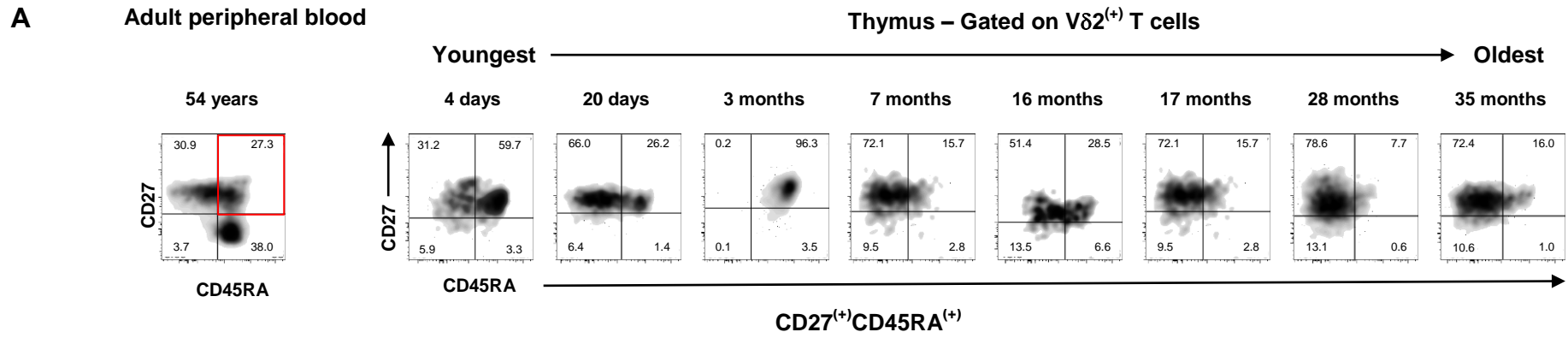


Figure 7.2 CD27/CD45RA expression on $V\delta 2^{(+)}$ T cells in the thymus.

(A) CD27/CD45RA flow cytometry density plots of $V\delta 2^{(+)}$ T cells from all eight thymic samples are shown and ranked by increasing age (left to right). Age is indicated above the associated plot. Percentage in each quadrant is indicated. A typical peripheral blood CD27/CD45RA profile is shown for comparison (far left). (B) The percentage of “naïve” cells (as defined by $CD27^{(+)CD45RA^{(+)}$) for thymic $V\delta 2$ T cells from thymus and peripheral blood. Red lines indicate median values. Statistical differences were assessed using the Mann–Whitney U test with p-values indicated.

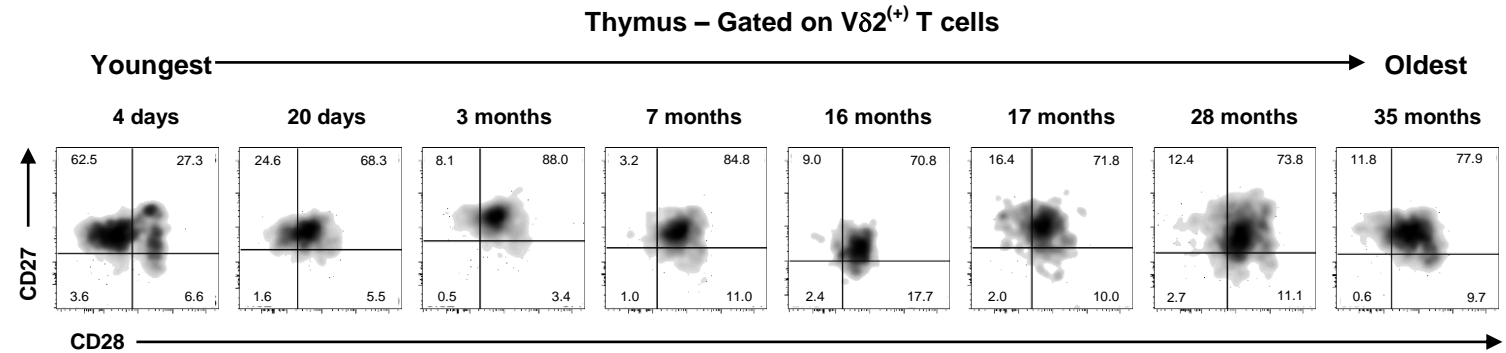
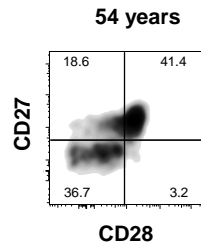
7.4 CD28/CD27 analysis of V γ 9V δ 2 T cells in the neonatal thymus

The eight thymus samples were next assessed for expression of CD28 and CD27 (as previously described). The microarray data and PSM analysis had tentatively suggested that a [CD27⁽⁺⁾CD28⁽⁺⁾] phenotype ($\gamma\delta^{28+}$) could be at one end (possibly at the start) of a pathway of V γ 9V δ 2 T cell differentiation. Consistent with this, in 7/8 samples the $\gamma\delta^{(28+)}$ subset was the major population observed (Figure 7.3A). Furthermore, the median percentage of this subset in the thymus (72.8%) was significantly higher than that observed in the blood of healthy adults (57.0%; $p = 0.035$) (Figure 7.3B). Nonetheless, in the very youngest thymus (Age=4 days) the [CD28⁽⁻⁾CD27⁽⁺⁾] subset predominated, again suggesting that the $\gamma\delta^{(28+)}$ subset was unlikely to represent a “naïve” V γ 9V δ 2 T cell population.

7.5 CCR7/CD62L analysis of V γ 9V δ 2 T cells in the neonatal thymus.

V γ 9V δ 2 T cells in the eight neonatal thymus samples were next assessed for CCR7 and CD62L expression, as a [CCR7⁽⁺⁾CD62L⁽⁺⁾] subset had previously been suggested to be a “naïve” subset. However, there was no evidence for this from this analysis; median levels of [CCR7⁽⁺⁾CD62L⁽⁺⁾] cells being 2.4% in the thymus, compared with 1.9% in the adult blood (Figure 7.4). Instead, most cells were CCR7⁽⁻⁾ with a generally CD62L⁽⁻⁾ phenotype. A caveat to this conclusion is a reminder that FACS staining for both CCR7 and CD62L can be problematic.

A Adult peripheral blood



B

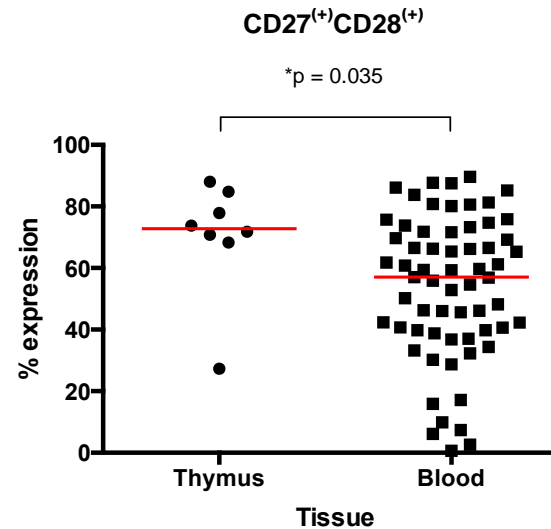


Figure 7.3 CD27/CD28 expression on Vδ2⁽⁺⁾ T cells in the thymus.

(A) CD27/CD28 flow cytometry density plots of Vδ2⁽⁺⁾ T cells from all eight thymic samples are shown and ranked by increasing age (left to right). Age is indicated above the associated plot. Percentage in each quadrant is indicated. A typical peripheral blood CD27/CD28 Vδ2 profile is shown for comparison (far left). (B) A comparison of the percentage of CD27⁽⁺⁾CD28⁽⁺⁾ cells in thymus is shown relative to the same cells in peripheral blood. Red lines indicate median values. Statistical differences were assessed using the Mann–Whitney U test with p-values indicated.

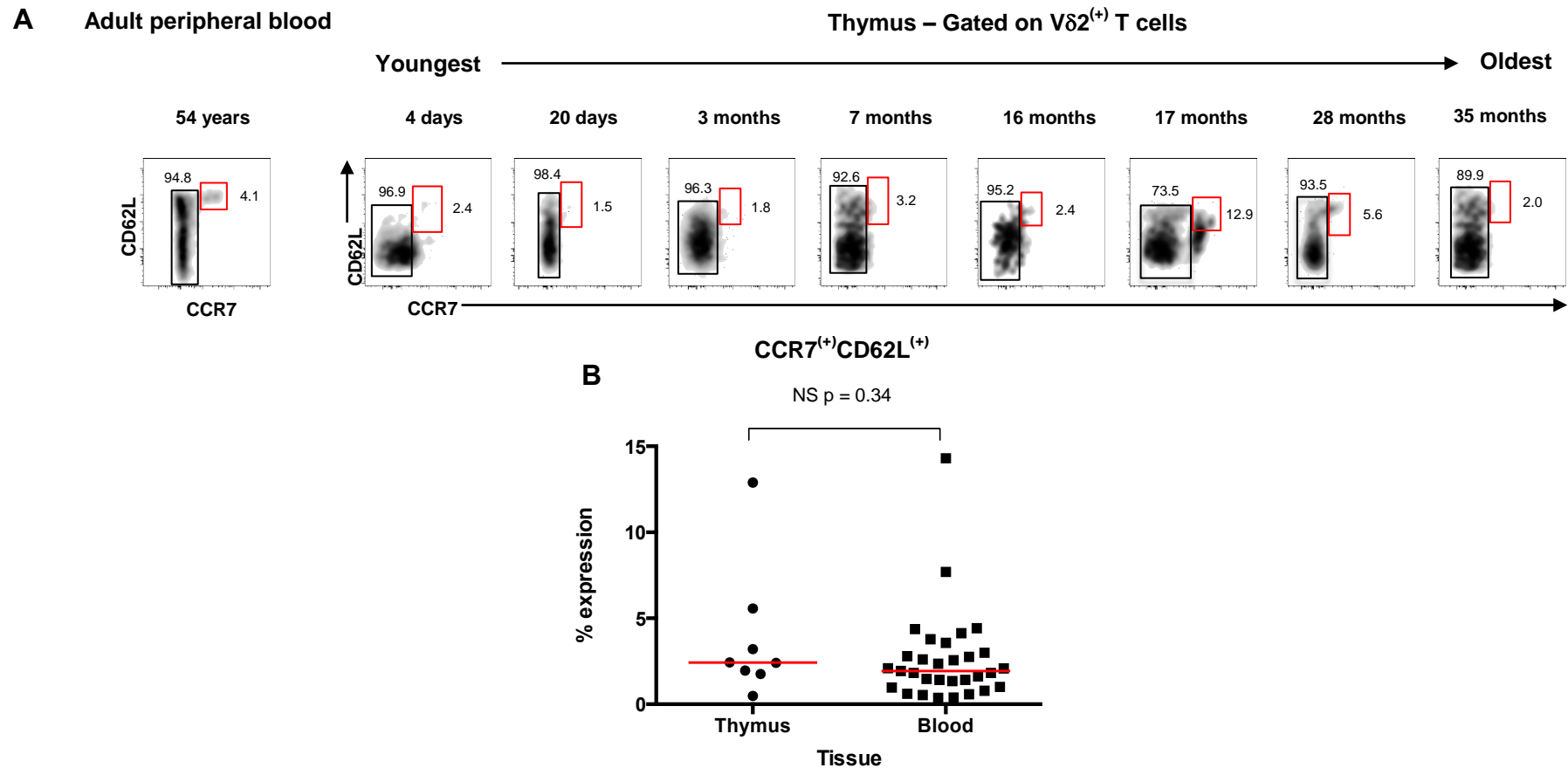


Figure 7.4 A comparison of CCR7/CD62L expression on V δ 2⁽⁺⁾ T cells in the thymus.

(A) CCR7/CD62L flow cytometry density plots of V δ 2⁽⁺⁾ T cells from all eight thymic samples are shown and ranked by increasing age (left to right). Age is indicated above the associated plot. Percentage in each quadrant is also indicated. A typical peripheral blood CCR7/CD62L V δ 2 profile is shown for comparison (far left). (B) A comparison of the percentage of “naïve” phenotype (as defined by CCR7⁽⁺⁾CD62L⁽⁺⁾) in thymic V δ 2 T cells is shown relative to the same cells in peripheral blood. Red lines indicate median values. Statistical differences were assessed using the Mann–Whitney U test with p-values indicated.

7.6 A novel population of cells exist in the neonatal thymus

The final method of analysis for $V\gamma 9V\delta 2$ T cells in the neonatal thymus samples involved assessment of CD27 and CD11a expression. In the peripheral blood of adults, the majority of cells are $CD11a^{(Hi)} CD27^{(+ \text{ or } -)}$ (but not $CD27^{(Hi)}$), with only a few cells (< 5%) showing the proposed $[CD27^{(Hi)} CD11a^{(Lo)}]$ phenotype of a “naïve” $V\gamma 9V\delta 2$ T cell (De Rosa *et al.* 2004)(Figure 7.5). By contrast, CD27/CD11a staining in the eight neonatal thymus samples showed a significantly different profile in that the majority of cells (in all cases) displayed a $CD27^{(+)}$ (but not $CD27^{(Hi)}$) and $CD11a^{(Lo)}$ phenotype (Figure 7.5). This $[CD27^{(+)} CD11a^{(Lo)}]$ subset has no obviously comparable population in the adult blood, which may suggest that these cells are in some way more “immature” than those in the periphery. Figure 7.6 shows CD27/CD11a plots from a neonatal thymus and adult blood to illustrate this point. It is tempting to speculate that the $CD27^{(Hi)}$ populations are comparable (circled in red), although no direct evidence yet exists to support this.

7.7 CD27 and CD11a define two $V\gamma 9V\delta 2$ T cell thymic populations

As it was possible to consistently define two populations of $V\gamma 9V\delta 2$ thymocytes with CD27 and CD11a, these populations were assessed for further marker expression. Figure 7.5 shows thymus $V\gamma 9V\delta 2$ T cell population 1 $[CD27^{(+)} CD11a^{(Lo)}]$ and thymus $V\gamma 9V\delta 2$ population 2 $[CD27^{(Hi)} CD11a^{(+)}]$ in two different thymus samples (#7 and #8) assessed for expression of CCR7, CD62L, CD45RA CD16 and CD28.

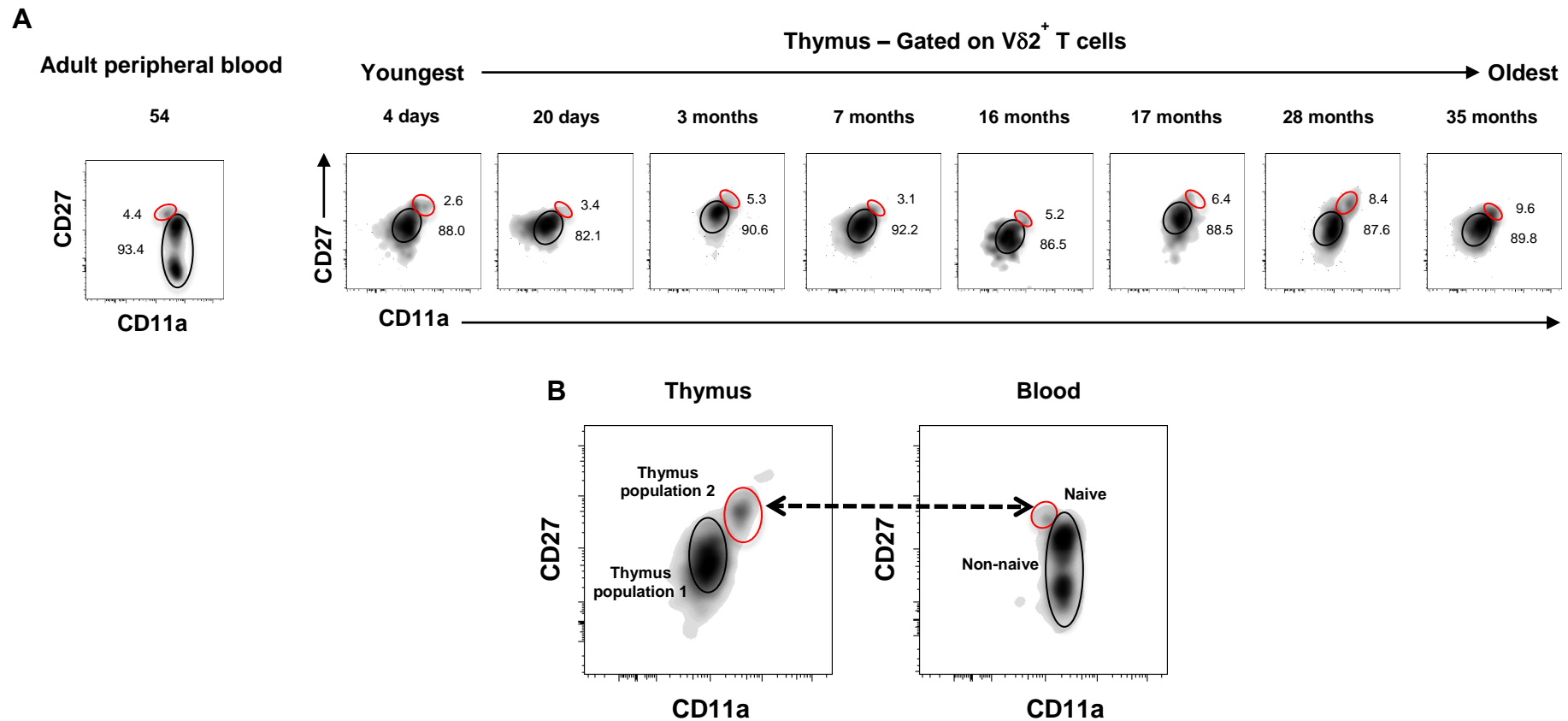


Figure 7.5 CD27/CD11a expression on $V\delta 2^{(+)}$ T cells in the thymus

CD27/CD11a flow cytometry density plots of $V\delta 2^{(+)}$ T cells from all eight thymic samples are shown and are ranked by increasing age (left to right) (A). Age of each patient is indicated above the associated plot. Percentage in each quadrant gate is also indicated. A typical peripheral blood CD27/CD11a profile is shown for comparison (far left). (B) Density plots showing CD27 and CD11a expression on $V\delta 2^{(+)}$ T cells from representative plots in neonatal thymus and adult blood. Density plots reveal two distinct subsets in the thymus that are difficult to relate to the typical populations seen in adult peripheral blood. Thymus population 1 = $[CD27^{(+)}CD11a^{(Lo)}]$ and thymus population 2 = $[CD27^{(Hi)}CD11a^{(+)}]$. Peripheral blood “naïve” population = $[CD27^{(Hi)}CD11a^{(Lo)}]$, non-“naïve” = $[CD27^{(+/-)}CD11a^{(Hi)}]$.

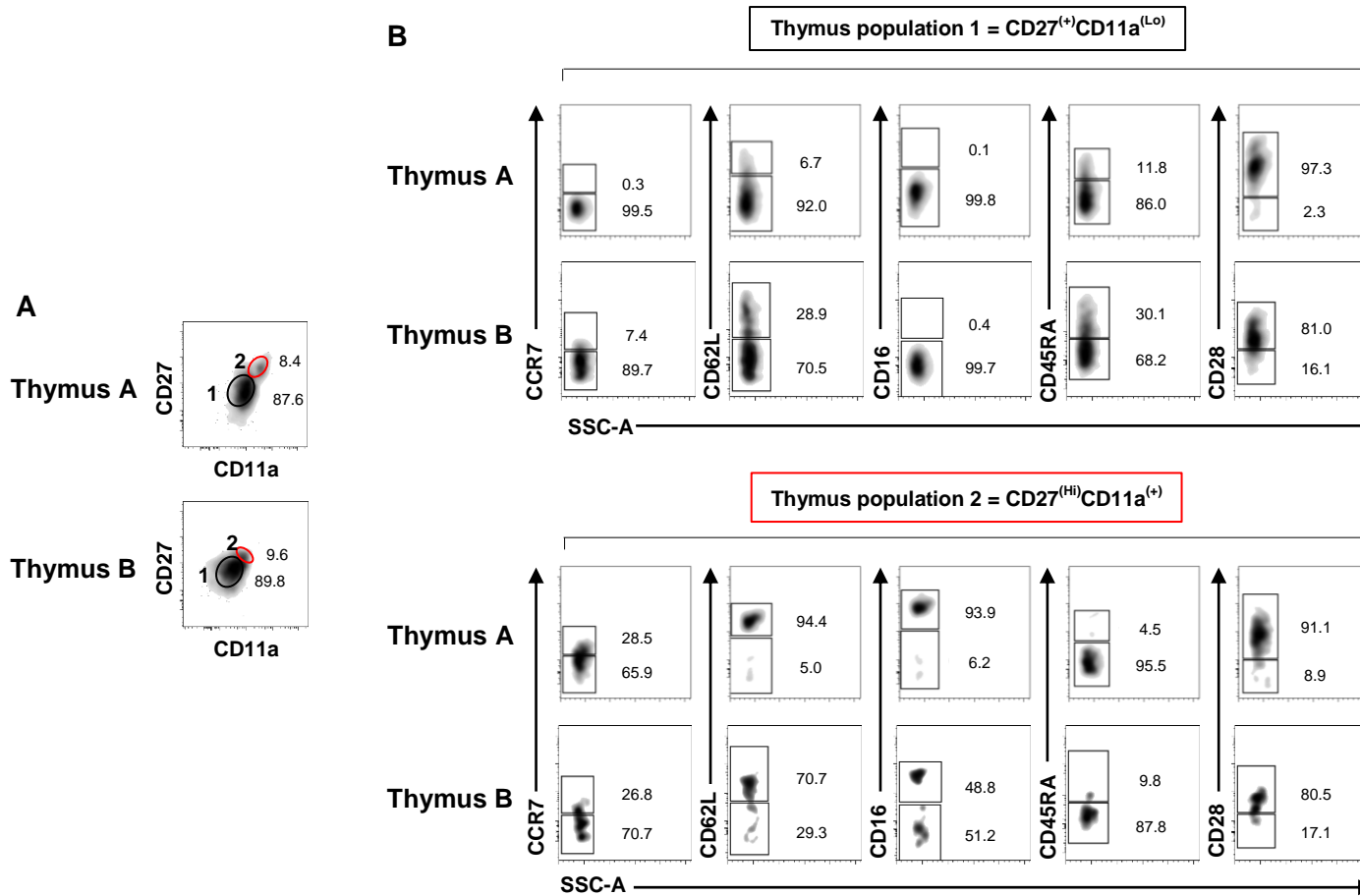


Figure 7.6 CD27 and CD11a define two distinct thymic V δ 2⁽⁺⁾ T cell subsets.

(A) Flow cytometry density plots showing two distinct thymic V δ 2⁽⁺⁾ T cell populations; Population 1 = [CD27⁽⁺⁾CD11a^(Lo)] (outlined in black) and Population 2 = [CD27^(Hi)CD11a⁽⁺⁾] (outlined in red) in two representative thymus samples (Thymus A and Thymus B). (A) Each thymus population (1 and 2) shown in (B) is characterised by surface markers CCR7, CD62L, CD16, CD45RA and CD28.

Interestingly, population 2 express significantly higher levels of CCR7, CD62L and CD16 compared to population 1 (Figure 7.6 and 7.7), but similar levels of CD45RA and CD28. The high levels of CD16 were particularly surprising for thymic-populations as it is typically described as a late effector marker in cytotoxic T cells. However, the consistently high levels of CD16 expression on population 2 seemed to confirm that the expression of CD16 might have a functional significance in the small [CD27^(Hi) CD11a⁽⁺⁾] subset.

7.8 Summary

In summary, it is apparent that classically-defined “naïve” V γ 9V δ 2 T cells are not obviously identifiable in the human neonatal thymus. Many of the suggested “naïve” phenotypes identify thymic populations that are similar in proportion to those seen in adult blood. Nonetheless, two distinct V γ 9V δ 2 T cell populations are present in all thymic samples, characterised as [CD27⁽⁺⁾CD11a^(Lo)] and [CD27^(Hi)CD11a⁽⁺⁾] that have distinct marker expression profiles. The smaller [CD27^(Hi)CD11a⁽⁺⁾] subset perhaps represent the closest comparison to a “naïve” subset found in adult blood and perhaps are cells about to be released into the peripheral blood. By contrast, the [CD27⁽⁺⁾CD11a^(Lo)] subset may represent a subset at a very early stage of thymic development.

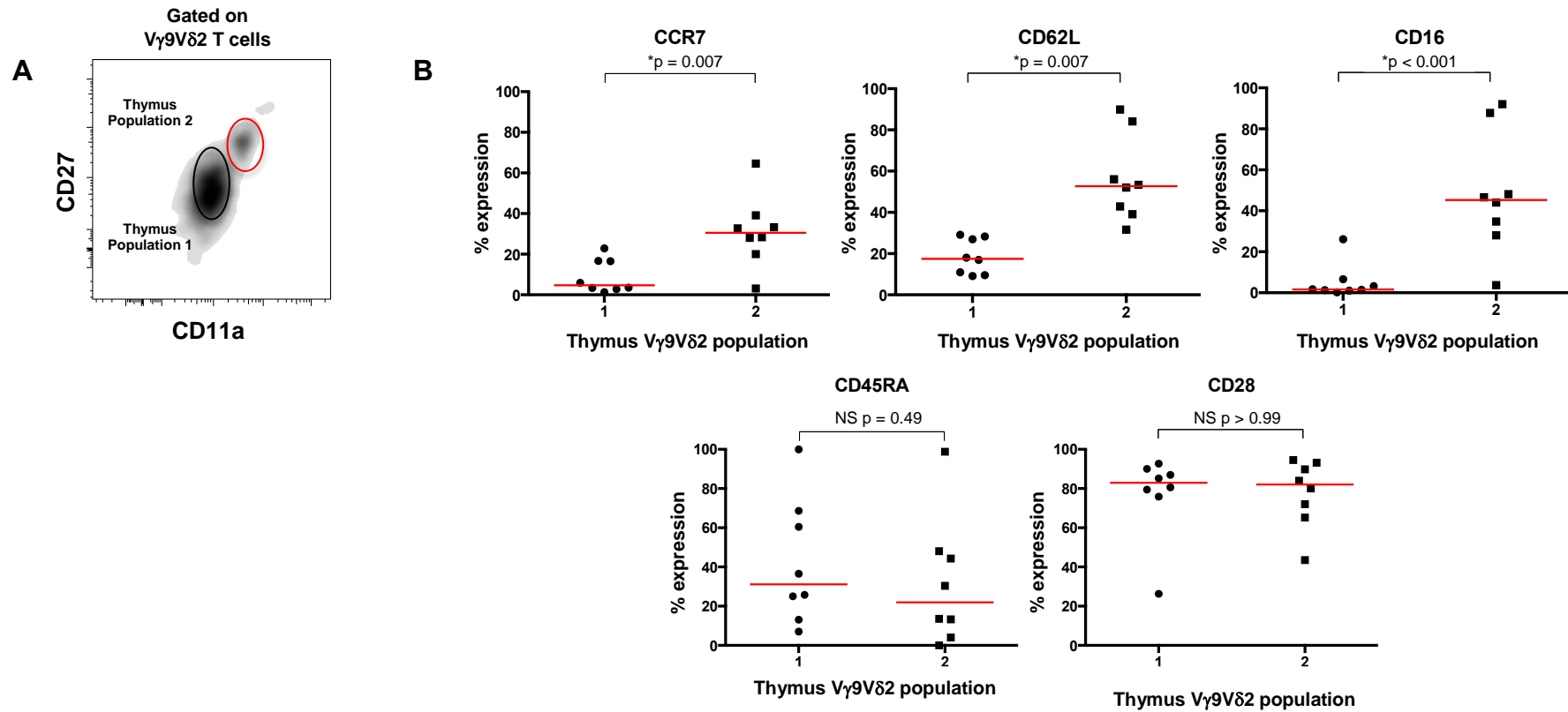


Figure 7.7 A comparison of surface marker expression on thymic $V\delta 2^{(+)}$ T cells.

(A) A flow cytometry density plot highlights the two main $V\delta 2^{(+)}$ T cell populations found in the thymus. (B) Relative expression of surface markers; CCR7, CD62L, CD16, CD27, CD45RA and CD28 are compared in the two major thymus populations; Population 1 = $[CD27^{(+)CD11a^{(Lo)}}]$ and population 2 = $[CD27^{(Hi)}CD11a^{(+)}]$ in (B). Red lines represent median values. Statistical differences were assessed using the Mann–Whitney U test with p-values indicated.

Chapter 8

$\gamma\delta$ T cell changes in bisphosphonate-related osteonecrosis of the jaw (BRONJ)

Chapter 8 $\gamma\delta$ T cell changes in bisphosphonate-related osteonecrosis of the jaw (BRONJ)

8.1 Introduction

The final chapter presents preliminary data investigating $\gamma\delta$ T cells in a small cohort of eight patients with a history of bisphosphonate-related osteonecrosis of the jaw (BRONJ). The pilot study was designed to investigate whether there was any evidence to suggest that $\gamma\delta$ T cells were implicated in BRONJ by comparing $\gamma\delta$ T cell number and phenotype to healthy controls, and to other patients exposed to bisphosphonates but without osteonecrosis. As previously discussed, the lack of access to BRONJ jaw tissue samples due to the current non-interventional treatment protocols in the UK, precludes any in-depth investigations on these cells within tissue samples. Therefore the pilot study was limited to looking and characterising $\gamma\delta$ T cells (V γ 9V δ 2 and V δ 1⁽⁺⁾) in the peripheral blood. Three different control groups were used; healthy volunteers with no previous exposure to bisphosphonates (n=63); osteoporotic patients taking oral bisphosphonates (n=5) and a group of osteoporotic patients on yearly intravenous bisphosphonate therapy (n=5).

8.2 BRONJ patient cohort

Eight BRONJ patients were recruited to the pilot study, two being male and six being female with a median age of 58.5 (range 46-88 years) (Table 8.1).

BRONJ patient	Sex (M/F)	Age (Years)	Country of Birth	Ethnicity	Bisphosphonate	Route of administration	Dose (mg)	Reason for prescription	Interval (Days)	Time on medication (Months)	Currently taking Bisphosphonate (Y/N)
1	F	88	UK (Northern Europe)	White - British	Aledronic acid	Oral	70	Osteoporosis	Weekly	46	Y
2	F	46	UK (Northern Europe)	White - British	Zoledronic acid	Intravenous	4	Breast cancer	Monthly	9	N
3	F	78	Cyprus (Southern Europe)	Turkish-Cypriot	Pamidronate	Intravenous	30	Osteoporosis	Bi-annually	36	Y
4	F	55	Kenya (Eastern Africa)	Indian/Burmese	Aledronic acid	Oral	70	Osteoporosis	Weekly	178	N
5	F	52	Jamaica (Caribbean)	Afro-Caribbean	Aledronic acid	Oral	70	Osteoporosis	Weekly	48	N
6	M	62	UK (Northern Europe)	White-British	Zoledronic acid	Intravenous	4	Multiple myeloma	Monthly	84	Y
7	F	53	UK (Northern Europe)	Greek-Cypriot	Aledronic acid	Oral	70	Osteoporosis	Weekly	60	Y
8	M	81	Italy (Southern Europe)	White - European	Clodronate	Oral	1600	Multiple myeloma	Daily	24	N

Table 8.1 BRONJ cohort bisphosphonate details.

Summary table of the eight BRONJ patients recruited for the study. The table details general patient demographics including; age, gender, country of birth (geographical sub-region) and ethnicity. Details regarding cumulative bisphosphonate exposure is described including; bisphosphonate drug, route of administration, dose, reason for prescription, length of time of drug prescription, and whether patients were still taking bisphosphonates at the time of blood analysis.

The majority of BRONJ patients (5/8) had taken bisphosphonates as a post-menopausal osteoporotic therapy and the majority of these (4/5) were on the less potent oral form of the medication. The remaining three BRONJ patients were prescribed bisphosphonates to prevent bone loss as a complication of multiple myeloma and breast cancer, with only two of these three patients prescribed the most potent monthly intravenous bisphosphonate regimen. In terms of cumulative bisphosphonate exposure, BRONJ patients were prescribed bisphosphonates for between 24 and 178 months in the oral group and for between 9 and 84 months in the intravenous group with an overall median exposure of 47 months. Half of the BRONJ cohort (4/8) continued to take, or continued to have bisphosphonates administered, despite the diagnosis of BRONJ.

8.3 Control groups

BRONJ patients were compared to three different control groups all with no previous history of BRONJ that included; non-bisphosphonate exposed healthy volunteers (n=63; Male=31, Female=32; Age range 3-69 years); oral bisphosphonate patients with no BRONJ (n=5; Male=1, Female=4, Age range 56-79 years) and intravenous bisphosphonate patients (n=5; Male=1, Female=4; Age range 64-81 years) (Table 8.2). Individuals within the healthy volunteer cohort that were > 50 years (n=16) were also considered as a separate sub-group in order to better age-match this group to the other typically older control groups.

	Sex (M/F)	Age (Years)	Country of Birth	Ethnicity	Bisphosphonate	Route of administration	Dose (mg)	Reason for prescription	Interval (Days)	Time on medication (Months)	Currently taking Bisphosphonate (Y/N)
1	F	81	UK (Northern Europe)	White – British	Zoledronic acid	IV	5	Osteoporosis	365	36	Y – 3 Annual infusions
2	F	64	Cyprus (Southern Europe)	Greek-Cypriot	Zoledronic acid	IV	5	Osteoporosis	365	24	Y – 2 Annual Infusions
3	M	78	India (Southern Asia)	Asian – Indian	Aledronic acid (12m) Zoledronic acid (28m)	IV	70 (Oral) / 5 (IV)	Osteoporosis	7 (Oral) / 365 (IV)	40	Y – Mixture of oral and IV bisphosphonates
4	F	75	UK (Northern Europe)	White – British	Pamidronate	IV	30	Osteoporosis	90	125	Y
5	F	79	Grenada (Caribbean)	Black – Afro-Caribbean	Zoledronic acid	IV	5	Osteoporosis	365	46	Y – 4 previous doses
6	M	56	Ireland (Northern Europe)	White – Irish	Aledronic acid	Oral	70	Osteoporosis	7	84	Y
7	F	72	UK (Northern Europe)	White – British	Aledronic acid	Oral	70	Osteoporosis	7	144	Y
8	F	79	UK (Northern Europe)	White – British	Aledronic acid	Oral	70	Osteoporosis	7	96	Y
9	F	63	UK (Northern Europe)	White – British	Aledronic acid	Oral	70	Osteoporosis	7	60	N – Recently stopped
10	F	73	UK (Northern Europe)	White – British	Aledronic acid	Oral	70	Osteoporosis	7	132	Y

Table 8.2 Bisphosphonate control group details.

Summary table of the ten patients recruited for study as a control group being exposed to therapeutic bisphosphonates without BRONJ. The table details patient demographics including; age, sex, country of birth (geographical sub-region) and ethnicity. Details regarding cumulative bisphosphonate exposure is described including; bisphosphonate drug, route of administration, dose, reason for prescription, length of time of drug prescription and whether patients were still taking bisphosphonates at the time of blood analysis. IV=Intravenous, Y=Yes, N=No, M=Male and F=Female.

8.4 BRONJ disease and treatment.

In all eight of the BRONJ patients, osteonecrosis was in the mandible and had mainly occurred following a dental extraction (7/8) (Table 8.3). Exposed BRONJ lesions were evident in 5/8 patients and in the worst case had lasted up to 117 months (9.75 years). Exposure size ranged from 0-25mm on examination and BRONJ stage ranged from 0-3. Treatment and management of each BRONJ case was very much dependent on the clinician, but in all cases was treated conservatively. No interventional surgery was carried out to remove necrotic bone and the only operative procedures were limited to the removal of loose symptomatic bone sequestrae and local curettage of debris from lesions on a symptomatic basis. Pentoxifylline and α -tocopherol (Vitamin E) were frequently used in combination with tetracycline and chlorhexidine antimicrobial agents (Figure 8.3).

8.5 Pain and quality of life related issues in BRONJ.

Only 2/8 BRONJ patients reported pain at the time of interview/examination and both of these patients rated their pain at 4/10 (numeric pain rating scale) (Table 8.4). BRONJ patients were also asked to recall their worst pain with 5/10 patients recalling at least one episode of severe pain (9 or 10 score). However, in one affected individual, no BRONJ lesion associated pain was ever reported and they remained totally asymptomatic throughout the disease course. The vast majority of BRONJ affected patients (7/8) reported that their eating had been affected by the condition and 5/8 were symptomatically aware of infection, typically due to a bad taste or drainage of pus from the lesion. Other symptoms reported included; food trapping in the lesion, referred pain to the ear, sharp bone exposed and numbness in the lip and chin.

BRONJ patient	Precipitating factor	Reason for extraction	Site	Bone exposed (Y/N)	Size of exposure (mm)	BRONJ stage	Exposure period (Months)	Systemic antimicrobials prescribed	Surgery/curettage	Topical treatment	Current BRONJ drug therapy
1	Dental extraction	Irreversible pulpitis	Mandible	Y	8	1	46	Y - Penicillin V, Amoxicillin, Co-amoxiclav and Tetracycline	Local curettage / Sequestrae removal	Y - Chlorhexidine - topical /mouthwash application	Pentoxyfylline, Vitamin E, Tetracycline
2	Dental extraction	Chronic apical periodontitis	Mandible	Y	24	3	9	Y - Amoxicillin	Local curettage / sequestrae removal	Y - Chlorhexidine - topical /mouthwash application	N
3	Dental extraction	Chronic apical periodontitis	Mandible	Y	5	1	36	Y- Tetracycline	N	Y - Chlorhexidine - topical /mouthwash application	Pentoxyfylline, Vitamin E, Tetracycline
4	Dental extraction	Chronic apical periodontitis	Mandible	N	0	0	3	Y- Tetracycline	Local curettage / sequestrae removal	Y - Chlorhexidine - topical /mouthwash application	Pentoxyfylline, Vitamin E, Tetracycline
5	Dental extraction	Chronic apical periodontitis	Mandible	Y	5	3	48	Y – Penicillin V	Local curettage / sequestrae removal	Y - Chlorhexidine - topical /mouthwash application	Pentoxyfylline, Vitamin E, Tetracycline
6	Dental extraction	Caries/Root fracture	Mandible	Y	25	2	84	Y- Tetracycline	N	Y - Chlorhexidine - topical /mouthwash application	N
7	Dental extraction	Periodontitis	Mandible	N	0	0	117	N – But on long-term antibiotics Penicillin V since January 1988	N	Y - Chlorhexidine - topical /mouthwash application	N
8	Periapical infection	NA – Teeth still in situ	Mandible	N	0	0	0	Y - Amoxicillin	N	Y - Chlorhexidine - topical /mouthwash application	N

Table 8.3 BRONJ disease details and treatment summary.

A summary of BRONJ disease in the eight recruited patients in the study. Details in the table include; precipitating factor, jaw site, BRONJ stage, as well as exposure period and size. The treatment received by each patient in terms of systemic antimicrobials or drugs, topical therapies and surgery is detailed. BRONJ stage (0-3) is stated in line with AAOMS staging criteria. Y=Yes, N=No.

BRONJ patient	Painful at present (Y/N)	Pain at present-Numeric pain rating scale (1-10)	Worst pain-Numeric pain rating scale (Recalled) (1-10)	Eating affected (Y/N)	Aware of infection (Y/N)	Pathological jaw fracture	Reported symptoms
1	N	0	9	Y – Mouth painful	Y-Intraoral Pus drainage through exposure	N	Bad taste, Previously painful
2	N	0	9	Y – Food trapping	Y – Intraoral Pus drainage through exposure	N	Occasional electric pain, food trapping and Bad taste
3	Y	4	7	Y – Mouth uncomfortable	N	N	Referred soreness and pain to ear
4	N	0	10	Y – Previously only able to eat soft food and drinking through straw	N	N	Sleep affected
5	Y	4	10	Y – Mouth generally uncomfortable	Y – Intraoral Pus drainage through exposure	N	Numbness in lip and paraesthesia in jaw
6	N	0	9	Y – Food trapping	N	N	Sharp bone, food packing, bad taste
7	N	0	0	N	Y – Intraoral Pus drainage through exposure	N	None
8	N	0	3	Y-Avoids eating on affected side	Y – Intraoral Pus drainage through exposure	N	None

Table 8.4 Pain and Quality of life issues in BRONJ patients

Factors relating to quality of life in BRONJ including reported numeric pain rating scale (1-10) for pain at present as well as the worst recalled pain. Qualitative data recorded from these patients included whether or not eating was affected and whether patients were aware of symptoms of infection. Other symptoms reported by this patient group were also recorded. Y=Yes, N=No.

8.6 V γ 9V δ 2 T cells are significantly depleted in BRONJ patients.

Initially, the relative percentages of both V γ 9V δ 2 and V δ 1⁽⁺⁾ T cells was determined in the eight BRONJ patients as a percentage of total lymphocyte number and compared to the three different control groups. All groups with previous exposure to bisphosphonates, including the BRONJ cohort, showed evidence of significant depletion in V δ 2/CD3(%) when compared to healthy controls with no previous bisphosphonate exposure ($p < 0.01$) (Figure 8.1). BRONJ patients had a median level of expression of 0.10% (range 0.00-0.21%), with those patients in the oral bisphosphonate group having a value of 0.07% (range 0.04-0.11%) and those in the IV bisphosphonate control group having a value of 0.13% (range 0.03-0.29%). By contrast, healthy volunteers showed a median level of expression of 2.15%, (range 0.25-21.91%).

Interestingly, there were no significant statistical differences ($p > 0.05$) between any of the BRONJ or bisphosphonate control groups although interestingly the three lowest V δ 2/CD3(%) were all found in BRONJ patients ($< 0.09\%$). This suggested that patients taking both oral and intravenous forms of bisphosphonates have depleted V γ 9V δ 2 T cell numbers in their peripheral blood compared to healthy controls.

The lowest median age in the healthy cohort (33 years) compared to the BRONJ cohort (58.5years), IV bisphosphonate control group (78 years), and oral bisphosphonate control group (72 years) might suggest that peripheral blood depletion of V γ 9V δ 2 T cells may simply be related to age rather than bisphosphonate intake. However when comparisons were made with only older

healthy volunteers > 50 years (n=16, median age 57 years), V γ 9V δ 2 T cells continued to be significantly depleted in BRONJ patients, (0.10% vs. 1.49%, p = 0.002) (Figure 8.1A).

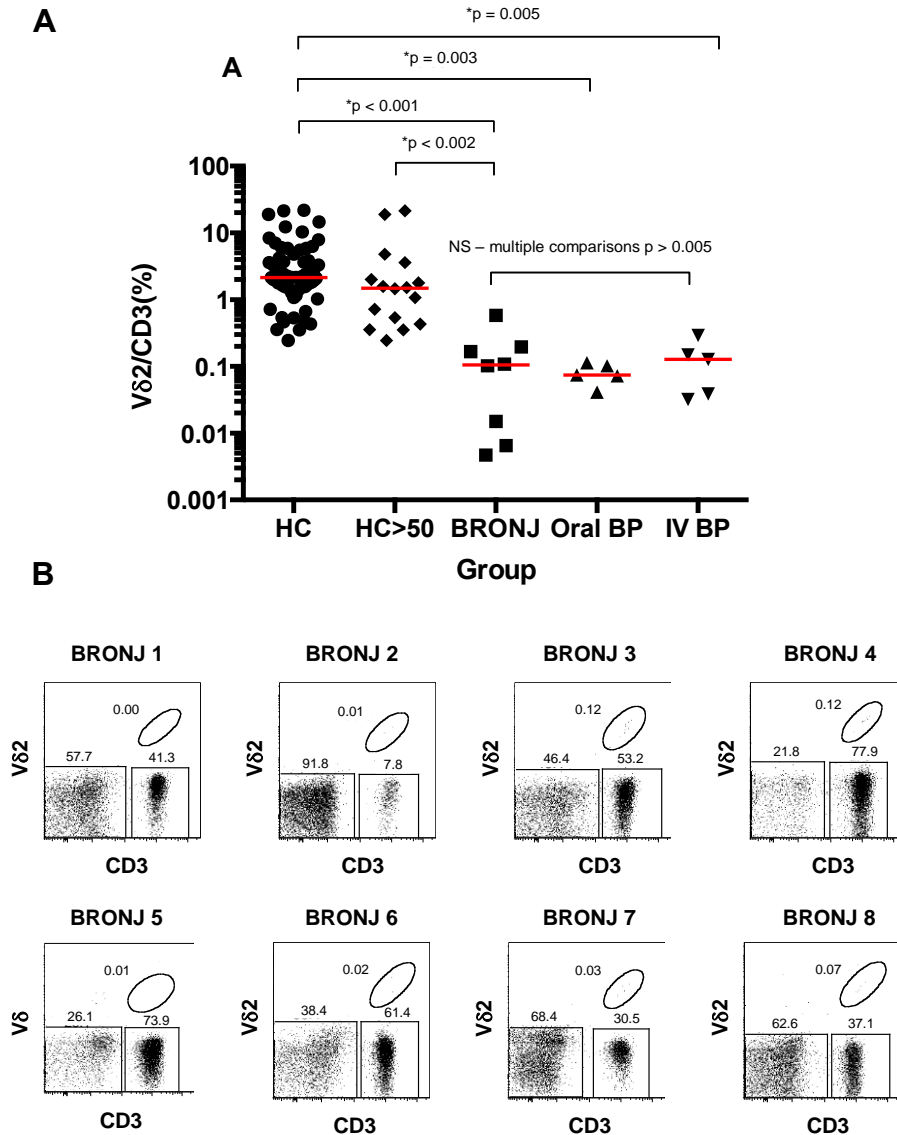


Figure 8.1 V δ 2/CD3(%) depletion in BRONJ patients and in patients on long-term bisphosphonate therapy.

(A) Graph shows V γ 9V δ 2 T cells expressed as a percentage of total CD3⁽⁺⁾ lymphocytes in the peripheral blood of different study groups; Healthy controls (HC), Healthy control >50 years (HC >50), Bisphosphonate-related osteonecrosis of the jaw patients (BRONJ), Oral bisphosphonate therapy patients (Oral BP) and Intravenous bisphosphonate therapy patients (IV BP). Red lines represent median values with statistical differences assessed using Kruskal-Wallis test (ANOVA) and multiple comparison post-hoc testing with Bonferroni correction (p-values are indicated). (B) Two-dimensional flow cytometry dot plots of all eight BRONJ patients showing depleted V δ 2⁽⁺⁾CD3⁽⁺⁾ T cell populations in peripheral venous blood samples. Percentage figures are stated next to adjacent gate.

8.7 $V\delta 1^{(+)}$ T cells show no evidence of depletion in BRONJ patients compared to all other control groups.

Following the observation that $V\gamma 9V\delta 2$ T cells are depleted in the BRONJ patient group, the levels of $V\delta 1/CD3(\%)$ were also determined to investigate whether there might also be differences in these cells. Figure 8.2 shows that the median percentages of $V\delta 1/CD3(\%)$ in BRONJ patients is 1.95% (range 0.29-5.19%). This compares to each of the respective control groups as follows; oral BP group 1.76% (range 0.12-4.56); IV BP group 0.75% (range 0.22-1.80%); and healthy non-exposed controls 0.79% (range 0.16-4.74). There were no significant differences between any of these groups ($p > 0.05$).

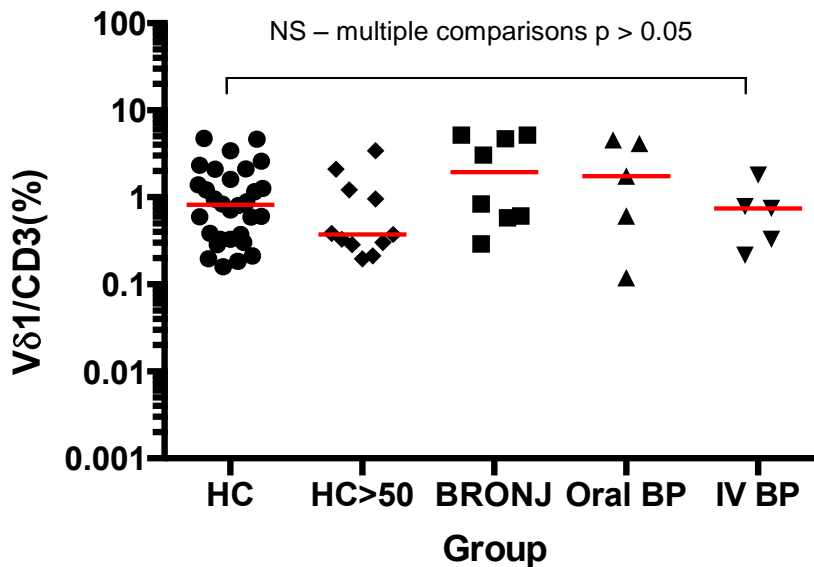


Figure 8.2 $V\delta 1^{(+)}$ T cells show no evidence of depletion in BRONJ patients and in patients on long-term bisphosphonate therapy.

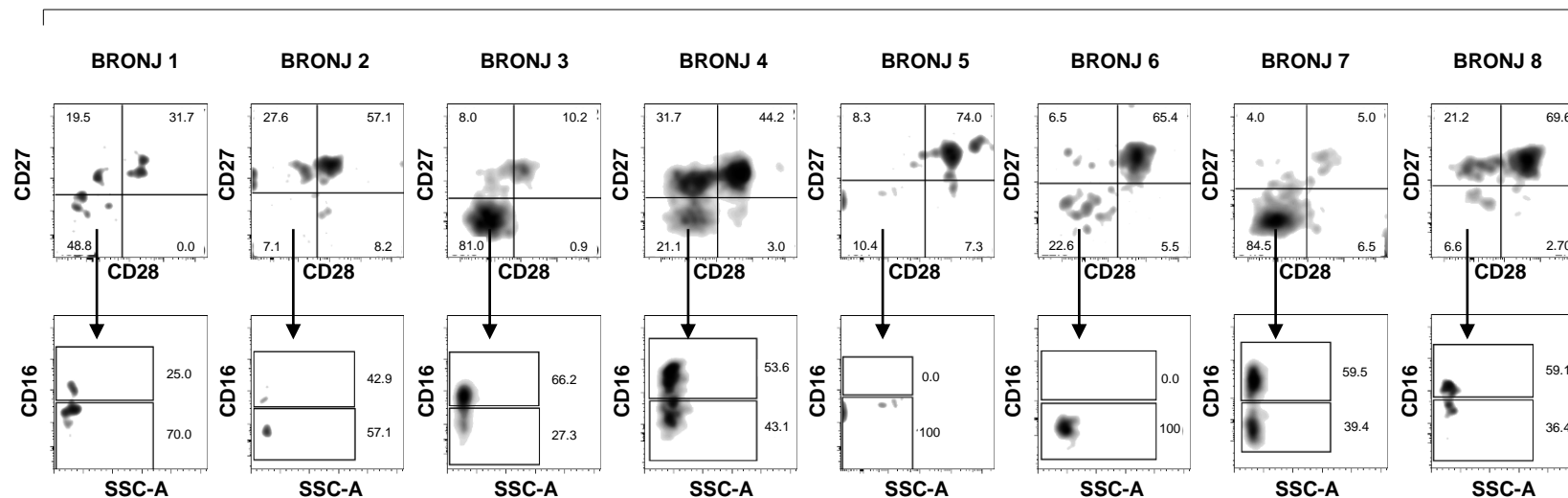
Graph shows $V\delta 1^{(+)}$ T cells expressed as a percentage of total $CD3^{(+)}$ lymphocytes in the peripheral blood of different study groups; Healthy controls (HC), Healthy control > 50 years (HC> 50), Bisphosphonate-related osteonecrosis of the jaw patients (BRONJ), Oral bisphosphonate therapy patients (Oral BP) and Intravenous bisphosphonates therapy patients (IV BP). Red lines represent median values with statistical differences assessed using Kruskal-Wallis test (ANOVA) and multiple comparison post-hoc testing with Bonferroni correction.

Comparison to older healthy controls (> 50 years) also failed to show significant differences between these groups. Thus, there is no evidence to support any significant changes in the proportion of V δ 1⁽⁺⁾ T cells in the blood of BRONJ patients or in patients taking different forms of bisphosphonates.

8.8 No evidence for a predominating V γ 9V δ 2 T cell phenotype in BRONJ patients

The phenotypic signature based on CD28, CD27 and CD16 was determined for V γ 9V δ 2 T cells from each individual in each of the individual cohorts to investigate whether a particular signature was characteristic of BRONJ disease or bisphosphonate treatment. It might be hypothesised that in patients who are on long-term bisphosphonate therapy, that persistent activation might lead to an effector phenotype (i.e. phenotypic signatures 4,5 or 6). However, there were no obvious dominant signatures in any of the groups (Figure 8.3). In the eight BRONJ patients, five out of the six phenotypic signatures were observed (i.e. phenotypic signatures 1,2,2,2,3,4,6,6) (Figure 8.3). Similarly, in the intravenous bisphosphonate control group the predominance of a particular phenotypic signature could not be determined, with all five individuals having a different phenotypic signature i.e. 1,2,3,4 and 5 (Figure 8.4). This wide spectrum of observed phenotypes was also observed in the oral bisphosphonate control group who had phenotypic signatures 2,3,3,4 and 6 (Figure 8.5). Therefore the idea that V γ 9V δ 2 T cell depletion is associated with polarisation to a particular phenotype is not supported by these data and instead is consistent with V γ 9V δ 2 T cell phenotypes being relatively stable over time and not affected by long-term antigen exposure or activation.

A

V γ 9V δ 2 T cell profiles from eight BRONJ patients

B

	BRONJ 1	BRONJ 2	BRONJ 3	BRONJ 4	BRONJ 5	BRONJ 6	BRONJ 7	BRONJ 8
V δ 2/CD3(%)	0.01	0.09	0.21	0.15	0.01	0.00	0.10	0.20
Gender (M/F)	F	F	F	F	F	M	F	M
Phenotypic signature group (1-6)	4	2	6	3	1	2	6	2
Reason for BP prescription	Osteoporosis	Breast cancer	Osteoporosis	Osteoporosis	Osteoporosis	Multiple myeloma	Osteoporosis	Multiple myeloma
Route (Oral/IV)	Oral	IV	Oral	IV	Oral	Oral	IV	Oral
Drug (Route)	AA (Oral)	ZOL (IV)	AA (Oral)	ZOL (IV)	AA (Oral)	AA (Oral)	ZOL (IV)	AA (Oral)
Time on medication (months)	46	9	36	178	48	84	60	24

Figure 8.3 Range of V γ 9V δ 2 T cell phenotypes in BRONJ patients.

Flow cytometry density plots are shown for each individual BRONJ patient (1-8) (A). V γ 9V δ 2 T cell phenotypes are shown using surface markers CD28, CD27 with CD16 expression shown for the CD27⁻CD28⁻ subset. Linked table (B) shows details of V δ 2/CD3(%), gender, phenotypic signature, bisphosphonate drug, route of administration and length of time on medication for each individual BRONJ patient. SSC-A=Side scatter–Area, AA=Aledronic acid, ZOL=Zoledronate, IV=Intravenous, M=Male and F=Female.

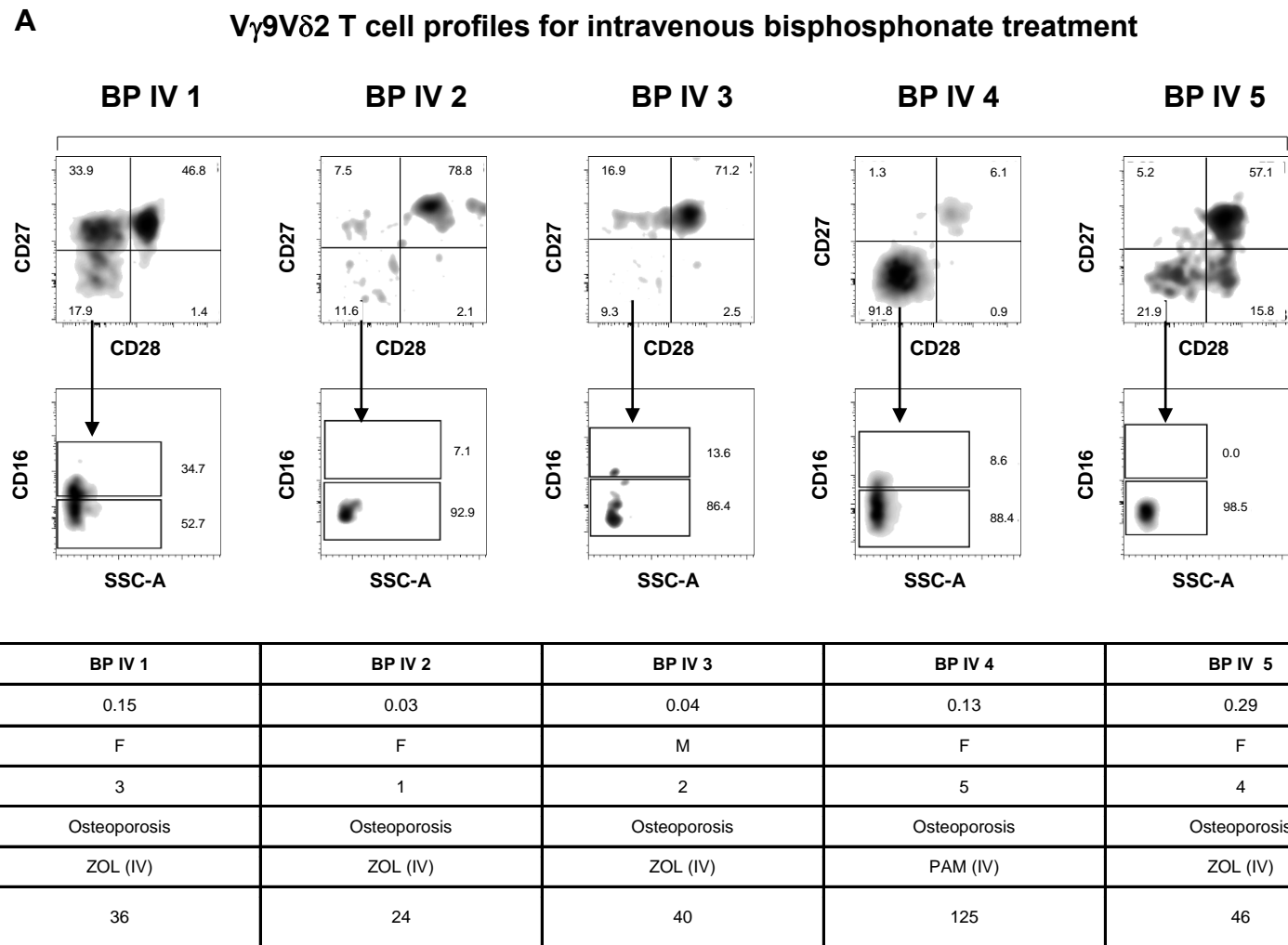


Figure 8.4 Range of $V\gamma 9V\delta 2$ T cell phenotypes in osteoporotic patients taking intravenous bisphosphonates.

Flow cytometry density plots are shown for each individual osteoporotic patient taking intravenous bisphosphonates (BP IV 1-5) (A). $V\gamma 9V\delta 2$ T cell phenotypes are shown using surface markers CD28 and CD27 with CD16 expression shown for the CD27⁽⁻⁾CD28⁽⁻⁾ subset. Linked table (B) shows details of $V\delta 2/CD3(\%)$, gender, phenotypic signature, bisphosphonate drug, route of administration and length of time on medication for each individual patient. AA = Aledronic acid, ZOL = Zoledronate, IV = Intravenous, M=Male and F=Female.

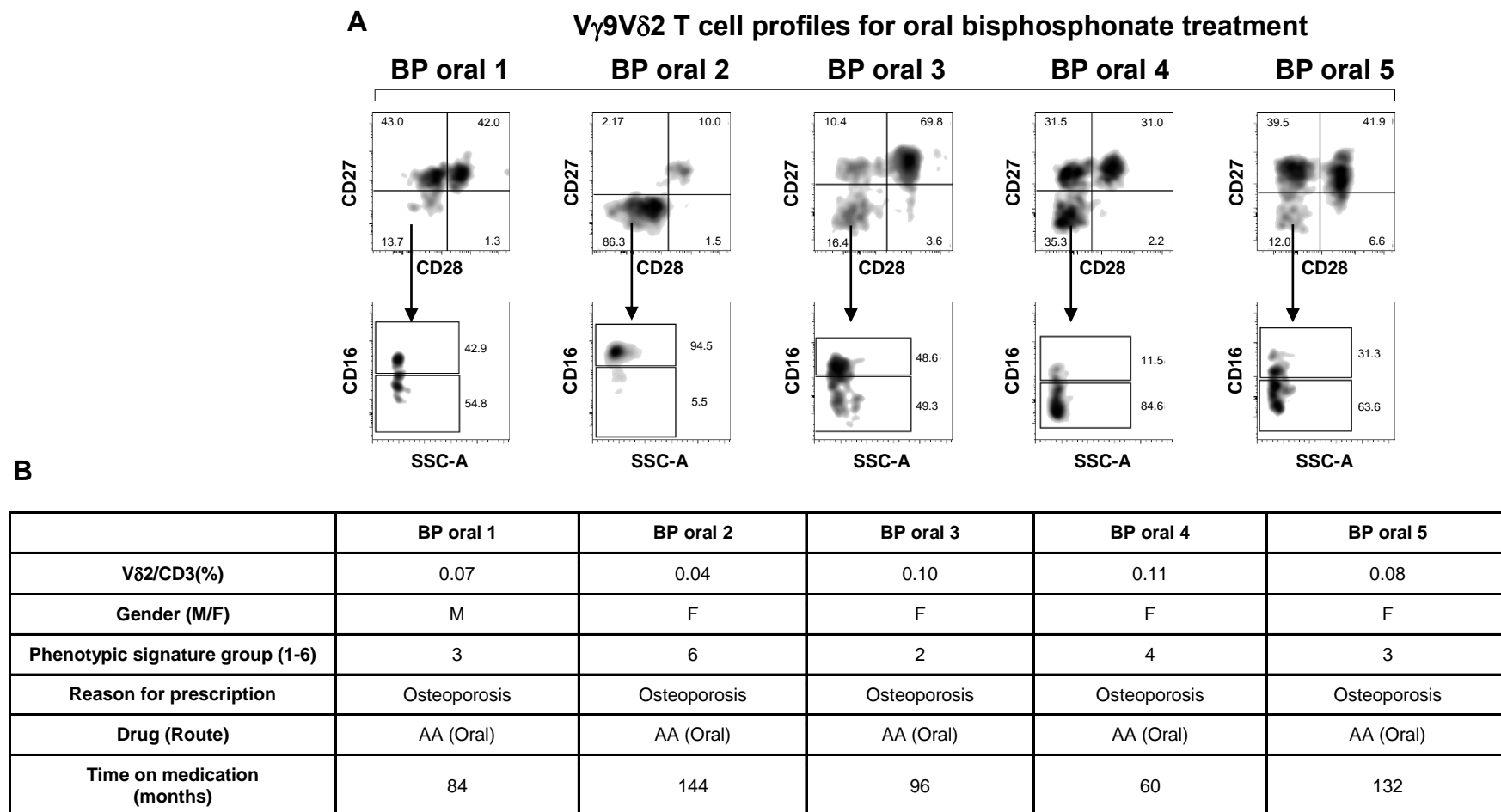


Figure 8.5 Range of V γ 9V δ 2 T cell phenotypes in osteoporotic patients taking oral bisphosphonates.

Flow cytometry density plots are shown for each individual osteoporotic oral bisphosphonate patient (BP oral 1-5) (A). V γ 9V δ 2 T cell phenotypes are shown using surface markers CD27 and CD28 with CD16 expression shown for the CD27⁽⁻⁾CD28⁽⁻⁾ subset. Linked table (B) shows details of V δ 2/CD3(%), gender, phenotypic signature, bisphosphonate drug, route of administration and length of time on medication for each individual patient. SSC-A = Side scatter-Area, BP = Bisphosphonate, AA = Aledronic acid, M=Male and F=Female.

8.9 Summary

This final chapter presents evidence that $V\gamma 9V\delta 2$ T cells are depleted in BRONJ patients. In all eight of the BRONJ patients, $V\gamma 9V\delta 2$ T cells were severely depleted compared to age matched healthy controls with no apparent effect on $V\delta 1^{(+)}$ T cells. However $V\gamma 9V\delta 2$ T cell depletion was also observed in bisphosphonate-treated patients both on oral and intravenous forms of the medication, suggesting that the $V\gamma 9V\delta 2$ T cell depletion is a consequence of bisphosphonate use, rather than a feature of the disease. In addition, we also observed no signatory $V\gamma 9V\delta 2$ T cell phenotype associated with either BRONJ or bisphosphonate use. The lack of a bias towards the $\gamma\delta^{(16+)}$ phenotype suggests that simple activation of $V\gamma 9V\delta 2$ T cells is not sufficient to drive differentiation of $V\gamma 9V\delta 2$ T cells to different phenotypes, even if the activating signal is long-term. Finally, the chapter also highlights the range of symptoms in BRONJ patients and that the condition can range from periods of severe pain to those who are apparently unaffected symptomatically by the condition.

Chapter 9

Discussion and Future work

Chapter 9 Discussion

Human $V\gamma 9V\delta 2$ T cells are a heterogeneous population of cells with a high degree of functional plasticity and suggested roles in a number of disease processes including bisphosphonate-related osteonecrosis of the jaw (BRONJ) (Dieli *et al.* 2001, Kalyan and Kabelitz 2013, Kalyan *et al.* 2013). Our understanding of these unconventional T cells has been somewhat hindered by a failure to develop a consistent system of nomenclature and system of phenotypic characterisation. Therefore, the results in this thesis propose the use of CD28, CD27 and CD16 as more useful markers in the phenotypic characterisation of $V\gamma 9V\delta 2$ T cells which can be used to identify six different $V\gamma 9V\delta 2$ T cell “phenotypic signatures” at the level of the individual that predict different functional capabilities and offers a potential novel solution to the challenges of predicting responses to $V\gamma 9V\delta 2$ T cell immunotherapeutic interventions.

The thesis also examined $V\gamma 9V\delta 2$ T cell subsets in human neo-natal thymuses in an attempt to understand subsets present early in development. However, the hypothesised early/naïve subsets seen in the blood failed to be identified in the thymus with only a minority of naïve surface markers expressed by thymocytes. The study does however identify two thymic subsets; $[CD27^{(+)}CD11a^{(Lo)}]$ and $[CD27^{(Hi)}CD11a^{(+)}]$ with a possible role in antigen presentation, which is subsequently discussed.

The newly-defined phenotypic system is also shown to be appropriate for the characterisation of the $V\delta 1^{(+)}$ T cell population which in contrast to $V\gamma 9V\delta 2$

T cells is characterised by a high proportion of “naïve” cells. Finally, some preliminary evidence is discussed showing that V γ 9V δ 2 T cell depletion is a feature of patients on long-term nitrogen containing bisphosphonate therapy including those with a diagnosis of BRONJ.

9.1 CD45RA is not a reliable marker for accurate representation of V γ 9V δ 2 T cells

One of the main conclusions of the thesis, is the limitations that the conventionally-used markers (CD27 and CD45RA) have in consistently failing to describe discrete V γ 9V δ 2 T cell subsets. Indeed, in reviewing the literature, it appears that the surface markers CD27 and CD45RA have been used to subset V γ 9V δ 2 T cells without particular justification or rationale and appearing to be a carry over of markers and descriptors commonly used to describe $\alpha\beta$ T cell subsets (Hamann *et al.* 1997, Hintzen *et al.* 1993).

The results of this study indicate that CD27 and CD45RA clearly better define four distinct subsets in conventional $\alpha\beta$ T cells compared to V γ 9V δ 2 T cells, where in particular, the wide range of expression levels make use of the CD45RA surface marker problematic. The fact that populations are not clearly identifiable using the CD27 and CD45RA surface markers, suggests that gating of these populations is likely to be variable in studies using this method leading to inconsistent estimates of the subsets. The reasons explaining why CD45RA expression is less pronounced on V γ 9V δ 2 T cells than on $\alpha\beta$ T cells from the same individual are unclear, but may be due to differences in the level of transcription or translation of the marker in the different T cell subtypes or due to post-translational processing in V γ 9V δ 2 T cells that removes/downregulates

surface expression of the marker. This practical limitation of CD45RA as a phenotypic marker has to date not been addressed in the literature and raises the question whether it is the most appropriate marker to use in describing V γ 9V δ 2 T cell subsets.

Questions are also raised as to the usefulness of CD45RA with respect to the apparent over-estimation of the “naïve” V γ 9V δ 2 T cell subset [CD27⁽⁺⁾CD45RA⁽⁺⁾], despite these same markers satisfactorily identifying “naïve” $\alpha\beta$ T cells (Hintzen *et al.* 1993, Hamann *et al.* 1997). This finding echoes the beliefs of others in the field who have also questioned the use of [CD27⁽⁺⁾CD45RA⁽⁺⁾] as a useful “naïve” cell descriptor due to its overestimation of this population in comparison to the much lower estimates (typically < 5%) when other “naïve” marker combinations are used e.g. CD27^(Hi)CD11a^(Lo) (De Rosa *et al.* 2004, Morita *et al.* 2007). Clearly, this suggests that there is a need to re-evaluate the findings and implications of studies that report a high percentage of $\gamma\delta^{(N)}$ cells when using [CD27⁽⁺⁾CD45RA⁽⁺⁾] (Dieli *et al.* 2003b, Caccamo *et al.* 2006).

The low numbers or relative absence of “naïve” V γ 9V δ 2 T cells in adult peripheral blood suggest that they convert to a non-“naïve” phenotype very early in life (Parker *et al.* 1990). This conversion likely occurs due to early environmental and/or infectious challenge, that results in an isoprenoid-mediated expansion of the population and conversion to an activated phenotype (Parker *et al.* 1990, De Rosa *et al.* 2004). Therefore, the fact that V γ 9V δ 2 T cells respond to commonly found isoprenoid molecules have lead many to speculate that these cells use their TCR as a form of pattern recognition receptor. Furthermore, the fact that these cells do not recognise

specific antigen epitopes, makes them very different to conventional MHC-restricted $\alpha\beta$ T cells that only recognise their specific cognate antigen. Additionally, and once more in contrast to $\alpha\beta$ T cells, the low levels of CCR7 expression on $V\gamma 9V\delta 2$ T cells observed in this study implies that the majority are unable to recirculate through secondary lymphoid tissue, again suggesting that they do not sample antigen in the same way as conventional T cells.

In bringing these observations together, it is apparent that the use of the terms “naïve” and “memory” as defining terms for $V\gamma 9V\delta 2$ T cell subsets, whilst being appropriate in describing the stages of $\alpha\beta$ T cell differentiation, may not be appropriate in describing unconventional $V\gamma 9V\delta 2$ T cell populations. Instead, $V\gamma 9V\delta 2$ T cells are perhaps better thought of as cells with developing states of “effector potential” that have predictable characteristics once activated.

9.2 $V\gamma 9V\delta 2$ T cells are better identified using CD28, CD27, and CD16

A thorough re-evaluation of all $V\gamma 9V\delta 2$ T cells surface markers (that had been previously utilised to identify distinct $V\gamma 9V\delta 2$ T cell subsets in other studies) suggested that a combination of CD28, CD27 and CD16 represented a robust and reliable methodology for the characterisation of $V\gamma 9V\delta 2$ T cells. This allowed all non-naïve $V\gamma 9V\delta 2$ T cells from all individuals to be described as belonging to one of four subsets; $\gamma\delta^{(28+)}$ cells [CD28⁽⁺⁾CD27⁽⁺⁾]; $\gamma\delta^{(28-)}$ cells [CD28⁽⁻⁾CD27⁽⁺⁾]; $\gamma\delta^{(16-)}$ cells [CD28⁽⁻⁾CD27⁽⁻⁾CD16⁽⁻⁾]; and $\gamma\delta^{(16+)}$ cells [CD28⁽⁻⁾CD27⁽⁻⁾CD16⁽⁺⁾]. Clearly, whilst CD28, CD27 and CD16 more readily identify distinct subsets it is also important to consider, the biological significance of

their expression to help explain the functional differences between the different subsets.

For conventional $\alpha\beta$ T cells, it is now generally accepted that effective T cell signalling not only requires TCR activation through recognition of MHC-associated antigen (signal-1) but also requires the co-stimulatory molecules such as, CD27 and CD28, to provide an additional “signal 2” to facilitate effective T cell activation when bound to their respective ligands (CD70-CD27) and (CD80/CD86-CD28). These molecules have been shown to be important in generating effective survival and proliferative responses in conventional T cells (Hintzen *et al.* 1993), but also more recently in human $V\gamma 9V\delta 2$ T cells (Ribot *et al.* 2012). It therefore follows that the relative expression levels of CD27 and CD28 on $V\gamma 9V\delta 2$ T cell subsets may help us to define functionally distinct subsets; e.g. cells expressing both co-stimulatory receptors [CD28⁽⁺⁾CD27⁽⁺⁾] $\gamma\delta^{(28+)}$ cells, one of the receptors [CD28⁽⁻⁾CD27⁽⁺⁾] $\gamma\delta^{(28-)}$ cells, or when both are absent [CD28⁽⁻⁾CD27⁽⁻⁾] $\gamma\delta^{(28-27-)}$. In further characterising $V\gamma 9V\delta 2$ T cells lacking both co-stimulatory receptors, CD16, an Fc-receptor (Fc γ RIIIa/b) typically found on cytotoxic CD8 T cells and NK cells, was used to further discriminate $V\gamma 9V\delta 2$ T cells with cytotoxic effector function in the [CD28⁽⁻⁾CD27⁽⁻⁾] subset. Therefore, the combined use of the well-characterised co-stimulatory molecules (CD27/CD28) in conjunction with a well-established marker of cytotoxic function (CD16) seem to provide an improved method of subsetting $V\gamma 9V\delta 2$ T cells.

Whilst all $V\gamma 9V\delta 2$ T cell subsets demonstrated the ability to readily produce T_H1-associated cytokines on stimulation (IFN- γ and TNF- α), there was evidence that the three CD28⁽⁻⁾ subsets showed increased cytotoxic potential as judged by a

number of a number of cytotoxic markers e.g. perforin, granulysin and granzyme B, with increased levels of expression particularly in the $\gamma\delta^{(16-)}$ and $\gamma\delta^{(16+)}$ subsets. Further differences were also observed in the proliferative potential of the subsets, with higher capacity in $\gamma\delta^{(28+)}$ and $\gamma\delta^{(28-)}$ subsets compared to $\gamma\delta^{(16-)}$ and $\gamma\delta^{(16+)}$ subsets. Having established a better definition of V γ 9V δ 2 T cell subsets it was apparent that they had distinct functional characteristics in terms of their proliferative potential, cytokine-secreting capacity, and cytotoxic function. Clearly, the differences in function of different subsets would predict that an individual's response to infectious challenge and cancer will be different depending on the relative proportion of V γ 9V δ 2 T cell subsets i.e. their phenotypic signature.

9.3 Significant individual-to-individual variation in the proportions of the four newly-defined V γ 9V δ 2 T cell subsets identifies at least six signature profiles

The $\gamma\delta$ T cell subset distribution of different individuals varies significantly. Indeed, healthy individuals can be sub-divided into at least six signature profiles, with differing proportions of each subset in each profile. As the four subsets differ in terms of their functional attributes, it follows that the different V γ 9V δ 2 T cell phenotypic signatures predict distinct V γ 9V δ 2 T cell functional potentials for different individuals. Thus, immunotherapeutic strategies that attempt to expand or activate V γ 9V δ 2 T cells will have different outcomes in individuals with different signature profiles. This in turn suggests that patient stratification into V γ 9V δ 2 T cell signature profiles would maximise the benefits of V γ 9V δ 2 T cell therapy aimed at a particular functional outcome. For example,

individuals with a predominance of $\gamma\delta^{(28+)}$ cells and $\gamma\delta^{(28-)}$ cells (phenotypic signatures 1-3) are likely to have more robust proliferative responses in comparison to those with a predominance of the $\gamma\delta^{(16-)}$ and $\gamma\delta^{(16+)}$ subsets with strong cytotoxic responses (phenotypic signatures 4-6). Clearly, our ability to predict V γ 9V δ 2 T cell responses has potential to allow more accurate forecast of V γ 9V δ 2 T cell immunotherapy success which at present is relatively unpredictable in terms of treatment success and improving survival outcome (Meraviglia *et al.* 2010, Wilhelm *et al.* 2003). Extending this concept further, a knowledge of an individual's V γ 9V δ 2 T cell profile may also be predictive of their own ability to mount protective V γ 9V δ 2 T cell responses to infectious challenge or tumours.

9.4 The $\gamma\delta^{(28+)}$ cell subset may retain the potential to develop into IL-17-secreting V γ 9V δ 2 T cells.

Unlike either human $\alpha\beta$ T cells, or mouse $\gamma\delta$ T cells, human $\gamma\delta$ T cells do not readily display IL-17-secreting capacity. Indeed, a lengthy and complicated activation regime *in vitro* is required to generate even a few IL-17-secreting V γ 9V δ 2 T cells (Caccamo *et al.* 2011b, Ness-Schwickerath and Morita 2011). Despite this, several studies have reported IL-17-secreting V γ 9V δ 2 T cells in certain diseases including tuberculosis and HIV (Peng *et al.* 2008, Fenoglio *et al.* 2009) (suggesting not only that V γ 9V δ 2 T cells can adopt this cytokine-secreting state, but also that they may have functional implications for disease progression).

Interestingly, the microarray gene expression analysis of the four newly-defined V γ 9V δ 2 T cell subsets suggest that the $\gamma\delta^{(28+)}$ cell subset may retain the ability

to develop IL-17-secreting potential as it differentially expresses three genes; *CCR6*, *RORC*, and *IL-23R*, which are implicated in the development of an IL-17-secreting phenotype. Moreover, the surface expression of CCR6 identifies a distinct sub-population of $\gamma\delta^{(28+)}$ cells lacking expression of CX3CR1 (Fractalkine receptor) which is strongly expressed by $CCR6^{(-)} \gamma\delta^{(28+)}$ cells, and all $\gamma\delta^{(28-)}$, $\gamma\delta^{(16-)}$ and $\gamma\delta^{(16+)}$ cells. CX3CR1 is a chemokine receptor that binds the chemokine CX3CL1 (fractalkine) and is believed to be important in the adhesion and migration of lymphocytes into tissues in a number of inflammatory diseases (Imai *et al.* 1997, Cockwell *et al.* 2002). It is produced in endothelial cells as a membrane adhesion protein as well as existing as a secreted chemotactic factor (Imaizumi *et al.* 2004). Thus, this $CCR6^{(+)} \gamma\delta^{(28+)}$ cell subset may represent an IL-17-secreting $V\gamma9V\delta2$ T cell progenitor population with reduced ability to migrate to the tissues, although the functional significance of the mutually exclusive expression of CCR6 and CX3CR1 clearly requires more in-depth study. Therefore, the characterisation of this subset, and investigation of whether it can be induced to adopt an IL-17-secreting phenotype under certain activation conditions is an obvious area of future potential research (see future work).

It would also be interesting to see whether this $CCR6^{(+)}CX3CR1^{(-)} \gamma\delta^{(28+)}$ subset is present in all individuals. If not, studies that attempted to generate IL-17-secreting $V\gamma9V\delta2$ T cells from donors that lacked this population would have revealed predictably negative results. In addition, if IL-17 producing subsets are not present in all individuals this also has implications in terms of predicting risk of IL-17-mediated inflammatory diseases e.g. rheumatoid arthritis and

psoriasis where IL-17 secreting $V\gamma 9V\delta 2$ T cells are believed to be key in the pathogenesis of disease (Laggner *et al.* 2011, Hu *et al.* 2012).

9.5 Mutually exclusive CCR6 and CX3CR1 expression in $V\gamma 9V\delta 2$ T cells identify an important differentiation stage in their functional biology

The mutually exclusive relationship between the chemokine receptors CCR6 and CX3CR1 appears to identify two non-overlapping $V\gamma 9V\delta 2$ T cells subsets; [CCR6⁽⁺⁾CX3CR1⁽⁻⁾] with a proposed IL-17 producing potential, and a second [CCR6⁽⁻⁾CX3CR1⁽⁺⁾] subset expressing the opposite pattern of chemokine receptors. Whilst the identification of a subset with potential IL-17 producing ability is interesting, nevertheless it is clear that the majority of $V\gamma 9V\delta 2$ T cells in the peripheral blood typically adopt a T_{H1} phenotype in preference to differentiation into T_{H17} -like, IL-17-producing subsets. It is therefore possible that the transition between the [CCR6⁽⁺⁾CX3CR1⁽⁻⁾] and [CCR6⁽⁻⁾CX3CR1⁽⁺⁾] populations within the $\gamma\delta^{(28+)}$ subset may signify an important developmental step in $\gamma\delta$ T cell biology. Indeed, it may represent the branch-point at which cells can either progress down a T_{H1} or a T_{H17} pathway as the expression of CCR6 on $V\gamma 9V\delta 2$ T cell subsets has previously been identified as a potential surface marker of cells with IL-17 producing potential (Caccamo *et al.* 2011a)(Figure 9.1).

Clearly, $V\gamma 9V\delta 2$ T cells show a typical preference to adopt a cytotoxic T_{H1} potential, as CX3CR1⁽⁺⁾ cells also upregulate granzyme B, granulysin and perforin directly associated with a cytotoxic phenotype. It is therefore possible that the [CCR6⁽⁺⁾CX3CR1⁽⁻⁾] subset is a “plastic” population, that has potential to

differentiate into many different phenotypic populations, but preferentially assumes a cytotoxic T_H1-like phenotype. Indeed, it has been proposed in a recent review that cells with an IL-17-producing potential are preferentially polarised to a T_H1-like phenotype following repeated or specific antigen exposure (Ness-Schwickerath and Morita 2011). The authors also postulate that IL-17 production might be restored in these “switched” V γ 9V δ 2 T cells if they are exposed to IL-17 priming cytokines (IL-1 β , IL-6, IL-23 and TGF- β) perhaps in particular inflammatory or niche tissue environments in specific diseases (Ness-Schwickerath and Morita 2011). This suggests that despite the majority of T_H17-like V γ 9V δ 2 T cells switching to a T_H1 phenotype, they retain a “memory” of their IL-17 secreting ability that can be restored in tissue sites of infection and in cancer where many of these aforementioned “IL-17 priming cytokines” are produced in the local environment during inflammation (Figure 9.1).

9.6 The $\gamma\delta^{(28+)}$ cell subset has a distinct chemokine receptor expression profile.

The results from both the microarray data and flow cytometry surface marker analysis also revealed that the $\gamma\delta^{(28+)}$ cell subset had a distinct chemokine receptor profile when compared to the other three subsets. As well as the aforementioned expression of CCR6, a significant proportion of the $\gamma\delta^{(28+)}$ cell subset also expressed both CCR2 and CCR5. These chemokine receptors have been shown to be important in the migration of both V δ 1 and V γ 9V δ 2 T cells towards tumour and inflammatory sites in murine experimental models of

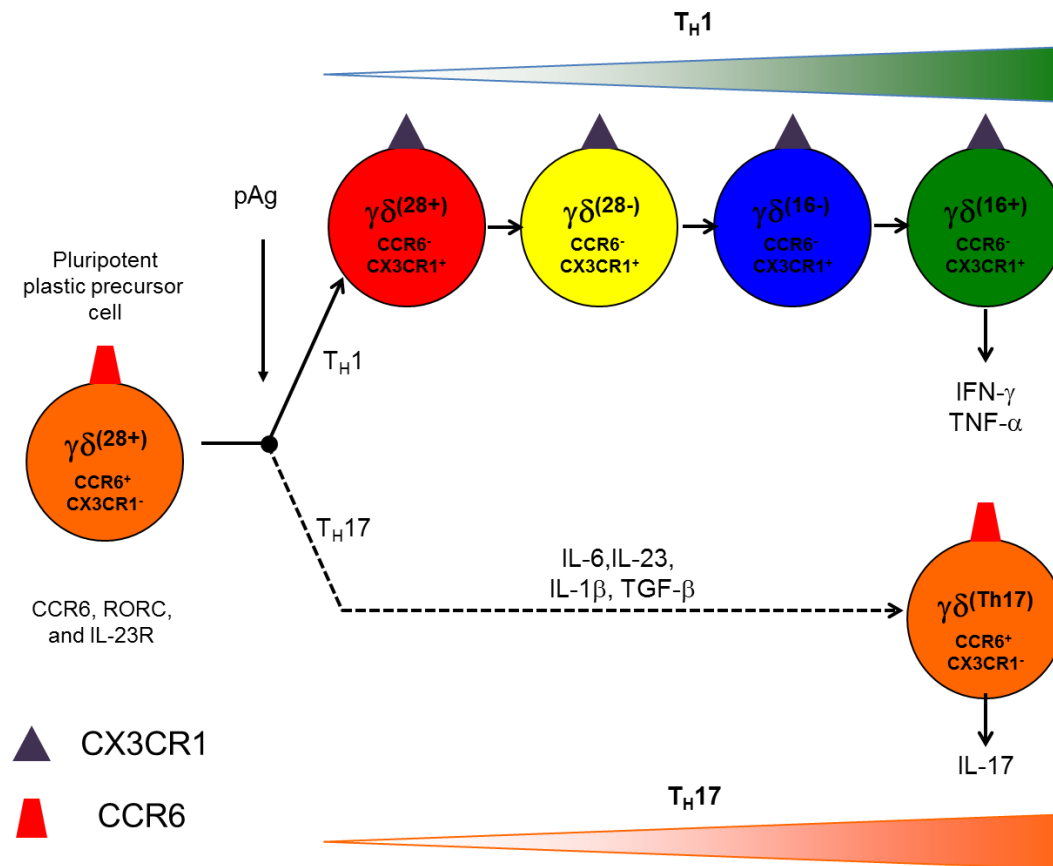


Figure 9.1 The $\gamma\delta(28^+)$ subset may represent a “plastic” population that can differentiate into cells with both T_H1 -like and T_H17 -like cytokine properties

$\gamma\delta(28^+)$ cells are made up of two further subsets with opposing patterns of chemokine receptor expression profiles i.e. $\gamma\delta(28^+)$ [CCR6⁽⁺⁾CX3CR1⁽⁻⁾] and $\gamma\delta(28^+)$ [CCR6⁽⁻⁾CX3CR1⁽⁺⁾] populations. Whilst the majority of $V\gamma9V\delta2$ T cells adopt a T_H1 -like expression profile, it is possible that the $\gamma\delta(28^+)$ [CCR6⁽⁺⁾CX3CR1⁽⁻⁾] subset represents a population that can differentiate under certain conditions into T_H17 -like cells with IL-17 producing capability.

malignant melanoma and as observed in human hepatocellular/colorectal cancer patients (Lança *et al.* 2013, Bouet-Toussaint *et al.* 2008). Previous studies have shown wide variation in the levels of CCR2 expression (15-58%) as well as CCR5 expression (59-98%) on human $\gamma\delta$ T cells with higher levels compared to conventional $\alpha\beta$ T cells (Meraviglia *et al.* 2011), perhaps suggesting an inherent increased ability of $\gamma\delta$ T cells in general to home to inflammatory/tumour sites compared to conventional $\alpha\beta$ T cells. A further study showed high levels of CCR2/CCR5 on CD27⁽⁻⁾ effector V γ 9V δ 2 T cell subsets (Dieli *et al.* 2003b) which is in contrast to the findings of this study that observe the highest levels of CCR2 and CCR5 on the $\gamma\delta^{(28+)}$ subset.

This would suggest that $\gamma\delta^{(28+)}$ cells show the highest homing potential to peripheral inflamed and tumour tissue sites despite having the lowest cytotoxic potential. However, further investigation to determine the expression of the inflammatory chemokine receptors CCR2 and CCR5 on [CCR6⁽⁺⁾CX3CR1⁽⁻⁾] and [CCR6⁽⁻⁾CX3CR1⁽⁺⁾] $\gamma\delta^{(28+)}$ subsets will allow us to better define these subsets in terms of their ability to home to inflammatory environments.

9.7 KIR proteins are expressed at high levels in the $\gamma\delta^{(16+)}$ subset

Two of the KIR family of proteins; Killer-cell immunoglobulin-like receptors 3 and 4 (*KIR2DL3* and *KR2DL4*), were expressed significantly higher in $\gamma\delta^{(16+)}$ cells compared to the three CD16⁽⁻⁾ subsets, with gene expression increasing across subsets. Our knowledge of these immunoregulatory genes is mainly derived from the study of NK cells and to date they have not been extensively studied in

V γ 9V δ 2 T cells. Therefore, the significance of an increasing level of expression of these genes across the subsets (i.e. $\gamma\delta^{(28+)} \rightarrow \gamma\delta^{(16+)}$) is not clear.

KIR2DL3 is an inhibitory receptor that inhibits cytotoxic signals through its two ITIM domains. It is expressed at higher levels in the subsets that display increased cytotoxic potential suggesting that it may be an in-built “control switch” that help to regulate cytotoxic responses (Rajagopalan and Long 2012). By contrast, KIR2DL4 is not expressed on the majority of V γ 9V δ 2 T cells (Lesport *et al.* 2011) being an atypical KIR protein expressed inside endosomes with little or no surface expression. KIR2DL4 shows extensive evolutionary conservation and has been proposed to have both inhibitory and activatory potential (Ponte *et al.* 1999, Rajagopalan *et al.* 2001). However on balance, it is considered to have a net stimulatory effect despite its single ITIM tail. KIR2DL4 promotes only weak cytotoxic activation, but in contrast its expression promotes a strong pro-inflammatory effect by increasing cytokine responses e.g. IFN- γ , TNF- α , IL-1 β and IL-6 (Rajagopalan and Long 2012). The expression of these KIR proteins clearly warrants further investigation along with cell surface characterisation of subsets to investigate whether their expression is similar to NK cells where these proteins have been predominantly studied (Rajagopalan *et al.* 2006, Rajagopalan and Long 2012). Interestingly, HLA-G is the only known ligand for KIR2DL4 and has been shown to be produced by tumours leading to an increase in serum HLA-G in these patients. Clearly, an increased understanding of the mechanisms that regulate V γ 9V δ 2 T cell cytotoxicity and cytokine secretion is central to our understanding of V γ 9V δ 2 T cell function in disease. In addition, it also has potential to assist in

developing more efficient cytotoxic V γ 9V δ 2 T cell immunotherapies against cancer.

9.8 Phenotypic subsets remain stable over time and suggest a homeostatic mechanism of control

In the analysis of V γ 9V δ 2 T cell from healthy volunteers, it was clear that a particular subset was not dominant in older individuals, suggesting that V γ 9V δ 2 T cells remained relatively stable throughout life, with a slight reduction in percentage (relative to total lymphocytes) with increasing age. The latter is consistent with studies that have also found a steady depletion of V γ 9V δ 2 T cells with increasing age (Parker *et al.* 1990, Caccamo *et al.* 2006, Michishita *et al.* 2011). In addition, there were no statistically significant differences found in V γ 9V δ 2 T cell percentage between sexes at different ages, which again is supported by published findings (Cairo *et al.* 2010). However, this finding is contradicted by one large study that found that V γ 9V δ 2 T cells were depleted with age more significantly in males (Caccamo *et al.* 2006). Results presented in this study also suggest that ethnicity, sub-region/continent of birth and the development status of country of birth did not significantly affect V γ 9V δ 2 T cell percentage in the peripheral blood. This however is not fully supported by other subset studies that have previously found an increase in V δ 2/CD3(%) in a Caucasian cohort compared to an African American cohort (Cairo *et al.* 2010). Indeed, another study also showed there to be significant variation in $\gamma\delta$ /CD3(%) depending on the country of the participating individual, with higher percentages found in Asian (Non-Japanese) and Turkish participants compared to Japanese and Swedish recruited cohorts (Esin *et al.* 1996).

The percentage of each V γ 9V δ 2 T cell phenotypic subset *also* appeared to be relatively stable over time with the only significant change being a decrease in the $\gamma\delta^{(28-)}$ subset in the oldest compared to youngest volunteers. All other subsets remained relatively stable with no significant changes found across the age ranges. This suggests that V γ 9V δ 2 T cell subsets are under some sort of homeostatic control. This relative stability over time is perhaps surprising, as it might be assumed that effector subsets might increase with age due to increased and cumulative antigen exposure. If it is also assumed that V γ 9V δ 2 T cells undergo a linear and progressive pattern of differentiation i.e. $\gamma\delta^{(28+)} \rightarrow \gamma\delta^{(28-)} \rightarrow \gamma\delta^{(16-)} \rightarrow \gamma\delta^{(16+)}$ and that thymic output is minimal after adolescence, then replenishment of subsets must occur independent of thymic output and perhaps via a stem or “memory” type population subset.

A range of phenotypic signatures were also found in the bisphosphonate-treated and BRONJ patients which demonstrates that despite continued activation of V γ 9V δ 2 T cells, and depletion from the blood that a shift towards an effector-dominated phenotypic signature does not occur. A final observation to support the notion that homeostatic regulation controls the stability of V γ 9V δ 2 T cell subsets over time was from a healthy 33 year-old female with signature #6 who was phenotyped on three separate occasions over a 12-month period without any notable changes in her V γ 9V δ 2 T cell subset signature.

9.9 A model for V γ 9V δ 2 T cell differentiation

There are three datasets of experimental evidence that relate to the construction of a model that explains V γ 9V δ 2 T cell differentiation and the adoption of certain functional qualities.

1. The microarray data suggested that the four newly-defined subsets were not equally as different from one another. Instead, it suggested that the two most different subsets were the $\gamma\delta^{(28+)}$ cell subset and the $\gamma\delta^{(16+)}$ cell subset. This could be taken to mean that these two populations are at either end of a differentiation pathway, which is visually supported by CD27/CD28 FACS dot plots (which appear to suggest a transition from $\gamma\delta^{(28+)}$ cells to $\gamma\delta^{(28-)}$ cells to $\gamma\delta^{(16+/-)}$ cells). An interesting additional observation is the relative lack of differences between the $\gamma\delta^{(28-)}$ and $\gamma\delta^{(16-)}$ cell subsets. This suggests that these two subsets may in fact represent a transitional state in which features of the $\gamma\delta^{(28+)}$ cell subset are lost while features of the $\gamma\delta^{(16+)}$ cell subset are gained. This would imply that there are two main V γ 9V δ 2 T cell phenotypes; the $\gamma\delta^{(28+)}$ subset and $\gamma\delta^{(16+)}$ subset, with transitional cells bridging these two effector states.

2. In support of the microarray data, the probability state modelling performed using the GemStone software also suggested two well-defined effector states that are defined as the $\gamma\delta^{(28+)}$ and $\gamma\delta^{(16+)}$ subsets. Taking the many healthy individuals together (which is an important feature of this software) we were able to observe a CD28⁽⁺⁾CD16⁽⁻⁾ phase and a CD28⁽⁻⁾CD16⁽⁺⁾ phase in practically all samples. The transition between these two phases differed slightly between individuals, but generally followed the following pattern; downregulation of CD28, downregulation of CD27, upregulation of CD16, upregulation of CD45RA.

3. An important prediction of a model of V γ 9V δ 2 T cell differentiation in which cells transition (presumably as a result of either an in-built differentiation

program, or in response to microbial activation) from a $\gamma\delta^{(28+)}$ cell phenotype, through a series of transitional stages, to a $\gamma\delta^{(16+)}$ cell phenotype is that the older a person is, the higher you would expect the $\gamma\delta^{(16+)}/\gamma\delta^{(28+)}$ ratio to be. It may also suggest that living in an environment with an increased risk of serious infection (such as in developing countries with low economic status), would also lead to higher $\gamma\delta^{(16+)}/\gamma\delta^{(28+)}$ ratios. However, our data show no evidence for this. Age, country of birth, and economic status were not significantly correlated with an increased $\gamma\delta^{(16+)}/\gamma\delta^{(28+)}$ ratio. The failure to show this predicted age-related change may be due to the relatively modest sample size (63 individuals) or the fact that the sampled healthy volunteer population is taken from individuals who have spent the majority of their life in the UK and may not have had exposure to the specific infections that drive $V\gamma 9V\delta 2$ T cell differentiation to a predominant phenotype. Nonetheless, there is no evidence from demographic data to support an age-dependent transition through a $\gamma\delta^{(28+)}$ cell to $\gamma\delta^{(28-)}$ cell to $\gamma\delta^{(16-/+)}$ cell pathway.

A model for $V\gamma 9V\delta 2$ T cell differentiation that is consistent with these three datasets suggests that an individual's $V\gamma 9V\delta 2$ T cell signature profile is in a fairly stable state over long periods of time. The nature of a $V\gamma 9V\delta 2$ T cell naïve population (see later) is still open to debate, but presuming that all non-naïve subsets differentiate from a precursor of this type, one could envisage a scenario in which the early activation of naïve $V\gamma 9V\delta 2$ T cells generates a spectrum of mature $V\gamma 9V\delta 2$ T cells with a range of "effector potentials" (Figure 9.2). On the two extremes of this spectrum are, on one hand, the $\gamma\delta^{(28+)}$ subset, which retains a high proliferative capacity and is capable of a certain degree of plasticity in cytokine production, but which has little cytotoxic potential. At the

other extreme is the $\gamma\delta^{(16+)}$ subset, which has lost proliferative potential and plasticity of cytokine function, but has upregulated robust cytotoxic capacity.

Perhaps the system is designed to provide a good quantity of all cell types, but in certain cases (for example in the presence of certain microbes) may be polarised to one extreme or the other. Once established, the stable signature profile of an individual must be actively maintained despite exposure to constant bacterial infections. Presumably active effector cells leave the pool of cells with “effector potential” when they are required to participate in anti-microbial responses. There may then be some sort of stem cell activity, which homeostatically restores the signature profile to its original state. Whether the signature profile does change over time is unclear from the data presented here, and would require a longitudinal study. However, it remains possible that certain infections may push the signature profile in one direction or the other. This remains to be tested.

9.10 CD27 and CD11a represent the most reliable naïve cell markers

One continued area of debate, is the size and most appropriate phenotypic surface markers for a “naïve” subset of $V\gamma 9V\delta 2$ T cells. It is apparent from our data that estimates of the naïve subset using CD45RA i.e. $(CD27^{(+)CD45RA^{(+)})$ are much higher (approximately 23%) compared to estimates using alternative naïve surface marker combinations e.g. $[CD27^{(Hi)}CD11a^{(Lo)}]$, $[CD27^{(Hi)}CCR7^{(+)}]$ or $[CCR7^{(+)CD62L^{(+)}]$ which estimate the “naïve” subset consistently at < 5%. Studies by De Rosa and Morita also support these findings and suggest that

CD27 and CD45RA grossly overestimate the naïve subset size (De Rosa *et al.* 2004, Morita *et al.* 2007).

Phenotypic studies by Morita and co-workers estimate the size of the naïve subset to be 1.8% and hence to represent a very small subset in adult peripheral blood that is frequently absent and often difficult to identify (Puan *et al.* 2009, Morita *et al.* 2007). This led us to consider the best markers to use to describe “naïve” and non-“naïve” subsets. Care must be taken when using CCR7, as staining is clone and condition-dependent. This finding is supported by a technique research paper which also concluded that expression of chemokine markers in general is temperature and technique sensitive (Berhanu *et al.* 2003). Another of the naïve markers; CD62L, has also been shown to be variable in some studies and can be totally lost from the cell surface as a result of prolonged transportation and temperature variations (De Rosa *et al.* 2004). This led us to the conclusion that the use of [CD27^(Hi)CD11a^(Lo)] was the most reliable way to identify “naïve” cell markers in peripheral blood. Further work on “naïve” V γ 9V δ 2 T cells is planned (see below).

9.11 Naïve cell surface markers do not predominate in the thymus.

Our knowledge of the earliest stages of human V γ 9V δ 2 T cell development in the thymus is limited by the lack of a direct equivalent population in murine experimental models. Indeed, we know very little about the phenotype of these early subsets, how they develop and whether there is any evidence of pre-commitment in the thymus as is seen for the various mouse $\gamma\delta$ T cell subsets.

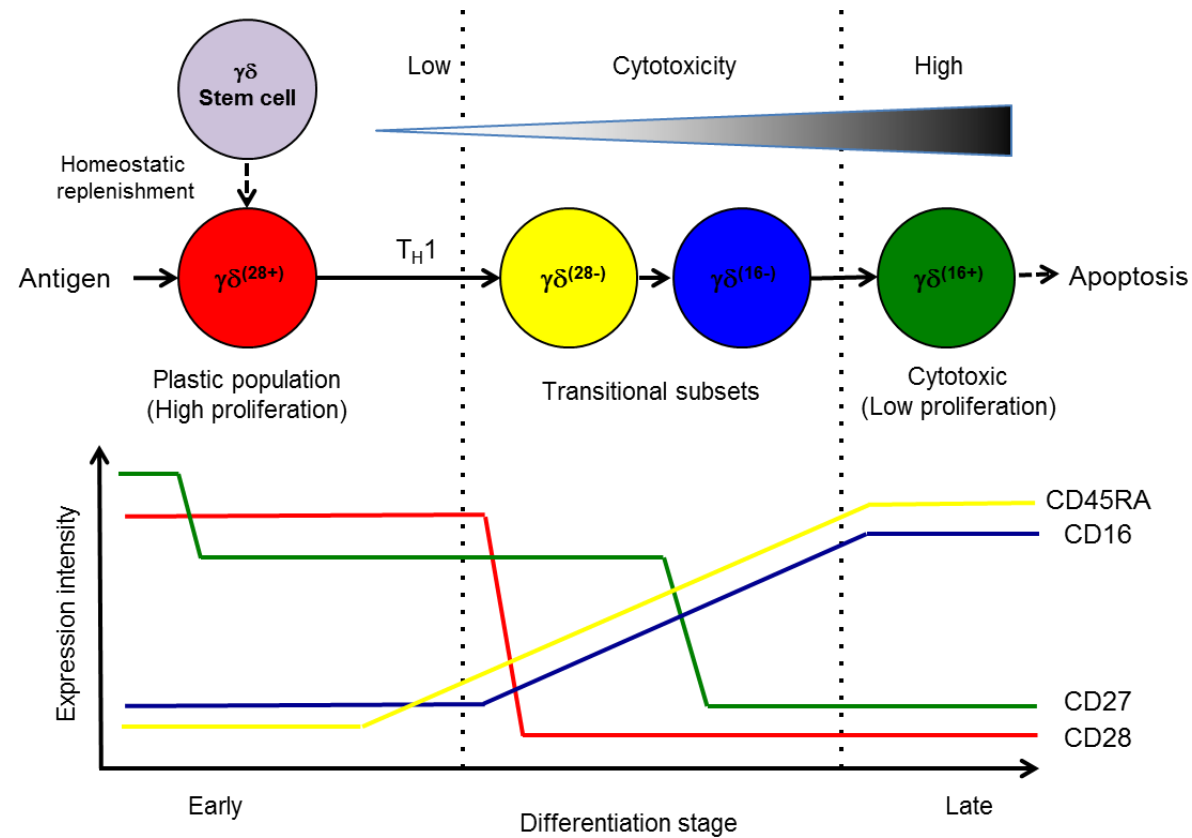


Figure 9.2 V γ 9V δ 2 T cell differentiation model

V γ 9V δ 2 T cells appear to differentiate in a linear pattern of differentiation sequentially from $\gamma\delta^{(28+)} \rightarrow \gamma\delta^{(28-)} \rightarrow \gamma\delta^{(16-)} \rightarrow \gamma\delta^{(16+)}$. Consistent stable subsets [$\gamma\delta^{(28+)}$ and $\gamma\delta^{(16+)}$] at the start and end of differentiation with transitional subsets [$\gamma\delta^{(28-)}$ and $\gamma\delta^{(16-)}$] observed with intermediate functional properties as cells move between the two effector states. V γ 9V δ 2 T cells appear to preferentially adopt a T_H1 cytokine profile, possibly due to continued antigen stimulation and exposure to Phosphoantigen. Despite this dynamic process, the size of V γ 9V δ 2 T cell subsets appear to remain relatively stable with time suggesting that homeostatic mechanisms are in place, that replenish the V γ 9V δ 2 T cell pool. A “stem cell” subset may help to replenish V γ 9V δ 2 T cell pools lost due to apoptosis.

Previous studies have suggested that human V γ 9V δ 2 T cells undergo peripheral activation and expansion very early in life with disappearance of naïve phenotypes and a predominance of memory and effector phenotypes as a result of early antigen exposure (Parker *et al.* 1990, De Rosa *et al.* 2004). Indeed, with the process of thymic involution in young adult life it is somewhat surprising that there are any “naïve” phenotypes remaining in the peripheral blood of adults which hints at an ongoing role for the thymus well into adult life. There is still uncertainty as to the most representative surface markers to describe the “naïve” V γ 9V δ 2 T cell subset (De Rosa *et al.* 2004, Morita *et al.* 2007, Dieli *et al.* 2003b) Therefore, eight neo-natal thymus samples were investigated to examine $\gamma\delta$ T cells during development. As expected, V δ 1⁽⁺⁾ T cells were the predominant $\gamma\delta$ T cell subset in the thymus with higher percentages found in the thymus compared to peripheral blood, where V γ 9V δ 2 T cells predominated. This was in agreement with several other studies, which also consistently found this same relationship (Parker *et al.* 1990, McVay and Carding 1999).

We hypothesised that V γ 9V δ 2 T cells should largely display “naïve” surface markers in their organ of origin before their release into the peripheral blood. However, surprisingly there did not seem to be a predominance of typical “naïve” surface markers expressed on V γ 9V δ 2 T cells in the thymus with the majority of samples analysed showing similar expression levels to the same subset in peripheral blood.

This suggests a number of possibilities. One explanation may be that V γ 9V δ 2 thymocytes are exposed to phosphoantigen within the thymus. Alternatively it is

possible that antigen-exposed cells in the periphery re-circulate back through the thymus. Indeed, thymic re-circulation of mature T cells has previously been described, but only a small minority of T cells show potential to return to the thymus after initial release (Sprent and Surh 2009, Nobrega *et al.* 2013) although re-circulation through the thymus has been observed to occur more commonly in neonates (Sprent and Surh 2009, Nobrega *et al.* 2013). Finally, it is also possible that the “naïve” phenotype that we see in the blood is a developmental stage that occurs during late thymic development and consequently is only expressed on a small proportion of cells immediately before leaving the thymus. Indeed, this is supported by one study suggesting that CD45 isoforms show dynamic switching at different stages of thymic development and that CD45RA is only expressed at a late stage of thymic development (Fujii *et al.* 1992).

Therefore, the identity of the true “naïve” phenotype was not clarified directly from observing the predominant thymocyte phenotypes, as the T cell markers conventionally considered as “naïve” i.e. CCR7, CD62L and CD45RA clearly were not predominant. It was however apparent that two consistently-observed subsets were present in the thymus; a predominant CD27⁽⁺⁾CD11a^(Lo) subset ($\approx 90\%$ of total thymocytes) and a smaller CD27^(Hi)CD11a⁽⁺⁾ subset ($\approx 10\%$). This pattern of CD27 and CD11a was very different to the subsets present in the peripheral blood, which made comparison of similar subsets in the different tissues difficult. In the peripheral blood CD27^(Hi)CD11a^(Lo) characterises the presumed “naïve” subset, with the majority of non-naïve cells expressing CD11a at high levels (CD11a^(Hi)). The differences in patterns of expression made it impossible to be sure as to the relationship of these subsets. However, within the thymus, it was apparent that the smaller CD27^(Hi)CD11a⁽⁺⁾ subset did

express significantly higher levels of the naïve surface markers CCR7 and CD62L and also surprisingly higher levels of CD16 in comparison to CD27⁽⁺⁾CD11a^(Lo) cells. The expression of CD16, usually considered as a cytotoxic marker, raises questions as to its presence on a thymic subset. One explanation for this is that CD16 might be indicative of V γ 9V δ 2 T cells or cytotoxic cells that have antigen presenting potential (Wu *et al.* 2009) Indeed, two separate studies have suggested that CD16 may be key receptor in both phagocytosis and subsequent antigen presentation specifically in V γ 9V δ 2 T cells (Wu *et al.* 2009, Kang *et al.* 1987) The increased expression of CCR7 and CD62L found on this same CD27^(Hi)CD11a⁽⁺⁾ subset add further weight to a potential role as possible precursors to an antigen presenting subset by indicating an ability to enter lymph nodes.

9.12 Higher frequency of the [CD27^(Hi)CD11a^(Lo)] subset in the V δ 1⁽⁺⁾ T cell population compared to V γ 9V δ 2 T cells may reflect differences in $\gamma\delta$ T cell development.

The higher representation of a so-called “naïve” [CD27^(Hi)CD11a^(Lo)] population as well as increased CD45RA expression, were clear differences between V δ 1⁽⁺⁾ and V γ 9V δ 2 T cell subsets. However, the functional significance of this difference is uncertain. Indeed, these results echo the findings of DeRosa and co-workers who also similarly found higher levels of the naïve phenotype [CD45RO⁽⁻⁾CD27^(Hi)CD11a^(Lo)] in V δ 1⁽⁺⁾ T cells in comparison with V γ 9V δ 2 T cells (De Rosa *et al.* 2004). This study goes on to postulate that this may reflect a difference in how V δ 1⁽⁺⁾ and V γ 9V δ 2 T cells are produced and maintained throughout life. They suggest that V δ 1⁽⁺⁾ and V γ 9V δ 2 T cells develop at

different times, in a similar manner to different subsets of murine $\gamma\delta$ T cells (Carding and Egan 2002). They propose that $V\gamma9V\delta2$ T cells develop at or around birth and home to peripheral sites, where they are subsequently maintained by proliferation of existing cells as opposed to the thymic generation of new “naïve” cells. This would explain the relatively low levels of “naïve” $V\gamma9V\delta2$ T cells in adult peripheral blood. By contrast, the relatively large $V\delta1^{(+)}$ naïve T cell population observed in adult blood might hint at the thymus having a significant on-going role in the production of new “naïve” $V\delta1^{(+)}$ cells well into adult life. However, the presence of naïve $V\gamma9V\delta2$ T cells in some individuals suggests that there is also potential for replenishment of the $V\gamma9V\delta2$ T cell pool by the thymus.

9.13 Depletion of $V\gamma9V\delta2$ T cells in the peripheral blood is characteristic of patients on long-term bisphosphonates including BRONJ

One of the consistent findings in all patients with a history of bisphosphonate exposure (including BRONJ patients), was the significant depletion of the $V\gamma9V\delta2$ T cell subset from the peripheral blood. This depletion is in agreement with another study which also found specific reduction of this T cell subset in patients exposed to oral and intravenous bisphosphonate therapy (Rossini *et al.* 2012). The most likely explanation for this finding is that chronic bisphosphonate therapy and repeated TCR activation leads to Fas-mediated apoptosis and a consequent depletion of the $V\gamma9V\delta2$ T cell subsets from the peripheral blood. This effect is likely to be an immunoregulatory mechanism that limits the activation of $V\gamma9V\delta2$ T cells after repeated activation (Gan *et al.*

2001). Therefore V γ 9V δ 2 T cell depletion does not appear to be specifically pathognomonic of BRONJ disease, but may simply be an associational change that occurs in all patients receiving long-term bisphosphonate therapy (Kalyan *et al.* 2013).

An alternative possibility, is that V γ 9V δ 2 T cell depletion is a clinical sign that is indicative of its direct role in disease causation and a necessary factor in the development of BRONJ. It is possible that the observed loss of peripheral blood V γ 9V δ 2 T cells might result due to the net movement of these cells from the peripheral blood to the jaws/peripheral tissues. This possibility, is further supported by recent evidence demonstrating that there were 4-5 times more V γ 9V δ 2 T cells found in BRONJ tissue histology samples compared to non-bisphosphonate osteonecrotic control tissues (Mawardi H 2013). This suggests that V γ 9V δ 2 T cells may home to the local sites of BRONJ in the disease process and that they may have a key role in initiating and sustaining the disease. Indeed, the preferential homing of V γ 9V δ 2 T cells to the tissues may be taking place due to the upregulation of the skin/mucosal homing marker (α 4 β 7) which has been shown to occur following phosphoantigen stimulation of V γ 9V δ 2 T cells (McCarthy *et al.* 2013). Therefore it is likely that bisphosphonates as well as oral bacteria which both indirectly increase phosphoantigen production will also have similar effects on V γ 9V δ 2 T cells. Clearly, the potential additional activation of V γ 9V δ 2 T cells by oral bacteria may help explain the fact that osteonecrosis only occurs in the jaws where these necessary conditions exist. The presence of activated V γ 9V δ 2 T cells and the subsequent release of pro-inflammatory cytokines (e.g. IFN- γ and TNF- α) at tissue sites may also be important in priming conventional $\alpha\beta$ T cells in the

tissues to a Th1 phenotype and further amplifying the local inflammatory response (McCarthy *et al.* 2013).

If this is the case, then the loss of peripheral blood V γ 9V δ 2 T cells may be a potential useful risk indicator for the development of BRONJ and perhaps a useful chairside test to predict those most at risk of developing BRONJ.

9.14 Limitations of experimental data

9.14.1 Proliferation assay

A limitation of the V γ 9V δ 2 T cell proliferation data presented in section 4.4 is that, by simply comparing starting and end phenotypes after culture, it is not possible to conclude whether changes observed are due to the proliferation of individual V γ 9V δ 2 T cell subsets or whether individual cells also change their surface marker expression and phenotype as a result of culture.

An alternative approach to analysis of the current data would be to display the phenotype of each of the individual rounds of division of V γ 9V δ 2 T cells to determine which of the subsets at 5-days had divided and proliferated the most. However this method also fails to account for any shifts in phenotypes and changes in surface marker expression that occur due to culture and stimulation.

Therefore, in order to resolve this in future work, each of the four V γ 9V δ 2 T cell subsets i.e. $\gamma\delta^{(28+)}$, $\gamma\delta^{(28-)}$, $\gamma\delta^{(16-)}$, $\gamma\delta^{(16+)}$ could be cell sorted and cultured with HMB-PP and IL-2 over 5-days to assess both proliferative potential as well as phenotype stability. However, these cultures would also require non-V δ 2

accessory cells to be added back into cultures in order to enable successful proliferation and effective V γ 9V δ 2 T cell expansion.

9.14.2 Cytokine production

A criticism of the use of PMA and ionomycin for determining cytokine secreting potential is that they generate a “non-physiological” cytokine release because it by-passes surface marker stimulation. PMA diffuses through the cell membrane and activates Protein kinase C (PKC) with ionomycin generating calcium release, which is a necessary factor in NFAT signalling (Manicassamy et al. 2006). An additional problem with PMA and ionomycin stimulation is that it can affect the expression of surface molecules including CD3 and therefore makes gating using flow cytometry potentially a problem. This highlights the absolute need for isotype and unstimulated controls in setting appropriate positive gates. However, it represents a useful method to determine the differential *ex vivo* cytokine release potential of V γ 9V δ 2 T cell subsets.

An alternate, more physiological method would be the use of anti-CD3 and/or anti-CD28 whereby activation of cells and cytokine production is triggered through surface molecules. A final alternate “more physiological” cell activation would be to use a phosphoantigen (HMB-PP or IPP) to stimulate cells.

Future experimental work could compare *ex vivo* (PMA/Ionomycin) stimulation with the aforementioned alternate stimulation protocols to determine whether there are differences in the types and amount of V γ 9V δ 2 T cell cytokine production when cells are activated in different ways and by different mechanisms.

Intracellular cytokine staining only measures the amount of cytokine produced inside each cell which does not necessarily equate to the amount of cytokine released into extracellular environment with the potential to exert a physiological/pathological effect. Therefore, whilst representing a useful method to compare the relative cytokine production in each V γ 9V δ 2 T cell subset, it may not truly represent the net cytokine output which is influenced by cytokine release, as well as the local tissue environment.

9.14.3 Age vs. Tissue (Thymus)

One of the most fundamental problems in comparing the phenotype of V γ 9V δ 2 T cells in the blood and the thymus was that, thymic samples were only available from children in the first few years of life who were undergoing corrective cardiac operations, whereas peripheral venous blood samples were taken from a predominantly adult population. Therefore, the comparison of circulating versus thymic V γ 9V δ 2 T cells was made between cells at different stages of development as well as from different individuals of different ages. However, whilst not directly comparable, the analysis of thymic V γ 9V δ 2 T cells was used to identify the “naïve” V γ 9V δ 2 T cell phenotype as it is thought that the thymus is an immune privileged site that is protected from infection. It was therefore postulated that the phenotype of V γ 9V δ 2 T cells in this organ might reveal the true “naïve” phenotype before release into the circulation and peripheral tissues.

Ideally, the comparison between thymic and circulating V γ 9V δ 2 T cells in neonates/infants within the same individual will allow more robust conclusions to be

made. It therefore represents a potential avenue of future research although this would require a new ethical approval to facilitate this.

9.14.4 Critical appraisal of PSM

Conventional understanding of T cell differentiation suggests that V γ 9V δ 2 T cells differentiate through distinct phenotypic stages, with naïve cells populating the thymus, central memory cells patrolling the blood and effector cells located in the tissues. These different T cell effector states are widely accepted and there is a presumption that T cells including V γ 9V δ 2 T cells also differentiate along this linear pathway and eventually undergo apoptosis in the tissues as cells become senescent. Whilst there is some *in vitro* experimental evidence to support this premise (Dieli et al. 2003b), the stages of development and phenotypes of V γ 9V δ 2 T cells have been carried over from conventional T cell without much evidence to support this.

Models derived using PSM are based on the input of “rules” or presumptions as to the direction of surface marker change during differentiation and the number of levels or intensity of surface markers as cells differentiate from an early or “naïve” phenotype to a late effector phenotype. Therefore, it generates average models by combining phenotypic signatures right across the spectrum from multiple samples. Whilst being a useful tool in averaging heterogeneous V γ 9V δ 2 T cell populations, a disadvantage is that the resulting model hides the extremes in phenotypic signature that occur in some individuals (phenotype 1 and 6). PSM, however, does allow the relationship of surface markers to be assessed visually along a differentiation pathway and would support a linear pattern of differentiation from $\gamma\delta^{(28+)} \rightarrow \gamma\delta^{(28-)} \rightarrow \gamma\delta^{(16-)} \rightarrow \gamma\delta^{(16+)}$. In support of this

pathway, it would appear that there are three major population subsets when visualised on a CD28/CD27 bivariate flow cytometry plot, which seem to suggest transition from CD28⁽⁺⁾CD27⁽⁺⁾ to CD28⁽⁻⁾CD27⁽⁻⁾ via an intermediate CD27⁽⁺⁾CD28⁽⁻⁾ population.

By contrast to the linear model of differentiation is the observation that individual phenotypic signatures appear to remain relatively stable over time. This might suggest that a linear pattern of differentiation is incorrect because we do not see an age dependent accumulation of late effector phenotypes i.e. increased $\gamma\delta^{(16+)}$ cells with increasing age. Alternatively, this might support a discrete model of differentiation, where an individual's phenotypic signature is established by V γ 9V δ 2 T cell subsets, which are in turn established interdependently of each other and tightly controlled by homeostatic control. Interestingly, the differentiation pathway of V γ 9V δ 2 T cells and conventional T cells seems to be different when modelled using PSM and raises the question as to whether terms and surface markers used for conventional $\alpha\beta$ T cells are also appropriate for V γ 9V δ 2 T cells.

Whilst the stimulation of cell sorted subsets with phosphoantigen and IL-2 over several days of culture might indicate the potential direction of V γ 9V δ 2 T cell subset differentiation *in vitro*, it is unclear as to the significance and relationship of cell subsets in the different tissue compartments *in vivo*. Furthermore, whether or not differentiation occurs in only one direction along a linear pathway or whether change between subsets is far more dynamic and possibly reversible is a question that still remains unanswered.

9.15 Future work

The experimental evidence presented in this thesis raises a number of new avenues of future research both in the biology of human V γ 9V δ 2 T cells as well as in our understanding of BRONJ.

Firstly, one of the most interesting and potentially significant observations of the thesis was the mutually exclusive surface expression of CCR6 and CX3CR1 on the V γ 9V δ 2 $\gamma\delta^{(28+)}$ T cell subset, dividing this population into two populations i.e. $\gamma\delta^{(28+)} \text{ CCR6}^{(+)}\text{CX3CR1}^{(-)}$ and $\gamma\delta^{(28+)} \text{ CCR6}^{(-)}\text{CX3CR1}^{(+)}$ V γ 9V δ 2 T cells. This finding, in addition to the fact that three important IL-17-associated genes (*CCR6*, *IL-23R* and *RORC*) are differentially expressed at higher levels in $\gamma\delta^{(28+)}$ T cells, raises questions as to whether further phenotypic division of the $\gamma\delta^{(28+)}$ subset based on CCR6 and CX3CR1 surface expression may be useful in identifying cells with IL-17 producing ability. Indeed, further characterisation of the $\text{CCR6}^{(+)}\text{CX3CR1}^{(-)}$ and $\text{CCR6}^{(-)}\text{CX3CR1}^{(+)}$ $\gamma\delta^{(28+)}$ subsets is warranted to determine whether differential expression of these chemokine receptors has a biological significance in terms of differences in cytokine-producing ability as well as chemokine receptor and cytotoxic protein expression.

At present, the field does not have a clear understanding as to how human $\gamma\delta$ T cells make IL-17. Thus, further understanding of the priming conditions that would lead to IL-17 production and the phenotypic characterisation of cells with this potential would markedly improve our insight into diseases in which V γ 9V δ 2 T cells make IL-17. This could be investigated by testing whether the culture of $\text{CCR6}^{(+)} \gamma\delta^{(28+)}$ V γ 9V δ 2 T cells in the presence of phosphoantigen (IPP), IL-17 priming cytokines (IL-1 β , IL-6, IL-23 and TGF- β) and accessory cells (dendritic

cells or monocytes) might preferentially polarise this specific subset to an IL-17 producing phenotype. Comparison could then be made to the other CCR6⁽⁻⁾ subsets i.e. from the $\gamma\delta^{(28+)}$, $\gamma\delta^{(28-)}$, $\gamma\delta^{(16-)}$ and $\gamma\delta^{(16+)}$ populations, and with populations from the neonatal thymus. The latter comparison is potentially important as it is likely that cells from younger individuals may retain greater ability to adopt different phenotypes.

Indeed, there is clearly a need to confirm in a larger number of individuals, the V γ 9V δ 2 T cell population phenotypes present in the thymus to further our understanding of both the phenotypic changes that occur during development and also perhaps in defining early populations with plastic potential. Whilst we have identified two distinct thymic subsets based on CD27 and CD11a i.e. [CD27⁽⁺⁾CD11a^(Lo)] and [CD27^(Hi)CD11a⁽⁺⁾], the lack of directly comparable subsets in comparison to the peripheral blood phenotype makes it difficult to determine the relationship of these subsets. Therefore it would be beneficial to also investigate the surface expression of CCR6 and CX3CR1 on thymic V γ 9V δ 2 T cells, given the differential expression of these same markers on the presumed earliest $\gamma\delta^{(28+)}$ subset in peripheral blood. Following on from this, it would subsequently be possible to sort different thymic V γ 9V δ 2 T cell subsets based on different putative naïve surface marker combinations to identify cell subsets with potential to be polarised to different effector populations (i.e. T_H1, T_H2, T_H17 etc). A better understanding of the functional potential of these early subsets would lead to increased understanding of V γ 9V δ 2 T cell plasticity generally.

Finally, the recruitment of a larger cohort of BRONJ patients will help in confirming the finding that V γ 9V δ 2 T cells are depleted in peripheral blood.

Examination of BRONJ tissue samples is clearly needed to confirm whether or not there are increased or reduced V γ 9V δ 2 T cell numbers within the tissues i.e. whether the peripheral blood depletion is due to net movement of V γ 9V δ 2 T cells to the jaw lesions or reflects the activation induced cell death due to chronic stimulation. Clearly, either increase or reduction of V γ 9V δ 2 T cells in the tissues can lead to loss of normal tissue homeostasis and potential to directly influence the disease process.

References

- AAOMS (2007) American Association of Oral and Maxillofacial Surgeons position paper on bisphosphonate-related osteonecrosis of the jaws. *J Oral Maxillofac Surg*, 65(3), 369-76.
- Aas, J. A., Paster, B. J., Stokes, L. N., Olsen, I. and Dewhirst, F. E. (2005) Defining the normal bacterial flora of the oral cavity. *J Clin Microbiol*, 43(11), 5721-32.
- Abate, G., Eslick, J., Newman, F. K., Frey, S. E., Belshe, R. B., Monath, T. P. and Hoft, D. F. (2005) Flow-cytometric detection of vaccinia-induced memory effector CD4⁽⁺⁾, CD8⁽⁺⁾, and gamma delta TCR⁽⁺⁾ T cells capable of antigen-specific expansion and effector functions. *J Infect Dis*, 192(8), 1362-71.
- European Medicines Agency (2011) Questions and answers on the review of bisphosphonates and atypical stress fractures. Outcomes of nine procedures under Article 20 of Regulation (EC) No 726/2004 and of one procedure under Article 31 of Directive 2001/83/EC.
- Allen, M. R. and Burr, D. B. (2008) Mandible matrix necrosis in beagle dogs after 3 years of daily oral bisphosphonate treatment. *J Oral Maxillofac Surg*, 66(5), 987-94.
- Allen, M. R. and Burr, D. B. (2009) The pathogenesis of bisphosphonate-related osteonecrosis of the jaw: so many hypotheses, so few data. *J Oral Maxillofac Surg*, 67(5 Suppl), 61-70.
- Almeida, A. R., Rocha, B., Freitas, A. A. and Tanchot, C. (2005) Homeostasis of T cell numbers: from thymus production to peripheral compartmentalization and the indexation of regulatory T cells. *Semin Immunol*, 17(3), 239-49.
- Altman, R. D., Johnston, C. C., Khairi, M. R., Wellman, H., Serafini, A. N. and Sankey, R. R. (1973) Influence of disodium etidronate on clinical and laboratory manifestations of Paget's disease of bone (osteitis deformans). *N Engl J Med*, 289(26), 1379-84.
- Angelini, D. F., Borsellino, G., Poupot, M., Diamantini, A., Poupot, R., Bernardi, G., Poccia, F., Fournié, J. J. and Battistini, L. (2004) FcγRIII discriminates between 2 subsets of Vγ9Vδ2 effector cells with different responses and activation pathways. *Blood*, 104(6), 1801-7.
- Antiabong, J. F., Boardman, W., Moore, R. B., Brown, M. H. and Ball, A. S. (2013) The oral microbial community of gingivitis and lumpy jaw in captive macropods. *Res Vet Sci*, 95(3), 996-1005.
- Aragon-Ching, J. B., Ning, Y. M., Chen, C. C., Latham, L., Guadagnini, J. P., Gulley, J. L., Arlen, P. M., Wright, J. J., Parnes, H., Figg, W. D. and Dahut, W. L. (2009) Higher incidence of Osteonecrosis of the Jaw (ONJ) in patients with metastatic castration resistant prostate cancer treated with anti-angiogenic agents. *Cancer Invest*, 27(2), 221-6.

Arancibia, S. A., Beltrán, C. J., Aguirre, I. M., Silva, P., Peralta, A. L., Malinarich, F. and Hermoso, M. A. (2007) Toll-like receptors are key participants in innate immune responses. *Biol Res*, 40(2), 97-112.

Badros, A., Weikel, D., Salama, A., Goloubeva, O., Schneider, A., Rapoport, A., Fenton, R., Gahres, N., Sausville, E., Ord, R. and Meiller, T. (2006) Osteonecrosis of the jaw in multiple myeloma patients: clinical features and risk factors. *J Clin Oncol*, 24(6), 945-52.

Bamias, A., Kastiris, E., Bamia, C., Moulopoulos, L. A., Melakopoulos, I., Bozas, G., Koutsoukou, V., Gika, D., Anagnostopoulos, A., Papadimitriou, C., Terpos, E. and Dimopoulos, M. A. (2005) Osteonecrosis of the jaw in cancer after treatment with bisphosphonates: incidence and risk factors. *J Clin Oncol*, 23(34), 8580-7.

Bansal, R. R., Mackay, C. R., Moser, B. and Eberl, M. (2012) IL-21 enhances the potential of human $\gamma\delta$ T cells to provide B-cell help. *Eur J Immunol*, 42(1), 110-9.

Bassett, C. A., Donath, A., Macagno, F., Preisig, R., Fleisch, H. and Francis, M. D. (1969) Diphosphonates in the treatment of myositis ossificans. *Lancet*, 2(7625), 845.

Bedogni, A., Saia, G., Bettini, G., Tronchet, A., Totola, A., Bedogni, G., Ferronato, G., Nocini, P. F. and Blandamura, S. (2011) Long-term outcomes of surgical resection of the jaws in cancer patients with bisphosphonate-related osteonecrosis. *Oral Oncol*, 47(5), 420-4.

Bennouna, J., Bompas, E., Neidhardt, E. M., Rolland, F., Philip, I., Galéa, C., Salot, S., Saiagh, S., Audrain, M., Rimbart, M., Lafaye-de Micheaux, S., Tiollier, J. and Négrier, S. (2008) Phase-I study of Innacell gammadelta, an autologous cell-therapy product highly enriched in V γ 9V δ 2 T lymphocytes, in combination with IL-2, in patients with metastatic renal cell carcinoma. *Cancer Immunol Immunother*, 57(11), 1599-609.

Berhanu, D., Mortari, F., De Rosa, S. C. and Roederer, M. (2003) Optimized lymphocyte isolation methods for analysis of chemokine receptor expression. *J Immunol Methods*, 279(1-2), 199-207.

Bhagat, G., Naiyer, A. J., Shah, J. G., Harper, J., Jabri, B., Wang, T. C., Green, P. H. and Manavalan, J. S. (2008) Small intestinal CD8⁽⁺⁾TCRgammadelta⁽⁺⁾NKG2A⁽⁺⁾ intraepithelial lymphocytes have attributes of regulatory cells in patients with celiac disease. *J Clin Invest*, 118(1), 281-93.

Biasotto, M., Chiandussi, S., Dore, F., Rinaldi, A., Rizzardi, C., Cavalli, F. and Di Lenarda, R. (2006) Clinical aspects and management of bisphosphonates-associated osteonecrosis of the jaws. *Acta Odontol Scand*, 64(6), 348-54.

Bisdas, S., Chambron Pinho, N., Smolarz, A., Sader, R., Vogl, T. J. and Mack, M. G. (2008) Bisphosphonate-induced osteonecrosis of the jaws: CT and MRI spectrum of findings in 32 patients. *Clin Radiol*, 63(1), 71-7.

Bonacina, R., Mariani, U., Villa, F. and Villa, A. (2011) Preventive strategies and clinical implications for bisphosphonate-related osteonecrosis of the jaw: a review of 282 patients. *J Can Dent Assoc*, 77, b147.

Bouet-Toussaint, F., Cabillic, F., Toutirais, O., Le Gallo, M., Thomas de la Pintièrre, C., Daniel, P., Genetet, N., Meunier, B., Dupont-Bierre, E., Boudjema, K. and Catros, V. (2008) V γ 9V δ 2 T cell-mediated recognition of human solid tumors. Potential for immunotherapy of hepatocellular and colorectal carcinomas', *Cancer Immunol Immunother*, 57(4), 531-9.

Brandes, M., Willimann, K., Lang, A. B., Nam, K. H., Jin, C., Brenner, M. B., Morita, C. T. and Moser, B. (2003) Flexible migration program regulates $\gamma\delta$ T-cell involvement in humoral immunity. *Blood*, 102(10), 3693-701.

Brandes, M., Willimann, K. and Moser, B. (2005) Professional antigen-presentation function by human gammadelta T Cells. *Science*, 309(5732), 264-8.

Brinkmann, V., Reichard, U., Goosmann, C., Fauler, B., Uhlemann, Y., Weiss, D. S., Weinrauch, Y. and Zychlinsky, A. (2004) Neutrophil extracellular traps kill bacteria. *Science*, 303(5663), 1532-5.

Burchett, S. K., Corey, L., Mohan, K. M., Westall, J., Ashley, R. and Wilson, C. B. (1992) Diminished interferon-gamma and lymphocyte proliferation in neonatal and postpartum primary herpes simplex virus infection. *J Infect Dis*, 165(5), 813-8.

Caccamo, N., Dieli, F., Wesch, D., Jomaa, H. and Eberl, M. (2006) Sex-specific phenotypical and functional differences in peripheral human V γ 9V δ 2T cells. *J Leukoc Biol*, 79(4), 663-6.

Caccamo, N., La Mendola, C., Orlando, V., Meraviglia, S., Todaro, M., Stassi, G., Sireci, G., Fournié, J. J. and Dieli, F. (2011b) Differentiation, phenotype, and function of interleukin-17-producing human V γ 9V δ 2 T cells. *Blood*, 118(1), 129-38.

Cairo, C., Armstrong, C. L., Cummings, J. S., Deetz, C. O., Tan, M., Lu, C., Davis, C. E. and Pauza, C. D. (2010) Impact of age, gender, and race on circulating $\gamma\delta$ T cells. *Hum Immunol*, 71(10), 968-75.

Carding, S. R. and Egan, P. J. (2002) Gammadelta T cells: functional plasticity and heterogeneity, *Nat Rev Immunol*, 2(5), 336-45.

Casetti, R., Agrati, C., Wallace, M., Sacchi, A., Martini, F., Martino, A., Rinaldi, A. and Malkovsky, M. (2009) Cutting edge: TGF- β 1 and IL-15 Induce FOXP3⁽⁺⁾ gammadelta regulatory T cells in the presence of antigen stimulation, *J Immunol*, 183(6), 3574-7.

Cendron, D., Ingoure, S., Martino, A., Casetti, R., Horand, F., Romagné, F., Sicard, H., Fournié, J. J. and Poccia, F. (2007) A tuberculosis vaccine based on phosphoantigens and fusion proteins induces distinct $\gamma\delta$ and $\alpha\beta$ T cell responses in primates. *Eur J Immunol*, 37(2), 549-65.

Chrcanovic, B. R., Reher, P., Sousa, A. A. and Harris, M. (2010) Osteoradionecrosis of the jaws--a current overview--part 1: Physiopathology and risk and predisposing factors. *Oral Maxillofac Surg*, 14(1), 3-16.

Cockwell, P., Calderwood, J. W., Brooks, C. J., Chakravorty, S. J. and Savage, C. O. (2002) Chemoattraction of T cells expressing CCR5, CXCR3 and CX3CR1 by proximal tubular epithelial cell chemokines. *Nephrol Dial Transplant*, 17(5), 734-44.

Cooper, M. D. and Alder, M. N. (2006) The evolution of adaptive immune systems. *Cell*, 124(4), 815-22.

D'haese, J., Van De Velde, T., Komiyama, A., Hultin, M. and De Bruyn, H. (2010) Accuracy and Complications Using Computer-Designed Stereolithographic Surgical Guides for Oral Rehabilitation by Means of Dental Implants: A Review of the Literature. *Clin Implant Dent Relat Res*.

D'Souza, C. D., Cooper, A. M., Frank, A. A., Mazzaccaro, R. J., Bloom, B. R. and Orme, I. M. (1997) An anti-inflammatory role for $\gamma\delta$ T lymphocytes in acquired immunity to Mycobacterium tuberculosis. *J Immunol*, 158(3), 1217-21.

Daha, M. R. (2010) Role of complement in innate immunity and infections, *Crit Rev Immunol*, 30(1), 47-52.

Danilova, N. (2006) The evolution of immune mechanisms, *J Exp Zool B Mol Dev Evol*, 306(6), 496-520.

De Rosa, S. C., Andrus, J. P., Perfetto, S. P., Mantovani, J. J., Herzenberg, L. A. and Roederer, M. (2004) Ontogeny of gamma delta T cells in humans, *J Immunol*, 172(3), 1637-45.

Di Mitri, D., Azevedo, R. I., Henson, S. M., Libri, V., Riddell, N. E., Macaulay, R., Kipling, D., Soares, M. V., Battistini, L. and Akbar, A. N. (2011) Reversible senescence in human CD4⁽⁺⁾CD45RA⁽⁺⁾CD27⁽⁻⁾ memory T cells, *J Immunol*, 187(5), 2093-100.

Diamond, T., Golombick, T., Manoharan, A., Kwan, Y. and Bryant, C. (2011) The impact of osteoporosis (as measured by lumbar spine quantitative computed tomography) on disease activity and survival in myeloma patients: a 13-year prospective study. *Am J Hematol*, 86(7), 617-9.

Dieli, F., Ivanyi, J., Marsh, P., Williams, A., Naylor, I., Sireci, G., Caccamo, N., Di Sano, C. and Salerno, A. (2003a) Characterization of lung $\gamma\delta$ T cells following intranasal infection with Mycobacterium bovis bacillus Calmette-Guérin. *J Immunol*, 170(1), 463-9.

Dieli, F., Poccia, F., Lipp, M., Sireci, G., Caccamo, N., Di Sano, C. and Salerno, A. (2003b) Differentiation of effector/memory V γ 9V δ 2 T cells and migratory routes in lymph nodes or inflammatory sites, *J Exp Med*, 198(3), 391-7.

Dieli, F., Troye-Blomberg, M., Farouk, S. E., Sireci, G. and Salerno, A. (2001) Biology of $\gamma\delta$ T cells in tuberculosis and malaria', *Curr Mol Med*, 1(4), 437-46.

Dieli, F., Vermijlen, D., Fulfaro, F., Caccamo, N., Meraviglia, S., Cicero, G., Roberts, A., Buccheri, S., D'Asaro, M., Gebbia, N., Salerno, A., Eberl, M. and Hayday, A. C. (2007) Targeting human $\gamma\delta$ T cells with zoledronate and interleukin-2 for immunotherapy of hormone-refractory prostate cancer. *Cancer Res*, 67(15), 7450-7.

Doran, K. S., Banerjee, A., Disson, O. and Lecuit, M. (2013) Concepts and mechanisms: crossing host barriers. *Cold Spring Harb Perspect Med*, 3(7).

Durie, B. G., Katz, M. and Crowley, J. (2005) Osteonecrosis of the jaw and bisphosphonates. *N Engl J Med*, 353(1), 99-102; discussion 99-102.

Esin, S., Shigematsu, M., Nagai, S., Eklund, A., Wigzell, H. and Grunewald, J. (1996) 'Different percentages of peripheral blood $\gamma\delta^{(+)}$ T cells in healthy individuals from different areas of the world. *Scand J Immunol*, 43(5), 593-6.

Fedele, S., Porter, S. R., D'Aiuto, F., Aljohani, S., Vescovi, P., Manfredi, M., Arduino, P. G., Broccoletti, R., Musciotto, A., Di Fede, O., Lazarovici, T. S., Campisi, G. and Yarom, N. (2010) Nonexposed variant of bisphosphonate-associated osteonecrosis of the jaw: a case series. *Am J Med*, 123(11), 1060-4.

Fenoglio, D., Poggi, A., Catellani, S., Battaglia, F., Ferrera, A., Setti, M., Murdaca, G. and Zocchi, M. R. (2009) $V\delta 1$ T lymphocytes producing IFN- γ and IL-17 are expanded in HIV-1-infected patients and respond to *Candida albicans*. *Blood*, 113(26), 6611-8.

Ficarra, G., Beninati, F., Rubino, I., Vannucchi, A., Longo, G., Tonelli, P. and Pini Prato, G. (2005) Osteonecrosis of the jaws in periodontal patients with a history of bisphosphonates treatment. *J Clin Periodontol*, 32(11), 1123-8.

Fisch, P., Oettel, K., Fudim, N., Surfus, J. E., Malkovsky, M. and Sondel, P. M. (1992) MHC-unrestricted cytotoxic and proliferative responses of two distinct human $\gamma\delta$ T cell subsets to Daudi cells, *J Immunol*, 148(8), 2315-23.

Foxman, E. F., Campbell, J. J. and Butcher, E. C. (1997) Multistep navigation and the combinatorial control of leukocyte chemotaxis. *J Cell Biol*, 139(5), 1349-60.

Fujii, Y., Okumura, M., Inada, K., Nakahara, K. and Matsuda, H. (1992) CD45 isoform expression during T cell development in the thymus. *Eur J Immunol*, 22(7), 1843-50.

Fye, K. H., Terasaki, P. I., Moutsopoulos, H., Daniels, T. E., Michalski, J. P. and Talal, N. (1976) Association of Sjögren's syndrome with HLA-B8. *Arthritis Rheum*, 19(5), 883-6.

Gan, Y. H., Wallace, M. and Malkovsky, M. (2001) Fas-dependent, activation-induced cell death of $\gamma\delta$ T cells. *J Biol Regul Homeost Agents*, 15(3), 277-85.

Garant, P. R. (1976) Light and electron microscopic observations of osteoclastic alveolar bone resorption in rats monoinfected with *Actinomyces naeslundii*. *J Periodontol*, 47(12), 717-23.

Garetto, L. P., Chen, J., Parr, J. A. and Roberts, W. E. (1995) Remodeling dynamics of bone supporting rigidly fixed titanium implants: a histomorphometric comparison in four species including humans. *Implant Dent*, 4(4), 235-43.

Germann, A., Oh, Y. J., Schmidt, T., Schön, U., Zimmermann, H. and von Briesen, H. (2013) Temperature fluctuations during deep temperature cryopreservation reduce PBMC recovery, viability and T-cell function. *Cryobiology*, 67(2), 193-200.

Girardi, M., Oppenheim, D. E., Steele, C. R., Lewis, J. M., Glusac, E., Filler, R., Hobby, P., Sutton, B., Tigelaar, R. E. and Hayday, A. C. (2001) Regulation of cutaneous malignancy by $\gamma\delta$ T cells, *Science*, 294(5542), 605-9.

Haig, N. A., Guan, Z., Li, D., McMichael, A., Raetz, C. R. and Xu, X. N. (2011) Identification of self-lipids presented by CD1c and CD1d proteins. *J Biol Chem*, 286(43), 37692-701.

Hamann, D., Baars, P. A., Rep, M. H., Hooibrink, B., Kerkhof-Garde, S. R., Klein, M. R. and van Lier, R. A. (1997) Phenotypic and functional separation of memory and effector human CD8⁽⁺⁾ T cells, *J Exp Med*, 186(9), 1407-18.

Hamzaoui, K. (2011) Th17 cells in Behçet's disease: a new immunoregulatory axis. *Clin Exp Rheumatol*, 29(4 Suppl 67), S71-6.

Han, Z. H., Palnitkar, S., Rao, D. S., Nelson, D. and Parfitt, A. M. (1997) Effects of ethnicity and age or menopause on the remodeling and turnover of iliac bone: implications for mechanisms of bone loss. *J Bone Miner Res*, 12(4), 498-508.

Hansen, T., Kirkpatrick, C. J., Walter, C. and Kunkel, M. (2006a) Increased numbers of osteoclasts expressing cysteine proteinase cathepsin K in patients with infected osteoradionecrosis and bisphosphonate-associated osteonecrosis--a paradoxical observation? *Virchows Arch*, 449(4), 448-54.

Hansen, T., Kunkel, M., Springer, E., Walter, C., Weber, A., Siegel, E. and Kirkpatrick, C. J. (2007) Actinomycosis of the jaws--histopathological study of 45 patients shows significant involvement in bisphosphonate-associated osteonecrosis and infected osteoradionecrosis. *Virchows Arch*, 451(6), 1009-17.

Hansen, T., Kunkel, M., Weber, A. and James Kirkpatrick, C. (2006b) Osteonecrosis of the jaws in patients treated with bisphosphonates - histomorphologic analysis in comparison with infected osteoradionecrosis. *J Oral Pathol Med*, 35(3), 155-60.

Harly, C., Guillaume, Y., Nedellec, S., Peigné, C. M., Mönkkönen, H., Mönkkönen, J., Li, J., Kuball, J., Adams, E. J., Netzer, S., Déchanet-Merville, J., Léger, A., Herrmann, T., Breathnach, R., Olive, D., Bonneville, M. and Scotet, E. (2012) Key implication of CD277/butyrophilin-3 (BTN3A) in cellular stress sensing by a major human $\gamma\delta$ T-cell subset', *Blood*, 120(11), 2269-79.

- Harper, R. P. and Fung, E. (2007) Resolution of bisphosphonate-associated osteonecrosis of the mandible: possible application for intermittent low-dose parathyroid hormone [rhPTH(1-34)]. *J Oral Maxillofac Surg*, 65(3), 573-80.
- Havran, W. L. (2000) A role for epithelial $\gamma\delta$ T cells in tissue repair. *Immunol Res*, 21(2-3), 63-9.
- Hayday, A. C., Roberts, S. and Ramsburg, E. (2000) $\gamma\delta$ T cells and the regulation of mucosal immune responses. *Am J Respir Crit Care Med*, 162(4 Pt 2), S161-3.
- Hellstein, J. W. and Marek, C. L. (2004) Bis-phossy jaw, phossy jaw, and the 21st century: bisphosphonate-associated complications of the jaws. *J Oral Maxillofac Surg*, 62(12), 1563-5.
- Hintzen, R. Q., de Jong, R., Lens, S. M., Brouwer, M., Baars, P. and van Lier, R. A. (1993) Regulation of CD27 expression on subsets of mature T-lymphocytes. *J Immunol*, 151(5), 2426-35.
- Hoff, A. O., Toth, B. B., Altundag, K., Johnson, M. M., Warneke, C. L., Hu, M., Nooka, A., Sayegh, G., Guarneri, V., Desrouleaux, K., Cui, J., Adamus, A., Gagel, R. F. and Hortobagyi, G. N. (2008) Frequency and risk factors associated with osteonecrosis of the jaw in cancer patients treated with intravenous bisphosphonates. *J Bone Miner Res*, 23(6), 826-36.
- Holtmeier, W. (2003) Compartmentalization $\gamma\delta$ T cells and their putative role in mucosal immunity. *Crit Rev Immunol*, 23(5-6), 473-88.
- Hsieh, B., Schrenzel, M. D., Mulvania, T., Lepper, H. D., DiMolfetto-Landon, L. and Ferrick, D. A. (1996) *In vivo* cytokine production in murine listeriosis. Evidence for immunoregulation by $\gamma\delta^{(+)}$ T cells. *J Immunol*, 156(1), 232-7.
- Hu, C., Qian, L., Miao, Y., Huang, Q., Miao, P., Wang, P., Yu, Q., Nie, H., Zhang, J., He, D., Xu, R., Chen, X., Liu, B. and Zhang, D. (2012) Antigen-presenting effects of effector memory V γ 9V δ 2 T cells in rheumatoid arthritis. *Cell Mol Immunol*, 9(3), 245-54.
- Hudu, S. A., Malik, Y. A., Niazlin, M. T., Harmal, N. S., Adnan, A., Alshrari, A. S. and Sekawi, Z. (2013) Antibody and immune memory persistence post infant hepatitis B vaccination. *Patient Prefer Adherence*, 7, 981-6.
- Hviid, L., Akanmori, B. D., Loizon, S., Kurtzhals, J. A., Ricke, C. H., Lim, A., Koram, K. A., Nkrumah, F. K., Mercereau-Puijalon, O. and Behr, C. (2000) High frequency of circulating $\gamma\delta$ T cells with dominance of the V δ 1 subset in a healthy population. *Int Immunol*, 12(6), 797-805.
- Imai, T., Hieshima, K., Haskell, C., Baba, M., Nagira, M., Nishimura, M., Kakizaki, M., Takagi, S., Nomiyama, H., Schall, T. J. and Yoshie, O. (1997) Identification and molecular characterization of fractalkine receptor CX3CR1, which mediates both leukocyte migration and adhesion. *Cell*, 91(4), 521-30.

- Imaizumi, T., Yoshida, H. and Satoh, K. (2004) Regulation of CX3CL1/fractalkine expression in endothelial cells. *J Atheroscler Thromb*, 11(1), 15-21.
- Inokuma, M. S., Maino, V. C. and Bagwell, C. B. (2013) Probability state modeling of memory CD8⁽⁺⁾ T-cell differentiation. *J Immunol Methods*, 397(1-2), 8-17.
- Inoue, S., Niikura, M., Mineo, S. and Kobayashi, F. (2013) Roles of IFN- γ and $\gamma\delta$ T Cells in Protective Immunity Against Blood-Stage Malaria. *Front Immunol*, 4, 258.
- Ismail, A. S., Behrendt, C. L. and Hooper, L. V. (2009) Reciprocal interactions between commensal bacteria and $\gamma\delta$ intraepithelial lymphocytes during mucosal injury. *J Immunol*, 182(5), 3047-54.
- Jameson, J., Ugarte, K., Chen, N., Yachi, P., Fuchs, E., Boismenu, R. and Havran, W. L. (2002) A role for skin $\gamma\delta$ T cells in wound repair. *Science*, 296(5568), 747-9.
- Jensen, P. E. (2007) Recent advances in antigen processing and presentation. *Nat Immunol*, 8(10), 1041-8.
- Ji, X., Pushalkar, S., Li, Y., Glickman, R., Fleisher, K. and Saxena, D. (2012) Antibiotic effects on bacterial profile in osteonecrosis of the jaw. *Oral Dis*, 18(1), 85-95.
- Junquera, L. and Gallego, L. (2008) Nonexposed bisphosphonate-related osteonecrosis of the jaws: another clinical variant? *J Oral Maxillofac Surg*, 66(7), 1516-7.
- Kabelitz, D. (2008) Small molecules for the activation of human $\gamma\delta$ T cell responses against infection. *Recent Pat Antiinfect Drug Discov*, 3(1), 1-9.
- Kabelitz, D., Bender, A., Schondelmaier, S., Schoel, B. and Kaufmann, S. H. (1990) A large fraction of human peripheral blood $\gamma\delta^{(+)}$ T cells is activated by Mycobacterium tuberculosis but not by its 65-kD heat shock protein. *J Exp Med*, 171(3), 667-79.
- Kalyan, S. and Kabelitz, D. (2013) Defining the nature of human $\gamma\delta$ T cells: a biographical sketch of the highly empathetic. *Cell Mol Immunol*, 10(1), 21-9.
- Kalyan, S., Quabius, E. S., Wiltfang, J., Mönig, H. and Kabelitz, D. (2013) 'Can peripheral blood $\gamma\delta$ T cells predict osteonecrosis of the jaw? An immunological perspective on the adverse drug effects of aminobisphosphonate therapy. *J Bone Miner Res*, 28(4), 728-35.
- Kang, Y. H., Carl, M., Watson, L. P. and Yaffe, L. (1987) Immunoultrastructural studies of human NK cells: II. Effector-target cell binding and phagocytosis. *Anat Rec*, 217(3), 290-304.

Kapp, J. A., Kapp, L. M., McKenna, K. C. and Lake, J. P. (2004) $\gamma\delta$ T-cell clones from intestinal intraepithelial lymphocytes inhibit development of CTL responses *ex vivo*. *Immunology*, 111(2), 155-64.

Khan, A. A., Sándor, G. K., Dore, E., Morrison, A. D., Alsahli, M., Amin, F., Peters, E., Hanley, D. A., Chaudry, S. R., Dempster, D. W., Glorieux, F. H., Neville, A. J., Talwar, R. M., Clokie, C. M., Al Mardini, M., Paul, T., Khosla, S., Josse, R. G., Sutherland, S., Lam, D. K., Carmichael, R. P., Blanas, N., Kendler, D., Petak, S., St-Marie, L. G., Brown, J., Evans, A. W., Rios, L., Compston, J. E. and Surgeons, C. A. o. O. a. M. (2008) Canadian consensus practice guidelines for bisphosphonate associated osteonecrosis of the jaw. *J Rheumatol*, 35(7), 1391-7.

Khan, S. A., Kanis, J. A., Vasikaran, S., Kline, W. F., Matuszewski, B. K., McCloskey, E. V., Beneton, M. N., Gertz, B. J., Sciberras, D. G., Holland, S. D., Orgee, J., Coombes, G. M., Rogers, S. R. and Porras, A. G. (1997) Elimination and biochemical responses to intravenous alendronate in postmenopausal osteoporosis. *J Bone Miner Res*, 12(10), 1700-7.

Kimmel, D. B. (2007) Mechanism of action, pharmacokinetic and pharmacodynamic profile, and clinical applications of nitrogen-containing bisphosphonates. *J Dent Res*, 86(11), 1022-33.

King, D. P., Hyde, D. M., Jackson, K. A., Novosad, D. M., Ellis, T. N., Putney, L., Stovall, M. Y., Van Winkle, L. S., Beaman, B. L. and Ferrick, D. A. (1999) Cutting edge: protective response to pulmonary injury requires $\gamma\delta$ T lymphocytes. *J Immunol*, 162(9), 5033-6.

Kistowska, M., Rossy, E., Sansano, S., Gober, H. J., Landmann, R., Mori, L. and De Libero, G. (2008) Dysregulation of the host mevalonate pathway during early bacterial infection activates human TCR $\gamma\delta$ cells. *Eur J Immunol*, 38(8), 2200-9.

Krimmel, M., Ripperger, J., Hairass, M., Hoefert, S., Kluba, S. and Reinert, S. (2013) Does dental and oral health influence the development and course of bisphosphonate-related osteonecrosis of the jaws (BRONJ)? *Oral Maxillofac Surg*.

Kroca, M., Tärnvik, A. and Sjöstedt, A. (2000) The proportion of circulating gammadelta T cells increases after the first week of onset of tularaemia and remains elevated for more than a year. *Clin Exp Immunol*, 120(2), 280-4.

Kunzmann, V., Smetak, M., Kimmel, B., Weigang-Koehler, K., Goebeler, M., Birkmann, J., Becker, J., Schmidt-Wolf, I. G., Einsele, H. and Wilhelm, M. (2012) Tumor-promoting versus tumor-antagonizing roles of $\gamma\delta$ T cells in cancer immunotherapy: results from a prospective phase I/II trial. *J Immunother*, 35(2), 205-13.

Kuroshima, S., Go, V. A. and Yamashita, J. (2012) Increased numbers of nonattached osteoclasts after long-term zoledronic acid therapy in mice. *Endocrinology*, 153(1), 17-28.

Kyrgidis, A., Vahtsevanos, K., Koloutsos, G., Andreadis, C., Boukovinas, I., Teleioudis, Z., Patrikidou, A. and Triaridis, S. (2008) Bisphosphonate-related osteonecrosis of the jaws: a case-control study of risk factors in breast cancer patients. *J Clin Oncol*, 26(28), 4634-8.

Laggner, U., Di Meglio, P., Perera, G. K., Hundhausen, C., Lacy, K. E., Ali, N., Smith, C. H., Hayday, A. C., Nickoloff, B. J. and Nestle, F. O. (2011) Identification of a novel proinflammatory human skin-homing V γ 9V δ 2 T cell subset with a potential role in psoriasis. *J Immunol*, 187(5), 2783-93.

Landesberg, R., Cozin, M., Cremers, S., Woo, V., Kousteni, S., Sinha, S., Garrett-Sinha, L. and Raghavan, S. (2008) Inhibition of oral mucosal cell wound healing by bisphosphonates. *J Oral Maxillofac Surg*, 66(5), 839-47.

Landesberg, R., Eisig, S., Fennoy, I. and Siris, E. (2009) Alternative indications for bisphosphonate therapy. *J Oral Maxillofac Surg*, 67(5 Suppl), 27-34.

Landesberg, R., Woo, V., Cremers, S., Cozin, M., Marolt, D., Vunjak-Novakovic, G., Kousteni, S. and Raghavan, S. (2011) Potential pathophysiological mechanisms in osteonecrosis of the jaw. *Ann N Y Acad Sci*, 1218, 62-79.

Lança, T., Costa, M. F., Gonçalves-Sousa, N., Rei, M., Grosso, A. R., Penido, C. and Silva-Santos, B. (2013) Protective role of the inflammatory CCR2/CCL2 chemokine pathway through recruitment of type 1 cytotoxic $\gamma\delta$ T lymphocytes to tumor beds. *J Immunol*, 190(12), 6673-80.

Lazarovici, T. S., Yahalom, R., Taicher, S., Elad, S., Hardan, I. and Yarom, N. (2009) Bisphosphonate-related osteonecrosis of the jaws: a single-center study of 101 patients. *J Oral Maxillofac Surg*, 67(4), 850-5.

Lesport, E., Baudhuin, J., Sousa, S., LeMaout, J., Zamborlini, A., Rouas-Freiss, N., Carosella, E. D. and Favier, B. (2011) Inhibition of human $\gamma\delta$ T-cell antitumoral activity through HLA-G: implications for immunotherapy of cancer. *Cell Mol Life Sci*, 68(20), 3385-99.

Libri, V., Azevedo, R. I., Jackson, S. E., Di Mitri, D., Lachmann, R., Fuhrmann, S., Vukmanovic-Stejic, M., Yong, K., Battistini, L., Kern, F., Soares, M. V. and Akbar, A. N. (2011) Cytomegalovirus infection induces the accumulation of short-lived, multifunctional CD4⁽⁺⁾CD45RA⁽⁺⁾CD27⁽⁺⁾ T cells: the potential involvement of interleukin-7 in this process. *Immunology*, 132(3), 326-39.

Locke, N. R., Stankovic, S., Funda, D. P. and Harrison, L. C. (2006) TCR gamma delta intraepithelial lymphocytes are required for self-tolerance. *J Immunol*, 176(11), 6553-9.

Lugassy, G., Shaham, R., Nemets, A., Ben-Dor, D. and Nahlieli, O. (2004) Severe osteomyelitis of the jaw in long-term survivors of multiple myeloma: a new clinical entity. *Am J Med*, 117(6), 440-1.

Malizos, K. N., Karantanas, A. H., Varitimidis, S. E., Dailiana, Z. H., Bargiotas, K. and Maris, T. (2007) Osteonecrosis of the femoral head: etiology, imaging and treatment. *Eur J Radiol*, 63(1), 16-28.

Manetti, R., Parronchi, P., Giudizi, M. G., Piccinni, M. P., Maggi, E., Trinchieri, G. and Romagnani, S. (1993) Natural killer cell stimulatory factor (interleukin 12 [IL-12]) induces T helper type 1 (Th1)-specific immune responses and inhibits the development of IL-4-producing Th cells. *J Exp Med*, 177(4), 1199-204.

Maniar, A., Zhang, X., Lin, W., Gastman, B. R., Pauza, C. D., Strome, S. E. and Chapoval, A. I. (2010) Human $\gamma\delta$ T lymphocytes induce robust NK cell-mediated antitumor cytotoxicity through CD137 engagement. *Blood*, 116(10), 1726-33.

Manicassamy, S., Sadim, M., Ye, R. D. and Sun, Z. (2006) Differential roles of PKC-theta in the regulation of intracellular calcium concentration in primary T cells', *J Mol Biol*, 355(3), 347-59.

Marolt, D., Cozin, M., Vunjak-Novakovic, G., Cremers, S. and Landesberg, R. (2011) Effects of Pamidronate on Human Alveolar Osteoblasts *In Vitro*. *J Oral Maxillofac Surg*.

Martínez-Borra, J., González, S. and López-Larrea, C. (2012) The origin of the bacterial immune response. *Adv Exp Med Biol*, 738, 1-13.

Marx, R. E. (1983) Osteoradionecrosis: a new concept of its pathophysiology. *J Oral Maxillofac Surg*, 41(5), 283-8.

Marx, R. E. (2003) Pamidronate (Aredia) and zoledronate (Zometa) induced avascular necrosis of the jaws: a growing epidemic. *J Oral Maxillofac Surg*, 61(9), 1115-7.

Marx, R. E. (2008) Uncovering the cause of "phossy jaw" Circa 1858 to 1906: oral and maxillofacial surgery closed case files-case closed. *J Oral Maxillofac Surg*, 66(11), 2356-63.

Mavrokokki, T., Cheng, A., Stein, B. and Goss, A. (2007) Nature and frequency of bisphosphonate-associated osteonecrosis of the jaws in Australia. *J Oral Maxillofac Surg*, 65(3), 415-23.

Mawardi H, I. I., Alnatour A, Jun-O J, Giro G, Kajiya M, , Yu Q, Woo S and Kawai T (2013) $\gamma\delta$ T cells in Bisphosphonate-Induced Osteonecrosis of the Jaw, in *IADR*, Seattle, Washington, USA Thursday, 21st March 2013: 8am-9:30 a.m. Location: Room 602 (Washington State Convention Center) Presentation Type: Oral Session, IADR,

McCarthy, N. E., Bashir, Z., Vossenkämper, A., Hedin, C. R., Giles, E. M., Bhattacharjee, S., Brown, S. G., Sanders, T. J., Whelan, K., MacDonald, T. T., Lindsay, J. O. and Stagg, A. J. (2013) Proinflammatory $V\delta 2^{(+)}$ T cells populate the human intestinal mucosa and enhance IFN- γ production by colonic $\alpha\beta$ T cells. *J Immunol*, 191(5), 2752-63.

McCutcheon, J. A., Yee, H., Hayashi, R., Licari, B., Lombardo, D., Rosenberg, P. A. and Phelan, J. (2004) Identification of $\gamma\delta$ T lymphocytes in human periapical lesions. *Oral Microbiol Immunol*, 19(2), 106-10.

McLeod, N. M., Patel, V., Kusanale, A., Rogers, S. N. and Brennan, P. A. (2011) Bisphosphonate osteonecrosis of the jaw: a literature review of UK policies versus international policies on the management of bisphosphonate osteonecrosis of the jaw. *Br J Oral Maxillofac Surg*, 49(5), 335-42.

McVay, L. D. and Carding, S. R. (1999) Generation of human $\gamma\delta$ T cell repertoires, *Crit Rev Immunol*, 19(5-6), 431-60.

Meraviglia, S., Caccamo, N., Guggino, G., Tolomeo, M., Siragusa, S., Stassi, G. and Dieli, F. (2010) Optimizing tumor-reactive $\gamma\delta$ T cells for antibody-based cancer immunotherapy, *Curr Mol Med*, 10(8), 719-26.

Meraviglia, S., El Daker, S., Dieli, F., Martini, F. and Martino, A. (2011) $\gamma\delta$ T cells cross-link innate and adaptive immunity in Mycobacterium tuberculosis infection. *Clin Dev Immunol*, 2011, 587315.

Merigo, E., Manfredi, M., Meleti, M., Corradi, D. and Vescovi, P. (2005) Jaw bone necrosis without previous dental extractions associated with the use of bisphosphonates (pamidronate and zoledronate): a four-case report. *J Oral Pathol Med*, 34(10), 613-7.

Mhaskar, R., Redzepovic, J., Wheatley, K., Clark, O. A., Miladinovic, B., Glasmacher, A., Kumar, A. and Djulbegovic, B. (2010) Bisphosphonates in multiple myeloma. *Cochrane Database Syst Rev*, (3), CD003188.

Michishita, Y., Hirokawa, M., Guo, Y. M., Abe, Y., Liu, J., Ubukawa, K., Fujishima, N., Fujishima, M., Yoshioka, T., Kameoka, Y., Saito, H., Tagawa, H., Takahashi, N. and Sawada, K. (2011) Age-associated alteration of $\gamma\delta$ T-cell repertoire and different profiles of activation-induced death of V δ 1 and V δ 2 T cells, *Int J Hematol*, 94(3), 230-40.

Migliorati, C. A., Woo, S. B., Hewson, I., Barasch, A., Elting, L. S., Spijkervet, F. K., Brennan, M. T. and Bisphosphonate Osteonecrosis Section, O. C. S. G., M. International Association of Supportive Care in Cancer (MASCC)/International Society of Oral Oncology (ISOO) (2010) A systematic review of bisphosphonate osteonecrosis (BON) in cancer. *Support Care Cancer*, 18(8), 1099-106.

Miksad, R. A., Lai, K. C., Dodson, T. B., Woo, S. B., Treister, N. S., Akinyemi, O., Bihle, M., Maytal, G., August, M., Gazelle, G. S. and Swan, J. S. (2011) Quality of life implications of bisphosphonate-associated osteonecrosis of the jaw. *Oncologist*, 16(1), 121-32.

Mombaerts, P., Arnoldi, J., Russ, F., Tonegawa, S. and Kaufmann, S. H. (1993) Different roles of alpha beta and $\gamma\delta$ T cells in immunity against an intracellular bacterial pathogen. *Nature*, 365(6441), 53-6.

Morita, C. T., Jin, C., Sarikonda, G. and Wang, H. (2007) Nonpeptide antigens, presentation mechanisms, and immunological memory of human V γ 9V δ 2 T cells: discriminating friend from foe through the recognition of prenyl pyrophosphate antigens. *Immunol Rev*, 215, 59-76.

Mukasa, A., Hiromatsu, K., Matsuzaki, G., O'Brien, R., Born, W. and Nomoto, K. (1995) Bacterial infection of the testis leading to autoaggressive immunity triggers apparently opposed responses of alpha beta and $\gamma\delta$ T cells, *J Immunol*, 155(4), 2047-56.

Munk, M. E., Gatrill, A. J. and Kaufmann, S. H. (1990) Target cell lysis and IL-2 secretion by $\gamma\delta$ T lymphocytes after activation with bacteria, *J Immunol*, 145(8), 2434-9.

Ness-Schwickerath, K. J. and Morita, C. T. (2011) Regulation and function of IL-17A- and IL-22-producing $\gamma\delta$ T cells. *Cell Mol Life Sci*, 68(14), 2371-90.

Nicolatou-Galitis, O., Papadopoulou, E., Sarri, T., Boziari, P., Karayianni, A., Kyrtonis, M. C., Repousis, P., Barbounis, V. and Migliorati, C. A. (2011) Osteonecrosis of the jaw in oncology patients treated with bisphosphonates: prospective experience of a dental oncology referral center. *Oral Surg Oral Med Oral Pathol Oral Radiol Endod*, 112(2), 195-202.

Nobrega, C., Nunes-Alves, C., Cerqueira-Rodrigues, B., Roque, S., Barreira-Silva, P., Behar, S. M. and Correia-Neves, M. (2013) T cells home to the thymus and control infection. *J Immunol*, 190(4), 1646-58.

Nussbaumer, O., Gruenbacher, G., Gander, H., Komuczki, J., Rahm, A. and Thurnher, M. (2013). Essential requirements of zoledronate-induced cytokine and $\gamma\delta$ T cell proliferative responses. *J Immunol*, 191(3), 1346-55.

O'Ryan, F. S. and Lo, J. C. (2012) Bisphosphonate-related osteonecrosis of the jaw in patients with oral bisphosphonate exposure: clinical course and outcomes. *J Oral Maxillofac Surg*, 70(8), 1844-53.

Okada, R., Kondo, T., Matsuki, F., Takata, H. and Takiguchi, M. (2008) Phenotypic classification of human CD4⁽⁺⁾ T cell subsets and their differentiation. *Int Immunol*, 20(9), 1189-99.

Olson, W. C., Smolkin, M. E., Farris, E. M., Fink, R. J., Czarkowski, A. R., Fink, J. H., Chianese-Bullock, K. A. and Slingluff, C. L. (2011) Shipping blood to a central laboratory in multicenter clinical trials: effect of ambient temperature on specimen temperature, and effects of temperature on mononuclear cell yield, viability and immunologic function, *J Transl Med*, 9, 26.

Oltz, E. M. (2001) Regulation of antigen receptor gene assembly in lymphocytes', *Immunol Res*, 23(2-3), 121-33.

Pang, D. J., Neves, J. F., Sumaria, N. and Pennington, D. J. (2012) Understanding the complexity of $\gamma\delta$ T-cell subsets in mouse and human. *Immunology*, 136(3), 283-90.

Parker, C. M., Groh, V., Band, H., Porcelli, S. A., Morita, C., Fabbi, M., Glass, D., Strominger, J. L. and Brenner, M. B. (1990) Evidence for extrathymic changes in the T cell receptor gamma/delta repertoire. *J Exp Med*, 171(5), 1597-612.

Patel, S., Choyee, S., Uyanne, J., Nguyen, A., Lee, P., Sedghizadeh, P., Kumar, S., Lytle, J., Shi, S. and Le, A. (2012) Non-exposed bisphosphonate-related osteonecrosis of the jaw: a critical assessment of current definition, staging, and treatment guidelines. *Oral Dis.* Oct; 18(7): 625-3.

Peng, M. Y., Wang, Z. H., Yao, C. Y., Jiang, L. N., Jin, Q. L., Wang, J. and Li, B. Q. (2008) Interleukin 17-producing gamma delta T cells increased in patients with active pulmonary tuberculosis, *Cell Mol Immunol*, 5(3), 203-8.

Perera, M. K., Carter, R., Goonewardene, R. and Mendis, K. N. (1994) Transient increase in circulating gamma/delta T cells during Plasmodium vivax malarial paroxysms', *J Exp Med*, 179(1), 311-5.

Pido-Lopez, J., Imami, N. and Aspinall, R. (2001) Both age and gender affect thymic output: more recent thymic migrants in females than males as they age. *Clin Exp Immunol*, 125(3), 409-13.

Ponte, M., Cantoni, C., Biassoni, R., Tradori-Cappai, A., Bentivoglio, G., Vitale, C., Bertone, S., Moretta, A., Moretta, L. and Mingari, M. C. (1999) Inhibitory receptors sensing HLA-G1 molecules in pregnancy: decidua-associated natural killer cells express LIR-1 and CD94/NKG2A and acquire p49, an HLA-G1-specific receptor, *Proc Natl Acad Sci U S A*, 96(10), 5674-9.

Pozzi, S., Marcheselli, R., Sacchi, S., Baldini, L., Angrilli, F., Pennese, E., Quarta, G., Stelitano, C., Caparotti, G., Luminari, S., Musto, P., Natale, D., Broglia, C., Cuoghi, A., Dini, D., Di Tonno, P., Leonardi, G., Pianezze, G., Pitini, V., Polimeno, G., Ponchio, L., Masini, L., Musso, M., Spriano, M., Pollastri, G. and Linfomi, G. I. S. (2007) Bisphosphonate-associated osteonecrosis of the jaw: a review of 35 cases and an evaluation of its frequency in multiple myeloma patients. *Leuk Lymphoma*, 48(1), 56-64.

Puan, K. J., Low, J. S., Tan, T. W., Wee, J. T., Tan, E. H., Fong, K. W., Chua, E. T., Jin, C., Giner, J. L., Morita, C. T., Goh, C. H. and Hui, K. M. (2009) Phenotypic and functional alterations of V γ 9V δ 2 T cell subsets in patients with active nasopharyngeal carcinoma. *Cancer Immunol Immunother*, 58(7), 1095-107.

Rajagopalan, S., Bryceson, Y. T., Kuppusamy, S. P., Geraghty, D. E., van der Meer, A., Joosten, I. and Long, E. O. (2006) Activation of NK cells by an endocytosed receptor for soluble HLA-G. *PLoS Biol*, 4(1), e9.

Rajagopalan, S., Fu, J. and Long, E. O. (2001) Cutting edge: induction of IFN- γ production but not cytotoxicity by the killer cell Ig-like receptor KIR2DL4 (CD158d) in resting NK cells. *J Immunol*, 167(4), 1877-81.

Rajagopalan, S. and Long, E. O. (2012) KIR2DL4 (CD158d): An activation receptor for HLA-G. *Front Immunol*, 3, 258.

Reid, I. R., Brown, J. P., Burckhardt, P., Horowitz, Z., Richardson, P., Trechsel, U., Widmer, A., Devogelaer, J. P., Kaufman, J. M., Jaeger, P., Body, J. J., Brandi, M. L., Broell, J., Di Micco, R., Genazzani, A. R., Felsenberg, D., Happ, J., Hooper, M. J., Ittner, J., Leb, G., Mallmin, H., Murray, T., Ortolani, S., Rubinacci, A., Saaf, M., Samsioe, G., Verbruggen, L. and Meunier, P. J. (2002) Intravenous zoledronic acid in postmenopausal women with low bone mineral density. *N Engl J Med*, 346(9), 653-61.

Ribot, J. C., Debarros, A., Mancio-Silva, L., Pamplona, A. and Silva-Santos, B. (2012) B7-CD28 costimulatory signals control the survival and proliferation of murine and human $\gamma\delta$ T cells via IL-2 production. *J Immunol*, 189(3), 1202-8.

Ribot, J. C., deBarros, A., Pang, D. J., Neves, J. F., Peperzak, V., Roberts, S. J., Girardi, M., Borst, J., Hayday, A. C., Pennington, D. J. and Silva-Santos, B. (2009) CD27 is a thymic determinant of the balance between i IFN- γ and interleukin 17-producing $\gamma\delta$ T cell subsets. *Nat Immunol*, 10(4), 427-36.

Roelofs, A. J., Jauhainen, M., Mönkkönen, H., Rogers, M. J., Mönkkönen, J. and Thompson, K. (2009) Peripheral blood monocytes are responsible for $\gamma\delta$ T cell activation induced by zoledronic acid through accumulation of IPP/DMAPP. *Br J Haematol*, 144(2), 245-50.

Roelofs, A. J., Thompson, K., Ebetino, F. H., Rogers, M. J. and Coxon, F. P. (2010) Bisphosphonates: molecular mechanisms of action and effects on bone cells, monocytes and macrophages. *Curr Pharm Des*, 16(27), 2950-60.

Rogers, M. J., Gordon, S., Benford, H. L., Coxon, F. P., Luckman, S. P., Monkkonen, J. and Frith, J. C. (2000) Cellular and molecular mechanisms of action of bisphosphonates. *Cancer*, 88(12 Suppl), 2961-78.

Romagnani, S. (2004) The increased prevalence of allergy and the hygiene hypothesis: missing immune deviation, reduced immune suppression, or both? *Immunology*, 112(3), 352-63.

Rossini, M., Adami, S., Viapiana, O., Fracassi, E., Ortolani, R., Vella, A., Zanotti, R., Tripi, G., Idolazzi, L. and Gatti, D. (2012) Long-term effects of amino-bisphosphonates on circulating $\gamma\delta$ T cells. *Calcif Tissue Int*, 91(6), 395-9.

Ruggiero, S. L., Mehrotra, B., Rosenberg, T. J. and Engroff, S. L. (2004) Osteonecrosis of the jaws associated with the use of bisphosphonates: a review of 63 cases. *J Oral Maxillofac Surg*, 62(5), 527-34.

Ryan-Payseur, B., Frencher, J., Shen, L., Chen, C. Y., Huang, D. and Chen, Z. W. (2012) Multieffector-functional immune responses of HMBPP-specific V γ 9V δ 2 T cells in nonhuman primates inoculated with *Listeria monocytogenes*. *J Immunol*, 189(3), 1285-93.

Saito, H., Kranz, D. M., Takagaki, Y., Hayday, A. C., Eisen, H. N. and Tonegawa, S. (1984) A third rearranged and expressed gene in a clone of cytotoxic T lymphocytes. *Nature*, 312(5989), 36-40.

- Saldanha, S., Shenoy, V. K., Eachampati, P. and Uppal, N. (2012) Dental implications of bisphosphonate-related osteonecrosis. *Gerodontology*.
- Sallusto, F., Lenig, D., Förster, R., Lipp, M. and Lanzavecchia, A. (1999) Two subsets of memory T lymphocytes with distinct homing potentials and effector functions. *Nature*, 401(6754), 708-12.
- Sarathy, A. P., Bourgeois, S. L. and Goodell, G. G. (2005) Bisphosphonate-associated osteonecrosis of the jaws and endodontic treatment: two case reports. *J Endod*, 31(10), 759-63.
- Scalise, F., Gerli, R., Castellucci, G., Spinozzi, F., Fabietti, G. M., Crupi, S., Sensi, L., Britta, R., Vaccaro, R. and Bertotto, A. (1992) Lymphocytes bearing the $\gamma\delta$ T-cell receptor in acute toxoplasmosis. *Immunology*, 76(4), 668-70.
- Seghaye, M. C., Heyl, W., Grabitz, R. G., Schumacher, K., von Bernuth, G., Rath, W. and Duchateau, J. (1998) The production of pro- and anti-inflammatory cytokines in neonates assessed by stimulated whole cord blood culture and by plasma levels at birth. *Biol Neonate*, 73(4), 220-7.
- Shao, L., Huang, D., Wei, H., Wang, R. C., Chen, C. Y., Shen, L., Zhang, W., Jin, J. and Chen, Z. W. (2009) Expansion, reexpansion, and recall-like expansion of $V\gamma 9V\delta 2$ T cells in smallpox vaccination and monkeypox virus infection. *J Virol*, 83(22), 11959-65.
- Shen, Y., Zhou, D., Qiu, L., Lai, X., Simon, M., Shen, L., Kou, Z., Wang, Q., Jiang, L., Estep, J., Hunt, R., Clagett, M., Sehgal, P. K., Li, Y., Zeng, X., Morita, C. T., Brenner, M. B., Letvin, N. L. and Chen, Z. W. (2002) Adaptive immune response of $V\gamma 9V\delta 2^{(+)}$ T cells during mycobacterial infections. *Science*, 295(5563), 2255-8.
- Smith, R., Russell, R. G., Bishop, M. C., Woods, C. G. and Bishop, M. (1973) Paget's disease of bone. Experience with a diphosphonate (disodium etidronate) in treatment. *Q J Med*, 42(166), 235-56.
- Sol, M. A., Tkaczuk, J., Voigt, J. J., Durand, M., Sixou, M., Maurette, A. and Thomsen, M. (1998) Characterization of lymphocyte subpopulations in periapical lesions by flow cytometry. *Oral Microbiol Immunol*, 13(4), 253-8.
- Sprent, J. and Surh, C. D. (2009) Re-entry of mature T cells to the thymus: an epiphenomenon? *Immunol Cell Biol*, 87(1), 46-9.
- Stumpe, M. R., Chandra, R. K., Yunus, F. and Samant, S. (2009) Incidence and risk factors of bisphosphonate-associated osteonecrosis of the jaws. *Head Neck*, 31(2), 202-6.
- Terpos, E., Sezer, O., Croucher, P. I., García-Sanz, R., Boccadoro, M., San Miguel, J., Ashcroft, J., Bladé, J., Cavo, M., Delforge, M., Dimopoulos, M. A., Facon, T., Macro, M., Waage, A., Sonneveld, P. and Network, E. M. (2009) The use of bisphosphonates in multiple myeloma: recommendations of an expert panel on behalf of the European Myeloma Network. *Ann Oncol*, 20(8), 1303-17.

Thiébaud, D., Sauty, A., Burckhardt, P., Leuenberger, P., Sitzler, L., Green, J. R., Kandra, A., Zieschang, J. and Ibarra de Palacios, P. (1997) An *in vitro* and *in vivo* study of cytokines in the acute-phase response associated with bisphosphonates. *Calcif Tissue Int*, 61(5), 386-92.

Tlaskalová-Hogenová, H., Stepánková, R., Hudcovic, T., Tucková, L., Cukrowska, B., Lodinová-Zádníková, R., Kozáková, H., Rossmann, P., Bártová, J., Sokol, D., Funda, D. P., Borovská, D., Reháková, Z., Sinkora, J., Hofman, J., Drastich, P. and Kokesová, A. (2004) Commensal bacteria (normal microflora), mucosal immunity and chronic inflammatory and autoimmune diseases. *Immunol Lett*, 93(2-3), 97-108.

Tosi, P., Zamagni, E., Cangini, D., Tacchetti, P., Di Raimondo, F., Catalano, L., D'Arco, A., Ronconi, S., Cellini, C., Offidani, M., Perrone, G., Ceccolini, M., Brioli, A., Tura, S., Baccarani, M. and Cavo, M. (2006) Osteonecrosis of the jaws in newly diagnosed multiple myeloma patients treated with zoledronic acid and thalidomide-dexamethasone. *Blood*, 108(12), 3951-2.

Tramonti, D., Andrew, E. M., Rhodes, K., Newton, D. J. and Carding, S. R. (2006) Evidence for the opposing roles of different $\gamma\delta$ T cell subsets in macrophage homeostasis. *Eur J Immunol*, 36(7), 1729-38.

Underhill, D. M. and Goodridge, H. S. (2012) Information processing during phagocytosis. *Nat Rev Immunol*, 12(7), 492-502.

Vincent, M. S., Roessner, K., Lynch, D., Wilson, D., Cooper, S. M., Tschopp, J., Sigal, L. H. and Budd, R. C. (1996) Apoptosis of Fashigh CD4⁽⁺⁾ synovial T cells by borrelia-reactive Fas-ligand(high) $\gamma\delta$ T cells in Lyme arthritis, *J Exp Med*, 184(6), 2109-17.

Wang, E. P., Kaban, L. B., Strewler, G. J., Raje, N. and Troulis, M. J. (2007) Incidence of osteonecrosis of the jaw in patients with multiple myeloma and breast or prostate cancer on intravenous bisphosphonate therapy. *J Oral Maxillofac Surg*, 65(7), 1328-31.

Weinberg, A., Song, L. Y., Wilkening, C., Sevin, A., Blais, B., Louzao, R., Stein, D., Defechereux, P., Durand, D., Riedel, E., Raftery, N., Jesser, R., Brown, B., Keller, M. F., Dickover, R., McFarland, E., Fenton, T. and Group, P. A. C. W. (2009) Optimization and limitations of use of cryopreserved peripheral blood mononuclear cells for functional and phenotypic T-cell characterization. *Clin Vaccine Immunol*, 16(8), 1176-86.

Wesch, D., Glatzel, A. and Kabelitz, D. (2001) Differentiation of resting human peripheral blood $\gamma\delta$ T cells toward Th1 or Th2 phenotype. *Cell Immunol*, 212(2), 110-7.

Wilhelm, M., Kunzmann, V., Eckstein, S., Reimer, P., Weissinger, F., Ruediger, T. and Tony, H. P. (2003) $\gamma\delta$ T cells for immune therapy of patients with lymphoid malignancies. *Blood*, 102(1), 200-6.

Willcox, C. R., Pitard, V., Netzer, S., Couzi, L., Salim, M., Silberzahn, T., Moreau, J. F., Hayday, A. C., Willcox, B. E. and Déchanet-Merville, J. (2012) Cytomegalovirus and tumor stress surveillance by binding of a human $\gamma\delta$ T cell antigen receptor to endothelial protein C receptor. *Nat Immunol*, 13(9), 872-9.

Wood, J., Bonjean, K., Ruetz, S., Bellahcène, A., Devy, L., Foidart, J. M., Castronovo, V. and Green, J. R. (2002) Novel antiangiogenic effects of the bisphosphonate compound zoledronic acid. *J Pharmacol Exp Ther*, 302(3), 1055-61.

Worku, S., Gorse, G. J., Belshe, R. B. and Hoft, D. F. (2001a) Canarypox vaccines induce antigen-specific human $\gamma\delta$ T cells capable of IFN- γ production. *J Infect Dis*, 184(5), 525-32.

Worku, S., Troye-Blomberg, M., Christensson, B., Björkman, A. and Fehniger, T. (2001b) Activation of T cells in the blood of patients with acute malaria: proliferative activity as indicated by Ki-67 expression. *Scand J Immunol*, 53(3), 296-301.

Worley, R. J. (1981) Age, estrogen, and bone density. *Clin Obstet Gynecol*, 24(1), 203-18.

Wu, Y., Wu, W., Wong, W. M., Ward, E., Thrasher, A. J., Goldblatt, D., Osman, M., Digard, P., Canaday, D. H. and Gustafsson, K. (2009) Human $\gamma\delta$ T cells: a lymphoid lineage cell capable of professional phagocytosis. *J Immunol*, 183(9), 5622-9.

Wypij, J. M., Fan, T. M., Fredrickson, R. L., Barger, A. M., de Lorimier, L. P. and Charney, S. C. (2008) *In vivo* and *in vitro* efficacy of zoledronate for treating oral squamous cell carcinoma in cats. *J Vet Intern Med*, 22(1), 158-63.

Yokobori, N., Schierloh, P., Geffner, L., Balboa, L., Romero, M., Musella, R., Castagnino, J., De Stéfano, G., Alemán, M., de la Barrera, S., Abbate, E. and Sasiain, M. C. (2009) CD3 expression distinguishes two $\gamma\delta$ T cell receptor subsets with different phenotype and effector function in tuberculous pleurisy. *Clin Exp Immunol*, 157(3), 385-94.

Zervas, K., Verrou, E., Teleioudis, Z., Vahtsevanos, K., Banti, A., Mihou, D., Krikelis, D. and Terpos, E. (2006) Incidence, risk factors and management of osteonecrosis of the jaw in patients with multiple myeloma: a single-centre experience in 303 patients. *Br J Haematol*, 134(6), 620-3.

Chapter 10 Appendices

10.1 Ethics - Favourable opinion



Health Research Authority

NRES Committee London - City & East

Bristol Research Ethics Committee Centre
Whitefriars
Level 3, Block B
Lewins Mead
Bristol
BS1 2NT

Telephone: 01173421386
Facsimile: 01173420445

29 May 2013

Mr Paul Ryan
Wellcome Trust / Faculty of Dental Surgery Research Training Fellow
Queen Mary University of London,
Barts and The London School of Medicine and Dentistry
6th Floor Dental Institute
Turner Street
London
E1 2AT

Dear Mr Ryan

Study title: An investigation into the role of Gamma delta T-cells and Oral bacteria in Bisphosphonate-related osteonecrosis of the jaw.
REC reference: 13/LO/0548
Protocol number: 3.0
IRAS project ID: 92597

Thank you for your letter of 21 May 2013, responding to the Committee's request for further information on the above research and submitting revised documentation.

The further information was considered in correspondence by a sub-committee of the REC. A list of the sub-committee members is attached.

Confirmation of ethical opinion

On behalf of the Committee, I am pleased to confirm a favourable ethical opinion for the above research on the basis described in the application form, protocol and supporting documentation as revised, subject to the conditions specified below.

We plan to publish your research summary wording for the above study on the NRES website, together with your contact details, unless you expressly withhold permission to do so. Publication will be no earlier than three months from the date of this favourable opinion letter. Should you wish to provide a substitute contact point, require further information, or wish to withhold permission to publish, please contact the Co-ordinator Mr Rajat Khullar, nrescommittee.london-cityandeast@nhs.net.

Ethical review of research sites

NHS sites

The favourable opinion applies to all NHS sites taking part in the study, subject to management permission being obtained from the NHS/HSC R&D office prior to the start of the study (see "Conditions of the favourable opinion" below).

Non-NHS sites

I am pleased to confirm that the favourable opinion applies to the following research site, subject to site management permission being obtained prior to the start of the study at the site (see under 'Conditions of the favourable opinion below').

Research Site	Principal Investigator / Local Collaborator
Blizard Institute, Queen Mary University of London	Mr Paul Ryan

Conditions of the favourable opinion

The favourable opinion is subject to the following conditions being met prior to the start of the study.

Management permission or approval must be obtained from each host organisation prior to the start of the study at the site concerned.

Management permission ("R&D approval") should be sought from all NHS organisations involved in the study in accordance with NHS research governance arrangements.

Guidance on applying for NHS permission for research is available in the Integrated Research Application System or at <http://www.rdforum.nhs.uk>.

Where a NHS organisation's role in the study is limited to identifying and referring potential participants to research sites ("participant identification centre"), guidance should be sought from the R&D office on the information it requires to give permission for this activity.

For non-NHS sites, site management permission should be obtained in accordance with the procedures of the relevant host organisation.

Sponsors are not required to notify the Committee of approvals from host organisations

It is the responsibility of the sponsor to ensure that all the conditions are complied with before the start of the study or its initiation at a particular site (as applicable).

Approved documents

The final list of documents reviewed and approved by the Committee is as follows:

<i>Document</i>	<i>Version</i>	<i>Date</i>
Covering Letter		26 March 2013
Evidence of insurance or indemnity		30 July 2012
Investigator CV		04 January 2013
Letter from Sponsor		11 March 2013
Email letter of invitation to participant	1.0	18 February 2013
Other: Summary CV for supervisor (student research)		04 January 2013
Other: Evidence of professional registration: Dentist GDC82525	1.0	26 March 2013
Other: Data collection sheets for all groups		
Other: Non NHS SSI Form		
Participant Consent Form: Healthy Participants	4.0	16 May 2013
Participant Consent Form: BRONJ Patients	4.0	16 May 2012
Participant Consent Form: Non-BRONJ Jaw Infections	4.0	16 May 2013
Participant Consent Form: Bisphosphonate Clinic	4.0	16 May 2013
Participant consent form – Retention of samples	4.0	16 May 2013
Participant Information Sheet: Healthy Participants	4.0	16 May 2013
Participant Information Sheet: BRONJ Patients	4.0	16 May 2013
Participant Information Sheet: Non-BRONJ Jaw Infections	4.0	16 May 2013
Participant Information Sheet: Bisphosphonate Clinic	4.0	16 May 2013
Protocol	4.0	16 May 2013
REC application		26 March 2013
Referees or other scientific critique report		18 February 2013
Response to Request for Further Information		21 May 2013
Summary/Synopsis	1.0	26 March 2013
Summary/Synopsis	2.0	18 May 2013
Healthy volunteer – Data collection sheet	3.0	18 February 2013
Group 1 BRONJ patients – Data collection sheet	3.0	18 February 2013
Group 2 Non- BRONJ related jaw infections – Data collection sheet	3.0	18 February 2013
Groups 3,4+5 – BRONJ control group data collection sheet	4.0	16 May 2013

Statement of compliance

The Committee is constituted in accordance with the Governance Arrangements for Research Ethics Committees and complies fully with the Standard Operating Procedures for Research Ethics Committees in the UK.

After ethical review

Reporting requirements

The attached document “*After ethical review – guidance for researchers*” gives detailed guidance on reporting requirements for studies with a favourable opinion, including:

- Notifying substantial amendments
- Adding new sites and investigators
- Notification of serious breaches of the protocol
- Progress and safety reports
- Notifying the end of the study

The NRES website also provides guidance on these topics, which is updated in the light of changes in reporting requirements or procedures.

Feedback

You are invited to give your view of the service that you have received from the National Research Ethics Service and the application procedure. If you wish to make your views known please use the feedback form available on the website.

Further information is available at National Research Ethics Service website > After Review

13/LO/0548	Please quote this number on all correspondence
-------------------	---

We are pleased to welcome researchers and R & D staff at our NRES committee members' training days – see details at <http://www.hra.nhs.uk/hra-training/>

With the Committee's best wishes for the success of this project.

Yours sincerely



pp Dr Arthur T. Tucker
Chair

Email: nrescommittee.london-cityandeast@nhs.net

Enclosures: List of names and professions of members who were present at the meeting and those who submitted written comments

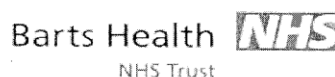
"After ethical review – guidance for researchers"

Copy to: Mr Gerry Leonard, Queen Mary University of London

10.2 Patient information sheets

Example of healthy volunteer patient information sheet is shown (Similar forms were used for other control groups).

REC REF 13/LO/0548



Patient Information Sheet

<p>Project Title:</p> <p>Bisphosphonate-related osteonecrosis of the jaw and the Immune system</p> <p>Healthy Participants</p> <p>Name of Researcher: Mr Paul Ryan</p>
--

INVITATION TO PARTICIPATE

We would like to **invite you** to take part in a research study which we think may be important. Before you decide you need to **understand** why the research is being done and what it would **involve for you**. Please **take time to read** the following information carefully. **Talk to others** about the study if you wish.

The information which follows tells you about the study. It is important that you **understand what is in this leaflet**. It tells you what will happen to you if you decide to take part.

Whether or not you decide to take part is entirely your choice.

Part 1: Tells you the **purpose of this study** and what will happen to you if you take part.

Part 2: Gives you more **detailed information** about the conduct of the study).

Please feel free to **ask any questions** about the research and we will try our best to answer them. **Take time to decide** whether or not you wish to take part.

Date 18.02.13 Version 3.0 Healthy Participants

When completed, 1 for patient; 1 for researcher site file; 1 (original) to be kept in medical notes

Bisphosphonate-related osteonecrosis of the jaw and the Immune system

Part 1

What the research is about?

This research aims at investigating **an uncommon side-effect** of a particular medication called a bisphosphonate. A side-effect of this drug is osteonecrosis of the jaw, where the jaw bone becomes damaged and dies. The cause of the condition is **poorly understood**.

We are interested in studying whether this condition is due to changes in your mouth bacteria and white blood cells that are important in your **immune system**. We would like to understand why a small minority of patients experience the side-effect whilst others remain unaffected.

Why have I been asked to take part?

You have been invited to participate in this study because you are a healthy individual. We are inviting healthy volunteers to provide a blood sample with their consent to test the effect of the bisphosphonate medication on blood cells in the laboratory.

What is osteonecrosis of the jaw?

Osteonecrosis of the jaw is an **uncommon side-effect** of bisphosphonates and is experienced by approximately between 1 and 5 patients in every 100 patients receiving the intravenous form of this medication.

In the disease, healthy bone tissue in the jaw becomes damaged and dies. This can lead to pain, swelling, infection and loose teeth. Other symptoms include numbness or heaviness in your jaw. The condition is **poorly understood** but tooth removal (extraction), gum disease, denture problems and dental treatment can increase the risk.

Do I have to take part?

No, it is up to you to decide. You are **free to withdraw at any time**, without giving a reason.

What will I have to do?

If you agree to take part in the study and following informed consent, you will be asked to:

1. Provide a **sample of blood** (Around three tablespoons or up to 50ml). (5 minutes).

In addition, some questions will be asked about you and your general health. This will be collected on information sheets and will be anonymised

What are the benefits of taking part?

You are unlikely to benefit directly from this research yourself but we hope it will benefit patients affected with bisphosphonate-related osteonecrosis of the jaw in the future.

Date 18.02.13 Version 3.0 Healthy Participants

When completed, 1 for patient; 1 for researcher site file; 1 (original) to be kept in medical notes

Are there any drawbacks to taking part?

The risks involved in this study are **minimal**. Very occasionally, blood tests can be associated with bleeding, bruising or infection at the site where the blood is taken. However this is usually only a minor discomfort and resolves quickly after the test.

What if there is a problem?

Any complaint about the way you have been dealt with during the study or any possible harm you might suffer will be addressed. The detailed information on this is given in Part 2.

Will my taking part in the study be kept confidential?

Yes, we will follow ethical and legal practice and all information about you will held securely in accordance with the terms of the Data Protection Act 1998.

What happens if I have further questions?

If you have any questions concerning the study please **feel free to ask us**. We can provide you with further information if you wish. Contact names and numbers are given below. **You do not have to join the study.**

If the information in Part 1 has interested you and you are considering participation, please read the additional information in Part 2 before making any decision.

Part 2: Information Sheet

What if relevant new information becomes available?

This is a non-interventional study we do not anticipate a situation whereby we would be ethically obliged to halt this study.

What will happen if I want to withdraw from the study?

You are under no obligation to take part in this study and are free to withdraw from it at any time. There is no long term follow-up commitment. If you subsequently inform us that you wish to withdraw from the study, we will destroy all your identifiable samples, but we may still use the data collected /analysed up to your withdrawal.

What if there is a problem?

We believe this study is basically safe and do not expect you to suffer harm or injury. In the unlikely event that you are harmed as a result of your participation in the study, Queen Mary University of London has agreed that you will be compensated, provided that, on the balance of probabilities, an injury was caused as a direct result of the procedures you received during the course of the study. These special compensation arrangements apply where an injury is caused to you that would not have occurred if you were not in the study. These arrangements do not affect your right to pursue a claim through legal action.

Complaints

If you have a concern about any aspect of this study, you should ask to speak to the researchers who will do their best to answer your questions (contact number below). You can also contact the Patient Advisory Liaison Service (PALS) if you have any concerns regarding your care, or as an initial point of contact if you have a complaint. Please telephone 020 7377 6335, or e-mail pals@bartshealth.nhs.uk. If you remain unhappy and wish to complain formally, you can do this through the NHS Complaints Procedure.

Will my taking part in this study be kept confidential?

All information collected about you during the research will be kept strictly confidential in accordance with the Data Protection Act 1998.

Everyone who takes part in the study will be assigned a code number. Information that allows you to be identified (e.g. your name and address) will be separated from the rest of your data and stored separately with only your assigned code number linking the two. All tissue samples and data collection sheets relating to the study will only be labelled with the code number. Only senior researchers involved in this study will be able to link your name to your clinical samples and data.

Your name will not be used in any reports or publications about the study.

Date 18.02.13 Version 3.0 Healthy Participants

When completed, 1 for patient; 1 for researcher site file; 1 (original) to be kept in medical notes

What will happen to any samples I give?

The blood will be taken specifically for research purposes in the clinic. All research samples will be labelled with your personal identifier code. They will then be securely transferred for analysis to the laboratories at Queen Mary University of London.

Where possible, samples will be analysed immediately or alternatively stored securely in freezers prior to analysis. Only researchers directly involved with this research project will have access to your samples. If you decide at any time to withdraw your data or samples from the study, your samples can be traced, removed from storage and destroyed. Samples will not be transferred outside the UK. It is unlikely that this study will provide information that is significant to you personally.

What will happen to my data and clinical samples after the study?

If you agree, your data, blood and tissue samples will be kept after this study has finished for use in future research projects. The samples will only be released to recognised researchers locally or from elsewhere whose project has undergone ethical and scientific review within the UK. The researchers may be given access to some information about your health, but will not be given any personal information that can be used to identify you.

What will happen to the results of the research study?

We plan to publish the results in a health/science journal as well as at Scientific conferences so others can learn from the results of the study. If you wish to know about any general results and publications, please let us know and we will keep you updated on the results of the study.

Who is organising and funding the research?

This research is jointly funded through The Royal College of Surgeons of England and The Wellcome Trust and will take place at Queen Mary, University of London. Neither your Doctor nor Research Clinicians are being paid for including you in the study

Who has reviewed the study?

All research in the NHS is looked at by independent group of people, called a Research Ethics Committee to protect your safety, rights, wellbeing and dignity. This study has been reviewed and given favourable opinion by London City and East Research Ethics Committee.

What happens if you are worried or if there is an emergency?

You will always be able to contact an investigator to discuss your concerns and/or to get help:

Principal Investigator for Study: Mr Paul Ryan
Address: **Centre for Adult Oral Health, 6th Floor Dental Hospital, London E1 2AT**
Telephone number: **0207 882 7156 / 8668** Email **p.l.ryan@qmul.ac.uk**

You will be given a copy of the information sheet and a copy of the consent form to keep. Copies will also be kept in the medical notes as well as retained by the Principal Investigator.

Date 18.02.13 Version 3.0 Healthy Participants
When completed, 1 for patient; 1 for researcher site file; 1 (original) to be kept in medical notes

10.3 Data collection sheets

10.3.1 Healthy volunteers



Bisphosphonate-related osteonecrosis of the jaw – An immunological based disease

Healthy volunteers- Data collection sheet

Date:	Systemic illnesses (List):
Pt Code:	Other Medications (List):
Sex: M/F	Previous Infections: Malaria / TB / HIV /Hep
Age:	Other infections:
Ethnicity:	Recent Antibiotics: Y/N
Countries resident outside UK:	Smoking: Y/N
Previous Bisphosphonates / RANKL inhibitors: Y/N	- Number - Years

10.3.2 BRONJ group



Bisphosphonate-related osteonecrosis of the jaw – An immunological based disease

Group 1- BRONJ patients- Data collection sheet

Date:	Systemic illnesses (List):
Pt Code:	Other Medications (List):
Sex: M/F	Previous Infections: Malaria / TB / HIV /Hep
Age:	Other infections:
Ethnicity:	Recent Antibiotics: Y/N
Countries resident outside UK:	Smoking: Y/N – No. Years
Bisphosphonate	
Drug:	Time on medication (weeks):
Route: Oral /IV	Reason for prescription:
Dose:	Fever after initial dose: Y/N
Dose interval (weeks):	Previous RANKL inhibitors (Denosumab): Y/N
BRONJ	
Pre-BP dental screen: Y/N	Reported symptoms:
Tingling prior to BRONJ: Y/N	Associated dental /pulpal infection periodontitis: Y/N + Details
BRONJ: Y/N Bone Exposed: Y/N	Precipitated by extraction /surgical extraction/oral surgery: Y/N + Details
Site: Mandible / Maxilla	Other reported precipitating factors:
Stage (AAOMS 2009): 1 / 2 / 3 / 4	Radiation therapy to Head + Neck: Y/N
Related to tooth site:	Radiographic signs:
Exposure period (weeks):	Treatment to date:
Pathological fracture: Y/N	<ul style="list-style-type: none"> • Topical Y/N • Antimicrobials Y/N • Surgery Y/N
Sinus tract: Y/N (Intra/extra-oral drainage)	
Eating affected: Y/N	
Painful: Y/N	
<p>0 - 10 VAS Numeric Pain Distress Scale</p> <p>No pain Moderate pain Unbearable pain</p> <p>0 1 2 3 4 5 6 7 8 9 10</p>	

10.4 Gene microarray- All differentially expressed genes.

All differentially expressed genes are indicated from the microarray of V γ 9V δ 2 T cell subsets. Comparison are made between each individual V γ 9V δ 2 T cell subset as well as between subsets compared to all other grouped subsets.+-

10.4.1 All differentially expressed genes in $\gamma\delta^{(28+)}$ v. $\gamma\delta^{(28-)}$.

Genes are ranked by fold difference and all have a fold difference >2 and p < 0.05 with values stated in the table below. Genes in red are higher in $\gamma\delta^{(28+)}$.

$\gamma\delta^{(28+)}$ vs. $\gamma\delta^{(28-)}$	Symbol	Fold change	p-value
1	<i>CCR6</i>	3.5	<0.0001
2	<i>GZMK</i>	3.2	0.0002
3	<i>LTB</i>	2.7	0.0001
4	<i>DPP4</i>	2.5	0.0001
5	<i>CD28</i>	2.5	0.0001
6	<i>LTB</i>	2.4	0.0001
7	<i>RORC</i>	2.3	0.0001
8	<i>IL23R</i>	2.2	0.0001
9	<i>MFGE8</i>	2.1	0.0001
10	<i>MYC</i>	2.1	0.01
11	<i>INADL</i>	2.1	0.0001
12	<i>FAM102A</i>	2.0	0.0001
13	<i>FGFBP2</i>	6.1	0.011
14	<i>GPR56</i>	5.4	0.03
15	<i>GPR56</i>	5.0	0.0007
16	<i>PRSS23</i>	4.6	<0.0001
17	<i>GZMB</i>	4.3	0.0001
18	<i>GZMH</i>	3.9	<0.0001
19	<i>GNLY</i>	3.3	0.0002
20	<i>FLJ20699</i>	3.0	<0.0001
21	<i>TTC38</i>	2.9	<0.0001
22	<i>OSBPL5</i>	2.5	<0.0001
23	<i>JAZF1</i>	2.5	<0.0001
24	<i>ZEB2</i>	2.5	<0.0001
25	<i>CES1</i>	2.4	0.02
26	<i>RAP2A</i>	2.3	<0.0001
27	<i>OSBPL5</i>	2.3	<0.0001
28	<i>ILMN_1856480</i>	2.3	0.02
29	<i>CYBRD1</i>	2.2	<0.0001
30	<i>ITGB1</i>	2.2	<0.0001
31	<i>KLRF1</i>	2.0	<0.0001
32	<i>ITGAM</i>	2.0	<0.0001
33	<i>LOC731007</i>	2.0	<0.0001

10.4.2 Differentially expressed genes in $\gamma\delta^{(28-)}$ vs. $\gamma\delta^{(16-)}$.

Genes are ranked by fold difference and all have a fold difference > 2 and p < 0.05 with values stated in the table below. Genes in red are higher in $\gamma\delta^{(28-)}$.

$\gamma\delta^{(28-)}$ vs. $\gamma\delta^{(16-)}$	Symbol	Fold change	p-value
1	<i>CD27</i>	10.3	<0.0001
2	<i>LOC441763</i>	2.6	<0.0001
3	<i>LOC100008588</i>	2.3	<0.0001
4	<i>LOC100008589</i>	2.3	<0.0001
5	<i>LOC100133565</i>	2.2	<0.0001
6	<i>LOC100134364</i>	2.2	<0.0001
7	<i>TYROBP</i>	2.2	<0.0001
8	<i>LOC100132394</i>	2.1	<0.0001
9	<i>LOC728499</i>	2.4	<0.0001
10	<i>CD8A</i>	2.3	<0.0001
11	<i>C5orf28</i>	2.3	<0.0001

10.4.3 Differentially expressed genes in $\gamma\delta^{(16-)}$ v. $\gamma\delta^{(16+)}$

Genes are ranked by fold difference and all have a fold difference > 2 and p < 0.05 with values stated in the table below. Genes in red are higher in $\gamma\delta^{(16-)}$.

$\gamma\delta^{(16-)}$ vs. $\gamma\delta^{(16+)}$	Symbol	Fold change	p-value
1	<i>SSBP3</i>	6.1	<0.0001
2	<i>LOC646674</i>	5.0	<0.0001
3	<i>LSP1</i>	4.6	<0.0001
4	<i>CD3E</i>	4.4	<0.0001
5	<i>ABCA2</i>	3.8	0.0005
6	<i>PPDPF</i>	3.5	<0.0001
7	<i>LOC641972</i>	3.4	<0.0001
8	<i>LOC400174</i>	3.4	<0.0001
9	<i>FLNA</i>	3.2	<0.0001
10	<i>BSG</i>	3.2	<0.0001
11	<i>LOC401002</i>	3.1	<0.0001
12	<i>AES</i>	3.1	<0.0001
13	<i>PKM2</i>	3.1	<0.0001
14	<i>SMARCC2</i>	3.0	<0.0001
15	<i>GATAD2B</i>	3.0	<0.0001
16	<i>LSP1</i>	2.8	0.006
17	<i>INO80E</i>	2.8	<0.0001
18	<i>LY6E</i>	2.7	<0.0001
19	<i>CHCHD10</i>	2.7	<0.0001
20	<i>VAMP2</i>	2.7	<0.0001
21	<i>LOC407835</i>	2.7	<0.0001
22	<i>PABPC1</i>	2.6	<0.0001
23	<i>CTSD</i>	2.6	<0.0001
24	<i>FAM100A</i>	2.6	<0.0001
25	<i>PACS1</i>	2.5	<0.0001
26	<i>SH3BP1</i>	2.5	0.0001
27	<i>FKBP1A</i>	2.5	<0.0001
28	<i>FKSG30</i>	2.5	0.001
29	<i>LSP1</i>	2.5	<0.0001
30	<i>BANF1</i>	2.5	<0.0001
31	<i>MGRN1</i>	2.4	<0.0001
32	<i>DCAF15</i>	2.4	<0.0001
33	<i>PKN1</i>	2.4	<0.0001
34	<i>PFN1</i>	2.3	<0.0001
35	<i>PTMS</i>	2.3	<0.0001
36	<i>HMGA1</i>	2.3	<0.0001
37	<i>PARP10</i>	2.3	<0.0001
38	<i>JOSD2</i>	2.3	<0.0001
39	<i>GTF3C1</i>	2.3	<0.0001
40	<i>PKM2</i>	2.3	<0.0001
41	<i>ARHGEF1</i>	2.3	0.002
42	<i>IL32</i>	2.2	<0.0001
43	<i>PTMA</i>	2.2	<0.0001
44	<i>RAB5C</i>	2.2	<0.0001
45	<i>ARHGEF1</i>	2.2	0.0005
46	<i>LOC642489</i>	2.2	<0.0001
47	<i>CLPTM1</i>	2.2	<0.0001
48	<i>LOC644914</i>	2.2	0.01
49	<i>G6PD</i>	2.2	<0.0001
50	<i>KIR2DL3</i>	2.2	<0.0001
51	<i>PARP10</i>	2.2	<0.0001
52	<i>PA2G4</i>	2.2	<0.0001
53	<i>ARRB2</i>	2.2	<0.0001
54	<i>TSC22D4</i>	2.2	0.03
55	<i>ZMAT3</i>	2.1	0.0005
56	<i>APBB1IP</i>	2.1	<0.0001
57	<i>BAT2</i>	2.1	<0.0001
58	<i>C16orf56</i>	2.1	0.003
59	<i>MRPL2</i>	2.1	<0.0001
60	<i>SMARCB1</i>	2.1	<0.0001
61	<i>BAT1</i>	2.1	<0.0001
62	<i>PKM2</i>	2.1	<0.0001
63	<i>ABTB1</i>	2.1	<0.0001
64	<i>LOC642828</i>	2.1	<0.0001
65	<i>GPAA1</i>	2.1	<0.0001
66	<i>CNPY3</i>	2.1	0.001
67	<i>FAM108A2</i>	2.1	<0.0001
68	<i>FAM108A3</i>	2.0	0.009
69	<i>CNOT3</i>	2.0	<0.0001
70	<i>PNPLA2</i>	2.0	<0.0001
71	<i>BCL2L1</i>	2.0	0.0001
72	<i>GZMK</i>	4.8	<0.0001
73	<i>LOC100132761</i>	4.5	<0.0001

74	LOC100130332	3.6	<0.0001
75	CALML4	3.5	<0.0001
76	HLA-DQA1	3.4	<0.0001
77	MRPS25	3.0	<0.0001
78	ILMN_1873034	2.9	<0.0001
79	TPM2	2.9	<0.0001
80	FOSEB	2.9	<0.0001
81	LOC100132564	2.8	<0.0001
82	ILMN_1916256	2.7	<0.0001
83	CYB561	2.6	<0.0001
84	INTS1	2.6	<0.0001
85	CPSF1	2.5	<0.0001
86	GRAMD1A	2.5	<0.0001
87	NELF	2.4	<0.0001
88	LTB	2.4	<0.0001
89	DBN1	2.4	<0.0001
90	HEATR1	2.4	<0.0001
91	DPP7	2.3	<0.0001
92	ILMN_1823130	2.3	<0.0001
93	LRCH4	2.3	<0.0001
94	C7orf27	2.3	<0.0001
95	RNF126	2.3	<0.0001
96	HMHA1	2.2	<0.0001
97	ZDHHC11	2.2	<0.0001
98	TP53I13	2.2	<0.0001
99	SPSB3	2.2	<0.0001
100	ILMN_1819304	2.2	<0.0001
101	LRCH4	2.2	<0.0001
102	RASAL3	2.1	<0.0001
103	TPD52L2	2.1	<0.0001
104	ILMN_1879482	2.1	<0.0001
105	PIGQ	2.1	<0.0001
106	U2AF1L2	2.1	<0.0001
107	C21orf2	2.1	<0.0001
108	UPLP	2.1	<0.0001
109	LRSAM1	2.1	<0.0001
110	MIR1974	2.1	0.0001
111	PLA2G4B	2.1	<0.0001
112	E4F1	2.1	<0.0001
113	LOC731682	2.1	0.02
114	CARD11	2.1	<0.0001
115	IL15	2.1	0.0002
116	CYB561	2.0	<0.0001
117	PRR14	2.0	<0.0001
118	CERKL	2.0	<0.0001
119	SLC26A11	2.0	<0.0001
120	SCAP	2.0	<0.0001
121	SPRYD3	2.0	<0.0001
122	ABTB1	2.0	<0.0001
123	SIPA1	2.0	<0.0001

10.4.4 Differentially expressed genes in $\gamma\delta^{(28+)}$ v. $\gamma\delta^{(16-)}$

Genes are ranked by fold difference and all have a fold difference > 2 and $p < 0.05$ with values stated in the table below. Genes in red are higher in $\gamma\delta^{(28+)}$.

$\gamma\delta^{(28+)}$ vs. $\gamma\delta^{(16-)}$	Symbol	Fold change	p-value
1	CD27	12.9	0.003
2	GZMK	8.2	<0.0001
3	PDE4B	6.3	0.001
4	DUSP2	5.1	<0.0001
5	CSDA	4.2	0.001
6	MYC	4.1	0.001
7	LTB	4.1	<0.0001
8	RPS23	4.0	<0.0001
9	LTB	3.9	<0.0001
10	CCR6	3.8	0.02
11	TMEM14C	3.5	<0.0001
12	CXCR4	3.5	<0.0001
13	FAM46C	3.5	<0.0001
14	MYC	3.3	0.001
15	AXUD1	3.3	<0.0001
16	LOC100132673	3.3	<0.0001
17	LOC647307	3.3	0.03
18	ZFP36	3.2	<0.0001
19	LOC100129882	3.2	<0.0001

20	DPP4	3.2	0.02
21	CXCR4	3.1	<0.0001
22	VAV3	3.0	0.01
23	LOC100134364	3.0	<0.0001
24	IFITM3	3.0	0.08
25	LOC100008589	3.0	<0.0001
26	LOC100132394	3.0	<0.0001
27	SIPA1L2	2.9	0.032
28	LOC91561	2.9	<0.0001
29	RPLP0	2.8	<0.0001
30	MFGE8	2.8	0.001
31	LASS6	2.8	0.05
32	NR4A2	2.7	0.001
33	TNFAIP3	2.7	<0.0001
34	SIK1	2.7	0.01
35	LOC649049	2.7	<0.0001
36	CD28	2.7	0.0001
37	FAM118A	2.6	0.024
38	TIPARP	2.6	<0.0001
39	RORC	2.6	0.65
40	RPL13L	2.6	<0.0001
41	ISG20	2.6	<0.0001
42	LOC100131866	2.5	<0.0001
43	FAM102A	2.5	<0.0001
44	SCD	2.5	0.0013
45	CNN2	2.5	<0.0001
46	NINJ1	2.5	<0.0001
47	PDE4B	2.5	0.22
48	IRS2	2.4	0.0013
49	LOC642934	2.3	<0.0001
50	DUSP5	2.3	<0.0001
51	ZFP36L2	2.3	<0.0001
52	LOC253039	2.3	0.001
53	LOC645688	2.3	<0.0001
54	SLC7A5	2.3	<0.00010
55	METTL1	2.2	0.001
56	LOC148430	2.2	<0.0001
57	ADCY3	2.2	0.001
58	JUNB	2.2	<0.0001
59	MTP18	2.2	<0.0001
60	LOC440927	2.2	<0.0001
61	IL23R	2.2	0.0001
62	LOC388564	2.2	<0.0001
63	LOC729679	2.2	<0.0001
64	NR4A2	2.2	<0.0001
65	LOC642989	2.2	<0.0001
66	LOC642035	2.2	0.0001
67	CD7	2.2	<0.0001
68	DNAJB9	2.1	<0.0001
69	LOC127295	2.1	<0.0001
70	LRIG1	2.1	0.0013
71	IL18R1	2.1	<0.0001
72	LOC388339	2.1	<0.0001
73	BEXL1	2.1	<0.0001
74	LOC727984	2.1	<0.0001
75	C17orf45	2.1	<0.0001
76	FKBP5	2.1	<0.0001
77	STS-1	2.1	0.001
78	SLAMF1	2.1	0.001
79	TRAT1	2.1	<0.0001
80	LOC728820	2.1	<0.0001
81	RPL14	2.1	<0.0001
82	TCEAL4	2.0	<0.0001
83	LOC100132795	2.0	<0.0001
84	LOC729236	2.0	<0.0001
85	LOC645173	2.0	<0.0001
86	LOC388556	2.0	<0.0001
87	ZNF683	10.5	<0.0001
88	CD8A	10.2	<0.0001
89	CD8A	9.3	<0.0001
90	FGFBP2	8.4	<0.0001
91	GPR56	8.2	<0.0001
92	CX3CR1	7.6	<0.0001
93	CX3CR1	6.9	<0.0001
94	GPR56	6.6	<0.0001
95	PRSS23	5.9	<0.0001
96	PATL2	5.6	<0.0001
97	GZMB	5.5	<0.0001
98	KIR2DL1	5.4	<0.0001
99	LOC197135	5.2	<0.0001
100	GZMH	5.0	<0.0001
101	LOC100133678	5.0	<0.0001
102	HBB	4.8	<0.0001
103	KIR3DS1	4.6	<0.0001
104	GNLY	4.6	<0.0001

105	GNLY	4.4	<0.0001
106	ILMN_1913060	4.3	<0.0001
107	TTC38	4.2	<0.0001
108	GNLY	4.2	<0.0001
109	FLJ20699	4.0	<0.0001
110	HLA-DQA1	3.9	<0.0001
111	ITGAX	3.9	<0.0001
112	PDGFRB	3.6	<0.0001
113	LGALS1	3.5	<0.0001
114	PALLD	3.5	<0.0001
115	LAIR2	3.4	<0.0001
116	TXNDC3	3.3	<0.0001
117	JAZF1	3.3	<0.0001
118	AKR1C3	3.3	<0.0001
119	HBA2	3.3	<0.0001
120	ASCL2	3.2	<0.0001
121	CES1	3.1	<0.0001
122	ERBB2	3.1	<0.0001
123	KIR2DL1	3.1	<0.0001
124	CD8A	3.1	<0.0001
125	PATL2	3.1	<0.0001
126	LAIR2	3.1	<0.0001
127	RAP2A	3.0	<0.0001
128	SGCE	2.9	<0.0001
129	KIR2DL4	2.9	<0.0001
130	KIR2DL4	2.9	0.006
131	OSBPL5	2.8	<0.0001
132	ITGB1	2.8	<0.0001
133	KIR3DL3	2.8	<0.0001
134	RHOB	2.8	<0.0001
135	KIR2DS5	2.8	<0.0001
136	PTGDR	2.8	<0.0001
137	CYBRD1	2.8	<0.0001
138	ZEB2	2.7	<0.0001
139	RAB11FIP5	2.7	<0.0001
140	MIAT	2.7	<0.0001
141	PROK2	2.6	<0.0001
142	TSHZ3	2.6	<0.0001
143	SLC1A7	2.6	<0.0001
144	HBA2	2.6	<0.0001
145	OSBPL5	2.6	<0.0001
146	IFNG	2.6	<0.0001
147	ILMN_1856480	2.5	<0.0001
148	GARNL4	2.5	<0.0001
149	ITGB1	2.5	<0.0001
150	PTGDR	2.5	<0.0001
151	PRF1	2.5	<0.0001
152	CLDND2	2.5	<0.0001
153	OASL	2.5	<0.0001
154	LOC730024	2.5	<0.0001
155	PLOD1	2.4	<0.0001
156	KLRF1	2.4	<0.0001
157	GDPD5	2.4	<0.0001
158	ILMN_1819608	2.4	<0.0001
159	SIGLECP3	2.4	<0.0001
160	ITGB1	2.4	<0.0001
161	CACNA2D4	2.3	<0.0001
162	PRKAR1A	2.3	<0.0001
163	LOC728499	2.3	<0.0001
164	FLJ14213	2.3	<0.0001
165	CENPK	2.3	<0.0001
166	SPG11	2.3	<0.0001
167	VCL	2.3	<0.0001
168	LOC731007	2.3	<0.0001
169	CEP78	2.2	<0.0001
170	RHOBTB3	2.2	<0.0001
171	D4S234E	2.2	0.0001
172	ITGAM	2.2	<0.0001
173	CYBRD1	2.2	<0.0001
174	KIR3DL1	2.2	0.0001
175	ATPGD1	2.2	<0.0001
176	ATPGD1	2.2	<0.0001
177	AKR1C4	2.1	<0.0001
178	PHGDH	2.1	<0.0001
179	ZNF365	2.1	<0.0001
180	EPDR1	2.1	<0.0001
181	FGR	2.1	<0.0001
182	KIR2DS3	2.1	0.0001
183	PLEK	2.1	<0.0001
184	PODN	2.1	<0.0001
185	HLA-DRB4	2.1	0.0002
186	LOC23117	2.1	<0.0001
187	FAM46A	2.1	<0.0001
188	LOC642909	2.1	<0.0001
189	CEP78	2.0	<0.0001

190	ZDHC11	2.0	<0.0001
191	SUSD1	2.0	<0.0001
192	ZNF439	2.0	<0.0001
193	FNDC3B	2.0	<0.0001
194	LOC649143	2.0	<0.0001
195	NMUR1	2.0	<0.0001

10.4.5 Differentially expressed genes in $\gamma\delta^{(28+)}$ v. $\gamma\delta^{(16+)}$

Genes are ranked by fold difference and all have a fold difference > 2 and p < 0.05 with values stated in the table below. Genes in red are higher in $\gamma\delta^{(28+)}$.

$\gamma\delta^{(28+)}$ vs. $\gamma\delta^{(16+)}$	Symbol	Fold change	p-value
1	GZMK	37.1	<0.0001
2	CD27	16.5	<0.0001
3	LTB	9.2	<0.0001
4	LTB	7.2	<0.0001
5	LOC100132761	6.4	0.02
6	PDE4B	6.12	<0.0001
7	MYC	5.4	<0.0001
8	DUSP2	5.3	<0.0001
9	ILMN_1873034	5.3	<0.0001
10	MYC	4.6	<0.0001
11	CCR6	4.4	<0.0001
12	LOC100133565	4.3	0.03
13	FAM102A	4.0	<0.0001
14	LOC100008589	4.0	0.01
15	CNN2	3.9	0.0001
16	CD160	3.9	<0.0001
17	LOC148430	3.8	<0.0001
18	CSDA	3.7	<0.0001
19	LOC100132673	3.7	<0.0001
20	GRAMD1A	3.7	<0.0001
21	MFGE8	3.6	<0.0001
22	DPP4	3.6	<0.0001
23	HLA-DMA	3.6	0.02
24	SIPA1L2	3.6	<0.0001
25	LOC100008588	3.5	0.0004
26	LOC651149	3.5	<0.0001
27	TMEM14C	3.5	<0.0001
28	CD7	3.4	<0.0001
29	LOC100131866	3.4	<0.0001
30	LOC91561	3.3	<0.0001
31	UBASH3A	3.3	0.02
32	AXUD1	3.2	<0.0001
33	CYB561	3.2	<0.0001
34	ZFP36	3.1	0.0259
35	DPP7	3.1	<0.0001
36	C8orf55	3.1	<0.0001
37	FOSB	3.0	0.0001
38	LOC100130332	3.0	<0.0001
39	TRAT1	2.9	<0.0001
40	FAM118A	2.9	<0.0001
41	LOC442232	2.9	<0.0001
42	CD28	2.9	<0.0001
43	RPL14	2.9	<0.0001
44	SLC7A5	2.9	0.001
45	RNF126	2.9	<0.0001
46	LOC729679	2.8	<0.0001
47	CYB561	2.8	0.0001
48	HPCAL1	2.8	<0.0001
49	RPL13L	2.8	<0.0001
50	LOC286444	2.8	<0.0001
51	LOC644907	2.8	<0.0001
52	TP53I13	2.7	<0.0001
53	ILMN_1916904	2.7	<0.0001
54	LOC649049	2.7	<0.0001
55	MIR1974	2.7	<0.0001
56	SIPA1	2.7	<0.0001
57	C17orf45	2.7	<0.0001
58	RORC	2.7	<0.0001
59	ADCY3	2.7	<0.0001
60	FAM46C	2.6	<0.0001
61	C11orf2	2.6	<0.0001
62	MRPS25	2.6	<0.0001
63	PARP3	2.6	<0.0001

64	SIK1	2.6	<0.0001
65	LRCH4	2.6	<0.0001
66	CPSF1	2.6	<0.0001
67	PDE4B	2.5	0.002
68	NINJ1	2.5	<0.0001
69	UPLP	2.5	<0.0001
70	LOC100130562	2.5	<0.0001
71	UBAC2	2.5	<0.0001
72	P2RY11	2.5	<0.0001
73	LOC653156	2.5	<0.0001
74	SIRPG	2.5	<0.0001
75	SIRPG	2.4	<0.0001
76	INADL	2.4	<0.0001
77	NCK2	2.4	<0.0001
78	C7orf27	2.4	<0.0001
79	HEXDC	2.4	<0.0001
80	DYNLL2	2.4	<0.0001
81	LOC653737	2.4	0.008
82	CMTM7	2.4	<0.0001
83	FBL	2.4	<0.0001
84	IRF1	2.4	<0.0001
85	FAM102A	2.4	<0.0001
86	IL23R	2.4	<0.0001
87	SUSD3	2.4	<0.0001
88	LOC387825	2.4	<0.0001
89	SCAP	2.4	<0.0001
90	CCDC109B	2.4	<0.0001
91	INTS1	2.3	<0.0001
92	RPL13	2.3	<0.0001
93	SLAMF1	2.3	0.0001
94	TPD52L2	2.3	<0.0001
95	DUSP5	2.3	<0.0001
96	LOC441506	2.3	<0.0001
97	LOC100129685	2.3	<0.0001
98	LOC652624	2.3	<0.0001
99	LYL1	2.3	<0.0001
100	RORC	2.3	<0.0001
101	STS-1	2.3	0.02
102	C10orf35	2.3	<0.0001
103	CECR5	2.3	<0.0001
104	UROS	2.3	<0.0001
105	RPLP0	2.3	0.0001
106	WDR74	2.3	<0.0001
107	LOC391019	2.2	0.002
108	TCEAL4	2.2	<0.0001
109	MTP18	2.2	0.0003
110	VEGFB	2.2	<0.0001
111	VARS2	2.2	<0.0001
112	HMHA1	2.2	<0.0001
113	POLR3H	2.2	<0.0001
114	PDXK	2.2	0.003
115	LOC441013	2.2	<0.0001
116	IL18R1	2.2	0.001
117	ADORA2A	2.2	0.01
118	METTL1	2.2	<0.0001
119	LOC728431	2.2	<0.0001
120	ABLIM1	2.2	<0.0001
121	TMEM14C	2.2	<0.0001
122	SMAP2	2.2	<0.0001
123	RPS6KB2	2.2	<0.0001
124	LOC729742	2.2	<0.0001
125	LOC401676	2.2	<0.0001
126	SYPL1	2.2	<0.0001
127	BTBD2	2.2	<0.0001
128	LOC390354	2.2	<0.0001
129	DENND5A	2.2	0.0001
130	HNRPA1L-2	2.2	<0.0001
131	LOC728820	2.1	0.0001
132	C16orf58	2.1	<0.0001
133	LOC339192	2.1	<0.0001
134	RPL12P6	2.1	<0.0001
135	DGCR6	2.1	<0.0001
136	ISG20	2.1	<0.0001
137	IL23R	2.1	0.0001
138	PARP10	2.1	<0.0001
139	LOC100130562	2.1	<0.0001
140	C17orf70	2.1	<0.0001
141	CAPS	2.1	<0.0001
142	EMD	2.1	<0.0001
143	TUBA1C	2.1	<0.0001
144	LIMS1	2.1	<0.0001
145	LOC644511	2.1	<0.0001
146	LOC728820	2.1	<0.0001
147	LOC648249	2.1	<0.0001
148	LOC388564	2.1	<0.0001

149	SLC25A22	2.1	<0.0001
150	ALDOC	2.1	<0.0001
151	BMS1	2.1	<0.0001
152	B4GALT1	2.1	0.01
153	LOC440991	2.1	<0.0001
154	LOC653232	2.1	<0.0001
155	SPSB3	2.1	<0.0001
156	LOC728060	2.1	0.008
157	LOC100132795	2.1	<0.0001
158	SNORA24	2.1	<0.0001
159	NFE2L3	2.1	<0.0001
160	DIMT1L	2.1	<0.0001
161	KLHL22	2.1	0.03
162	LOC401115	2.1	<0.0001
163	STMN3	2.1	0.002
164	LOC389156	2.1	<0.0001
165	PTGES2	2.1	<0.0001
166	MFSD3	2.1	<0.0001
167	FAM173A	2.0	<0.0001
168	DPH5	2.0	0.0002
169	GNL1	2.0	<0.0001
170	TRMT1	2.0	<0.0001
171	LOC389156	2.0	<0.0001
172	CARD11	2.0	<0.0001
173	GTPBP6	2.0	<0.0001
174	C19orf66	2.0	<0.0001
175	AVP11	2.0	<0.0001
176	PRKCZ	2.0	<0.0001
177	RPS29	2.0	<0.0001
178	PUS1	2.0	<0.0001
179	LOC388556	2.0	<0.0001
180	DNAJB9	2.0	0.003
181	TRAF5	2.0	0.008
182	LOC158345	2.0	<0.0001
183	LOC388707	2.0	<0.0001
184	SPRYD3	2.0	<0.0001
185	FGFBP2	11.0	<0.0001
186	CX3CR1	10.0	0.0004
187	GPR56	9.9	<0.0001
188	CX3CR1	9.1	<0.0001
189	SSBP3	9.0	<0.0001
190	GPR56	8.0	0.0009
191	PRSS23	6.8	<0.0001
192	GZMB	6.8	<0.0001
193	LOC646674	6.5	<0.0001
194	TTC38	5.7	<0.0001
195	FLJ20699	5.4	<0.0001
196	GNLY	5.3	<0.0001
197	KIR2DL4	5.3	<0.0001
198	KIR2DL3	5.1	<0.0001
199	SPON2	4.9	0.03
200	RAP2A	4.7	0.01
201	LSP1	4.7	<0.0001
202	ZEB2	4.6	<0.0001
203	GZMH	4.5	<0.0001
204	ERBB2	4.3	<0.0001
205	CD3E	4.1	<0.0001
206	ABCA2	4.0	0.0002
207	LAIR2	4.0	<0.0001
208	GNLY	3.9	<0.0001
209	CYBRD1	3.7	<0.0001
210	FLNA	3.7	<0.0001
211	KIR3DL1	3.6	0.001
212	ITGB1	3.6	<0.0001
213	MGC52282	3.6	0.006
214	LAIR2	3.6	<0.0001
215	JAZF1	3.5	<0.0001
216	LOC400174	3.4	<0.0001
217	LOC401002	3.4	<0.0001
218	LOC641972	3.4	<0.0001
219	KIR2DL3	3.3	<0.0001
220	LYN	3.3	0.0105
221	PRF1	3.3	<0.0001
222	BSG	3.2	<0.0001
223	GATAD2B	3.2	<0.0001
224	CYBRD1	3.2	<0.0001
225	AES	3.2	<0.0001
226	LSP1	3.1	0.0009
227	VAMP2	3.0	<0.0001
228	SUSD1	3.0	0.0002
229	SMARCC2	3.0	<0.0001
230	ATPGD1	3.0	<0.0001
231	FAM100A	2.9	<0.0001
232	TSHZ3	2.9	<0.0001
233	EPDR1	2.9	<0.0001

234	TRK1	2.9	<0.0001
235	GDPD5	2.9	<0.0001
236	PKM2	2.8	<0.0001
237	PKN1	2.8	<0.0001
238	FKSG30	2.7	0.005
239	PFN1	2.7	<0.0001
240	LSP1	2.7	<0.0001
241	RAB11FIP5	2.7	<0.0001
242	LOC730024	2.7	<0.0001
243	OASL	2.7	<0.0001
244	SMAD7	2.7	<0.0001
245	FAM46A	2.7	0.0003
246	ASCL2	2.7	<0.0001
247	FLJ14213	2.6	<0.0001
248	OSBPL5	2.6	<0.0001
249	BCL9L	2.6	<0.0001
250	LY6E	2.6	<0.0001
251	FGF	2.6	<0.0001
252	ABI3	2.6	<0.0001
253	APOBEC3C	2.6	<0.0001
254	PTMS	2.6	<0.0001
255	C16orf56	2.6	<0.0001
256	SETBP1	2.6	<0.0001
257	SSBP3	2.5	<0.0001
258	MYO1G	2.5	<0.0001
259	INO80E	2.5	<0.0001
260	PACS1	2.5	<0.0001
261	PTPN12	2.5	<0.0001
262	SH3BGR13	2.5	<0.0001
263	APBB1IP	2.5	<0.0001
264	ARHGEF1	2.5	0.0004
265	FAM108A2	2.5	<0.0001
266	CEP78	2.5	0.04
267	CEP78	2.5	0.003
268	PTK2B	2.4	0.005
269	FNDC3B	2.4	<0.0001
270	LRRFIP1	2.4	<0.0001
271	LOC653438	2.4	<0.0001
272	CLPTM1	2.4	<0.0001
273	LOC729495	2.4	<0.0001
274	CTNNA1	2.4	<0.0001
275	PPDPF	2.4	0.02
276	FCAR	2.4	<0.0001
277	LOC407835	2.4	<0.0001
278	RAB5C	2.4	<0.0001
279	RPTOR	2.4	0.04
280	ACTB	2.4	<0.0001
281	RTN4	2.4	<0.0001
282	ZYX	2.3	<0.0001
283	RHOBTB3	2.3	<0.0001
284	FAM108A3	2.3	0.0004
285	SH3BP1	2.3	0.002
286	CTSD	2.3	0.0003
287	VCL	2.3	<0.0001
288	GTF3C1	2.3	<0.0001
289	FKBP1A	2.3	<0.0001
290	ITGAM	2.3	<0.0001
291	STXBP2	2.3	<0.0001
292	PARP10	2.3	<0.0001
293	PARP10	2.3	<0.0001
294	GNPTAB	2.3	<0.0001
295	PKN1	2.3	<0.0001
296	SEMA3E	2.3	<0.0001
297	AES	2.3	<0.0001
298	FNDC3B	2.3	<0.0001
299	FAR1	2.3	<0.0001
300	ADD3	2.3	0.0001
301	HSPA6	2.3	<0.0001
302	BANF1	2.3	<0.0001
303	PA2G4	2.3	<0.0001
304	LOC644988	2.3	<0.0001
305	DCAF15	2.3	<0.0001
306	RAB5C	2.3	<0.0001
307	ARHGEF1	2.3	0.0003
308	CENPT	2.3	<0.0001
309	G6PD	2.3	<0.0001
310	JOSD2	2.2	<0.0001
311	ADAMTS1	2.2	<0.0001
312	ADAM8	2.2	<0.0001
313	TSC22D4	2.2	0.02
314	OSBPL5	2.2	<0.0001
315	DUSP8	2.2	<0.0001
316	MYL12A	2.2	<0.0001
317	STIM1	2.2	<0.0001
318	LOC644914	2.2	0.02

319	GFI1	2.2	0.008
320	XRCC2	2.2	0.001
321	RTN4	2.2	<0.0001
322	DRAP1	2.2	<0.0001
323	GNAI2	2.2	<0.0001
324	FAM63A	2.2	<0.0001
325	CAPNS1	2.2	<0.0001
326	ZNF69	2.2	0.0001
327	ARRB2	2.2	<0.0001
328	ILMN_1872419	2.2	<0.0001
329	LOC729495	2.1	<0.0001
330	UBL3	2.1	<0.0001
331	FKBP14	2.1	0.004
332	LOC642489	2.1	0.0005
333	MGRN1	2.1	<0.0001
334	CEBPA	2.1	0.0001
335	PKM2	2.1	<0.0001
336	ACTN4	2.1	<0.0001
337	HCG2P7	2.1	<0.0001
338	CAPNS1	2.1	<0.0001
339	SSBP4	2.1	<0.0001
340	SASH3	2.1	<0.0001
341	PLEKHA1	2.1	0.002
342	CNOT3	2.1	<0.0001
343	PDZD4	2.1	<0.0001
344	GHDC	2.1	<0.0001
345	SLCO4C1	2.1	<0.0001
346	S1PR5	2.1	<0.0001
347	ILMN_1900734	2.1	0.0003
348	VCL	2.1	0.0000
349	SHROOM4	2.1	0.0000
350	CD3G	2.1	0.002
351	PTPN6	2.0	0.0000
352	PTPN12	2.0	0.0000
353	LSS	2.0	0.001
354	ILMN_1864166	2.0	0.0000
355	BAT1	2.0	0.0000
356	ACTR3	2.0	0.0000
357	LMF2	2.0	0.002
358	MBTD1	2.0	0.0000
359	SYTL1	2.0	0.0009

10.4.6 Differentially expressed genes in $\gamma\delta^{(28+)}$ v. Others (grouped)

Genes are ranked by fold difference and all have a fold difference > 2 and p < 0.05 with values stated in the table below. Genes in red are higher in $\gamma\delta^{(28+)}$ subset.

$\gamma\delta^{(28+)}$ v Others	Symbol	Fold change	p-values
1	GZMK	5.9	<0.0001
2	CCR6	4.0	<0.0001
3	LTB	4.0	<0.0001
4	LTB	3.7	<0.0001
5	PDE4B	3.6	<0.0001
6	MYC	3.2	<0.0001
7	DPP4	3.1	<0.0001
8	SIPA1L2	2.9	<0.0001
9	MYC	2.8	<0.0001
10	DUSP2	2.8	0.04
11	CD28	2.8	<0.0001
12	MFGE8	2.7	<0.0001
13	FAM102A	2.7	<0.0001
14	RORC	2.6	<0.0001
15	AXUD1	2.5	<0.0001
16	TMEM14C	2.5	<0.0001
17	CSDA	2.5	<0.0001
18	ILMN_1873034	2.5	<0.0001
19	LOC91561	2.4	0.01
20	FAM118A	2.4	<0.0001
21	IL23R	2.4	<0.0001
22	LOC100131866	2.3	<0.0001
23	SIK1	2.3	<0.0001
24	LOC148430	2.2	0.04
25	INADL	2.2	<0.0001
26	RPLP0	2.2	<0.0001
27	LOC651149	2.2	0.04
28	FAM46C	2.2	<0.0001

29	<i>LOC442232</i>	2.1	<0.0001
30	<i>RORC</i>	2.1	<0.0001
31	<i>RPL13L</i>	2.1	<0.0001
32	<i>ADCY3</i>	2.1	<0.0001
33	<i>IL23R</i>	2.1	<0.0001
34	<i>LOC649049</i>	2.1	<0.0001
35	<i>FAM102A</i>	2.0	<0.0001
36	<i>LASS6</i>	2.0	<0.0001
37	<i>ZNF683</i>	8.3	<0.0001
38	<i>FGFBP2</i>	8.2	<0.0001
39	<i>GPR56</i>	7.4	<0.0001
40	<i>CX3CR1</i>	7.3	0.03
41	<i>CX3CR1</i>	6.6	<0.0001
42	<i>GPR56</i>	6.2	<0.0001
43	<i>PRSS23</i>	5.8	<0.0001
44	<i>GZMB</i>	5.4	<0.0001
45	<i>TTC38</i>	4.2	<0.0001
46	<i>GNLY</i>	4.2	<0.0001
47	<i>FLJ20699</i>	4.2	<0.0001
48	<i>GZMH</i>	4.1	<0.0001
49	<i>LGALS1</i>	3.9	<0.0001
50	<i>GNLY</i>	3.6	<0.0001
51	<i>ERBB2</i>	3.5	<0.0001
52	<i>ZEB2</i>	3.5	<0.0001
53	<i>LAIR2</i>	3.4	<0.0001
54	<i>LAIR2</i>	3.1	<0.0001
55	<i>JAZF1</i>	3.0	<0.0001
56	<i>CYBRD1</i>	3.0	<0.0001
57	<i>ITGB1</i>	2.8	<0.0001
58	<i>ASCL2</i>	2.7	<0.0001
59	<i>OSBPL5</i>	2.6	<0.0001
60	<i>PRF1</i>	2.6	<0.0001
61	<i>TSHZ3</i>	2.5	<0.0001
62	<i>CYBRD1</i>	2.5	0.01
63	<i>LOC731007</i>	2.5	<0.0001
64	<i>RAB11FIP5</i>	2.4	<0.0001
65	<i>EPDR1</i>	2.4	<0.0001
66	<i>SUSD1</i>	2.4	<0.0001
67	<i>OSBPL5</i>	2.4	<0.0001
68	<i>ATPGD1</i>	2.3	0.03
69	<i>FLJ14213</i>	2.3	<0.0001
70	<i>LOC730024</i>	2.3	0.0200
71	<i>ITGAM</i>	2.2	<0.0001
72	<i>FGR</i>	2.1	<0.0001
73	<i>PTPN12</i>	2.1	<0.0001
74	<i>HSPA6</i>	2.1	<0.0001
75	<i>ADAMTS1</i>	2.1	<0.0001
76	<i>MYO1G</i>	2.1	0.01
77	<i>FNDC3B</i>	2.1	<0.0001
78	<i>VCL</i>	2.0	<0.0001
79	<i>GNPTAB</i>	2.0	<0.0001
80	<i>FNDC3B</i>	2.0	<0.0001
81	<i>RHOBTB3</i>	2.0	<0.0001

10.4.7 Differentially expressed genes in $\gamma\delta^{(28-)}$ vs. Others (grouped).

Genes are ranked by fold difference and all have a fold difference > 2 and $p < 0.05$ with values stated in the table below. Genes in red are higher in $\gamma\delta^{(28-)}$ subset.

$\gamma\delta^{(28-)}$ v Others	Symbol	Fold change	p-value
0			

10.4.8 Differentially expressed genes in $\gamma\delta^{(16-)}$ vs. Others (grouped).

Genes are ranked by fold difference and all have a fold difference > 2 and p < 0.05 with values stated in the table below. Genes in red are higher in $\gamma\delta^{(16-)}$ subset.

$\gamma\delta^{(16-)}$ v Others	Symbol	Fold change	p-value
1	<i>CD8A</i>	2.7	<0.0001
2	<i>PATL2</i>	2.6	<0.0001
3	<i>LOC197135</i>	2.4	<0.0001
4	<i>LOC728499</i>	2.1	<0.0001
5	<i>PATL2</i>	2.0	<0.0001
6	<i>CD8A</i>	2.0	<0.0001

10.4.9 Differentially expressed genes in $\gamma\delta^{(16+)}$ vs. Others (grouped).

Genes are ranked by fold difference and all have a fold difference > 2 and p < 0.05 with values stated in the table below. Genes in red are higher in $\gamma\delta^{(16+)}$ subset.

$\gamma\delta^{(16+)}$ vs. Others	Symbol	Fold change	p-value
1	<i>SSBP3</i>	7.6	<0.0001
2	<i>LOC646674</i>	5.4	<0.0001
3	<i>LSP1</i>	4.4	<0.0001
4	<i>ABCA2</i>	4.1	0.0002
5	<i>CD3E</i>	4.0	<0.0001
6	<i>FLNA</i>	3.4	<0.0001
7	<i>LOC401002</i>	3.3	<0.0001
8	<i>LOC400174</i>	3.3	<0.0001
9	<i>LOC641972</i>	3.2	<0.0001
10	<i>GATAD2B</i>	3.2	<0.0001
11	<i>AES</i>	3.0	<0.0001
12	<i>BSG</i>	3.0	<0.0001
13	<i>VAMP2</i>	2.9	<0.0001
14	<i>SMARCC2</i>	2.9	<0.0001
15	<i>LSP1</i>	2.9	0.003
16	<i>PKM2</i>	2.9	<0.0001
17	<i>PPDPF</i>	2.7	0.0009
18	<i>FAM100A</i>	2.7	<0.0001
19	<i>INO80E</i>	2.6	<0.0001
20	<i>LSP1</i>	2.6	<0.0001
21	<i>KIR2DL3</i>	2.6	<0.0001
22	<i>PACS1</i>	2.5	<0.0001
23	<i>PKN1</i>	2.5	<0.0001
24	<i>TTC38</i>	2.5	<0.0001
25	<i>ZEB2</i>	2.5	<0.0001
26	<i>C16orf56</i>	2.4	0.0001
27	<i>KIR2DL4</i>	2.4	0.006
28	<i>LOC407835</i>	2.4	<0.0001
29	<i>FKSG30</i>	2.4	0.011
30	<i>ARHGEF1</i>	2.4	0.001
31	<i>SH3BP1</i>	2.4	0.0004
32	<i>FCAR</i>	2.4	<0.0001
33	<i>LY6E</i>	2.4	<0.0001
34	<i>PFN1</i>	2.4	<0.0001
35	<i>FLJ20699</i>	2.3	0.03
36	<i>KIR2DL3</i>	2.3	0.03
37	<i>TSC22D4</i>	2.3	0.007
38	<i>BCL9L</i>	2.3	<0.0001
39	<i>GTF3C1</i>	2.3	<0.0001
40	<i>PARP10</i>	2.3	<0.0001
41	<i>PTMS</i>	2.3	<0.0001
42	<i>DCAF15</i>	2.3	<0.0001
43	<i>CLPTM1</i>	2.3	<0.0001
44	<i>CTSD</i>	2.3	<0.0001
45	<i>SEMA3E</i>	2.3	<0.0001
46	<i>ARHGEF1</i>	2.3	0.0004
47	<i>FKBP1A</i>	2.3	<0.0001
48	<i>PARP10</i>	2.2	<0.0001
49	<i>LRRFIP1</i>	2.2	<0.0001
50	<i>SMAD7</i>	2.2	0.003
51	<i>BANF1</i>	2.2	<0.0001

52	<i>RAB5C</i>	2.2	<0.0001
53	<i>APBB1IP</i>	2.2	<0.0001
54	<i>CENPT</i>	2.2	<0.0001
55	<i>FAM108A3</i>	2.2	0.002
56	<i>FAM108A2</i>	2.2	<0.0001
57	<i>LOC644914</i>	2.2	0.01
58	<i>FAM63A</i>	2.2	<0.0001
59	<i>PA2G4</i>	2.2	<0.0001
60	<i>SSBP3</i>	2.2	<0.0001
61	<i>MGRN1</i>	2.2	<0.0001
62	<i>JOSD2</i>	2.2	<0.0001
63	<i>ARRB2</i>	2.1	<0.0001
64	<i>PKN1</i>	2.1	<0.0001
65	<i>G6PD</i>	2.1	<0.0001
66		2.1	<0.0001
67	<i>STXBP2</i>	2.1	<0.0001
68	<i>BAT2</i>	2.1	<0.0001
69	<i>APOBEC3C</i>	2.1	<0.0001
70	<i>XRCC2</i>	2.1	0.0002
71	<i>ERBB2</i>	2.1	0.04
72	<i>LOC653438</i>	2.1	<0.0001
73	<i>PKM2</i>	2.1	<0.0001
74	<i>STIM1</i>	2.1	<0.0001
75	<i>GDPD5</i>	2.1	0.02
76	<i>MBTD1</i>	2.1	<0.0001
77	<i>RAB5C</i>	2.1	<0.0001
78	<i>SHROOM4</i>	2.1	<0.0001
79	<i>LOC642489</i>	2.0	0.0001
80	<i>ZNF69</i>	2.0	<0.0001
81	<i>ADD3</i>	2.0	0.01
82	<i>ITGB1</i>	2.0	0.01
83	<i>FKBP14</i>	2.0	0.03
84	<i>SH3BGL3</i>	2.0	0.004
85	<i>LOC729495</i>	2.0	<0.0001
86	<i>ABI3</i>	2.0	0.003
87	<i>ABTB1</i>	2.0	<0.0001
88	<i>LOC729495</i>	2.0	0.0005
89	<i>LOC644988</i>	2.0	<0.0001
90	<i>CD27</i>	12.4	0.004
91	<i>LOC100132761</i>	5.4	<0.0001
92	<i>LOC100132564</i>	4.0	0.0002
93	<i>ILMN_1873034</i>	4.0	0.001
94	<i>LOC100133565</i>	3.9	<0.0001
95	<i>CD160</i>	3.4	0.0006
96	<i>LOC100008588</i>	3.3	<0.0001
97	<i>GRAMD1A</i>	3.2	<0.0001
98	<i>CALML4</i>	3.1	<0.0001
99	<i>HLA-DMA</i>	2.9	0.01
100	<i>LOC100130332</i>	2.9	<0.0001
101	<i>CD7</i>	2.8	<0.0001
102	<i>HEATR1</i>	2.8	<0.0001
103	<i>DPP7</i>	2.8	<0.0001
104	<i>CYB561</i>	2.7	0.0004
105	<i>RNF126</i>	2.6	<0.0001
106	<i>MRPS25</i>	2.5	<0.0001
107	<i>C8orf55</i>	2.5	0.0005
108	<i>TP53I13</i>	2.5	0.0000
109	<i>CYB561</i>	2.4	0.0006
110	<i>SIPA1</i>	2.4	<0.0001
111	<i>LRCH4</i>	2.4	<0.0001
112	<i>CPSF1</i>	2.4	<0.0001
113	<i>RPL14</i>	2.3	0.0002
114	<i>INTS1</i>	2.3	<0.0001
115	<i>C7orf27</i>	2.3	<0.0001
116	<i>LOC653156</i>	2.2	0.02
117	<i>DBN1</i>	2.2	<0.0001
118	<i>LOC729679</i>	2.2	0.004
119	<i>C11orf2</i>	2.2	<0.0001
120	<i>HMHA1</i>	2.2	<0.0001
121	<i>HPCAL1</i>	2.2	0.0003
122	<i>UPLP</i>	2.2	0.0031
123	<i>LOC286444</i>	2.2	0.001
124	<i>C17orf45</i>	2.2	0.0001
125	<i>CERKL</i>	2.2	0.0001
126	<i>SCAP</i>	2.2	<0.0001
127	<i>LOC644907</i>	2.2	0.0001
128	<i>HEXDC</i>	2.2	<0.0001
129	<i>TPD52L2</i>	2.2	<0.0001
130	<i>UBAC2</i>	2.2	<0.0001
131	<i>CMTM7</i>	2.1	0.03
132	<i>SIRPG</i>	2.1	<0.0001
133	<i>BTBD2</i>	2.1	<0.0001
134	<i>CARD11</i>	2.1	<0.0001
135	<i>PARP10</i>	2.1	<0.0001
136	<i>IRF1</i>	2.1	0.0001

137	<i>ILMN_1823130</i>	2.1	0.03
138	<i>SIRPG</i>	2.0	0.02
139	<i>RPS6KB2</i>	2.0	<0.0001
140	<i>FBL</i>	2.0	<0.0001
141	<i>UROS</i>	2.0	<0.0001
142	<i>P2RY11</i>	2.0	0.02